EXPLORING POTENTIAL ANALGESIC TARGETS AND TOOLS FOR CHRONIC PAIN TREATMENT

Rayan Haroun Mohammed Abdalla

A thesis submitted for the degree of Doctor of Philosophy to University College London

Wolfson Institute for Biomedical Research (WIBR), Division of Medicine

UCL 2023

I. Declaration

I, Rayan Haroun, confirm that the work presented in this thesis is my own. Where information has been derived from other sources; I confirm that this has been indicated in the thesis.

II. Abstract

This thesis investigated two main topics. The first was the preclinical evaluation of various analgesic modalities for cancer-induced bone pain (CIBP). The second involved the potential application of chemogenetic tools for pain research.

I optimised and used an *in vivo* model of CIBP involving the injection of Lewis Lung Carcinoma cells into the intramedullary space of the femur of C57BL/6 mice or transgenic mice with C57BL/6 background. In this model, mice gradually reduce the use of the affected limb resulting in altered weight bearing. Symptoms of secondary cutaneous cold, heat, and mechanical sensitivity also manifest. Three potential analgesic modalities were assessed, which can be divided into three categories; targeting the $Na_V1.7$ voltage-gated Na^+ channel, targeting neuronal subsets (namely the μ-opioid receptor-expressing neurons and the sensory neurons that express $Na_V1.8$ channels), and finally, the dual targeting of two of the tumour-derived products (nerve growth factor (NGF) and tumour necrosis factor (TNF)). Results from these experiments indicated the congenital deletion or chemogenetic-based silencing of the $Na_V1.8$ expressing neurons reduced pain-like behaviour associated with CIBP. Moreover, dual inhibition of NGF and TNF resulted in an impressive reduction in CIBP-driven weight-bearing and prevented the development of secondary cutaneous heat hyperalgesia.

The second half of this work focused on modified ligand-gated ion channels, namely $PSAM^4$-GlyR and $PSAM^4$-5HT3. This work showed that expressing $PSAM^4$-GlyR in dorsal root ganglia (DRG) neurons and agonism with varenicline silences DRG neurons and elevates the withdrawal thresholds of mice in various sensory tests. Additionally, $PSAM^4$-GlyR activation in the $Na_V1.8$+ neurons reversed signs of mechanical, thermal, and cold sensitivity associated with neuropathic pain. Moreover, chemogenetic-based activation of specific neurons in the central amygdala was shown to increase pain thresholds. These techniques will be useful for studies investigating the effects of manipulating neuronal subsets.

III. Impact statement

Chronic pain persisting long after injury constitutes possibly the biggest clinical challenge of the twenty-first century, quantitatively and qualitatively. Analgesics that are currently on the market often fail to treat chronic pain effectively. Approximately a fifth of the world's population will endure excruciating forms of chronic pain while alive. As my thesis title indicates, my work mainly focused on finding ways to treat this chronic and purposeless pain.

A significant part of my work focussed on cancer-induced bone pain (CIBP), a condition that occurs in about 90% of patients with bone metastases. By evaluating the analgesic potential of several targets and/or tools, my work suggests analgesic options and opens doors for re-purposing some analgesics for the benefit of patients living with CIBP. By attempting to use chemogenetic tools for pain management, both centrally and peripherally, my work suggests that reversible gene therapy tools can be a safer alternative compared to gene knockout options for conditions where individual molecular targets fail. I believe that this work will positively impact academic research as well as clinical studies.

The results obtained during my Ph.D. have been presented at several national and international meetings and have been shared online. Additionally, a review article discussing the mechanisms of cancer has been published in Frontiers in Pain Research.

I, along with other students from UCL, have established a group called the ‘Students’ P.O.P’, which organises monthly seminars at UCL and discusses various science-related topics. I also took part in the ‘Patient Ambassador’ group, which is a group that tries to bridge the gap between the science that takes place within the BonePainII network and patients. Through this group, we talked to patients and patient advocates to help guide scientists and clinicians to what patients need the most. I also taught a lecture that focused on touch and proprioception to undergraduate students at UCL.

IV. Dedication

This work is dedicated to all the members of Haroun Mohammed Abdalla Dirar's family and my beloved country, Sudan.

V. Acknowledgements

I want to express my gratitude to Professor John Wood, my primary supervisor, for allowing me to pursue a Ph.D. in the Molecular Nociception Group. I sincerely appreciate all of his advice, support, and helpful suggestions. I also want to express my gratitude to Professor James Cox, my secondary supervisor, for his encouragement and for guiding me throughout my PhD. I also want to express my gratitude to Professor Fan Wang for having me in her lab at the Massachusetts Institute of Technology.

I would like to express my gratitude to all former and current members of the Molecular Nociception Group for their support. This has been a wonderful environment for doing a Ph.D. I would like to thank Sam Gossage for being my right hand during cancer-induced bone pain surgeries. Thanks to my fellow postdocs for their informative conversations and moral support during my Ph.D. Special thanks to Dr Naxi Tian, who has not only been an inspiring postdoc but also for being a best friend. Special thanks to Dr Manuel Arcangeletti for all the help and the patch clamping experiments for the chemogenetics project. I also would like to thank Dr Federico Iseppon for teaching me the Ca^{2+} imaging technique. I also want to thank Dr Ana Luiz for her help with the DRG exposure and for the emotional support. Thanks to Dr Marta Alves Simoes for teaching me the DRG culture. Thanks to Sonia Santana-Varela for teaching me the cancer-induced bone pain model and the behavioural tests. Thanks to Alex Fudge for the technical support.

Additionally, I want to thank Dr Jing Zhao for always answering my inquiries. I want to thank Dr Shafaq Sikandar for guiding me while writing my published review. I also would like to thank Dr Sara Caxaria for the µ-CT imaging. I want to thank Dr Iain Chessell and Dr Fraser Welsh for their kind donation of MEDI-578 (and its control) and etanercept. Thanks to all of the BonePainII network members for all the collaborations. Special thanks to Professor Anne-Marie Heegaard and Ulla Jakobsen for making my Ph.D. experience so wonderful. I want to express my gratitude to everyone who helped me get to this stage, especially the instructors and supervisors at UCL, the Chevening scholarship, King's College London, UCB, and the University of Khartoum. I'm grateful to my friends for always being there for me.

Finally, I would like to thank my parents for giving me the tools that brought me here and for supporting my academic life choices. I would like to thank my mom, who is my role model, for supporting me. A big thank you to my siblings for being there, sparing no effort to listen, and seeking solutions for any issues I faced, not only during my Ph.D. but also ever since I was born. Many thanks to my loving nieces and nephews for reminding me of what I am here for and that I have a loving family waiting for me in Sudan. Thanks to Rania Haroun for being my guardian angel and motivation engine and for helping me out in my moments of deepest despair. Thanks for planting the enthusiasm in me and for not letting me settle for less. Thanks to Ahmed Abdelrahman for his support. Thanks to my friends for always being there for me.

VI. Funding

I would like to thank the European Union's Horizon 2020 research and innovation program under the Marie Sklodowska-Curie grant agreement No 814244 for funding my Ph.D. I also would like to thank the Bogue Fellowship from UCL and Professor Fan Wang for funding my visit to MIT. I would like to thank cancer research UK (CRUK, grant number 185341) for funding a significant part of the work reported in my thesis.

"The project has received funding from the European Union's Horizon 2020 research and innovation programme under the Marie Sklodowska-Curie grant agreement No 814244".

VII. Publications

Haroun, R., Wood, J.N. and Sikandar, S. (2022). Mechanisms of cancer pain. Frontiers in Pain Research (Lausanne, Switzerland), [online] 3, p.1030899. doi:https://doi.org/10.3389/fpain.2022.1030899.

VIII. Table of Contents

IX. List of figures

X. List of tables

1. General introduction

1.1. Why is *pain* a problem?

1.1.1. The difference between nociception and pain

The word “pain” originates from Poinê, the Greek goddess of retribution (Duncan, 2017). In almost all eras and civilisations, pain has been equated with divine punishment. According to the International Association for the Study of Pain (IASP), *pain* is “An unpleasant sensory and emotional experience associated with, or resembling that associated with, actual or potential tissue damage” (Raja et al., 2020). The common meaning of pain, which refers to hardship and suffering in a larger sense, is very different from this description. The IASP terminology places the patient’s sentiments front and centre while highlighting the subjective character of pain and generating a specific, narrow definition that can be studied scientifically. Other definitions place more emphasis on how they serve a purpose, such as “pain is the unpleasant sensation that has evolved to motivate behaviour that avoids or minimises tissue damage or promotes recovery” (Wright, 2011). Looking deeper into the IASP pain definition, it appears that pain has two main components: sensory and emotional components. The presence of the emotional pain component explains the fact that the same stimulus can result in varying degrees of pain perception between individuals (Wilcox et al., 2015).

Pain has many resemblances with other senses. Firstly, pain is linked to receptors that detect damage or potential damage caused by various types of stimuli. These receptors are expressed on the free nerve endings that are distributed throughout the body. Secondly, once a noxious stimulus creates a message, this message is conveyed by specific nerves to the spinal cord. The nerves responsible for detecting noxious stimuli and conveying the message to the spinal cord are named primary afferent nociceptors (or first-order neurons). Within the spinal cord, the first-order neuron contacts the second-order neuron. The second-order neuron conveys pain messages to the higher brain centres via specific pathways. The higher brain centres to which the messages are conveyed include the brain stem reticular formation, thalamus, somatosensory cortex and limbic system. It is believed that pain perception relies mainly on the thalamus and cortex.

Even with this understanding, there remains an unanswered question; Why is pain felt? Firstly, pain serves as an early caution that prompts withdrawal from possibly dangerous stimuli. Secondly, pain from damaged tissue compels you to protect the injured area, aiding in the healing process by keeping a wound from getting worse. Thirdly, the annoying sensation of pain is a deterrent that instructs you not to repeat the action that caused the suffering in the first place. Patients who are born with congenital insensitivity to pain may suffer fatal, painless injuries, which highlights that pain is necessary for survival (Cox et al., 2006).

Nociception is not the same as pain. Charles Sherrington created the term "nociception" to differentiate between the physiological actions taking place in the nervous system and the subjective perception of pain (Levine, 2007). According to IASP, "the neural process of encoding noxious stimuli" constitutes the sole scope of nociception(Loeser & Treede, 2008). Without any associated pain, nociceptive alterations to behaviour and homeostasis can occur. On the other hand, pain can be felt even when peripheral nociceptors are not active in patients suffering from brain lesions or stroke (Henry et al., 2008). Since animals are unable to self-report their pain, many studies focus on studying nociception in animals (Corder et al., 2017). In these studies, nocifensive behaviours are regarded as being pain-like behaviours which could mean that the animal is likely experiencing pain. Despite the challenges related to studying the emotional component of pain experience, many research groups attempt to decode this element. For example, digging and burrowing behaviour can be used to evaluate 'well-being' in mouse models of arthritis to determine the impact of pain on daily activities (Chakrabarti et al., 2018).

The prevalence of nociception and pain-like behaviours in the natural world is evidence of their importance for survival. Even bacteria retrench when exposed to high pressure (Levina et al., 1999). Mammals, amphibians, reptiles, birds, and fish are vertebrates that have nociceptors, although cartilaginous fish do not have the unmyelinated afferents which are necessary for nociception in the majority of species (Smith & Lewin, 2009). Similarly, invertebrates, like *C. elegans,* also possess nociceptors (Elwood, 2011). Interesting species with reduced nociception have arisen as a result of evolution. Because of a $Na_V1.7$ variant which is strongly inhibited by protons to impede acid-driven action potential firing, the naked mole rat is not responsive to acid (Smith et al., 2011).

Sensitisation is a key component of nociception. Our nociceptors increase their responses when subjected to extended stimulation. Maladaptive sensitisation can cause excruciating, pointless agony (Gold & Gebhart, 2010). What causes these peculiar sensitivities to develop? Nociceptors in squid develop sensitisation after damage. If this sensitisation is stopped using an anaesthetic, an injured squid demonstrates diminished long-term survival due to delayed escape responses whenever exposed to predators in comparison to both uninjured squids and injured squids with preserved sensitisation. This is because an injured squid with blocked sensitisation finds it harder to escape from predators (Crook et al., 2014). Thus, pain plasticity is adaptive, providing a survival benefit, but it may go wrong over time, leading to chronic pathological pain.

1.1.2. Chronic (persistent) pain

A fifth of the global population suffers from chronic pain, and many individuals are resistant to treatment (Breivik et al., 2006). As our population ages, both the total number and percentage of people experiencing pain are rising (Freburger et al., 2009). The issue of pain constitutes possibly the biggest clinical challenge of the twenty-first century, quantitatively and qualitatively.

Chronic pain is defined as pain that lasts longer than three months (Treede et al., 2015). Multiple age-related and chronic diseases, such as cancer, diabetes, and arthritis, have the trait of persistent pain. One meta-analysis in the UK revealed that approximately 14.3% of the UK general population experiences moderate to severe chronic pain (Fayaz et al., 2016). It should come as no surprise that people with chronic pain have a lower quality of life, suffer from mental health issues, and lose their jobs. Chronic pain collectively places a substantial strain on the medical system and has a $300 billion annual economic cost in the US (Gaskin & Richard, 2012).

Short-lived pains, such as post-surgical pain, are successfully managed by current medicines, while persistent pain states are much more difficult to control. For instance, only one-third of people with persistent neuropathic pain, including shingles or diabetic neuropathy, obtain pain reduction with pregabalin (Derry et al., 2019). The most frequently prescribed analgesic, paracetamol, was found to be absolutely inefficacious for treating lower back pain in a systematic review (Saragiotto et al., 2016). Although there is less evidence to support their usage,

opioids, which seem to be very beneficial in treating acute or end-of-life pain, are frequently prescribed in the US for chronic pain (Stannard, 2018). Prescription opioids are now widely available as a result of excessive opioid prescription, which has led to an epidemic of opioid addiction. Over 80,000 individuals died because of opioid overdoses in the US alone in 2021, creating a tragedy of enormous humanitarian proportions (NIDA, 2023). Chronic Non-steroidal anti-inflammatory drugs (NSAIDs) use, which is widespread among older generations, is often strongly linked to mortality. The most probable reasons include gastric haemorrhage, renal failure, and enhanced cardiovascular problems (Marcum & Hanlon, 2010). As a result, there is a pressing unmet need for novel analgesics that are more effective than the currently existing ones, have fewer adverse effects, and provide a lower risk of addiction.

The Declaration of Montréal, released in 2010 by IASP, indicated that access to effective pain management is an important human right (International Pain Summit Of The International Association For The Study Of Pain, 2011). New therapeutic approaches to pain alleviation should be developed in order to address the issue of pain. It is important to identify and validate novel biological targets rationally. Therefore, we need to understand pain physiology and pathology to achieve this, and basic experimental research is the only way to accomplish this.

1.1.3. Theories attempting to explain pain

Galen, a Greek physician, was the first to conduct experimental research on pain. Galen believed that perhaps the malfunction in four humours is the cause of nerve irritation, which leads to pain. He demonstrated how sensory deficiencies result from cutting the spinal cord of piglets, implying the presence of an ascending somatosensory route (Cervero & Wood, 2020; Ochs, 2004). Avicenna, an Iranian scholar, came to the conclusion that pain could be distinguished from touch and temperature as a separate sense in the 11th century based on his clinical findings (Perl, 2007). The study of the nervous system anatomy continued throughout the Middle Ages, but it really took off during the Renaissance when Vesalius expanded on Galen's discoveries (Moayedi & Davis, 2013). However, it is Descartes who is now typically credited with founding the scientific study of pain. Descartes compared the nervous system to a machine in his Treatise on Man, wherein fire particles led animal spirits to travel down certain filaments to the

brain, which is the location where the pain is felt. The iconic drawing by La Forge, which combined Descartes' thesis with modern anatomical advancements, may thus be deemed the first scientific representation of pain (Figure 1) (Cervero & Wood, 2020).

The Specificity Theory of Pain was foreshadowed by Descartes' model. According to the Specificity Theory, pain is a distinct sense that travels via designated pathways from the peripheral sites to perception, with the intensity of the stimulus governing how much pain is felt. Lesion investigations provided evidence in favour of a distinct pain pathway. The anterolateral pathway for pain and temperature was discovered in the 19th century by cutting the spinal cord at various levels, but the posterior bundles were specialised for harmless mechano-sensation (Moayedi & Davis, 2013). A patient with a bullet wound to the grey matter of the spinal cord was described by Gowers, a doctor in London, as lacking the ability to feel pain and temperature while touch sensation remained intact (Moayedi & Davis, 2013). Charles Sherrington proposed the presence of nociceptors, special nerves devoted to sensing harmful stimuli and whose activation resulted in pain, which Ed Perl and colleagues finally discovered about fifty years later (Bessou & Perl, 1969b; Burgess & Perl, 1967; Levine, 2007).

Figure 1: Famous illustration by La Forge that was printed in Descartes' Treatise of Man. *Descartes' theory of the acute pain reaction is captured in this illustration. B) The man's foot is near the flames (A). The skin is pressed against*

the flames, which pull on the fibril or filament (C). This causes the opening of the pore (D and E) in which the fibril terminates in the brain. The pore opening allows animal spirits to enter the fibril from the cavity in the brain (F). The muscles are then triggered by the animal spirits to pull the foot away from the flames, which is what we now refer to as a nocifensive reflex or behaviour.

A major issue of the specificity theory is that it does not consider pain's cognitive and affective aspects. Accordingly, several other theories attempted to decode the intricacy of the pain sensation. In the 1800s, William Erb made the observation that powerful feelings are typically unpleasant and brought on by potent stimuli, leading him to hypothesise that pain was basically the emotional result of the strong stimulation of unspecialised somatosensory tracts. In syphilitic individuals with deteriorated dorsal columns, recurrent stimulation (up to 600 times) using ordinarily inconspicuous tactile stimuli resulted in excruciating pain (Moayedi & Davis, 2013). These studies prompted Alfred Goldscheider to postulate that for the pain to expand with the intensity of various sensory inputs, some sort of summing up must be taking place within the central nervous system (Moayedi & Davis, 2013). John Nafe built on the Intensity Theory in the late 1920s as a component of his "quantitative theory of feeling". According to him, certain patterns of input caused somatosensory perception to emerge; the pattern of firing of peripheral nerves encoded the nature of the stimulus and determined the nature of the accompanying experience (Nafe, 1929). This Pattern Theory's fundamental premise was that peripheral nerves are fundamentally all the same; the details of the structure and timing of the activity, rather than the nerve itself, are the determinants of the identity of the nerve. Wide dynamic range neurons were first found in the deep dorsal horn in the 1960s, which reinforced the criticism against the specificity theory (Mendell, 1966).

In the "harsh dispute" surrounding these opposing pain theories, the groundbreaking paper "Pain mechanisms: a new theory" was published, and it served as the basis for that debate (R. Melzack & P. D. Wall, 1965). Melzack and Wall start by introducing the works of the opposing sides, the Specificity Theory and the Pattern Theory. They presented a unique Gate Control mechanism that combined elements of both theories, recognising that the experimental evidence may support either explanation. However, they proposed that the substantia gelatinosa served as a gate that controlled which peripheral inputs reached the

brain. They acknowledged the presence of specialised nociceptive and tactile afferents. They also suggested that small nociceptive fibres tend to open the gate and large fibres close it. They also indicated that the entire system was controlled by descending inputs from the brain, explaining the clinical fact that pain frequently does not match the severity of the injury. Gate Theory was not the final word on the subject, despite its influence.

The debate over the selectivity of sensory neuron responses has been reignited by the development of *in vivo* imaging tools that allow for the simultaneous monitoring of the firing of large groups of cells (Emery & Wood, 2019). There is no doubt that research based on the Specificity Theory has been incredibly fruitful, leading to the identification of numerous distinct cell types, receptors, and ion channels that seem to transmit distinct sensations (Le Pichon & Chesler, 2014). Nonetheless, it is impossible to overlook the philosophical issues with the Specificity Theory. On the one hand, certain channels necessitate an integrator to create the total perception, eerily resembling a "Cartesian theatre" where the man-in-the-brain just perceives (Dennett, 1993). However, there needs to be a ceiling to specificity in order to avoid falling into the hypothesis that one neuron is necessary for each unique sensation (Gross, 2002). In their review (Emery & Wood, 2019), Emery and Wood acknowledged the existence of modality-specific nociceptive neurons being supported by data from electrophysiological, behavioural, molecular, and imaging research, but they highlighted that the general consensus in the study of pain is that most nociceptors are polymodal. They suggested that the environment definitely affects how often polymodality occurs. They explained by the suggestion that if a given stimulus is sufficiently powerful to produce tissue damage, or if experimental preparation causes such damage, the subsequent inflammatory response is likely to increase the number of receptive sensory neurons as well as modulate their modality sensitivity, hence raising the prevalence of polymodality. The disparity in results could demonstrate the extraordinary adaptability of peripheral sensory neurons in detecting noxious stimuli during pain states, both acute and chronic.

Since they most closely match the reality of patients' experiences, theories of pain that address both the central and emotional pain elements have had the greatest influence in the clinic. An example of these theories is the one proposed by Melzack (Casey, 2019). According to this theory, the behaviours that people

indulge in to protect themselves are not just natural responses to pain; rather, they are an integral component of the pain experience. The IASP definition of pain officially endorses this multidimensional perspective on pain. The importance of prior knowledge and experience has recently been acknowledged in relation to pain. Howard Fields emphasises the significance of expectations and contends that conflicting motivations will lessen pain (Fields, 2018). It is becoming more common to adopt a Bayesian perspective of the brain in pain, in which pain is viewed as an inference based on not only nociceptive inputs but also the expectancies obtained from previous experiences (Seymour, 2019). Just from this brief assessment, it is clear that there are many different ideas that attempt to account for pain. The conflicting theories and personalities can be challenging to integrate and to determine which theory is the most correct or instructive. It is obvious that there are specialised receptors, neurons, and ion channels. Nevertheless, it is also undeniably true that there are many internal and environmental elements that might affect how a painful stimulus feels.

We need to be careful not to conflate different levels of analysis or explanation. A theory to explain nociception is not equivalent to a theory to explain pain, and vice versa. The central mechanisms leading to the emotional component and perceptual elements of pain may be better explained by one hypothesis, whereas the peripheral mechanisms for detecting and sensing the stimuli may be best explained by another. While my PhD work aims to find novel analgesics, the work did not focus on the emotional aspects.

1.2. Nociception and pain: sensory biology

1.2.1. Peripheral nerves

To direct behavioural and homeostatic responses, sensory neurons in the periphery monitor alterations in both the internal milieu and the surroundings. Here, I will be concentrating on sensory neurons, particularly the ones implicated in nociception and pain and whose axons terminate in the skin. These cutaneous fibres, whose cell bodies are found in the dorsal root and trigeminal ganglia, supply inputs that power the conscious perception of touch, temperature, itch, as well as pain. At the peripheral nerve terminal, many types of ambient energy, such as thermal, mechanical, and chemical stimuli, are converted into electrical signals which travel up somatosensory tracts to be processed and recognised by the central nervous system (CNS). Muller, an anatomist, is typically recognised

for being the first to propose that various sensory nerves convey information about varying stimuli types. This idea, which he dubbed his Law of Specific Nerve Energies, served as a foundational justification for the Specificity Theory of Pain (Moayedi & Davis, 2013). Von Frey and others provided experimental evidence for such "labelled lines" by demonstrating that simulating minute "spots" of the human skin using pinpricks resulted in unique sensations of pressure, heat, cold, or pain. Notably, histologists had already characterised and given names to specialised end organs at nerve terminals, such as Pacinian corpuscles, Meissner's corpuscles, and others. Von Frey attempted to associate these structures with certain feelings based on his "spot" research (Perl, 2007). Physiologists working with homemade recording devices gained a lot of insightful knowledge about how peripheral nerves operate. In the 1920s, recordings from the peripheral nerves of frogs showed that different fibre types respond differently to varying types of stimuli (Adrian & Zotterman, 1926). Almost all neuroscience textbooks continue to use recordings (obtained by Gasser) of compound action potentials from the cat's saphenous nerve to classify various fibres depending on their conduction velocity, diameter, and extent of myelination (Table 1).

Sherrington, who introduced the word "nociceptor," first proposed the idea that a portion of peripheral nerves recognises unpleasant or damaging stimuli (Levine, 2007). Pain was specifically left out of the five Aristotelian senses, and so many psychologists and doctors continued to support the intensity and/or pattern theories well into the 20th century, which claimed that pain was caused by excessive bursts of regular activity in unspecialised nerves. On the other hand, Gasser demonstrated that A-delta and C fibres were linked to nocifensive reactions by activating or inhibiting activity in neurons participating toward certain elements of the compound action potential (Perl, 2007). As a result, nociception and thermoception are typically connected with Aδ and C fibres, whereas tactile and proprioceptive signals are provided by Aβ fibres (see Table 1). Nevertheless, it is currently understood that nociceptors include A-beta fibres and all other kinds of sensory nerves (Lawson et al., 2019). When a short-lasting painful stimulus is applied to human subjects, the faster A fibres and the slower C fibres, correspondingly, are responsible for the early sharp and late dull pain sensations (Lewis & Pochin, 1937).

Table 1: Peripheral nerve categorisation according to electrophysiological recordings from cats' sensory neurons.

The conventional classification of sensory afferents, according to action potential conduction speed, is influenced by diameter as well as myelination level. C- and Aδ-fibres have typically been largely linked to nociceptors. Presently, Aβ nociceptors are believed to also exist (Lawson et al., 2019).

Sensory neuron fibre class	Diameter (µm)	Myelination extent	Action potential conduction speed (m/s)	Functional specificity
Aβ	6-22	Heavy	30-120	Tactile, proprioception, nociception
Aδ	1-4	Light	5-25	Tactile, mechano-nociception, Cold
C	0.4-1.2	None	0.1-2	Nociception, heat, cold, tactile, Pruriception

Since they were very thin, putative nociceptors presented physiologists with a significant technical challenge when trying to record from a single C fibre. Zotterman came to the conclusion that the C fibre section, which had a high threshold for activation, transmitted pain after recording from the cat's entire lingual nerve (Zotterman, 1936). But a few years later, he noticed that C fibres seemed to react to minor tactile stimuli, and he made the assumption that these might be specialised tickle afferents (Zotterman, 1939).

Perl and colleagues found single C and Aδ fibres that fired solely in response to noxious stimuli by monitoring several hundreds of individual units methodically and objectively. Nevertheless, contrary to Zotterman, not all C fibres acted as nociceptors. The majority of the nociceptive C fibres exhibited "polymodal"

responses. High-threshold mechanical stimuli were the primary triggers for activating Aδ nociceptors, but some Aδ fibres also responded to innocuous brushing (Bessou & Perl, 1969a, 1969b; Burgess & Perl, 1967). Results from recordings from human volunteers undergoing microneurographic recording of individual afferent fibres indicated a correlation between noxious stimulus, C fibre response, and perception of pain (Cox et al., 2006). Clinical studies have confirmed that peripheral nociceptors are key for driving the conscious feeling of pain when stimulated with a mild electrical current (Konietzny et al., 1981). We should be cautious during the interpretation of such microneurographic investigations as we cannot be certain which fibre is being stimulated because of the size of the microelectrode tip in touch with the microscopic fibres (Wall & McMahon, 1985). However, there is little question that mammals have specialised fibres that can detect and encode painful sensations based on several decades worth of peripheral nerve recordings in humans and other species. But, it is still unclear how they contribute to various types of pathological and physiological pain.

1.2.2. The main molecular markers used to categorise sensory neurons

Ramon y Cajal first identified that neurons might be classified into a taxonomy of cell "types". He classified the different morphologies of neurons into distinct groups by carefully examining Golgi-stained nerve tissues. Modern neuroscience is built on the idea that there are many types of cells. In order to profile and categorise individual neurons, characteristics like appearance, developmental origin, and gene expression profile are frequently utilised. Relating the physiological and anatomical specialisations of sensory neurons to the plethora of proteins expressed has been a major burden for sensory biologists. It is now feasible to classify and manipulate specific sensory neuron subgroups in mice by detecting molecular "markers" that label subsets of afferents (Figure 2).

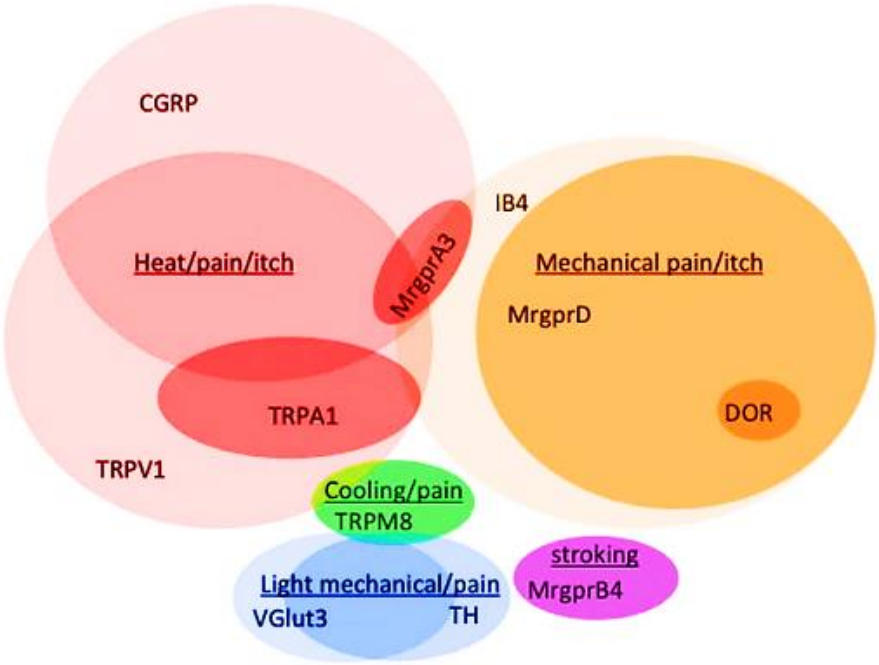

Figure 2: A Venn diagram summarising the prevalence of various molecular markers among a wide range of C fibre types as established by mouse genetic research. *The various molecularly-determined subtypes of sensory neurons and their functional specialisations are depicted in this Venn diagram. The main source of this categorisation is cell ablation research. Each circle symbolises a particular molecular marker, and each colour denotes a distinct modality. As a result, noxious heat necessitates cells that express TRPV1, CGRP, and TRPA1, whereas cooling is represented predominantly by neurons that express TRPM8, but that also express TRPV1. TRPV1: transient vanilloid receptor, CGRP: Calcitonin gene-related peptide, IB4: Isolectin B4, TH: Tyrosine hydroxylase, VGlut3: Vesicular glutamate transporter 3, Mrgpr: Mas-related G-protein-coupled receptor, DOR: delta opioid receptors. Adapted from (Le Pichon & Chesler, 2014).*

For instance, we can correlate the functional specialisations of specific sensory neurons using the neurochemical markers expressed. These biomarkers can be visualised through immunostaining. Densely myelinated sensory neurons, i.e. Aβ fibres, stain for neurofilament 200 (Lawson & Waddell, 1991), while small "dark" sensory neurons, i.e. C fibres, can be recognised by peripherin staining (Goldstein et al., 1991). It is important to mention that recent findings from rats' sensory neurons indicated that 23.9% of the neurofilament 200-positive neurons are unmyelinated and approximately 15.5% of the peripherin-expressing neurons are large myelinated neurons (Bae et al., 2015). The peptidergic and non-

peptidergic neurons are the main subgroups of presumptive nociceptors, but it is important to note that there is considerable overlap between these two subgroups. Neuropeptides like calcitonin gene-related peptide (CGRP) and Substance P are expressed by peptidergic neurons, whereas non-peptidergic neurons are distinguished by their isolectin B4 (IB4)-positivity (Emery & Ernfors, 2018). Sally Lawson's *ex vivo* and *in vivo* experiments showed that CGRP-expressing neurons make up C and Aδ fibres and constitute more than 50% of all nociceptors (Lawson et al., 2002; Lawson et al., 1996). Aδ mechanonociceptors innervating the hairy skin with circumferential ends were recently discovered by extracellular recording as well as Ca^{2+} imaging of CGRP-expressing afferents, highlighting the continued relevance and usefulness of these conventional neurochemical markers (Ghitani et al., 2017).

Deciphering the developmental origin of sensory neurons has been equally valuable. Transcription and growth factor molecular markers have been used to map the heterogeneity of low-threshold mechanosensors. For instance, low Tropomyosin receptor kinase B (TrkB) levels and expression of the transcription factor cMaf characterise the fast adapting low threshold mechanosensors, innervating the Meissner as well as Pacinian corpuscles (Wende et al., 2012). Conversely, Shox2 expression promotes the growth of TrkB-expressing neurons (Abdo et al., 2011; Emery & Ernfors, 2018). The Ginty laboratory has used molecular genetics to assess and characterise a sizable number of touch-related sensory neurons (Li et al., 2011). An intriguing illustration of how a few markers, when used in combination, can direct the fine-grained subdivision of a sensory neuron subset is how the Aβ low-threshold mechanoreceptors were defined and targeted utilising intersectional genetic methods depending on the fact that they co-express TrkC and Ret (Bai et al., 2015).

Predictably, ion channel genes, which are essential for the physiology of specialised sensory neurons, have demonstrated efficacy as markers. For instance, nociceptors were targeted using $Na_V1.8$, a Tetrodotoxin (TTX)-resistant Na^+ channel produced by C fibres possessing small diameter (L. Caroline Stirling et al., 2005). The vast majority of nociceptors are killed by diphtheria toxin-based removal of $Na_V1.8$-expressing neurons in a Cre-dependent manner, which eliminates the perception of mechanical, cold, as well as inflammatory pain (Abrahamsen et al., 2008) (see Chapter 4). The behaviour of animals which

express diphtheria toxin receptors driven by the promoter for heat-responsive ion channel transient receptor potential vanilloid 1 (Trpv1) shows that aversion to elevated temperatures is entirely eliminated after diphtheria toxin administration in adulthood (Pogorzala et al., 2013). Markers of ion channels have also been employed for "functional fingerprinting" in cultured sensory neurons. In this method, Ca^{2+} imaging is used to determine the response of cells to numerous channel-specific agonists, enabling the detection of groups depending on the distinctive "constellation" of molecules expressed rather than on the expression of one or two marker genes (Teichert et al., 2014).

Single-cell RNA sequencing has recently made it possible to categorise dorsal root ganglia (DRG) neurons objectively depending on the expression of tens of thousands of transcripts. The transcriptional profiles of 622 single mouse DRG neurons were examined by Patrick Ernfors' lab. This group divided the neurons into eleven distinct subsets by iterative principal component analysis that perfectly matched known categories of sensory neurons (Figure 3) (Usoskin et al., 2015). Subsequently, Linarsson examined 500,000 mouse nervous system cells and discovered a hierarchy of 17 subsets of sensory neurons (Zeisel et al., 2018). Unfortunately, these investigations only covered a small portion of the transcriptomes. Ten subcategories of sensory neurons were discovered by a greater-coverage analysis; this classification was supported by *in vivo* patch-clamp recordings, RNA extraction via the recording pipette, and subsequent analysis of the extracted RNA by reverse transcriptase polymerase chain reaction (PCR) (Li et al., 2018; C.-L. Li et al., 2016). One needs to keep in mind that sequencing depth, sampling techniques, and quality control have a significant impact on the final results, making single-cell transcriptomics not a magic bullet for sensory neuron taxonomy. The importance of analysing transcriptomes as opposed to the translatome is one of the most fundamental arguments. However, the value of these categorisation studies becomes more apparent when we consider how open-source single-cell transcriptome datasets aided scientists in hypothesis formulation. Underlying any count of cell subgroups are philosophical questions on what constitutes a biological "type". Taxonomists are cautioned against entering the trap of essentialism (Hull, 1965). For example, the thermal threshold of cold-sensing neurons, which is determined by expressing TRPM8, is actually set by simultaneous fluctuation in TRPM8 and K^+

channel expression levels (Madrid et al., 2009). This reality should not be obscured by the theoretical ease of a cell "type". Galanin, a possible marker of peptidergic nociceptors, has significant temporal variability, peaking after nerve damage and suggesting a pathogenic function (Bangash et al., 2018). As a result, clustering that relies on single-cell transcriptome implies that cell groups rely on a collection of multidimensional but statistically co-varying features, in such cases, expressed genes, even if "markers" offer an intuitive, binary means of defining cell identity. While I frequently refer to different taxonomies of DRG neurons in my thesis, it is important to remember these limitations.

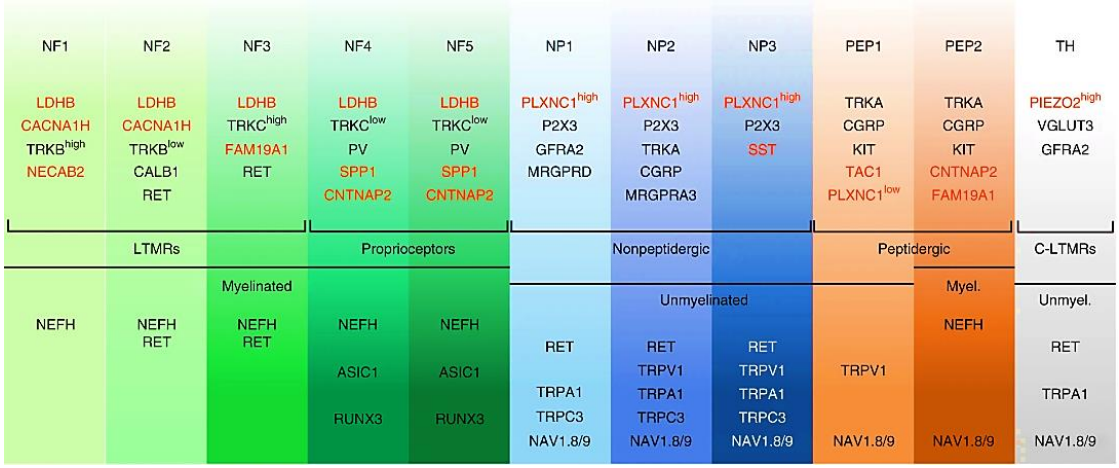

Figure 3: The foremost unbiased categorisation of DRG neurons obtained through single-cell RNA sequencing.

Ernfors and colleagues conducted single-cell RNA sequencing and classified sensory neurons by identifying eleven distinct subtypes, which are represented here in table form. Marker genes are displayed at the top, followed by functional ly significant molecules expressed in each subtype, including ion channels. Previously associated with myelinated DRG neurons, neurofilament heavy chain (Nefh) and parvalbumin (Pvalb) are expressed by the NF cluster. The expression of substance P (Tac1), TRKA (Ntrk1), and calcitonin gene-related peptide (CGRP, also known as Calca), previously associated with peptidergic nociceptors, was observed in the PEP cluster. Mrgprd and P2rx3 positivity, traditionally associated with non-peptidergic nociceptors, was detected in the NP cluster. The fourth cluster, designated TH, had a unique expression of tyrosine hydroxylase (Th), which has been characterised by a different subtype of unmyelinated neurons (Usoskin et al., 2015).

1.3. The experience of pain

The full pain experience has four essential components: transduction, transmission, modulation and perception (see Figure 4) (Khera & Rangasamy, 2021). Transduction is the process through which different stimuli of varying types (mechanical, thermal or chemical) are transformed into electrical signals. Transmission refers to all the relay functions that carry the message from the periphery where the damage (or potential damage) occurred to the brain centres responsible for pain perception. Modulation is the capacity of supraspinal neurons to influence nociceptive inputs. The influence that the supraspinal neurons could have on the nociceptive inputs can either facilitate the transmission of the pain signal to the higher CNS centres or hinder it. The fourth component of the pain experience is perception, which is the awareness of pain. Pain perception is subjective, allowing the individual to integrate the sensory messages into a coherent overall experience. Perception itself is attained by the complex interaction between several functions within the brain, such as attention, expectation, and interpretation (Urch, 2007). Unlike the preceding three pain processes (transduction, transmission and modulation), pain perception cannot be decoded using objective methods that rely on direct observation. Accordingly, even though it is possible to monitor the activity of the neurons involved in pain transmission, this does not allow researchers to determine whether or not the individual being investigated is experiencing pain.

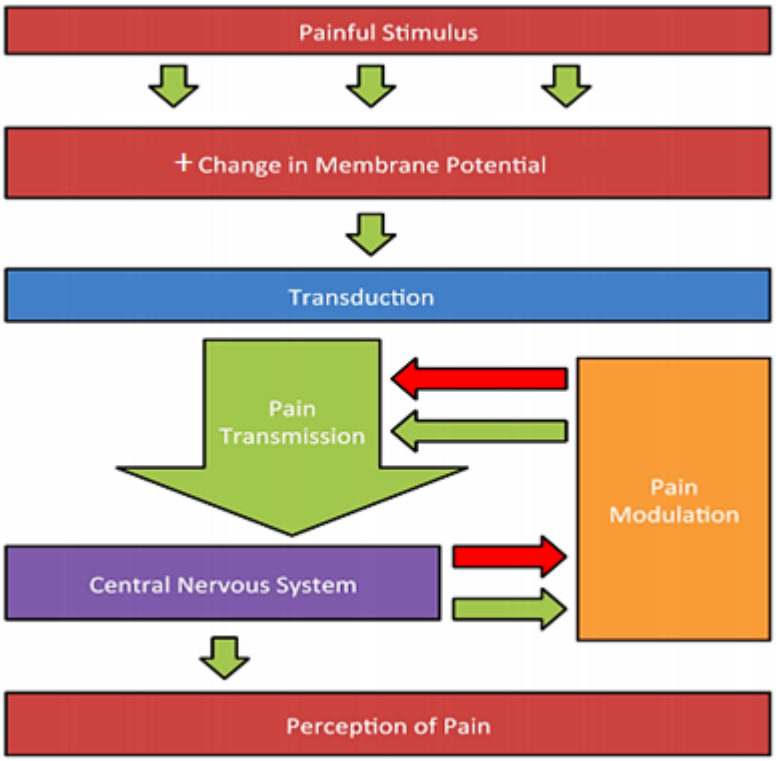

Figure 4: A schematic representation of the pain pathway with a particular focus on pain transduction. *The pain pathway has four main processes (Transduction, Transmission, Modulation and Perception). Transduction is the mechanism through which a noxious stimulus is converted into electrical impulses that are transmissible (via the process of transmission) to the central nervous system, where this signal is ultimately perceived as pain. The higher brain centres can modulate the transmission of pain (alter it) through the descending pain modulatory tracts, shown as green or red arrows indicating facilitation of transmission or inactivation of transmission, respectively. Adapted from (McEntire et al., 2016).*

1.3.1. The transduction of sensory information

Sensory neurons have developed to convert environmental energy into information that influences behaviour. Transducer molecules in the peripheral terminal are gated by thermal, mechanical, or chemical energy. On nociceptors, several receptors are responsible for performing the transduction process. Examples of these receptors include TRP channels, purinergic receptors for adenosine triphosphate (ATP), acid-sensing ion channels (ASICs) and a plethora of G protein-coupled receptors (GPCRs). Once a stimulus is applied, these transducers contribute to changing the depolarisation of the membrane potential (generator potential, which is the initial stage in the process of detecting a sensory

input) (McEntire et al., 2016). Understanding transducer molecules provides insight into the stimulus-specific responses that peripheral sensory neurons exert. This section highlights some of the transducer molecules.

1.3.1.1. Transient receptor potential (TRP) channels

The TRP family of channels comprises 28 members in mammals. Some TRP channels are referred to as thermo-TRPs because they are activated at varying temperatures. For example, some of them are activated by noxious heat (TRPV1 and TRPA1), non-noxious heat (TRPV3 and TRPV4), mild cooling (TRPM8), and noxious cold (TRPA1). Along with the ability of these channels to respond to the change in temperature, they can also respond to changes in the membrane potential, mechanical stimulation and chemical molecules (both endogenous and exogenous). The reason why certain plant compounds give rise to distinct temperature perceptions is a major question in sensory biology (Pérez de Vega et al., 2016). Even if the love of spicy cuisine is not universal, it appears that all cultures perceive chillies as "hot" and mint as "cold" (Guzmán & Bosland, 2017). Refer to Figure 5 to understand some of the reasons why we can make such distinctions. A few examples of the TRP channels will be listed below.

1.3.1.1.1. TRPV1

TRPV1 was cloned in 1997 by Caterina and Julius. Electrophysiological recording of recombinant TRPV1 demonstrated a non-specific cation channel which is opened by temperatures exceeding 43 °C, the psychophysical threshold for painful heat (Caterina et al., 1997). Experiments from TRPV1 knockout mice revealed little impairment in acute heat sensibility, despite the absence of the response to capsaicin and the impairment of inflammatory heat hyperalgesia (Caterina et al., 2000; Davis et al., 2000). This emphasises why the notion that compensating overexpression of other genes might compensate for the loss of function during development is a crucial proviso to gene knockout studies. It has recently been demonstrated that deleting TRPV1, TRPM3, and TRPA1 is required to eliminate the unpleasant heat sensation entirely (Vandewauw et al., 2018). Such findings highlight the redundant nature of sensory pathways, with channels balancing for one another, complicating the interpretation of typical perturbations of single genes. The discoveries related to the role of TRPV1 in somatosensation motivated scientists to test whether TRPV1 could be a potential analgesic target. Like all TRP channels, TRPV1 channels exist in one of three

states, open (short agonist exposure), closed (no agonist) or inactive (prolonged agonist exposure). Interestingly, not just TRPV1 antagonists but also direct agonists, such as capsaicin, were capable of generating an analgesic effect *in vivo*. The analgesic effect of capsaicin is a result of its capacity to desensitise the TRPV1 channel, as prolonged exposure to capsaicin causes the channel to transform into an inactive state, impeding activation via a Ca^{2+}-dependent mechanism. Capsaicin has been used for neuropathic pain with positive outcomes. Currently, agonists are more popular than antagonists for deactivating TRPV1 channels, particularly because old-generation TRPV1 antagonists caused substantial body temperature increases in clinical trial participants (Wong & Gavva, 2009). It is noteworthy that TRPV1 channels are also activated by acidification (Leffler et al., 2006).

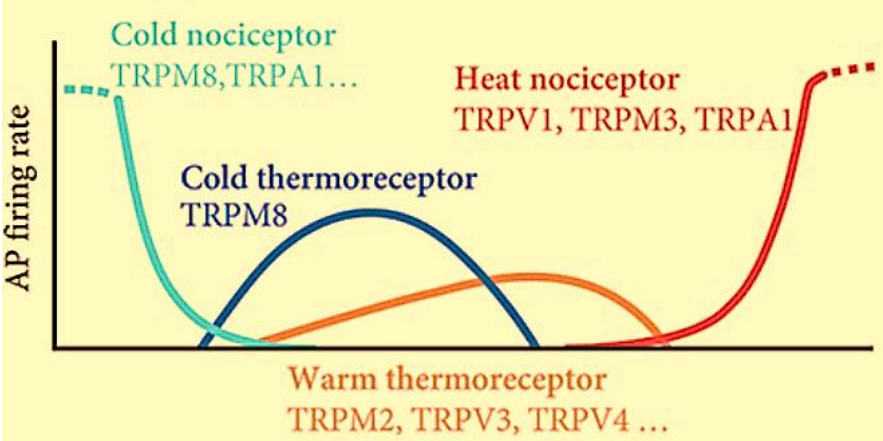

Figure 5: An illustration showing the TRP channels that have been hypothesised as the potential mediators of the thermal action potential firing in many classes of sensory afferents. *This diagram depicts the ion channels that are predicted to cause action potential discharge (y-axis) in several sensory neurons (presented in different colours) over a wide range of temperature bands, from cold to hot (x-axis). Temperature readings are withheld in order to avoid the appearance of precision. As a result, the detection of harmful heat is dependent on three TRP channels, which cause a dramatic rise in discharge as the temperature rises into the harm range. The ellipsis indicates that it is still unclear which transducers regulate unpleasant cold and harmless heat sensations. Obtained from (Viana & Voets, 2019).*

1.3.1.1.2. TRPM8

TRPM8 channels were first detected in the prostate, but they are also expressed by some sensory neurons that innervate skin, mucosa, lung epithelium, and other tissues. About 5% of sensory neurons express TRPM8, and these neurons include small unmyelinated C fibres and mildly myelinated A-delta fibres. TRPM8 can coexist with TRPV1 and/or CGRP in some sensory neurons. TRPM8 channels are triggered by innocuous cooling (temperatures between 10 and 28 degrees Celsius) and agonists like menthol and icilin. They also open when the plasma membrane depolarises. TRPM8-knockout mice are incapable of detecting/responding to innocuous cool temperatures, providing significant evidence supporting the relevance of TRPM8 in the experience of innocuous cooling (Dhaka et al., 2007). In addition, these mice are less sensitive to cold-induced hyperalgesia and acute cold than wild-type mice (Dhaka et al., 2007). Notably, TRPM8-deficient animals can still respond to temperatures below 0°C (Dhaka et al., 2007).

Regarding the role of TRPM8 in chronic pain conditions, TRPM8 in sensory neurons was found to contribute to cold allodynia after nerve injury or inflammation. Moreover, it was experimentally shown that activating (and then desensitising) TRPM8 channels reduces both evoked and inflammatory pain (Pérez de Vega et al., 2016).

1.3.1.2. Mechanosensors

The Piezo class of mechanically-gated ion channels was the last primary transducer group to be discovered. Using an RNAi screen, Piezo1 was identified as the channel responsible for the mechanically-triggered current observed in N2A cells. Large transmembrane receptors Piezo1 and Piezo2 can be regarded as *bona fide* mechanosensors since they react to pressure after being expressed in heterologous systems (Coste et al., 2010). Experiments conducted on mice lacking Piezo2 revealed that they lost the ability to respond to mild touch and proprioception. Piezo2 drives the rapidly-adapting currents in DRG neurons (Ranade, Woo, Dubin, Moshourab, Wetzel, Petrus, Mathur, Bégay, Coste, & Mainquist, 2014; Woo et al., 2015). Mutants devoid of human PIEZO2 have severe impairments in proprioception and discriminative touch (Chesler et al., 2016). Notably, Piezo2 alternative splicing generates channel variants with

distinct biophysical properties that are expressed in a variety of cell types (Szczot et al., 2017).

1.3.1.3. Acid-sensing ion channels (ASICs)

In the 1980s, proton-sensitive ion channels were found in DRG and trigeminal neurons. A group of proton-gated ion channels is named ASICs. The presence of ASICs in sensory neurons and small-diameter DRG neurons suggests they may be involved in pain sensation(Krishtal & Pidoplichko, 1981). ASICs and TRPV1 channels may play complementary functions in acid-evoked pain. ASICs are activated by mild and intense acidification, while TRPV1 is activated at lower pH levels. Amiloride, an ASIC blocker, relieves moderate acid-induced pain in healthy humans. The co-administration of amiloride and capsazepine to block ASICs and TRPV1 relieves acidification-induced pain when the pH falls below 6 (Leffler et al., 2006). Mambalgins, which are peptides obtained from venoms and can inhibit ASICs, were shown to have an analgesic effect in various pain models, including inflammatory and neuropathic pain (Brzezicki & Zakowicz, 2018). Because the release of protons characterises several pain conditions like inflammation (as protons are released following the damage of cells), fracture and tumour development, understanding the activation properties of ASICs is of great importance.

ASICs are members of the epithelial Na^+ channel (ENaC)/degenerin (DEG) ion channels superfamily. There are six subunits of ASIC, which are (ASIC1a, ASIC1b, ASIC2a, ASIC2b, ASIC3 and ASIC4). Upon activation, ASICs cause depolarisation by allowing Na^+ ions to enter the cell (Deval et al., 2010). Some reports suggested that ASICs can also be permeable to Ca^{2+} ions (Xiong et al., 2004). The degree of extracellular acidification that activates each ASIC differs depending on the subunits from which it is formed (Deval et al., 2010).

1.3.1.3.1. ASICs in the peripheral nervous system

In rodents, ASICs are present throughout the nervous system (central and peripheral). Within the peripheral nervous system and particularly the sensory nervous system, most ASICs are present. Nevertheless, in the CNS, ASIC1a and ASIC2 subunits are the dominant ones.

Since ASIC3 channels are extensively expressed in skeletal afferents (Ikeuchi et al., 2009; Molliver et al., 2005), this section will discuss the activation

characteristics of this channel. Unlike all ASICs that produce a fast-inactivating current, ASIC3 channels are distinguished from other ASICs in that they can generate a biphasic current in response to the acidification of the extracellular fluid (Waldmann et al., 1997). As a result of the sustained current, the depolarisation of the neuronal membrane is maintained, resulting in non-adapting pain. Notable is the fact that acidosis to pH values below pH=6 can occur in conditions like bone cancer and bone metastases (Mantyh et al., 2002).

1.3.1.3.2. ASICs in the central nervous system

Second-order neurons express ASIC1a and ASIC1a/2a. In addition to the profound expression levels of ASIC1a, ASIC2a and ASIC2b subunits in the dorsal horn of rats, the expression of both ASIC1a and ASIC2a is elevated following peripheral inflammation. Because of its involvement in central sensitisation, silencing ASIC1a in the spinal cord's dorsal horn reduces acute and chronic pain in animals (Deval et al., 2010).

1.3.1.3.3. The link between ASICs and analgesics

The inhibition of the activity of ASIC1a and ASIC3 channels contributes to the analgesic effects seen with NSAIDs by delaying the recovery of these ASICs from inactivation. The allosteric inhibition of ASICs by NSAIDs can be seen with the therapeutic doses of NSAIDs. Included among the NSAIDs that inhibit ASIC1a are flurbiprofen and ibuprofen. Also, salicylic acid, aspirin and diclofenac have the ability to stop the sustained current of ASIC3 (Voilley et al., 2001).

Analgesia is achieved when ASIC1a is inhibited in the dorsal horn using an intrathecal injection of PcTx1 or antisense oligonucleotide-based downregulation of ASIC1a. It is thought that the endogenous opioid system is implicated in this analgesia, as Met-enkephalin levels were raised in cerebrospinal fluid. Met-enkephalin may be indirectly elevated through spinal cord inhibitory interneurons expressing ASIC1a, which activate enkephalinergic neurons (Mazzuca et al., 2007).

1.3.1.4. Other transducers

This section will briefly list various transducers discovered and characterised in sensory neurons. These include additional TRP channel family members essential for thermosensation (Figure 5). According to reports (Bautista et al., 2007; Dhaka et al., 2007), TRPM2 is required for sensing innocuous warmth.

TRPA1 reacts to pungency and may be implicated in the perception of heat, cold, and mechanical stimuli (Brierley et al., 2009; Karashima et al., 2009; Vandewauw et al., 2018). Purinergic receptors, particularly P2X3, which are expressed on nociceptors and react to ATP released into the extracellular environment after cell disintegration, also play a role in injury response (Bele & Fabbretti, 2015). Background K^+ channels are a type of transducer whose closure reduces the outward leak of K^+ ions, causing the membrane to depolarise. For example, mechanically gated and temperature-responsive TREK1 and TRAAK modulate thresholds for warm and cold responsiveness (Noël et al., 2009). Notably, both damage and inflammation can influence the transcription and functionality of most transducers (Gold & Gebhart, 2010).

There are still many important questions that need to be answered. Despite the fact that Tmem120a channels have previously been proposed as the pore-forming subunit (Beaulieu-Laroche et al., 2020), the molecules underlying the gradually-adapting mechanical currents, which are thought to be responsible for unpleasant mechanical sensations, are unclear. Also, it is still unclear what role specific transducers play in chronic pain states and under what circumstances.

1.3.2. Electrogenesis

Peripheral sensory neurons have lengthy axons. For instance, Sauropod dinosaurs have 50-meter-long recurrent laryngeal nerves (Wedel, 2011). If neurons relayed sensory signals purely through the generator potential, graded depolarisations from original transducers would degrade quickly with distance due to axon cable properties. Peripheral nerves carry sensory information using self-propagating action potentials. The CNS receives information about the sensory stimuli via the magnitude, frequency, and temporal pattern of the action potentials. Consequently, the locations of molecular specialisation and regulation in peripheral sensory neurons are essential for impulse production and conduction.

Since 1865, Bernstein has been credited with defining the action potential time course. But the ionic cause of the modifications in membrane potential remained a mystery. After almost a century, Hodgkin and Huxley performed voltage-clamp recordings using the squid giant axon. They selected this approach specifically as the axon is characterised by its substantial thickness, which permitted the placement of an intracellular electrode (Hodgkin & Huxley, 1939). They were able

to locate a quick, voltage-driven Na^+ conductance that sparked the action potential by adjusting the holding potential and ion concentrations within the extracellular solution. They also suggested that the falling phase of the impulse was driven by an outward K^+ conductance that was both delayed and voltage-activated (Hodgkin & Huxley, 1952). While the action potential was convincingly simulated using computer modelling of these ionic components employing hand-cranked calculations, the physical makeup of the conductances stayed unidentified. The later discovery of substances like TTX, which only prevented the passage of the Na^+ current and not the K^+ current, indicated the possibility of the presence of specific pores or gates that allowed certain ions to enter or exit the cell (Narahashi et al., 1964). In the 1970s, the invention of the patch clamp enabled the observation of individual ion channel opening and closing in a cell-attached form, providing a firm molecular foundation for the physiological study of ion channels (Hamill et al., 1981; Neher & Sakmann, 1976). This section summarises some of the ion channels implicated in electrogenesis in the different sites of sensory neurons, including voltage-gated sodium ion (VGSC), K^+, and Ca^{2+} channels (VGCCs).

1.3.2.1. Voltage-gated sodium ion channels (VGSCs)

1.3.2.1.1. Structure and Function of VGSCs

There are two key structural components of VGSCs (β and α subunits). There are ten types of α subunits, nine of which are voltage-gated. The VGSCs possessing these voltage-gated α subunits are named (Na_V 1.1–1.9). In the 1980s, the α subunits of Na_V 1.1–1.9 were cloned, and they were found to be formed of approximately 2000 amino acids forming four domains (DI–DIV). Every domain has six transmembrane segments (S1–S6) (Bennett et al., 2019). Of these segments, (S1-S4) are important for voltage detection, while (S5-S6) form the pore through which ions can pass. It is thought that the positively charged amino acids present in S4 are crucial for voltage sensation. Voltage-dependent VGSCs have three states (open, closed, and inactive). VGSCs close during membrane hyperpolarisation. Upon depolarisation, they open and then rapidly inactivate (within milliseconds). The intracellular mouth of the channel pore is closed by the IFM motif in the inactive (fast) state, while it remains open in the closed state (Bennett et al., 2019). Slow inactivation occurs after extended

depolarisations and takes tens of seconds. Following the inactivation, the channel shifts to the closed state in a process known as re-priming (Bennett et al., 2019).

Regarding the β-subunits, they have four types that are composed of a terminal immunoglobulin-like domain, a transmembrane segment, and an intracellular segment. The way these β-subunits (1-4) form complexes with α subunits varies depending on the type of the β subunit. The association can be via disulfide bonds (β2 and β4) or non-covalent (β1 and β3). In general, β subunits play different roles, such as governing the state of the channel (Bouza & Isom, 2018).

1.3.2.1.2. Overview of the role of VGSCs in the action potential

Following signal transduction, a little membrane potential depolarisation occurs (Simard et al., 2007). At this stage, the role of the VGSCs starts as they are required for the amplification of the signals that the stimulus causes. The amplification of the stimulus signal might facilitate reaching the threshold, which subsequently allows the generation of an action potential. DRG neurons express both TTX-sensitive ($Na_V1.6$, $Na_V1.7$, $Na_V1.1$, and $Na_V1.3$) and TTX-resistant VGSCs ($Na_V1.8$ and $Na_V1.9$). The most important subtypes of VGSCs that contribute to the amplification of the signal step are $Na_V1.7$, $Na_V1.9$, and $Na_V1.3$. When the membrane potential reaches the threshold for action potential, an all-or-none action potential is generated. During the rising phase of the action potential, $Na_V1.6$, $Na_V1.7$ and $Na_V1.8$ are the key players (Bennett et al., 2019). See Figure 6 for the localisation of these VGSCs in the DRG neurons.

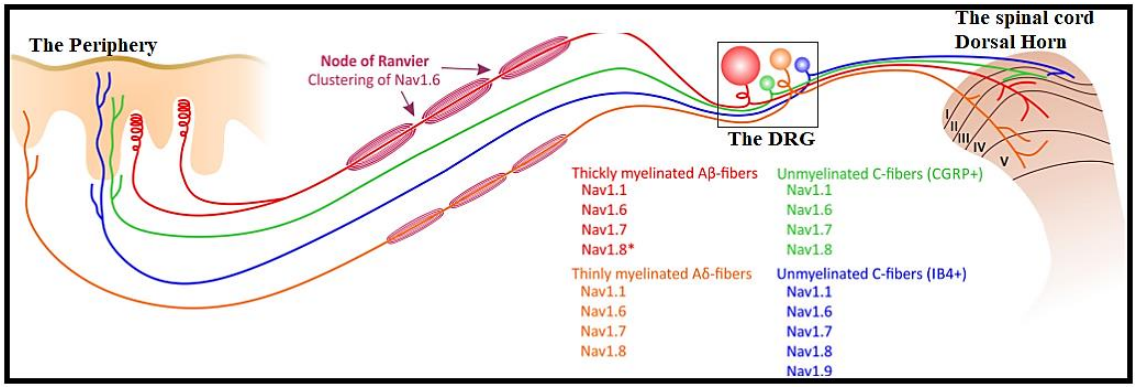

Figure 6: The subtypes of VGSCs present in the DRG neurons of mice. *Pseudo-unipolar morphology characterises primary afferents. The primary afferents innervate the periphery (the skin, for example), have the cell bodies at the DRG, and then synapse with the second-order neurons at the dorsal horn of the spinal cord. DRG neuron types determine where they terminate in the spinal*

*cord's dorsal horn (shown as roman numbers I, II, III, IV and V). Myelinated Aβ and Aδ fibres end at deeper laminae than unmyelinated fibres (lamina I and II). All DRG neuron subpopulations contain VGSCs $Na_V1.1$, $Na_V1.6$, and $Na_V1.7$. Small-diameter nociceptors with unmyelinated C fibres can be divided into two subtypes: peptidergic (CGRP+) and non-peptidergic (IB4+) neurons. $Na_V1.9$ channels are expressed on non-peptidergic fibres. * indicates that only a limited number of large-diameter neurons express $Na_V1.8$ at high levels. $Na_V1.6$ channels contribute to saltatory conduction at nodes of Ranvier. $Na_V1.6$ may play a role in non-myelinated axons too. Source: (Bennett et al., 2019).*

1.3.2.1.3. Examples of subtypes of Na^+ channels and their roles in pain

The distinct feature of $Na_V1.7$, $Na_V1.8$, and $Na_V1.9$ is their highly selective expression in the periphery. Since nociceptors are peculiar in their requirement to produce action potentials despite the presence of damaged tissue, co-expressing Na^+ channels that are redundant with one another could be a simple evolutionary fix. This is observed in mice lacking $Na_V1.8$, wherein the loss of function is mitigated by elevated TTX-sensitive currents, most likely caused by $Na_V1.7$ (Akopian et al., 1999). Since $Na_V1.7$ is necessary for human pain, it is a prospective target for analgesic drugs. This topic will be covered in more detail later (see Chapter 3). Similarly, the fact that the expression of $Na_V1.8$ channels is almost confined to DRG neurons makes it an attractive target, and it will be discussed in further detail in Chapter 4. Herein, I will discuss $Na_V1.3$, $Na_V1.6$ and $Na_V1.9$ channels, as data suggests their involvement in various chronic pain conditions.

1.3.2.1.3.1. $Na_V1.3$

Adult naive rats do not express $Na_V1.3$ channels, whereas neonatal rats do. Injury reactivates the expression of $Na_V1.3$ channels in small and large DRG neurons. After sciatic nerve axotomy, messenger RNA (mRNA) and protein studies showed $Na_V1.3$ re-expression. $Na_V1.3$ channels produce a fast-inactivating, rapidly-repriming TTX-sensitive current. Another property of these channels is slow closed-state inactivation. This feature permits the channel to generate substantial ramp current even with slow depolarisations (Bennett et al., 2019).

Following nerve damage, $Na_V1.3$ expression levels increase in less than a day and remain for weeks in rats. Increased $Na_V1.3$ levels are linked with spontaneous discharges (Liu et al., 1999) and allodynia in rats (Bennett et al., 2019). In order to characterise the role of $Na_V1.3$ in neuropathic pain, $Na_V1.3$ knockout/down mice were generated, and the pain responses were measured following neuropathic pain models. In several studies, the pain behaviours in $Na_V1.3$ knockout mice were almost indifferent to those of the wild-type mice. On the other hand, the knockdown of $Na_V1.3$ resulted in favourable outcomes in the spared nerve injury (SNI) model in rats by reducing the resulting neuropathic pain. One explanation could be that compensatory mechanisms develop in the knockout mice, unlike in the knockdown conditions (Bennett et al., 2019).

1.3.2.1.3.2. $Na_V1.6$

$Na_V1.6$, expressed mainly by neurons with large diameters, has rapid inactivation kinetics and accounts for nearly two-thirds of the cells' TTX-sensitive current. As shown in Figure 6, $Na_V1.6$ channels contribute to saltatory conduction at nodes of Ranvier. Viral-mediated conditional deletion of $Na_V1.6$ indicated the involvement of this channel in mechanical hypersensitivity following neuropathic pain (Chen et al., 2018).

1.3.2.1.3.3. $Na_V1.9$

The *SCN11A* gene encodes $Na_V1.9$ channels. Two reported patients with $Na_V1.9$ mutations were born oblivious to pain. These individuals possessed gain-of-function mutations in this channel, resulting in excessive firing at rest and prolonged depolarisation, which precludes impulse production (Leipold et al., 2013). Both small and large DRG neurons can express these channels. Expression of $Na_V1.9$ channels has been observed primarily in non-peptidergic DRG neurons with small diameters. However, $Na_V1.9$ channels are also present in the colon's peptidergic DRG neurons (Hockley et al., 2014). As humans lack the selection marker for non-peptidergic neurons, IB4 lectin, it is challenging to compare $Na_V1.9$ expression in peptidergic and non-peptidergic neurons. Within the DRG neurons, $Na_V1.9$ channels are found in the free nerve endings, nerve fibres, soma, and spinal cord terminals. $Na_V1.9$ channels are mainly found in the C fibres but have also been found in Aδ and Aβ fibres of nociceptors. Additionally, the nodes of Ranvier in myelinated fibres include $Na_V1.9$ channels. Human $Na_V1.9$ opens with weaker stimulation than rat $Na_V1.9$. The currents produced by

$Na_V1.9$ channels are resistant to TTX. In contrast to TTX-sensitive channels such as $Na_V1.7$, $Na_V1.9$ channels are active at hyperpolarised potentials, which is the most notable property of $Na_V1.9$ channels. Additionally, the $Na_V1.9$ currents are more persistent than those generated by $Na_V1.7$ and other TTX-sensitive channels. It is also significant to note that the kinetics of $Na_V1.9$ channel activation and inactivation differ from those of TTX-sensitive channels. Compared to the TTX-sensitive channels, $Na_V1.9$ demonstrates delayed activation and inactivation (Bennett et al., 2019). Therefore, $Na_V1.9$ channels are considered threshold channels mainly because their slow kinetics indicate that these channels do not participate in the action potential amplitude. Additionally, $Na_V1.9$ channels open at hyperpolarised potentials compared to other Na^+ channels, indicating that $Na_V1.9$ channels cause depolarisations at the resting membrane potential (Zhou et al., 2017). It is thought that $Na_V1.9$ channels are sensitised by inflammatory mediators (like prostaglandin E2 (PGE2)) and their signalling cascades (Rush & Waxman, 2004). This observation illustrates the important role of $Na_V1.9$ channels in enhancing the excitability of DRG neurons in diseases characterised by inflammation. Recent research by Katharina Zimmerman's team has shown that $Na_V1.9$ exhibits a significant gain-of-function with heating, causing this channel to initiate action potentials at high temperatures making these channels important for action potential generation in extreme conditions. In fact, $Na_V1.9$-deficient animals show significant impairment in heat hyperalgesia and spontaneous pain (Akopian et al., 1999; Priest et al., 2005).

1.3.2.2. K^+ channels

K^+ channels comprise 78 genes in the human genome and are functionally and molecularly diverse. Forty genes produce voltage-gated K^+ channel subunits, repolarising the membrane to de-inactivate Na^+ channels. They represent the chief drivers of the falling phase of the action potential (Tsantoulas & McMahon, 2014). Here, I will concentrate on the Shaker-like KV1 channels, a subfamily of delayed rectifier channels. They serve as excitability "brakes", preventing stimulus-driven depolarisations since modest membrane depolarisations trigger them. KV1.1 knockdown through small interfering RNA does, in fact, result in elevated excitability in sensory neuronal cultures classified as nociceptors due to their capsaicin sensitivity (Chi & Nicol, 2007). Additionally, KV1.1 knockout animals have decreased pain thresholds (heat and mechanical) and greater pain-

like behaviours on the formalin behavioural test (Clark & Tempel, 1998). Even though numerous KV1 channel mutations in humans have been reported, quantitative sensory testing is, as far as I am aware, infrequently carried out since ataxic or seizure symptoms frequently predominate (Manole et al., 2017; Sachdev et al., 2017).

1.3.2.3. Ca^{2+} channels

There are nine main types of Ca^{2+} channels expressed in vertebrates. These nine channels are grouped into three families known as Cav1, Cav2 and Cav3. Cav1 and Cav2 are known as high-voltage activated (HVA) as they only open in high depolarisations of the plasma membrane, while Cav3 is low-voltage activated (LVA) as it requires less depolarisation for opening (Dolphin, 2016). The Cav1 channels generate L-type Ca^{2+} currents in the nervous system and muscles (Striessnig et al., 2015). Regarding the Cav2 family, it has three main members, known as Cav2.1 (P/Q type Ca^{2+} currents), Cav2.2 (N-type Ca^{2+} currents) and Cav2.3 (R-type Ca^{2+} currents). The Cav3 family also has three main members, Cav3.1, Cav3.2 and Cav3.3, all supporting T-type Ca^{2+} currents (Zamponi et al., 2018).

HVA Ca^{2+} channels are 1:1:1 heteromultimers of Cavα1, Cavβ and Cavα2δ (Catterall, Goldin, et al., 2005; Wu et al., 2016). LVA Ca^{2+} channels solely contain the Cavα1 subunit. Cavα1 is the pore-forming unit, and it is capable of generating Ca^{2+} channels without the assistance of other subunits (Catterall, Perez-Reyes, et al., 2005). Cavβ subunits interact with Cavα1's cytoplasmic portion. Cavβ subunits protect the channel from ubiquitination, prevent protease degradation, and refine channel biophysics (Zamponi et al., 2018).

Biophysical features, pharmacological profiles, and expression patterns are unique to each Ca^{2+} channel type (Zamponi et al., 2018). Cav2.1 and Cav2.2 channels reside in presynaptic terminals and regulate neurotransmitter release (Westenbroek et al., 1992). Cav3 channels are positioned at neuron dendrites and somata and determine excitability (McKay et al., 2006). Pharmacological profiles characterise Ca^{2+} channel types: ω-conotoxins inhibit Cav2.2 channels (such as GVIA and MVIIA), SNX-482 blocks Cav2.3 channels, Nickel ion inhibits T- and R-type Ca^{2+} channels and dihydropyridines can block L-type channels (Zamponi et al., 2015). Cav3 channels regulate first-order neuron activation by causing rebound bursting (low-threshold spikes). Cav3 channels may also affect

dorsal horn interneuron firing. Therefore, the Cav3 channels play a key function in dorsal horn neurotransmission (Jacus et al., 2012). Cav3.2 channels are present in about a third of DRG neurons, with significant expression in low-threshold mechanical neurons (François et al., 2015) and knockdown reduces mechanical allodynia in preclinical neuropathic pain models (Bourinet et al., 2005). Cav2.2 channels are particularly important for nociceptive signal transmission because they control neurotransmitter release from dorsal horn neurons (Snutch, 2005). Intrathecal Cav2.2 blockers provide considerable analgesia (Diaz & Dickenson, 1997), and Cav2.2-null mice show reduced noxious responses (Hatakeyama et al., 2001).

Compared to other Ca^{2+} channels, Cavα2δ subunits are exclusively found in HVA Ca^{2+} channels; thus, they were evaluated for pain modulation because they are involved in channel trafficking. Gabapentinoids are used to treat neuropathic pain and target Cavα2δ (Field et al., 2007; Zamponi et al., 2018). Gabapentinoids' acute application has no effect on N-type Ca^{2+} channels or synaptic transmission. Chronic gabapentinoid use, on the other hand, seems to reduce the trafficking of N-type Ca^{2+} channels to the dorsal horn of the spinal cord, reducing neurotransmitter release (Zamponi et al., 2018). Specific toxins from venomous spiders and scorpions can block T-type Ca^{2+} channels; however, these poisons cannot cross the blood-brain barrier (Zamponi et al., 2018). ABT-639 was effective preclinically (Jarvis et al., 2014) but not therapeutically (Zamponi et al., 2018) as a T-type Ca^{2+} current blocker.

1.3.3. Transmission of nociceptive signals across synapses

Why do we rub the area where we have been hit? Melzack and Wall contend that the Gate Control Theory of Pain provides the solution. They suggested in 1965 that myelinated afferents conveying innocuous touch could stimulate interneurons within the spinal cord, leading to the suppression of synaptic transmission from nociceptors and thus decreasing pain (Ronald Melzack & Patrick D. Wall, 1965). Even though the precise details of the classic Gate Control Theory faced a lot of debates, the main idea remained popular. At the dorsal horn, incoming sensory information originating at the periphery is filtered and modified prior to reaching the brain (Todd, 2010). As a result, the peripheral drive is regulated in health and disease by the chemicals implicated in transmitting signals from the central termini of nociceptors.

Katz discovered the characteristics of rapid synaptic transmission around the mid-twentieth century (Del Castillo & Katz, 1954; Fatt & Katz, 1952). His findings showed that the release of a neurotransmitter is probabilistic, quantifiable and Ca^{2+}-dependent, which applies to other synapses, like those of the central terminals of sensory neurons. The primary fast neurotransmitter used by the sensory neurons at these synapses is glutamate. The release of neurotransmitters takes place as a result of the arrival of an action potential to the central terminals of sensory neurons, leading to voltage-gated Ca^{2+} channel activation, causing an influx of Ca^{2+}, which couples to the intracellular Ca^{2+}sensor, synaptotagmin, and causes synaptosomal-associated protein receptor protein (SNARE)-driven vesicular efflux of transmitter "packets," which bind post-synaptic receptors (Brunger et al., 2018).

Depending on the type of fibre, the dorsal horn's afferent terminals are divided into spinal segments and laminae (Figure 7). Neurotransmitters, substance P and glutamate, are used by nociceptors at their main synapses, found in laminae I and II of the dorsal horn. In contrast to controls, mice lacking Vglut2 (vesicular glutamate transporter) experience less pain associated with inflammation after receiving a neurokinin receptor antagonist, highlighting the necessity of co-release of both transmitters in the development of sensitive pain states (Lagerström et al., 2011). Interestingly, the shape of nociceptor termini within the spinal cord's dorsal horn differs depending on the body part from where they originate. For example, Mas-related G-protein coupled receptor (Mrgprd+) mechanonociceptors from plantar-derived fibres differ from those from the hairy skin, despite having similar peripheral projections. The increased nociceptor sensitivity of the paw may be explained by this polymorphism (Olson et al., 2017). Tactile information is transmitted by myelinated neurons, which typically synapse in layers III to IV. The Ginty team demonstrated the extraordinary complexity of the mechanosensory dorsal horn, which contains up to eleven different classes of interneurons that integrate information from the peripheral and CNS (Abraira et al., 2017).

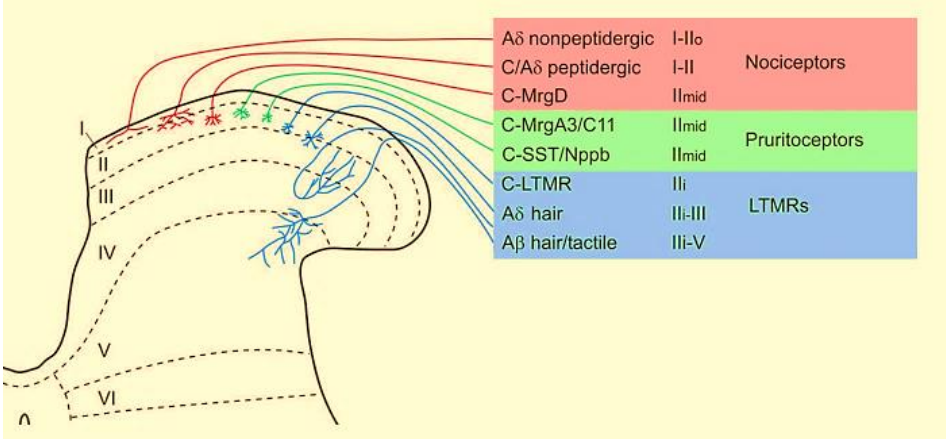

Figure 7: The projection of the primary sensory neurons within the dorsal horn of the spinal cord and the laminae where they terminate*. The table lists subsets of the main sensory neurons and their functional specialisations. The lines in the horizontal segment represent their core axons, which branch into multiple dorsal horn laminae. For instance, low-threshold mechanoreceptors (LTMRs) end predominantly in the deeper laminae, whereas nociceptors terminate principally in the surface laminae I and II. Pruritoceptors are the neurons responsible for the detection of itch. Since they are less well understood, the central terminals of warm- and cold-detecting neurons have been excluded from this list. Obtained from (Todd et al., 2018).*

Nociceptive afferents communicate with both the dorsal horn interneurons and the projection neurons in the spinal cord. Even though nociceptive projection neurons are located in layer I, the vast majority of neurons in layers I-III are interneurons with axons that terminate locally and engage in axo-axonic synapses with central terminals of afferent neurons (Todd, 2010). With the help of neurochemical markers like dynorphin and galanin, it is now possible to differentiate between different types of interneurons and target them with various genetic tools. Experiments using genetic ablation, for instance, demonstrated how inhibitory interneurons, which are distinguished by their synthesis of dynorphin, function to limit the activation of nociceptive excitatory neurons by Aβ fibres, so successfully gating mechanical pain transmission (Duan et al., 2014). The central terminals of sensory neurons are also controlled by descending regulation (will be covered in further detail in section 1.3.5). Even though I have centred the majority of the discussion around the spinal cord, it is possible that orofacial nociceptors and the parabrachial nucleus have direct monosynaptic

interactions that contribute to an increased sensation of pain. This is proposed as a potential explanation for the enhanced affective component of orofacial pain (Rodriguez et al., 2017).

1.3.4. Ascending pain pathways

Suppose the stimulation of the second-order neuron is high enough to generate an action potential. In that case, the action potential will propagate along the axon and convey the message to the brain via two major routes. The first tract is called the spinothalamo-cortical tract, which connects the dorsal horn to the cortex via the thalamus (giving rise to the sensory component of the overall pain experience). The cortical areas to which the spinothalamo-cortical tract projects are the primary somatosensory, secondary somatosensory, insular cortex, and cingulate cortex. The main role of the primary somatosensory cortex is detecting pain location, type, and intensity. On the other hand, the second somatosensory is implicated in learning and memory about the pain experience. The insular cortex is responsible for mediating the autonomous and motivational responses to pain. The cingulate cortex has a role in the integration and perception of pain, and it also helps the individual to select the appropriate action in response to pain. The second tract, named the parabrachial-limbic tract, connects lamina I to the lateral parabrachial area and from there to various centres, including the amygdala, the lateral bed nucleus of stria terminalis, and the paraventricular nucleus of the thalamus and the lateral and periventricular regions of the hypothalamus. The previously mentioned areas provide inputs to higher brain centres, such as the nucleus accumbens, insula as well as cingulate cortex. The paraventricular nucleus of the thalamus and the hypothalamus are implicated in the motivational components of pain. Additionally, the neurons connecting the lateral parabrachial area to the central nucleus of the amygdala aid in keeping the memory of painful situations to avoid them in the future. It is worth mentioning that the lateral parabrachial area also sends inputs to the periaqueductal gray (PAG), the rostral ventral medulla (RVM) and reticular areas of the medulla that are implicated in descending pain modulation (Todd et al., 2018).

There are three main types of second-order neurons. The first class is called the nociceptive-specific neurons (that get input from nociceptors with high thresholds and are specialised for noxious stimuli). The second class of projection neurons is called the wide-dynamic range neurons (which can receive input from any of

the primary afferent fibres and convey noxious and innocuous stimuli). The third class of neurons is the non-nociceptive neurons (which solely receive inputs from Aβ primary afferents and thereby function to convey innocuous stimuli) (Almeida et al., 2004).

1.3.5. Modulation

Over the past 50 years, numerous studies have proven that activating midbrain and medullary locations can influence nociception in both directions. The PAG, which receives information from higher brain areas, can activate a potent analgesic effect. The RVM, which serves as the final relay in the regulation of descending pain facilitation, has the ability to both facilitate and inhibit nociceptive inputs. Through these structures, cortical and subcortical regions can affect nociception (Ossipov et al., 2014). Additionally, interneurons within the spinal cord also impact nociceptive signal transmission. This section discusses these pain modulation mechanisms.

1.3.5.1. PAG and RVM

Reynolds showed that the electrical stimulation of the PAG causes significant analgesia in animals (Loyd & Murphy, 2009). Similar results were seen in humans. Interestingly, it was found that the analgesic effect produced after the electrical stimulation of the PAG is abolished by naloxone, a drug that antagonises opioid receptors (Lubejko et al., 2022). PAG modulates pain chiefly via the connection that the PAG has with the RVM, as studies in rats revealed that the PAG activation results in the excitation of RVM neurons, and accordingly, the nociceptive signal transmission is inhibited (Behbehani & Fields, 1979). Not only does the RVM receive inputs from the PAG but also from the thalamus, the parabrachial area and the noradrenergic locus coeruleus. The RVM represents the final common relay in descending pathways for pain modulation. The RVM projects to the dorsal horn of the spinal cord and the trigeminal nucleus caudalis (Loyd & Murphy, 2009). The net effect that the RVM can have on pain can be inhibitory or facilitatory. Fields et al. recorded from the RVM while conducting tail-flick experiments on rats using radiant heat. The results from the recordings showed that some cells had enhanced activity after applying the noxious stimulus and before the tail-flick, which they named ‘ON-cells’. Other cells stopped firing directly before the tail flick and were called ‘OFF-cells’ (Loyd & Murphy, 2009). Opioids have an inhibitory effect on the ‘ON cells’ and an excitatory effect on the

'OFF cells'. The excitation of the 'OFF-cells' by opioids is thought to be crucial and sufficient for the analgesic effect of opioids (Loyd & Murphy, 2009). ON-cells and OFF-cells' presence explains the fact that the PAG/RVM system can modulate pain either negatively or positively. The existence of an imbalance between pain inhibition and facilitation may, at least in part, explain why some patients have pathological pain (Ossipov et al., 2014). In animal models, it was found that ON-cell activity is potentiated by injury or inflammation. Additionally, any form of interference (pharmacological, neurochemical or physical) with the descending pain facilitation from the RVM attenuates the hyperalgesia leaving the protective pain reflexes unaffected (Ossipov et al., 2014). Human imaging highlighted that the activation of this region of the brainstem is linked explicitly to the development and maintenance of central sensitization (Michael et al., 2008).

1.3.5.2. Spinal serotonergic activity and pain modulation

In the RVM, there are serotonergic nuclei, GABAergic neurons (release gamma-aminobutyric acid (GABA)) and glycinergic neurons, which all send descending projections to the spinal cord. The nature of neurotransmitters of the ON and OFF-cells is still debatable. It is yet to be determined whether these cells are serotonergic, nonserotonergic or a mixture. Many studies have shown that activating descending projections from the RVM causes the release of serotonin at the dorsal horns of the spinal cord. The source of serotonin could be from the descending projection terminals or the interneurons (Bravo et al., 2019). Nevertheless, according to the receptor subtype that serotonin activates within the spinal cord, it can be either pronociceptive or antinociceptive (Cortes-Altamirano et al., 2018). All of these findings highlight the importance of serotonin in bidirectional pain modulation (Ossipov et al., 2014).

1.3.5.3. The role of descending noradrenergic neurons in the modulation of pain

The origins of the descending noradrenergic neurons in the dorsal horns of the spinal cord are A5, A6 (the locus coeruleus) and A7 (the Kölliker-Füse). All these areas have communications with the PAG and RVM (Ossipov et al., 2014). Many preclinical trials have illustrated that stimulating the noradrenergic nuclei or PAG and RVM, either chemically or electrically, induces the release of norepinephrine in the spinal cerebrospinal fluid, and the release of norepinephrine has an anti-nociceptive effect. Furthermore, the spinal administration of blockers of the α2-

adrenergic receptor blocks antinociception (Ossipov et al., 2014). Many preclinical studies highlighted that the activation of the α2-adrenergic receptor results in significant antinociception and that agonists of α2 adrenergic receptors produce synergistic analgesia with opioids (Ossipov et al., 2014). Similar results were obtained in humans, as spinal clonidine causes analgesia but not systemic clonidine (Eisenach et al., 1995; Eisenach et al., 1998). Unlike α2-adrenergic receptors, α1-adrenergic receptors' activation at the level of the spinal cord facilitates pain. In a study, opioid-induced hyperalgesia was linked to the noradrenergic neurons. This study found that the microinjection of 7.5 nmol of morphine in the A7 region facilitated the nocifensive tail and foot responses. Interestingly, it was found that these hyperalgesic responses are linked to the spinal projections of the noradrenergic A7 neurons and that α1 adrenoreceptors facilitate the pain. With the aid of selective blockers of α-adrenoceptors, it was revealed that, unlike α_1 adrenoreceptors, α2-adrenoceptors were found to have an anti-nociceptive effect. Therefore, it was concluded that morphine activates noradrenergic neurons from A7 that project to the dorsal horn of the spinal cord and these noradrenergic neurons result in opposite effects on nociception. Accordingly, methionine-enkephalin neurons that project from the RVM to A7 can facilitate or inhibit nociceptive responses (Holden et al., 1999). Some studies proposed that when there is nerve injury, the descending noradrenergic neurons enhance their activity in an attempt to dampen down the elevated nociceptive signals. The spinal α2-adrenergic receptors also have enhanced efficacy during injury (Muto et al., 2012). These findings may justify the efficacy of the serotonin/norepinephrine reuptake inhibitors in some chronic pain conditions (Arnold, 2007).

1.3.5.4. Spinal interneurons and pain modulation

The biggest set of neurons within the dorsal horn is the interneurons. Interneurons can be classified into two main categories; excitatory and inhibitory. Excitatory interneurons in the dorsal horn release glutamate as their main neurotransmitter, whereas the inhibitory interneurons release glycine or GABA as their neurotransmitter. Both excitatory and inhibitory interneurons act as regulators of the activity of the projection neurons. In an attempt to study the effect of the deletion of a large set of excitatory interneurons in the dorsal horn, conditional knockout mice were generated, which were Cre-dependent and

targeted the gene encoding for the testicular orphan nuclear receptor TR4. In these mice, a large set of the excitatory interneurons in the dorsal horn are absent, but the afferent neurons, the projection neurons and the inhibitory interneurons remain unaffected. This study showed that conditional knockout mice had reduced pain responses for behavioural assays that required supraspinal involvement (Wang et al., 2013). For example, there were impaired responses in the hot plate (and capsaicin-induced licking and other tests), which require licking behaviour that involves supraspinal processing along with spinal processing. On the other hand, the conditional knockout mice had comparable latency in the Hargreaves' (and other tests), which only require a withdrawal response that does not need a supraspinal involvement. An interesting finding was seen when the chronic-constriction injury (CCI) model was performed in these conditional knockout mice, as these mice did not show mechanical hypersensitivity but had heat hypersensitivity. These results indicated that the excitatory interneurons are functionally distinct (Wang et al., 2013).

Inhibitory interneurons have several functions. Some excitatory circuits within the spinal cord have the ability to carry signals from low-threshold afferent neurons and transmit them to pain projection neurons. If these circuits function, then pain will be felt even after a delicate touch in a condition called allodynia. However, under physiological conditions, inhibitory interneurons inhibit these circuits. Thereby, no pain should be felt after the application of a low-threshold stimulus. But, when the inhibitory neurons are inhibited (disinhibition), pain due to low-threshold stimuli becomes evident (Takazawa & MacDermott, 2010).

1.4. Chronic pain: a pathophysiological viewpoint

Chronic pain represents a group of various diseases that vary in their underlying mechanisms, just like cancer. For instance, one can categorise chronic pain as either inflammatory pain (caused by persistent inflammation) or neuropathic pain. The majority of pain states, however, exhibit characteristics of both (such as arthritis) or do not fit into either type (such as cancer pain) (Burma et al., 2017). From a clinical point of view, pain can be classified into nociceptive pain, inflammatory pain, or pathological pain. The initial phase of pain is named nociceptive pain. The pain that follows nociceptive pain is named inflammatory pain. Inflammatory pain helps the individual avoid causing further damage to the injury that has already occurred. Both nociceptive and inflammatory pain types

are considered protective. The third type is called pathological pain. Pathological pain is not considered protective as it is not to avoid damage or potential damage, and this type of pain is a challenge to patients and pharmaceutical research.

Nociceptive pain can be classified into two types: somatic pain and visceral pain. Somatic pain affects the skin, bones, ligaments, joints, and muscles. Visceral pain (soft tissue pain) occurs in internal organs. Inflammatory pain mainly occurs due to the activation of the immune system due to tissue damage or infection. The immune system then releases inflammatory mediators that increase the sensitivity of nociceptors to various types of stimuli. Although this pain is considered adaptive, it needs to be reduced in patients who suffer from lasting inflammation (like osteoarthritis patients). The mechanism by which inflammatory mediators increase the nociceptors' sensitivity will be explained in section 2.1.4.1.2. The third pain type is pathological pain, which is defined as pain that lasts after the tissue damage is resolved and can sometimes arise even in the absence of tissue damage. Pathological pain usually occurs due to alterations in the neurons (either peripherally or centrally), causing hyperalgesia and allodynia. Hyperalgesia is an exaggerated pain sensation to noxious stimuli, while allodynia is a pain sensation due to innocuous stimuli (Dai, 2016). Hyperalgesia has two major types: primary and secondary (Hsieh et al., 2015). Primary hyperalgesia occurs at the exact site of the injury, whereas secondary hyperalgesia occurs at a site other than the injury site. Accordingly, it is thought that primary hyperalgesia occurs due to alteration in the first-order neurons innervating the tissue, while secondary hyperalgesia takes place mainly due to central sensitisation. What drives the shift from acute pain to chronic pain is mainly neuronal plasticity. This plasticity can occur at almost any level of the circuitry of pain. The following section will discuss some proposed mechanisms contributing to the transition from acute to chronic pain.

1.4.1. Mechanisms that contribute to the transition from acute to chronic pain

The alterations that can occur in nociceptors can be classified into two categories; modulation or modification. Modulation stands for all the reversible alterations in the excitability of pain neurons (first, second and third-order neurons) that are derived by the post-translational modification of receptors and ion channels (i.e. the already present receptors and channels). Usually, post-translational

modifications occur due to the triggering of intracellular signal-transduction pathways. Modification, however, means any long-lasting change in pain circuitry. These long-lasting changes can be any changes in the expression of receptors, neurotransmitters or ion channels. Furthermore, modification includes any neuronal structure, connectivity or survival changes. One example of a modification is the change in cytoarchitecture, which then alters the properties of the normal responses to stimuli (Voscopoulos & Lema, 2010). Modification is probably the main neuronal alteration linked to the transition from acute to chronic pain.

There is a large number of substances that activate nociceptors and induce their modifications. Although these substances bind distinct receptors, the overall effects involve the activation of the exact intracellular signalling pathways that eventually activate protein kinase A (PKA) or protein kinase C (PKC) (Voscopoulos & Lema, 2010). Therefore, it is doubtful that inhibiting one sensitising agent could allow the prevention/elimination of peripheral sensitisation, and the same applies to central sensitisation (Voscopoulos & Lema, 2010).

Sensory neurons and the development of persistent pain

After tissue inflammation, nociceptors become more responsive to stimuli either by lowering their threshold or by becoming spontaneously active (Handwerker et al., 1987). Not only do regular nociceptors show greater activity, but also silent nociceptors become active during inflammation. Normally, silent nociceptors show no responses, but they become sensitised upon the release of inflammatory mediators. Also, the ion channels and the receptors for pain stimuli might be expressed in higher than normal amounts due to changes in the expression and trafficking of these receptors (Schmidt et al., 1995).

Neuropathic pain can result from injury in the peripheral or central nervous system. These lesions entail that the neurons develop a spontaneous activity or show enhanced responses to innocuous stimuli. This spontaneous activity occurs in nociceptors (C fibres and Aδ fibres) and Aβ fibres (e.g. due to $Na_V1.3$ expression) (Finnerup et al., 2020).

The role of N-methyl-d-aspartic acid (NMDA) receptors

The sustained firing of C-fibres is accompanied by the release of glutamate. Glutamate is the main excitatory neurotransmitter in the CNS. Glutamate released from central terminals of C-fibres can bind several receptors that can be ionotropic or metabotropic. The ionotropic receptors of glutamate include N-methyl-D-aspartic acid (NMDA), α-amino-3-hydroxy-5-methyl-4-isoxazole propionic acid (AMPA) receptors and kainate receptors. Kainate receptors were found to be expressed presynaptically in the dorsal horn of the spinal cord (Kerchner et al., 2001). During acute and transient pain conditions, glutamate released by the first-order neurons activates AMPA receptors and results in excitatory postsynaptic current (EPSC) generation in the second-order neuron. But, upon repetitive firing of C-fibres, EPSCs add up and eventually result in action potential firing. It was found that when C-fibres are excited electrically, this increases the excitability of spinal cord neurons in a fashion that is frequency-dependent, and this process is known as wind-up. Wind-up occurs due to the activation of NMDA receptors; magnesium ions usually block NMDA receptors, but the magnesium ion is removed upon continuous stimulation. It is proposed that the co-release of substance P and CGRP facilitates the detachment of magnesium ions (Eide, 2000). It is thought that NMDA receptors trigger many translational alterations in the second-order neurons that could be vital for chronic pain. NMDA receptor activation is also crucial for the descending inhibitory pathways from the higher brain centres to lamina II of the spinal cord. It was observed that long-term depression (LTD) of the synaptic transmission in the neurons of substantia gelatinosa is seen after the application of electrical stimulation of afferent Aδ fibres. This LTD was attenuated by the application of NMDA blockers. Despite the important role of NMDA receptors in the initiation and maintenance of pain, current blockers of NMDA receptors do not have the aimed-for clinical benefit, mainly due to the lack of specificity and the presence of many side effects. Luckily, low doses of NMDA blockers show favourable clinical responses, making their multi-modal analgesic strategies rational (Voscopoulos & Lema, 2010).

The role of glial cell activation and macrophage infiltration

Immune cells are activated in the CNS following trauma or injury to peripheral nerves, according to studies utilising animal models of inflammation, peripheral nerve injury, bone cancer pain, and spinal cord injury (Kyranou & Puntillo, 2012).

Reports indicate that the infiltration of macrophages into the DRG neurons innervating osteoarthritic knees in mice is linked to pain-like behaviour in these models and that the inhibition of M1-like macrophages by means of IL4-IL10 fusion protein or M2-like macrophages resulted in a good analgesic effect in mouse models of knee osteoarthritis (Ramin et al., 2021).

Microglial cells in the CNS have similar functions to the macrophages in the periphery. The activation of glial cells has a major contribution to pain. Glial cells are activated by many substances released from the central terminal of first-order neurons, including substance P and glutamate. Furthermore, glial cells can be activated by nitric oxide and prostaglandins derived from the second-order neurons. Upon activation, glial cells cause an upregulation of cyclo-oxygenase-2 (COX-2). In turn, COX-2 leads to the production of prostaglandin E2 (PGE2) and causes the release of several cytokines like interleukin-1, interleukin-6 and tumour necrosis factor-α (TNFα). The overall effect of all these substances is that they enhance the second-order neuron excitability, induce the sprouting of neurons, cause alterations in the connectivity of neurons and cause cell death (Voscopoulos & Lema, 2010). Glial activation was evident in many preclinical models of central demyelination and diabetes (Chu et al., 2021; Gonçalves et al., 2018). Glial cells can stimulate one another's activation, which increases nociceptive activation. In other words, pain is amplified and maintained through a positive feedback system (Kyranou & Puntillo, 2012). Studies have shown that P2X4 receptors are required for pain upon peripheral nerve injury (Tsuda et al., 2003). As only microglial cells within the spinal cord possess these purinergic receptors, these results entail the involvement of microglia in generating chronic pain.

Cyclo-oxygenase-2 (COX-2)

During inflammation and neuronal injuries, many transcriptional changes occur in the dorsal horn neurons. Among these transcriptional changes is COX-2 induction. The main reason for the enhanced expression of central COX-2 is interleukin-1β. If the expression of central COX-2 is enhanced, the peripheral

nerve block becomes insufficient to alleviate pain, and in these cases, the use of inhibitors of COX-2 or non-steroidal anti-inflammatory drugs is encouraged. The enhanced expression of COX-2 centrally results in central sensitisation, and some experiments showed that the use of COX-2 inhibitors administered intra-spinally resulted in a remarkable reduction in centrally-induced inflammatory pain hypersensitivity. As COX-2 eventually causes the production of PGE2, the effects of PGE2 cannot be separated from the upregulation of COX-2. Centrally, PGE2 can bind to EP1 or EP3 (subtypes of prostaglandin E receptors) expressed on sensory neurons. This leads to the activation of PKA and PKC and the phosphorylation of certain Na^+ channels on sensory neurons. The threshold of the neurons is then lowered, and the excitability of neurons is enhanced. In addition, PGE2 can activate the microglial production of IL-1β (Voscopoulos & Lema, 2010).

The role of inflammation

The initial phase of transition from acute to chronic pain is usually triggered by inflammation. Inflammation is one way that the body responds to tissue damage. The infiltration of several types of cells, like mast cells, macrophages, neutrophils, T-cells, basophils and keratinocytes, characterises inflammation. These cells produce and liberate inflammatory mediators, which in turn sensitise primary afferents. As mentioned above, as first-order neurons can also act as efferents, they can release substances that promote inflammation. This process is called neurogenic inflammation: inflammation of neuronal origin. Many substances are released locally during inflammation, including bradykinins, prostaglandins, protons, nerve growth factor (NGF), substance P and CGRP. The activation of GPCRs or tyrosine kinase receptors modulates the excitability of neurons as they can sensitive ion channels by phosphorylation, for example. Consequently, hyperalgesia and allodynia may occur as neurons will be ready to fire with stimuli intensities that are lower than the ones needed to generate an action potential in normal situations. The increased firing of the first-order neurons increases the neurotransmitter release at the central terminals of the afferent neurons, which could lead to hypersensitisation of the second-order neurons (Kyranou & Puntillo, 2012).

Neuroplasticity

An important event that is involved in the transition from acute to chronic pain is neuroplasticity. Neuroplasticity stands for the physical remodelling of the cytoarchitecture of neurons. While debatable(Polgár et al., 2005), some studies suggest that peripheral injuries that send a continuous array of pain inputs to the spinal cord cause the death of interneurons that function as modulators of nociceptive signals. Also, the glial cells present centrally cause a remodelling of the synapses between neurons, resulting in the augmentation of nociceptive transmission. Accordingly, the sensitivity of first-order neurons increases and thereby, these neurons become more responsive to stimuli and grow further connections to the projection neurons in the CNS. Shortly after these events, central sensitisation becomes evident. Central sensitisation involves several phenotypic changes in the dorsal horn neurons and the higher CNS centres (Voscopoulos & Lema, 2010).

Alterations in the inhibitory control within the spinal cord

To preserve the appropriate processing of sensory inputs, inhibitory interneurons communicate with other interneurons, the endings of primary nociceptors and/or projection neurons simultaneously (Millan, 2002; Neumann et al., 1996). The production of inhibitory neurotransmitters like glycine and GABA allows interneurons in the spinal cord to perform their inhibitory role. Neurotransmission at this level can be impacted by prolonged nociceptive stimulation brought on by inflammation and/or neuropathy in three different ways: 1) by reducing the number of sites that release GABA and glycine, 2) by reducing the number of receptors to which they bind, 3) by speeding up the removal of the inhibitory neurotransmitters from the synaptic cleft (Cherubini & Conti, 2001; Lee et al., 2009), and 4) GABAergic signaling disinhibition due to alterations in Cl^- homeostasis (Coull et al., 2003). Therefore, the cascade of events that result in persistent chronic pain may be influenced by the interneuron dysfunction brought on by decreased inhibitory control and enhanced stimulation. At the spinal cord, opioids can support the maintenance of an inhibitory effect (Mattia et al., 2006).

Alterations in the descending pain modulation

Chronic pain can result from decreased inhibitory input from the spinal regions and/or enhanced descending pain facilitation. Under ordinary conditions, fibres

that descend from supraspinal regions such as the cortex, midbrain, and brain stem to the spinal cord provide extra inhibitory input to spinal cord neurons within the dorsal horn as well as the central terminals of sensory neurons (Millan, 2002; Porreca et al., 2002; Urban & Gebhart, 1999; Watkins & Maier, 1999). For instance, fibres which descend from the PAG stimulate serotoninergic neurons inside the RVM or noradrenergic neurons in the reticular formation in the pons. Those descending neurons release serotonin and norepinephrine into the spinal cord. Both of these neurotransmitters can diminish the release of excitatory neurotransmitters by primary afferent fibres; hence, the projection neurons in the spinal cord will not be triggered to send noxious signals to the brain. Noradrenaline and serotonin-mediated antinociceptive effects can occur through the direct or indirect (through interneurons) inhibition of sensory neurons (Millan, 2002). Because it acts as an agonist on μ-receptors and inhibits serotonin and noradrenaline reuptake, tramadol has been suggested to treat minor pain in intensive care unit patients (Mattia et al., 2006). Nefopam, a non-opioid analgesic, works similarly by inhibiting dopamine, norepinephrine, and serotonin reuptake, preventing the transmission of nociceptive signals.

Also notable is the role of the RVM in the medulla as a crucial relay site for descending facilitatory actions on nociceptive signal transmission (Fields & Heinricher, 1985; Porreca et al., 2001). Descending facilitation can take place following the prolonged nociceptive inputs, as these inputs can stimulate descending pain facilitatory networks from the RVM, thereby augmenting pain signal transmission. As a result, long-term pain persistence may result in increased pain as a consequence of top-down effects on the spinal cord, which is another justification for treating pain as aggressively as possible in patients (Kyranou & Puntillo, 2012).

Descending pain facilitatory and inhibitory systems may work together to maintain sensory processing (Vanegas & Schaible, 2004; You et al., 2010). Illness, injury, or inflammation can disturb this balance; if facilitation is favoured, pain is exacerbated, whereas an elevation in inhibition might hide underlying pain, maintaining homeostasis (Ren & Dubner, 2002; Vanegas & Schaible, 2004; You et al., 2010). Xu et al. (Xu et al., 1999) observed that 30% of Sprague-Dawley rats did not experience neuropathic pain after spinal nerve ligation (SNL). Atipamezole, but not naloxone, caused touch and cold allodynia in these animals.

Notably, atipamezole (alpha2 antagonist) did not aggravate these symptoms in rats (Xu et al., 1999). This entails that lifting the tonic endogenous noradrenergic inhibitory control unmasked heightened pain (Xu et al., 1999). In a study (De Felice et al., 2011), SNL surgery caused allodynia in half of the Holtzman rats. Lidocaine-based inhibition of RVM activity reversed evoked hypersensitivity and caused conditioned place preference (CPP) in rats with allodynia owing to nerve damage. RVM lidocaine caused allodynia and conditioned place aversion (CPA) in pain-free SNL rats (De Felice et al., 2011). Selective suppression of RVM pain inhibitory neurons with μ-opioid agonist U69593 or spinal injection of α2-adrenergic antagonist yohimbine unmasked symptoms of increased pain in asymptomatic nerve-injured rats (De Felice et al., 2011). Electrophysiological experiments showed that 'pain-free' wounded rats had reduced RVM on-cell function and improved RVM off-cell function (De Felice et al., 2011). These data show that descending inhibition can protect against experimental neuropathic pain after damage (De Felice et al., 2011). In rats with tibial nerve transection, descending noradrenergic suppression delayed pain (Hughes et al., 2013). Blocking spinal α2-adrenergic receptors accelerated behavioural sensitisation, contralateral allodynia, and Fos expression in the spinal dorsal horn (Hughes et al., 2013). These results show that an efficient and functional descending noradrenergic pain inhibitory system prevents heightened aberrant pain and that a mismatch between pain suppression and facilitation might cause it.

In humans with pancreatic cancer, pain is usually experienced only at the late stages, likely because disease progression surpasses descending inhibition. In mouse models of pancreatic cancer, early systemic naloxone injection unmasks pain (Sevcik et al., 2006). The loss of diffuse noxious inhibitory controls (DNICs, a mechanism in which pain inhibits pain) (Le Bars et al., 1979) has also been linked to pain emergence. DNIC is integrated at the dorsal reticular nucleus (DRt), which connects with the PAG and RVM and projects to the spinal cord (Leite-Almeida et al., 2006; Lima et al., 2002). Persistent morphine treatment in rats reduced DNIC, increasing trigeminal neuron sensitivity to dural stimulation (Okada-Ogawa et al., 2009). Inactivating the RVM with lidocaine restored DNIC (Okada-Ogawa et al., 2009). This study demonstrates that elevated descending facilitation may be confused with loss of inhibition. It is unclear which pain modulation changes are more clinically relevant.

1.4.2. Animal models of chronic pain

Here, I use rodent models to examine the cell and molecular pathways causing human chronic pain problems. A decent preclinical pain model must meet two important criteria. The model must first exhibit behavioural characteristics that accurately represent the pertinent symptoms of the human pain situation. No single animal model can fully capture all the characteristics of human disease, but careful study of mouse models of chronic pain can and has taught us a lot. The second requirement for a good model is that it has good face validity, which means that it should be rooted in our best knowledge of how human pathology occurs and, preferably, try to emulate the time course of said pathological alterations (Gregory et al., 2013). Hyperalgesia, allodynia, as well as spontaneous pain are the three main signs of chronic pain (Jensen & Finnerup, 2014). Correlates of the first two are easily seen in rodents, where they manifest as lower reflex withdrawal thresholds, while spontaneous pain is more difficult to investigate. Hyperalgesia, a term used to describe greater pain in humans in reaction to typically unpleasant stimuli, is frequently connected to inflammatory pain. Allodynia is a characteristic of many neuropathic pain conditions in which patients experience pain that is elicited by typically benign stimuli. It is more difficult to differentiate between these two symptoms in mice since rodents cannot express their feeling of pain. The majority of behavioural tests detect hypersensitivity to stimuli that are classified as noxious or benign depending on industry standards and the trained experimenter's observations. The Hargreaves' Apparatus tracks variations in the duration to withdraw the paw from radiant heat, and is used to study heat hyperalgesia (Hargreaves et al., 1988). Von Frey hairs may be employed for the evaluation of primary and secondary mechanical hypersensitivity (Deuis et al., 2017). It is debatable whether the von Frey test assesses hyperalgesia or allodynia, as the von Frey test could still elicit withdrawal even during healthy conditions. Mechanical hyperalgesia, on the other hand, is evaluated by using the Randall-Selitto test, which could be applied to the tail or paw (Randall, 1957). It is worth mentioning that even a stimulus that is as innocuous as the application of a cotton swab to assess dynamic allodynia can still cause withdrawal in naive animals, calling into question the assumption that withdrawal is always nocifensive (Ranade, Woo, Dubin, Moshourab, Wetzel, Petrus, Mathur, Bégay, Coste, Mainquist, et al., 2014). Therefore, withdrawal reflexes cannot indicate whether an animal is truly in pain. For example, paw

withdrawal continues even in decerebrate rats (Woolf, 1984). Alternatively, researchers can employ the mouse grimace scale, for example (Langford et al., 2010). Similarly, a research paper utilised digging and burrowing behaviour as means of evaluating 'well-being' in mouse models of arthritis to determine the impact of pain on daily activities (Chakrabarti et al., 2018). Even though spinal reflexes are a simplistic method for pain assessment in mice, evaluating the quality of life through various indicators will, most probably, enhance translation.

Any behavioural test should be conducted carefully. Peculiarities of mouse biology and the experimenter can impact results and be a major confounding factor. For instance, male experimenters can cause stress-induced analgesia in mice (Sorge et al., 2014).

Inflammatory pain is technically the easiest model of all the states of chronic pain. It is possible to inject certain elements of the inflammation soup thought to be responsible for hyperalgesia, like PGE2. Alternatively, algogenic substances, such as Complete Freud's Adjuvant (CFA) or carrageenan, can be administered to the animal to evoke a much more widespread inflammatory response (Burma et al., 2017; Gregory et al., 2013). The drawback of these inflammatory models is that they have little clinical applicability because short-lasting pain caused by inflammation is not, in fact, a chronic pain condition but instead a type of physiological sensitisation to facilitate tissue repair. The fact that the formalin model has a second-phase response makes this model a particularly attractive inflammatory model, as this second phase can be regarded as a chronic pain condition (Dubuisson & Dennis, 1977). Other models that rely on eliciting a damaged state prior to administering an algogenic substance have been employed to decipher pain chronification. For instance, a study found that the manifestation of priming induced by carrageenan administration and the subsequent PGE2 injection requires primary afferent-derived brain-derived neurotrophic factor (BDNF) (Sikandar et al., 2018).

A number of nerve damage preparations initially created for use in rats but now frequently utilised in mice are applied to imitate neuropathic pain (Jaggi et al., 2011). There is, however, inter-lab variation in the behavioural alterations specific to each modality. Models of chemotherapy-elicited peripheral neuropathy involve injecting various chemotherapeutic agents like oxaliplatin, but treatments need to be continued for long periods to achieve pain (Flatters et al., 2017). In mice, pain

that comes with rheumatoid arthritis and osteoarthritis can be studied in mice, for example, with the well-known monoiodoacetate model (Pitcher et al., 2016). The models mentioned, however, are unable to describe numerous vital aspects of the pathologies, which include age effects. Recently, a non-invasive osteoarthritis model that involves the application of a mechanical load on joints has been developed, which recapitulates the disease progression and the suffering that patients experience throughout time (Ter Heegde et al., 2019).

Human tissue samples are a growing substitute for rodent pain models in pain research. For example, sensory neurons can be produced from induced pluripotent stem cells obtained from patients and then studied in a dish. Until now, such research has mostly concentrated on people who have inherited erythromelalgia or other genetically based chronic pain conditions (Meents et al., 2019). Unfortunately, it is clear that these studies will not tell us much about pathophysiological alterations that take place throughout the entire organism. I relied on mouse models for my PhD work reported here mainly because they can be used to combine systems neuroscience and molecular genetic techniques with well-characterised chronic pain models.

1.4.3. An overview of the role of the peripheral nervous system in chronic pain

The CNS is where pain is first consciously perceived. On the other hand, peripheral nociceptive input typically contributes to the sensory and emotional pain experience. Interestingly, withdrawing these peripheral inputs using local anaesthetics that inhibit VGSCs alleviates acute as well as chronic pain (Aguirre et al., 2012). Likewise, patients with mutations in the genes encoding for peripheral Na^+ channels that lead to congenital insensitivity to pain do not experience chronic pain, even though they encounter numerous injuries all across their lives, which would commonly evoke persistent pain (Cox et al., 2006). These findings indicate that peripheral sensory neurons play a crucial part in creating and sustaining persistent pain experiences. Peripheral sensitisation describes the mechanism in which immunogenic and inflammatory substances liberated following tissue damage engage their targets expressed on the nerves, enhancing their excitability. An *in vivo* imaging experiment showed the numerous changes in sensory neuron response characteristics that take place after being exposed to an "inflammatory soup" (Smith-Edwards et al.,

2016). Intriguingly, DRG transcriptomic characterisation, in conjunction with good behavioural phenotyping, has demonstrated the crucial role of immune responses in neuropathic pain, as demonstrated by the fact that depleting T cells or macrophages abolishes mechanical allodynia (Cobos et al., 2018). Trpv1, for example, will be directly sensitised by protons generated during tissue acidosis, which lowers the temperatures needed for its activation and causes a burning-like sensation (Tominaga et al., 1998). Other components of the soup interact with GPCRs or growth factor receptors to produce more prolonged modifications in sensory neurons.

However, what troubles patients the most is not sensitisation to unpleasant stimuli, as it is not difficult to avoid these triggers. But when patients experience mechanical allodynia, even gentle touch can cause pain; for these people, the simple brush of clothing against the skin can be excruciating. Piezo2 has recently been demonstrated to be necessary for tactile allodynia. Knocking out Piezo2 conditionally in the caudal half of the mouse by the use of Hoxb8 Cre prevented mechanical hypersensitivity following capsaicin as well as nerve injury (Murthy et al., 2018). The above mouse findings are backed by the convincing finding suggesting that humans with Piezo2 loss-of-function mutations also do not experience tactile allodynia upon applying capsaicin cream, emphasising the translational significance of Piezo2 for managing chronic pain. Ablating TrkB-expressing cells in adults implies that these low-threshold D-hair and fast adapting Aβ fine touch sensors are crucial for the development of dynamic, punctate, as well as static tactile allodynia during neuropathic pain states (Dhandapani et al., 2018). These findings show that mechanical allodynia requires peripheral input. Both damaged and intact nerves become hyper-excitable following a nerve injury, generating ectopic discharges that may be the cause of the spontaneous pain that most patients report as their main symptom. This shift in afferent excitability may be caused by alterations in the expression and activity of several voltage-gated channels, like $Na_V1.8$ (Gold et al., 2003; Roza et al., 2003).

A variety of molecular and cellular pathways may influence the aetiology and continuation of chronic pain. It must be emphasised, though, that a peripheral factor that has been determined to be essential for chronic pain may not necessarily represent a pathogenic cause. The mechanosensory input from the

TrkB neurons necessary for tactile allodynia is probably converted into pain by dysfunctional central circuits. It is important to differentiate between peripheral drive, that merely maintains chronic pain, and peripheral sensitisation, causing it. In the latter instance, although reducing ascending input by targeting the periphery may reduce pain, the pathologic alteration takes place upstream in the CNS.

1.4.4. Understanding the role of the central nervous system in chronic pain

Sherrington famously described *pain* as "the psychical adjunct of a protective reflex" (Lamont et al., 2000). The CNS implements the psychological aspects of pain, including perceptual, affective, and emotional reactions. The sensory-emotional experience of pain is frequently connected to nociceptor activity, but not always. Nociceptors recognise damage rather than pain. According to Melzack and Wall, the resulting incoming sensory information is subsequently "gated" and shaped at the cord and brain levels to provide a sense of pain. As a result, the following distinction between the core processes of pain is useful. First, pathologic central processes may amplify a peripheral input that contributes to pain. The second type of pain comes from central circuits that have been damaged initially on the periphery. Not to mention, there is pain that has a totally central cause. Clifford Woolf reported a rise in the flexion reflex evoked by noxious stimulation in rats with nerve damage while recording from motor efferents, which was driven by a central alteration in the spinal cord (central sensitisation involving NMDA receptors) (Woolf, 1983). This type of post-synaptic plasticity, known as central sensitisation, essentially involves the strengthening of post-synaptic receptors in an NMDA-receptor-based manner in order to enhance synaptic efficacy. (Woolf, 2018; Woolf & Thompson, 1991). Although the phrase "central sensitisation" has been misused frequently and has become a vague term for any core cause of persistent pain. Inhibiting peripheral nerve activity or NMDA receptor activation during surgery may help avoid phantom limb pain by stopping bursts of activity from causing post-synaptic sensitisation at the dorsal horn neurons, which were originally conveyed from the amputated limb (Reuben & Buvanendran, 2007).

The internal state of the organism, as well as the external context in which it is situated, have a significant impact on both the affective and perceptual aspects

of chronic pain. As an illustration, restricting food from mice can alleviate inflammatory pain because the impulse to alleviate hunger takes precedence over the pain (Alhadeff et al., 2018). Similarly, a human patient's level of arousal, acute stress, and emotional state all determine how intensely pain is felt (Perl, 2007).

According to the findings of a recent study, pain hypersensitivity that was conditioned by a previous painful experience within an identical setting could be found in male mice and humans, but it did not exist in females of either species (Martin et al., 2019). Patients with lower socioeconomic status have a significantly higher incidence of chronic pain (Macfarlane et al., 2009). Inevitably, less fortunate people are more likely to suffer from painful conditions such as injuries due to their jobs (Connolly et al., 2000). Prolonged exposure to stress causes brain alterations that weaken the reaction to cortisol, which in turn facilitates chronic pain (Hannibal & Bishop, 2014). The primary objective of fundamental biology research into nociception is to discover peripheral targets and mechanisms that contribute to the pathophysiology of pain. A successful translation, on the other hand, will necessitate knowledge of the fact that in humans, peripheral nociception is usually accompanied by a wide range of psychosocial and biological elements that work through central circuits.

1.4.5. Analgesics

Salicylic acid, the active component of willow bark, was discovered in the 19th century. Acetylated salicylic acid, also known as aspirin, was produced on a large scale by Bayer at the turn of the new century and quickly gained popularity for treating pain, especially rheumatoid arthritis (Wood, 2015). However, it was not until 1971 that Ferreira, Moncada, and Vane—for which Vane won the Nobel Prize—identified the mechanism of action of NSAIDs like aspirin. They discovered that aspirin inhibits cyclooxygenases (COX1 and COX2), enzymes necessary for the production of eicosanoids from arachidonic acid, including prostaglandin and thromboxane, which are known to cause pain (Ferreira et al., 1971). Since acetaminophen (also known as paracetamol) only has weak anti-inflammatory effects and does not seem to target COX2, it is typically not regarded as an NSAID. According to one study, TRPA1 is activated by acetaminophen metabolites (Andersson et al., 2011) and other suggests that it acts through cannabinoid receptor 1 receptors (Klinger-Gratz et al., 2018). Such

debates suggest that commonly used analgesics like acetaminophen probably have several interrelated modes of action that work together to produce analgesia.

Opiates have been utilised for pain relief since ancient times, just as willow bark. Opioids, which include both synthetic opioids like oxycodone and plant-derived opiates like morphine, are typically particularly successful at reducing short-term pain, such as that which follows surgery. They act as agonists for the opioid receptors. The neurological system contains endogenous opioids from four different families: nociceptin, enkephalins, -endorphins, and dynorphins. These peptides are created by enzymatically splicing bigger precursor molecules, which are then bundled into dense core vesicles. Preproenkephalin, for instance, can be cleaved into met or leu-enkephalin. Endogenous opioids, especially in so-called pain pathways, are generated as volume transmitters from axon terminals and diffuse to their corresponding receptors, which are often extrasynaptic. This reduces the activity of post-synaptic neurons (Corder et al., 2018). For instance, in a well-known study, Jon Levine and Howard Fields demonstrated that naloxone prevented the placebo effect in individuals with dental pain, indicating that endogenous opioid signalling is necessary for the occurrence of placebo analgesia (Levine et al., 1978).

Depending on how sensitive they are to various agonists, opioid receptors, which belong to the GPCRs superfamily, can be divided into four subtypes: mu, delta, kappa, and nociceptin. Although each subtype is encoded by a separate gene, their amino acid compositions can be up to 60% similar (Corder et al., 2018). All four subtypes communicate by inhibiting adenylate cyclase through the G-i/o pathway. The Gβγ subunit can open G-protein-coupled inwardly rectifying K^+ channels (GIRK K^+ channels), causing membrane hyperpolarisation, and directly block voltage-gated Ca^{2+} channels, preventing transmitter release (Corder et al., 2018). The mitogen-activated protein kinase cascade is one of the intracellular signalling pathways that is recruited by arrestin-bound opioid receptors which causes side effects like respiratory depression (Madariaga-Mazón et al., 2017). A recent study demonstrated that μ and δ co-localisation is unusual in the CNS, and even when they are co-expressed, the receptors operate separately (Dong Wang et al., 2018). These receptors are expressed by several other tissue areas that are not linked to pain. This justifies why opioid medicines can have a wide

range of side effects, such as respiratory depression, constipation, dependency and addiction, with the associated possibility of overdose. If the medications are administered for a long time, tolerance or even hyperalgesia may develop, highlighting the significance of creating novel analgesics that do not target the opioid system (Lyapustina & Alexander, 2015).

The ideal pain reliever would lessen pain quantitatively and controllably without causing side effects, tolerance, or addiction. Numerous pain-related ion channels have been targeted by small molecule inhibitors (e.g. against $Na_V1.7$); however, these inhibitors have so far shown limited efficacy (Emery et al., 2016). In contrast, monoclonal antibodies that sequester CGRP or antagonise its receptors have had great effectiveness in (e.g. for migraine and headache pain (Tso & Goadsby, 2017)). The pharmaceutical sector has also shown interest in using already-approved medications to alleviate pain. Cannabinoids have long been used by people who self-medicate their pain. With the rising social acceptance of these substances, their use may expand. It's interesting to note that James Cox and colleagues published a case study on a patient who had a microdeletion in a FAAH (fatty acid amide hydrolase) pseudogene, which disrupts FAAH function and, as a result, increases endocannabinoid levels, resulting in a phenotype free of pain and anxiety (Habib et al., 2019).

Several groups are actively investigating circuit-based approaches to pain management in the lab. Chronic pain has been treated in people by anterior cingulate cortex deep brain stimulation. Electrical stimulation randomly activates neurons; chemo- and optogenetic techniques, on the other hand, allow for more precise modification of circuit function. In a proof-of-concept investigation, the Gereau lab silenced bladder afferents using the inhibitory opsin archaeorhodopsin to treat a mouse model of persistent bladder pain (Samineni et al., 2017). A novel ivermectin-gated chloride channel was recently described by the Bennett group in a publication that could mute sensory neurons and alleviate neuropathic pain (Weir et al., 2017). The fact that this tool was expressed in sensory neurons as a result of viral infection is a benefit. See Chapter 6 for further information on the application of chemogenetic tools in pain research.

The sad reality is that most treatments—whether they include small compounds, biologics, or circuit-based technology—fail in clinical trials. The placebo effect, which oddly has been increasing year over year in clinical studies, contributes to this in part by making it more challenging to discern successful molecules (Tuttle et al., 2015). Therapeutic strategies that are effective in mice are frequently ineffective in people because of the homogeneity of inbred lab mice (Selman & Swindell, 2018). Nowadays, clinical trials are frequently randomised, double-blinded, pre-registered, and include predetermined outcome measures. Although most preclinical research is blinded, outcome measurements are frequently flexible, and randomisation processes may not be employed correctly. This gives plenty of leeway for post-event speculation. Numerous statistical reporting errors were discovered during a study of the literature in basic neuroscience publications that were published in reputable journals (Nieuwenhuis et al., 2011). A movement to address the reproducibility dilemma that started in psychology has recently spread to fundamental preclinical science, and publications are already publishing registered papers and calling for open access to data and analyses. I hope that these advancements are enough to broaden the translational bottleneck for moving analgesics from the bench to the clinic.

A type of evidence-based talking therapy called cognitive behavioural therapy (CBT) places a strong emphasis on the role that behaviour and conscious thought have in determining how we feel. The success of utilising CBT to treat emotional problems has led to the introduction of cognitive-behavioural principles into the therapy of chronic pain since pain is increasingly recognised as both a sensory and an emotional experience. In spite of significant methodological advancements in trial design and administration, the results of interdisciplinary pain management programmes inspired by CBT are at best modest. A hybrid CBT strategy that aims to simultaneously address pain and associated comorbidities shows promise in maximising treatment effectiveness and flexibility while the field searches for novel therapy possibilities (Tang, 2018).

2. The optimization and characterization of a mouse model of cancer-induced bone pain

2.1. Introduction

2.1.1. The problem of cancer-induced bone pain (CIBP)

Cancer survival rates have dramatically increased since the turn of the century with the advent of targeted and improved treatment strategies. On the other hand, the annual number of cancer cases worldwide is estimated to rise, leaving a growing problem of providing effective pain management for the side effects of cancer and its treatments. Between 30-50% of patients receiving curative-intent therapy and 75-90% of patients with advanced disease endure chronic pain that is strong enough to require opioid therapy (Teunissen et al., 2007; M. H. J. van den Beuken-van Everdingen et al., 2007). More than one-third of patients in disease remission will continue to report pain after curative treatment (M. H. van den Beuken-van Everdingen et al., 2007). The World Health Organization (WHO) Analgesic Ladder is frequently the first step in a paradigm for guiding clinicians to manage pain in a systemic manner. Over-the-counter analgesics comprise Step 1, and "weak" opioids (such as codeine) are escalated in Step 2, followed by the use of "strong" opioids in Step 3 to treat moderate-to-severe pain. Clinical professionals are urged to take non-pharmacologic pain management methods in Step 4 into account. The advantage of NSAID/opioid combination therapy is a reduction in overall opioid prescriptions, but data on its efficacy is conflicting (Haroun et al., 2022). Adjuvant therapies include anti-depressants (like duloxetine (Smith et al., 2013) and anticonvulsants like gabapentin and pregabalin (Mishra et al., 2012)), which are first or second-line analgesics for other chronic pain conditions, including painful neuropathies (Bates et al., 2019). Adjuvant analgesics, integrative therapeutic options (such as acupuncture (Lu et al., 2008)), as well as interventions (e.g. nerve block (Amr & Makharita, 2014)), and epidural or intrathecal analgesics (Haroun et al., 2022), can be considered at any stage of pain management even though they are not listed on the WHO ladder.

There remains a continuous debate regarding the suitability of these generalised WHO recommendations to adequately manage pain in a heterogeneous group of

patients that have a cancer diagnosis. The need to modify current pain management protocols in patients with cancer is indicated by reports that pain is the most common complaint leading to emergency unit visits by patients with cancer (Barbera et al., 2010; Batalini et al., 2017; Mayer et al., 2011). It was found that the bone is one of the most commonly reported pain sites, emphasising the importance of discovering new ways to control CIBP. Bone metastasis is estimated to occur in 65-75% of patients with advanced breast or prostate cancer and approximately 30-40% of patients with advanced lung cancer, all of which are among the most common cancers in terms of prevalence (Coleman, 2001). Bone metastasis adversely impacts the quality of life of patients and reduces their life expectancy. Bone pain and analgesic usage rise remarkably within a time frame of six months from the start of skeletal events (Brodowicz et al., 2017; von Moos et al., 2016).

This section gives an introduction to the bone, its structure and innervation. Following that, the current understanding of the mechanisms that lead to CIBP, both the peripheral and central nervous system mechanisms involved in CIBP, will be discussed.

2.1.2. Bone physiology

2.1.2.1. The structure of the bone

The human body contains about 200 bones. The bones have numerous purposes. For example, bones provide a hard skeleton that protects the internal organs. Furthermore, bones, tendons and muscles contribute to body movement. Additionally, bones perform numerous endocrine activities, such as controlling phosphate metabolism, increasing insulin release, and producing testosterone (Karsenty & Ferron, 2012).

Histologically speaking, there are two types of mature bone. The first type of bone is the dense and compact cortical bone, which forms the outer layer of bones. Trabecular bone is the second type and is less dense than cortical bone. The cortical bone is extremely resistant to bending and twisting. The rate of turnover of cortical bone is relatively slow. On the other hand, trabecular bone is essential for compression resistance and has a faster turnover rate than cortical bone (Kamioka et al., 2001).

2.1.2.2. The main cell types in the bone

In the bone tissue of adults, there are four main types of cells; osteoclast (responsible for bone resorption), osteoblasts (important for bone formation), bone-lining cells and osteocytes (main cell type that responds to mechanical loading) (Dudley & Spiro, 1961; Tatsumi et al., 2007). Moreover, osteocytes are the chief suppliers of receptor activator of nuclear factor κB ligand (RANKL) under mechanical loading conditions (Xiong et al., 2011). RANKL signaling results in bone resorption by promoting osteoclastogenesis (Boyce & Xing, 2008). Bone-lining cells are thought to contribute to bone remodelling as they form a cover over the resorption lacuna (Hauge et al., 2001).

2.1.2.3. Modelling and re-modelling of bones

The primary mechanism through which bones develop and change shape is bone modelling. The modelling of bone is not common in adults. During bone remodelling (also known as the virtuous circle), bone is either formed or resorbed, altering the bone structure (either by shaping or re-shaping). Bone remodelling is a lifelong process. While bone modelling influences the bone's structure, bone remodelling impacts the bone's properties (like mineralisation). In bone remodelling, both osteoclasts and osteoblasts act sequentially at the same spatial location, whereas in bone modelling, bone production and resorption can occur independently (so only one of them can take place) (Allen & Burr, 2014; Langdahl et al., 2016). Bone remodelling has five main steps: the activation of remodelling, bone resorption, resorption reversal, the formation of bone, and termination (See Figure 8).

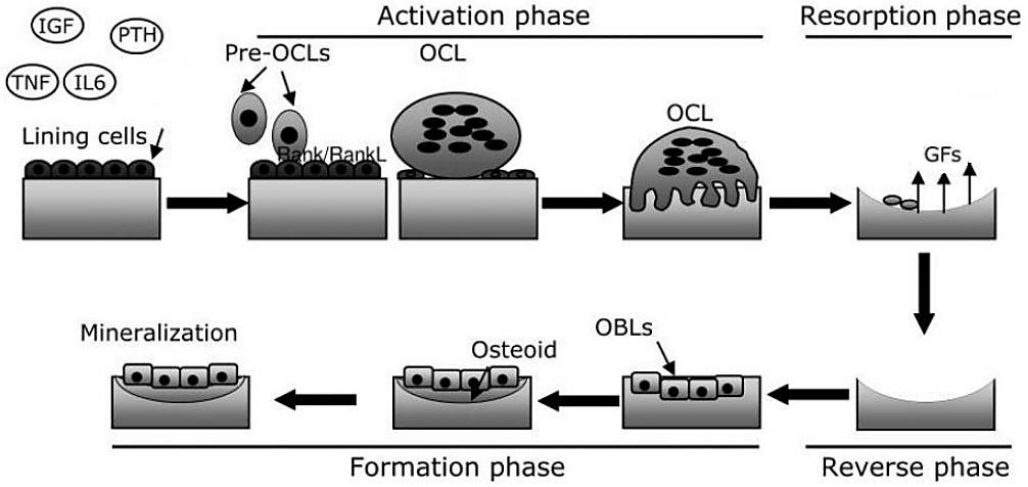

Figure: 8 The steps involved in remodelling of bone. *When various stimuli activate lining cells, which raise RANKL surface expression, bone remodelling can begin. The interaction between RANKL and its receptor, RANK (Receptor Activator of Nuclear B), causes the development of osteoclasts (Activation phase). Osteoclasts break down bone during the resorption phase, releasing substances like BMPs, TGF, and FGFs that attract osteoblasts to the site of the break. Osteoblasts, once recruited, create the new bone matrix and encourage its mineralization (Formation phase), completing the bone remodelling process. Abbreviations: Pre-OCLs (pre-osteoclasts); OCL (osteoclast); OBL (osteoblasts); TNF: tumour necrosis factor; IGF; (insulin growth factor); TNF (tumour necrosis factor); IL6 (interleukin 6); PTH (parathyroid hormone); GFs (growth factors). Adapted from (Rucci, 2008).*

2.1.2.4. The innervations of the bone

2.1.2.4.1. Development of a unified theory for nerves in bone

In 1868, Jean-Martin Charcot first hypothesised that the role of the nerves in the bones is trophic. His explanation was that the damage of nerves deprives the bones and joints of some necessary growth factors, which in turn results in the destruction of the bones. Charcot's principle became the basis for the neurotrophic theory to explain the role of nerves in the health of bones and joints. Following this theory came the neurotraumatic theory, which speculates that the loss of peripheral sensation because of nerve damage leads to recurring traumas that exceed the rate of healing. The third theory is the neurovascular theory. This theory was developed in the 1980s when it became evident that diabetic patients who suffer from neuropathy have increased blood flow in their joints. The neurovascular theory explains the association between neuropathy and vascular

tone. Because sympathetic nerves control the tone of blood vessels in the bones, neuropathy causes excessive blood flow to the bones. This local inflammation then results in bone resorption (Edmonds et al., 1985). In fact, all these three theories together contribute to explaining the actual role of nerves in the bone.

2.1.2.4.2. Classification of skeletal axons

The nerve branches that target the skeleton are predominantly unmyelinated or myelinated fibres with small or medium diameters of axons. These characteristics indicate that the neurons that target the skeleton are primary sensory neurons and postganglionic autonomic neurons (Brazill et al., 2019).

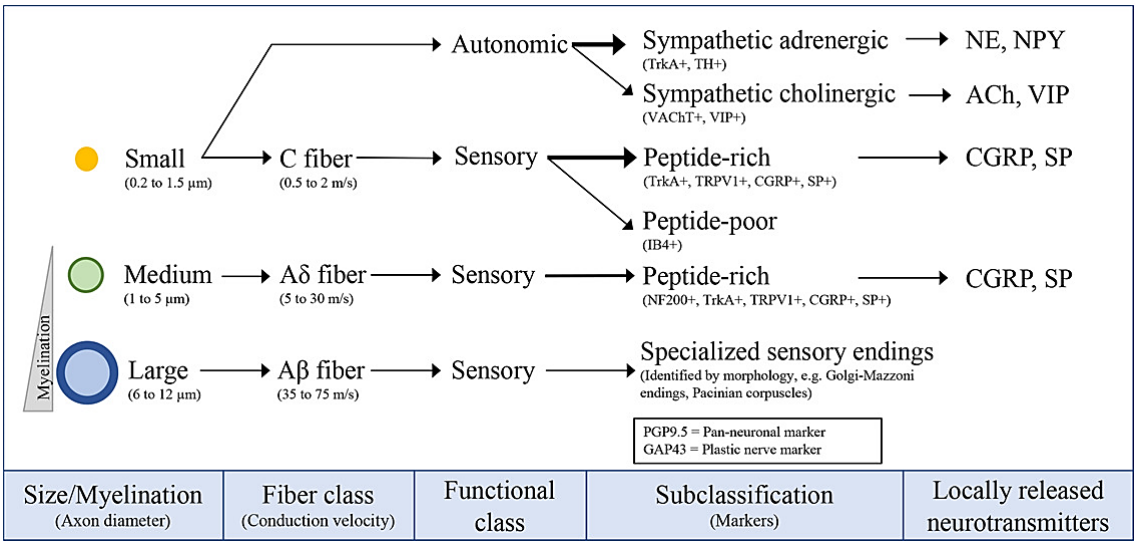

Figure 9: Skeletal axons classified. *Size and myelination conditions of bone-supplying peripheral nerve axons affect conduction speed. Most skeletal fibres are unmyelinated, small-diameter, slow-conducting axons (yellow). These include sympathetic, adrenergic or cholinergic, and sensory C fibres. Aδ fibres are minimally myelinated, medium-diameter (green), and conduct at 5 to 30 m/s. Aβ fibres are large-diameter, densely myelinated axons that conduct quickly (35 to 75 m/s), but these are rare in bone. Each fibre subclass has unique immunohistochemical markers. Sensory and autonomic small and medium-sized neurons can release neurotransmitters locally. TrkA = type 1 tyrosine kinase receptor; TH = tyrosine hydroxylase; VAChT = vesicular acetylcholine transporter; VIP = vasoactive intestinal peptide; TRPV1 = transient receptor potential cation channel subfamily V member 1; CGRP = calcitonin gene-related peptide; SP = substance P; IB4 = isolectin B4; NF200 = neurofilament 200; PGP9.5 = protein gene product 9.5; GAP43 = growth associated protein 43;*

NE = norepinephrine; NPY = neuropeptide Y; ACh = acetylcholine. Obtained from (Brazill et al., 2019).

2.1.2.4.2.1. Sensory nerves in bone

The DRG contains cell bodies of the sensory neurons that innervate bone, just as it contains the cell bodies of the main sensory neurons that innervate other body parts. In addition to transmitting signals from the periphery to the CNS, these neurons can also generate efferent signals. After tissue injury, neurogenic inflammation is a notable example of the efferent activity of sensory neurons. Neurons release neuropeptides such as CGRP and substance P during neurogenic inflammation. CGRP induces vasodilation, whereas substance P promotes plasma extravasation. Neurogenic inflammation is also evident in the bone (Brazill et al., 2019).

Experiments on rat bone indicated that following the application of noxious mechanical stimuli, the conduction velocities of nociceptors correspond to the conduction velocity of small unmyelinated C fibres (less than 2 m/s) and those of medium-sized myelinated Aδ fibres (between 2 and 12.5 m/s). Analysis of the nerves within the bone marrow revealed the absence of neurons with a large diameter. Large-diameter neurons with encapsulated ends that specifically detect vibration and pressure were nevertheless identified in the interosseous membranes separating bones. In humans, these large-diameter neurons were detected in the periosteum (a fibrous tissue that covers the surface of most bones in the body) of long bones (Brazill et al., 2019). Peptidergic sensory fibres express CGRP and substance P and are abundant in the bone of almost all vertebrates (Bjurholm et al., 1988). See Figure 9 for an explanation of the sensory and noradrenergic neurons innervating the bone.

Classically, the majority of studies investigating bone nociception have focused on the periosteum (Brazill et al., 2019), perhaps because the periosteum is more accessible and can be stimulated easily. The vast majority of periosteal neurons were poorly myelinated Aδ fibres and non-myelinated C-fibres, according to these investigations. Aδ fibres are associated with acute pain with a rapid onset, whereas C-fibres are associated with persistent pain. These neurons are sensitive to harmful chemical, mechanical, and thermal stimuli (Brazill et al.,

2019). Similarly, the stimulation of the periosteum causes pain in humans (Inman & deC. M. Saunders, 1944).

Compared to the periosteum, there has been far less research on bone marrow. However, myelinated Aδ fibres and non-myelinated C-fibres appear to be the most prevalent in the bone marrow. In contrast to the periosteum, Aβ fibres have not yet been found in the bone marrow. Normal activation of the nociceptors of the bone marrow is caused by an increase in intramedullary space pressure (Aielli et al., 2019). In humans, the rise in pressure of the intramedullary space is observed in disorders such as bone metastases (Haroun et al., 2022). In CIBP, the increase in pressure seems to play a central role as most tumours metastasize to the trabecular bone that is always present in the medullar cavity.

Notably, nociceptors in the periosteum and the bone marrow are typically polymodal (i.e., are responsive to multiple types of stimuli) and can fire in response to heat, cold, oxidative pressure, acidosis and other stimuli (Aielli et al., 2019).

2.1.2.4.2.2. Autonomic nerves in bone

Two major divisions comprise the autonomic nervous system: the sympathetic nervous system and the parasympathetic nervous system. Postganglionic neurons of the autonomic nervous system have conduction speeds comparable to those of C fibres. They are likewise similar to C fibres in that they have a small diameter and are unmyelinated. In general, the autonomic nervous system is responsible for regulating the body’s automatic responses to stimuli of external or internal origin. For instance, the sympathetic nervous system's responses to stress might influence bone metabolism (Aielli et al., 2019).

The majority of bone’s autonomic innervations are sympathetic neurons, and the expression of tyrosine hydroxylase (TH) is used to identify the postganglionic neurons of the sympathetic division of the nervous system. Notably, some cholinergic sympathetic postganglionic neurons have also been identified in the bone (Aielli et al., 2019). There is currently no evidence of parasympathetic innervations in bone (Aielli et al., 2019).

2.1.2.4.3. Pathways to the brain

Some studies have attempted to identify how the skeleton sends sensory signals to the CNS. Retrograde labelling of the sensory neurons that innervate the rat

tibia indicated that the somas are located in the ipsilateral lumbar DRGs (L1-L6) (Aielli et al., 2019). In a study that involved the noxious stimulation of the bone using a mechanical stimulus (drilling of rat tibial diaphysis), the brain areas associated with pain processing were retrogradely labelled (namely the thalamus, gracile nucleus and lateral parabrachial nucleus). In this study, Fos immunohistochemistry was used as a tool to identify the neurons that get activated within the spinal cord as a result of drilling. The results highlighted an essential distinction between the neurons engaged in acute bone pain (following mechanical stimulation) and acute cutaneous or visceral pain, with the spinoparabrachial pathway being the most critical tract for conveying acute mechanical bone pain. Contrarily, the spinothalamic tract is the chief route for conveying cutaneous pain signals, and the postsynaptic dorsal column pathway is the main pathway for transmitting visceral pain signals (Aielli et al., 2019). Since drilling the rat tibia activates neurons that synapse as superficially as laminae I and II in the spinal cord, painful drilling signals are transmitted to the lateral parabrachial nucleus.

In order to study sympathetic innervations in the bone marrow of a rat's femur, pseudorabies viruses were injected into the marrow space, and the infection sites were observed for several days following the injection. The identified central networks were not unique for the bone, and the sympathetic regulation of the bone was comparable to that of any other peripheral organ (i.e. through controlling vascular tone (Aielli et al., 2019)).

2.1.3. Events after bone metastases

The bone is typically an excellent target for metastasis due to its favourable biochemical and physiological characteristics. According to the "seed and soil theory" of Steven Paget, bone is good soil for the seed (Paget, 1989). Numerous cancer cell types, including prostate, breast, myeloma, thyroid, lung, and bladder cancer, are attracted to the bone as a potential site for metastasis. Multiple steps are required for cancer to metastasize. Cancer cells must first penetrate their surrounding tissues (local invasion). Second, cancer cells reach the bloodstream or lymphatic system (intravasation). Thirdly, it is essential that cancer cells remain alive while circulating in the blood. In the fourth step, termed extravasation, cancer cells leave the bloodstream and colonise the target tissue. Several genetic and epigenetic alterations encourage metastasis. The shape of sinusoids

(capillaries of the bone marrow) enables them to transport hematopoietic cells efficiently; however, the same property also facilitates the extravasation of cancer cells. RANKL in the bone functions as a chemoattractant to attract RANK-expressing cancer cells to the bone. As stated previously, cancer cells then begin to express receptors that are characteristic of hematopoietic cells. Chemokine receptor 4 (CXCR4) is one of these receptors; it binds stromal cell-derived factor 1 on osteoblasts and bone lining cells, hence enhancing the adhesive properties of cancer cells, which aids in metastasis. Consequently, cancer cells now possess the characteristics necessary to compete with hematopoietic cells for occupancy of the bone. After extravasation and bone occupation, cancer cells remain dormant and develop what is known as dormant micrometastasis. Cancer cells will remain in micrometastasis until they acquire the 'right' genetic/epigenetic changes, which permit the growth of these cells to eventually form macrometastasis (Haroun et al., 2022).

The tumour growth in the bone is described as a "vicious cycle" (Maurizi & Rucci, 2018; Roodman, 2004). According to X-ray images, there are two types of vicious cycles, and the classification depends on whether the tumour is osteosclerotic or osteolytic (Ibrahim et al., 2010). During a vicious osteosclerotic cycle, the alterations that occur in the virtuous cycle are accompanied by an increase in the growth factors in the osteoid. However, the mineralisation and the remodelling are inadequate, causing the bone to become mechanically incompetent and described as "woven" bone (Guise et al., 2006). On the other hand, osteolytic lesions that occur in bone metastases of many cancers, like breast and renal cancers (Hernandez et al., 2018), happen as a result of osteoclast hyperactivity (Roodman, 2004). Figure 10 summarises the vicious cycles of tumour growth in the bone. The protype for osteosclerotic cancers is prostate cancer, whereas breast cancer is the protype of osteolytic as breast cancer cells potentiate osteoclasts-induced bone degradation. In certain bone metastases, both osteolytic and osteosclerotic features are detected.

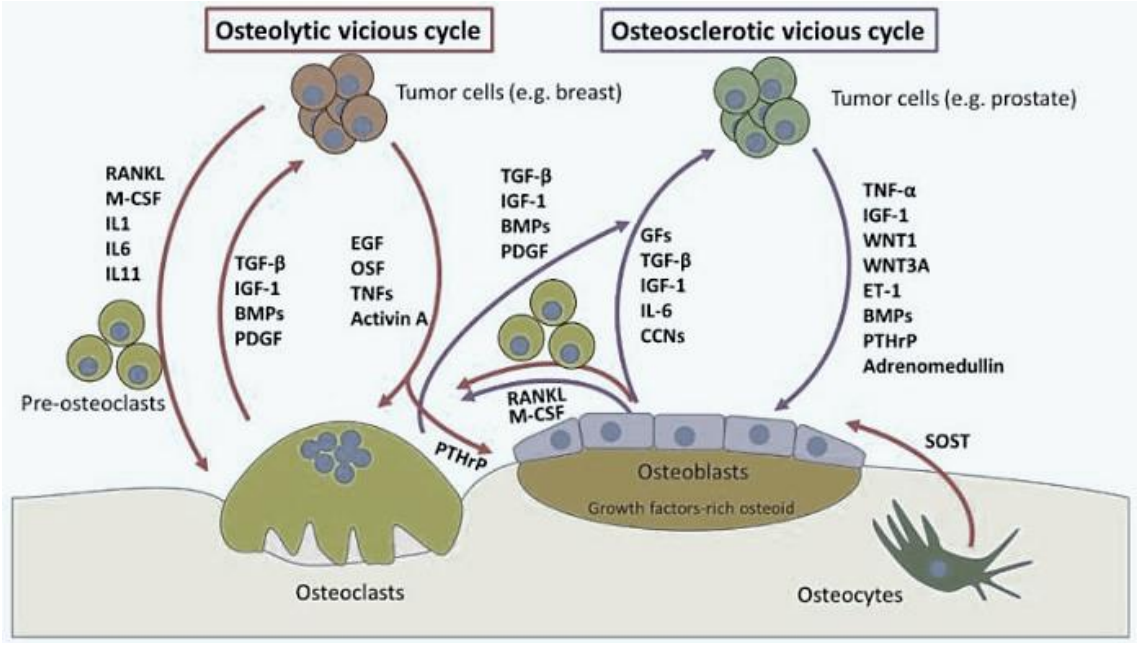

Figure 10: A schematic representation of the osteolytic and osteosclerotic vicious cycles. *The osteolytic cycle stands for any metastasising cancer cells that start to release factors that stimulate osteoclasts resulting in osteolysis (an example is breast cancer cells) upon arrival to the bone. Examples of factors that stimulate osteoclasts include epithelial growth factor (EGF), osteoclast stimulating factor (OSF), tumour necrosis factors (TNFs) and Activin A. Along with these substances, cancer cells also release factors that promote osteoclast differentiation, and these include receptor activator of nuclear factor-kB ligand (RANKL), macrophage-colony stimulating factor (M-CSF) and Interleukin (IL)-1, 6 and 11. The overall effect of these substances is the enhancement of differentiation of pre-osteoclasts into osteoclasts. The bone matrix has rich stores of growth factors (GFs) (like transforming growth factor (TGF)-β, insulin-like growth factor (IGF)-1, bone morphogenic proteins (BMPs) and platelet-derived growth factor (PDGF)). As a consequence of bone resorption, these factors are released, and they support tumour growth, so then cancer can cause more osteolysis resulting in a vicious osteolytic cycle. Osteocytes have a central role in the vicious cycle as they can secrete sclerostin (SOST) in the case of osteolytic cancers (particularly multiple myeloma). SOST has an inhibitory effect on osteoblast activity and the Wnt- β-catenin pathway. On the other hand, an osteosclerotic cycle is a cycle caused by the bone metastasis of cancer cells that generate osteosclerosis (these include prostate cancer cells). Osteosclerosis is achieved by the secretion of factors that stimulate osteoblasts by cancer cells.*

These factors include TNFα, IGF-1, Wingless-type MMTV integration site (WNT)1, WNT3A, Endothelin (ET)-1, BMPs, parathyroid hormone-related peptide (PTHrP) and adrenomedullin. The liberation of these factors results in the stimulation of osteoblast differentiation and osteoblast activity. It is worth mentioning that a secondary increased osteoclast activity accompanies the enhanced activity of osteoblasts as they release RANKL and M-CSF, which are important enhancers of osteoclastogenesis. The enhanced osteoclastogenesis results in the secretion of tumour growth–promoting factors that were mentioned in the osteolytic cycle. Not only can osteoclasts promote tumour growth, but also osteoblasts can do the same as they release an array of substances (like GFs, TGF-β, IGF-1, IL-6 and chemokines (CCNs)) that can stimulate cancer growth resulting in the closure of the vicious osteosclerotic cycle. In most cases, the vicious osteosclerotic cycle is also accompanied by osteolysis. Obtained from (Aielli et al., 2019).

2.1.4. Mechanisms of CIBP

In the microenvironment where the tumour grows in the bone, bone-innervating neurons and cancer and tumour-associated stromal cells can all contribute to CIBP through changes in bone homeostasis, structural and neurochemical reorganisation of sensory and sympathetic nerve fibres innervating bone, as well as the neurochemical reorganisation in the spinal cord. The use of animal models of CIBP has helped scientists unravel some of the mechanisms leading to this pain. Early models of CIBP relied on the administration of cancer cells into the left ventricle of mice, followed by migration of cancer cells in the general circulation to develop metastases at different tissue sites, including bone marrow (Yoneda et al., 1994). The main advantage of models relying on systemic administration of cancer cells is the replication of the clinical course of disease due to the fact that bone tumours usually develop as metastases rather than as primary tumours. However, significant disadvantages of such models include the poor predictability of metastatic sites and size, leading to insufficient reproducibility of disease progression across a cohort of animals. Another strategy is to directly administer cancer cells into the intramedullary space of a bone (e.g. the femur) in rodents (Arguello et al., 1988). The site of the injection of the cancer cells into the bone is then sealed to restrict tumour growth in the intramedullary space. In comparison to systemic administration of cancer cells,

CIBP models that involve direct injection in the bone facilitate the evaluation of tumour growth over time, radiological imaging, observation of bone degradation, examination of histopathologic changes, site-specific behavioural testing, as well as evaluation of neurochemical changes that take place at the tumour site, in DRGs and the CNS (Brown et al., 2005).

The ability to reproduce a chronic pain phenotype, as well as the cancer-induced bone remodelling, is critical to understanding the structural and neuronal mechanisms underlying CIBP (Coleman & Rubens, 1987; Mercadante & Fulfaro, 2007). In general, CIBP can be classified into two main branches, peripheral and central. The peripheral mechanisms causing CIBP can be subdivided into three main groups: acidosis, pain caused by tumour-derived products (like NGF), and neuropathic pain (Falk & Dickenson, 2014). Herein, these two mechanisms will be discussed.

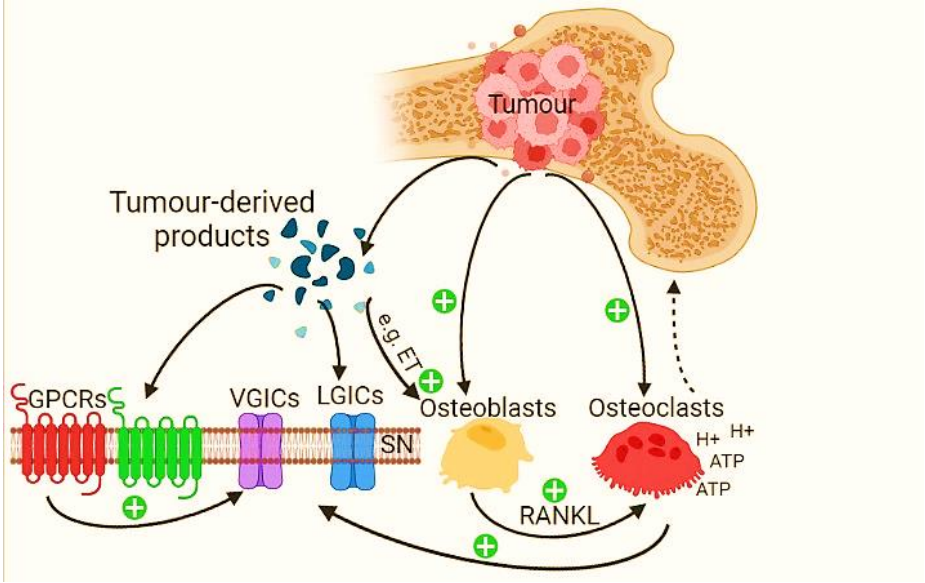

Figure 11: Cellular interactions in the bone microenvironment in CIBP. *Tumour cells release endothelin (ET), which interacts with osteoblasts via their appropriate receptors to stimulate the proliferation of osteoblasts. Activated osteoblasts release receptor activator of nuclear factor-kappa-B ligand (RANKL), which serves as a signal for osteoclast proliferation and maturation to enhance osteoclast-mediated bone matrix destruction (represented by the dashed arrow). Osteoclasts generate adenosine triphosphate (ATP) and acidosis by releasing protons, resulting in the activation of various receptors and ligand-gated ion channels (LGICs) like P2X receptors, transient receptor potential V1 receptors and acid-sensing ion channels type 3 expressed on bone innervating sensory*

neurons. Tumour cells, stromal cells and activated immune cells release a variety of mediators (such as endothelin, nerve growth factor, protons, and pro-inflammatory cytokines) that activate their respective receptors expressed on sensory neurons (SN) and thereby initiate the detection of noxious stimuli. GPCRs can sometimes indirectly sensitise various voltage-gated ion channels (VGICs) expressed on sensory neurons leading to a further potentiation of nociceptive signalling to the spinal cord. Osteolytic cancers (like breast cancer) activate osteoclasts, while osteosclerotic cancers (like prostate cancer) activate osteoblasts leading to a further potentiation of pain signal transmission.

2.1.4.1. Peripheral mechanisms of CIBP

The peripheral mechanisms of CIBP involve a long list of interacting mechanisms that can broadly be classified into three categories. The first is pain driven by acidosis. Second is pain caused by tumour-derived products. The third is the neuropathic pain originating from the peripheral nervous system. The three categories will be discussed here. See Figure 11 for a summary of some of the mechanisms involved in CIBP.

2.1.4.1.1. Acidosis

Acidosis is thought to be a key mechanism driving CIBP and is largely driven by disseminated tumour cells that dysregulate bone remodelling through osteomimicry of osteoblasts and osteoclasts (Akech et al., 2010; Andersen et al., 2007; Bellahcène et al., 2007). Many factors contribute to acidosis in bone cancer. The first cause is the Warburg effect, which is the tendency to ferment glucose to lactate, producing protons (Liberti & Locasale, 2016). In addition, cancer activates osteoclasts which in turn cause bone degradation by releasing protons to solubilise the mineralised bone matrix, liberating Ca^{2+} and phosphate ions to the bloodstream (Teti & Zallone, 2009). Upon the physiological activation of osteoclasts, the release of acids by osteoclasts during bone resorption is restricted to the bone matrix due to the tightly sealed sac called the resorption lacuna (Cappariello et al., 2014). After finishing bone resorption, osteoclasts normally release the lacunae and translocate to a close site or undergo apoptosis. However, in cancer, because the number and activity of osteoclasts increase dramatically, this tight regulation is disrupted, resulting in the leakage of protons, which might lead to the acidification of the bone marrow. Because the bone marrow is richly innervated with nociceptors possessing ASICs and TRP

channels (especially TRPV1), pain signals are generated (Nagae et al., 2007). TRPVs and ASICs are also present in the periosteum. Antagonists of TRPV1 and ASIC3 were shown to reduce CIBP (Haroun et al., 2022). A primary indicator of the important role of acidosis in CIBP is the finding that CIBP, as a result of breast cancer metastasis and multiple myeloma, was reduced by the use of vacuolar proton pump inhibitors (namely proton pump inhibitors) (Haroun et al., 2022).

2.1.4.1.2. Tumour-derived products

In addition to acidosis, several mediators released by cancer cells and their associated stromal cells contribute to CIBP. These include NGF, interleukin-1, TNFα, endothelin, PGE2 and others (Aielli et al., 2019). These mediators can contribute to CIBP both directly and indirectly. For instance, IL-1β enhances the expression of COX-2 by macrophages, which in turn amplifies prostaglandin synthesis. These prostaglandins can sensitise the primary afferent neurons by binding the prostanoid receptors expressed on terminals of bone-innervating neurons (Barrios-Rodiles & Chadee, 1998; Sabino et al., 2002). Furthermore, several factors at the site of bone metastasis, such as ROS, immune cell infiltration and activation, as well as tumour-induced cytotoxicity, result in the production of ATP following the death of bone marrow cells. When ATP is released, it binds its receptor P2X3 on sensory neurons leading to their activation and subsequent sensitisation (Aielli et al., 2019). The blockade of P2X3 receptors attenuated pain behaviours in a rat model of CIBP (Kaan et al., 2010). Herein, tumour-derived mediators like neurotrophins (such as NGF and BDNF), TNFα, Endothelins, interleukin 1- α (IL1-α), PGE2, and ATP will be discussed.

2.1.4.1.2.1. Neurotrophins

Examples of neurotrophins are NGF, BDNF, neurotrophin-3 (NT-3) and neurotrophin-4 (NT-4). Although all neurotrophins bind to p75, each one of them has its specific receptor as well. p75 is known as the low-affinity nerve growth factor receptor (LNGFR). Regarding the specific receptors, tropomyosin-related kinase (Trk)-A is the receptor for NGF, TrkB is the receptor for BDNF (as well as NT-4), and TrkC is the receptor for NT-3 (Chao, 2003). Neurotrophins bind their specific receptors with high affinity. In the bone marrow, neurotrophic tyrosine kinase receptor types 1-3 (TrkA, B and C) are located at the terminals of CGRP-positive neurons. NGF will be discussed thoroughly in section 5.1.1.1.

BDNF

NGF can increase the production of BDNF centrally, resulting in central sensitisation. Accordingly, much research now focuses on the general inhibition of Trk receptors (Thakkar & Acevedo, 2023). Interestingly, it was found that metastatic breast cancer cells and prostate cancer cells express NGF and BDNF in high levels. NGF and BDNF have several proalgesic effects that can involve the direct stimulation of nociceptors and triggering of macrophages to release TNFα, IL-6, IL-1β and PGE2 (Bruno et al., 2022; Haroun et al., 2022). The release of such inflammatory mediators can potentiate the pain responses, reinforce the vicious cycle (both types), and worsen the pain (Haroun et al., 2022).

2.1.4.1.2.2. PGE2

PGE2 is one of the products of the COX pathway. PGE2 has four main receptor subtypes; EP1, EP2, EP3 and EP4. All these receptors are GPCRs, and all of them are expressed on sensory neurons; they seem to play an important role in nociceptive signal transmission both at the peripheral level and the spinal cord level. Studies after the intraplantar injection of PGE2 suggested that PKA is crucial for the early phases of hyperalgesia, whereas PKCε is a key player in the late stages of hyperalgesia caused by PGE2 (Sachs et al., 2009). See figure 12.

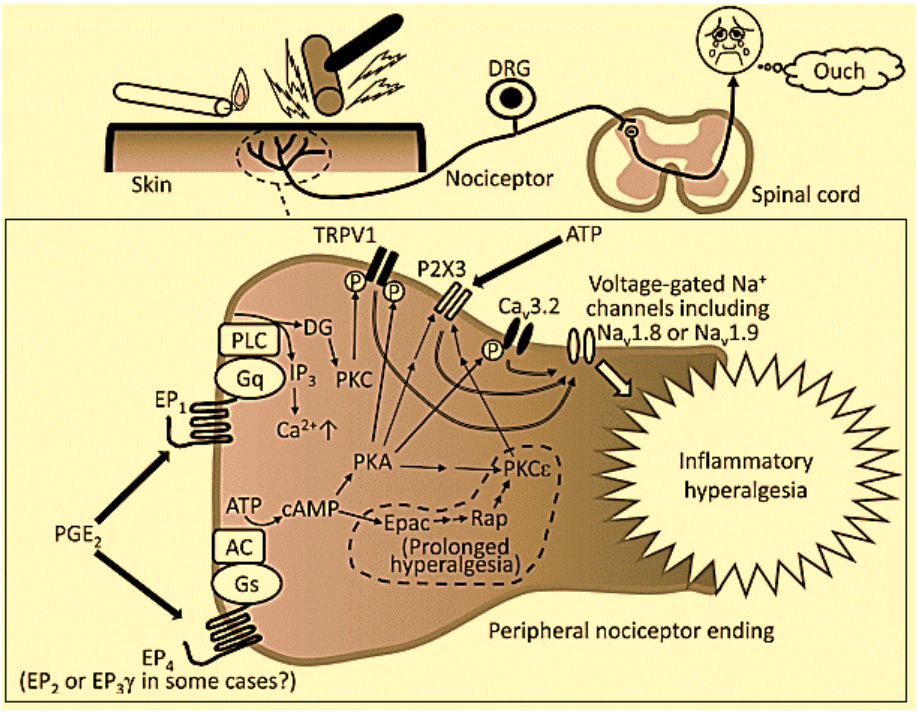

Figure 12: The suggested mechanisms for PGE2-mediated inflammatory hyperalgesia. *PGE2 has two main receptors on peripheral sensory neurons;*

EP1 and EP4 receptors. In peripheral nociceptors, the activation of EP1 by PGE2 activates Protein Kinase C (PKC), while the activation of EP4 receptors by PGE2 activates Protein Kinase A (PKA). EP1 receptors belong to the GPCR superfamily and are coupled to Gq, which activates phospholipase C (PLC), produces diacylglycerol (DG) and then activates PKC. On the other hand, EP4 receptors are coupled with Gs, which activates adenylyl cyclase (AC), which catalyses the transformation of adenosine triphosphate (ATP) into cAMP (cyclic adenosine monophosphate), which then activates PKA. In some instances, EP2 or EP3 receptors can drive PGE2-mediated PKA activation. In turn, PKA and PKC result in the sensitisation of many receptors and ion channels, like TRPV1 channels, P2X3 purinergic receptors, Cav3.2 Ca^{2+} channels and VGSCs (especially $Na_V1.8$ and $Na_V1.9$). The net effect of all these actions is inflammatory hyperalgesia. In conditions when there is prolonged inflammatory hyperalgesia, cAMP produced by AC activates EPAC, which eventually activates P2X3 via a pathway involving Rap and PKCε. Obtained from (Kawabata, 2011).

2.1.4.1.2.3. IL-1β

IL1-β is a pro-inflammatory cytokine. IL1-β has different receptors; type 1 receptor (IL-1RI) and type 2 receptor (IL-1 RII). IL-1RI is considered the most important receptor as it is the one that results in cell signalling after activation, unlike IL-1 RII. IL1-β can play roles in pain sensation both directly and indirectly. The fact that IL1-β can activate the nociceptors from the skin in less than 1 minute *in vitro* suggested that IL1-β could be having a direct effect on nociceptors (Ren & Torres, 2009). This direct effect is mediated by the activation of TRPV1, Na^+ channels, GABA receptors, and NMDA receptors (reviewed in (Schäfers & Sorkin, 2008)). Also, *in vitro*, IL1-β was shown to increase the release of CGRP from cutaneous nociceptors in rats (Oprée & Kress, 2000). One of the indirect mechanisms by which IL1-β contributes to pain sensation involves increasing the transcription of NGF (Safieh-Garabedian et al., 1995). IL1-β can also increase the release of Prostaglandin, Interleukin-6, substance P, and MMP9 (Economides et al., 2003; Inoue et al., 1999; Kawasaki et al., 2008; Samad et al., 2001).

2.1.4.1.2.4. ET-1

Endothelin-1 (ET-1) belongs to the family of endothelins, which consists of ET-1, ET-2 and ET-3 peptides. Endothelins exert their effects by acting on two types of receptors known as ET_A and ET_B. These two receptors belong to the GPCR

superfamily. ET_A is highly expressed in vascular smooth muscle cells (causing contraction). On the other hand, ET_B is primarily present in endothelial cells (it relaxes vascular smooth muscle cells) (Khodorova et al., 2009).

The effects of ET-1 on peripheral sensory neurons include the elevation of the intracellular concentration of Ca^{2+} (Figure 13) and the stimulation of PKC (Plant et al., 2007; Zhou et al., 2002). ET_B receptors are primarily expressed in DRG satellite cells and ensheathing Schwann cells (Pomonis et al., 2001), where they trigger the production and release of PGE2 (Koyama et al., 1999). Additionally, ET_B receptors are expressed on keratinocytes. The activation of ET_B receptors was shown to enhance the release of β-endorphin from keratinocytes and generate local analgesia (Khodorova et al., 2003).

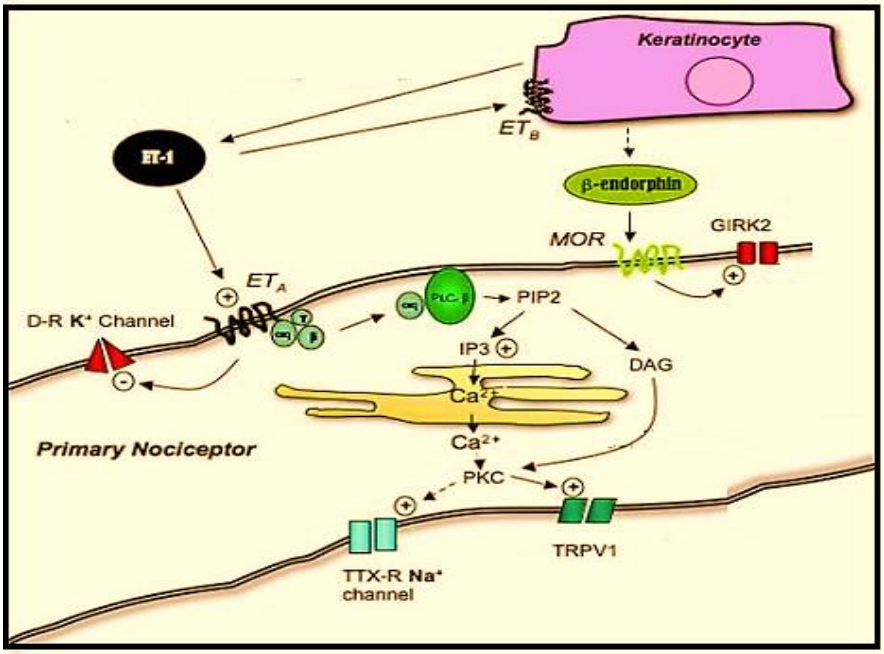

Figure 13: A cartoon depicting the effects of ET-1 on the nerve terminals of sensory neurons and epidermal keratinocytes. *When ET-1 activates ETA receptors (GPCR) expressed on sensory neurons, it modifies the activity of several ion channels. Firstly, ETA receptors inhibit delayed rectifier (D-R) type K^+ channels. Secondly, TTX-R Na^+ channels and TRPV1 channels are likely activated through protein kinase C (PKC)-mediated phosphorylation. The activation of ETA receptors by ET-1 results in the release of calcium ions (Ca^{2+}) from intracellular stores, which causes the activation of PKC (and probably PKA). ETB receptors are expressed on keratinocytes. Keratinocytes release β-endorphin as well as ET-1. β-endorphin activates μ-opiate receptors (MOR) on*

sensory neurons. The downstream effects of MOR activation include the potentiation of the currents of G protein-coupled inward rectifier K^+ channels (GIRK2). As GIRK2 causes K^+ to leave the cells, it results in hyperpolarisation, and hence the excitability of neurons is diminished (Circled + or – signs denote stimulation or inhibition, respectively). Abbreviations: PLC (phospholipase C), TTX-R (tetrodotoxin–resistant), PIP2 (phosphatidylinositol 4,5-bisphosphate), TRPV1 (transient receptor potential V1), IP3 (inositol trisphosphate). Obtained from (Khodorova et al., 2009).

2.1.4.1.2.5. ATP

ATP is one of the mediators that is generated during inflammation, and it is abundant in malignant tissues. ATP receptors are known as purinergic receptors. Purinergic receptors have two primary signalling mechanisms. The first type of receptors belongs to the GPCR superfamily (P2Y), and the second type comprises ligand-gated ion channels (P2X) (Puchałowicz et al., 2014). Under physiological settings, cutaneous nerves have significant concentrations of P2X3 receptors, whereas the periosteum and mineralised bone are nearly devoid of P2X3. This information was obtained by analysing mice femurs. In line with these findings, in a mouse model of CIBP (characterised by significant skin and skeletal hypersensitivity), inhibiting P2X3 with an antibody reduces skin hypersensitivity (as measured by the von Frey test), whereas skeletal pain-like behaviours remained mostly unchanged (Guedon et al., 2016). In contrast, it was discovered that nociceptors are positive for P2X3 in the DRG neurons that innervate the rat tibia in rat models of CIBP. In this investigation, systemic administration of the P2X3 and P2X2/3 antagonist AF-353 reduced CIBP without significantly affecting cancer-induced bone destruction. The reversal of CIBP was determined by the reversal of mechanical hypersensitivity (von Frey test) and the improvement in weight-bearing test outcomes (Tian et al., 2023).

The disparity in outcomes between these studies could be attributed to the different animal species utilised. Additionally, the variation may be attributable to the different types of bone analysed in the research projects.

2.1.4.1.3. Neuropathic pain

Multiple causes, including increased intraosseous pressure, sprouting, and nerve damage, contribute to the neuropathic pain component of CIBP. Numerous preclinical models of neuropathic pain have indicated that nerve compression can

result in pain (Austin et al., 2012; Yalcin et al., 2014). In addition, CIBP is characterised by the sprouting of sensory and sympathetic fibres, and it is thought that NGF plays a role in this nerve sprouting, as many preclinical models showed that ectopic sprouting and neuroma formation were prevented upon blocking NGF (Jimenez-Andrade et al., 2011). Moreover, analyses of biomarkers at the level of the DRGs indicate that markers of neuropathic pain/ nerve injury are detected. These biomarkers include activating transcription factor 3 (ATF3). Furthermore, macrophage infiltration is also detected at the level of the DRGs in rodent models of CIBP, an observation that characterises neuropathic pain models (Peters et al., 2005). These similarities between CIBP and neuropathic models suggest that CIBP has a neuropathic pain element. This section focuses on the neuropathic element of CIBP.

2.1.4.1.3.1. Pressure

The increase in the intraosseous pressure could contribute to CIBP. Several preclinical models of neuropathic pain have demonstrated that pressing the nerves can cause pain. Most of the pressure-based neuropathic models rely on either cuffing or partially compressing nerve bundles. For instance, in animal models, spinal cord compression generates mechanical hyperalgesia in the front and hind limbs (Yu et al., 2013), and spinal cord compression occurs in about 5% of patients with metastatic cancer, mainly presenting as back pain (Cole & Patchell, 2008). The increase in the intraosseous pressure is sensed by mechanoreceptors (Nencini & Ivanusic, 2017) and mechanotransducing osteocytes, leading to pain signal generation. One of the suggested mechano-transducing ion channels is Piezo2. Significant data suggest that Piezo2 aids in the transduction of low-threshold mechanical stimuli (Florez-Paz et al., 2016; Ikeda et al., 2014; Ikeda & Gu, 2014; Ranade, Woo, Dubin, Moshourab, Wetzel, Petrus, Mathur, Bégay, Coste, Mainquist, et al., 2014; Woo et al., 2015; Woo et al., 2014). In addition, emerging pieces of evidence highlight the role of Piezo2 channels as transducers of noxious mechanical stimuli. The currents generated by Piezo2 are potentiated by bradykinin, which is often thought to drive inflammation-induced mechanical hypersensitivity (Dubin et al., 2012). Furthermore, mouse studies indicate that knocking Piezo2 down in the DRG neurons alleviates the mechanical hypersensitivity that results from skin inflammation but leaves thermal hypersensitivity unaffected (Singhmar et al.,

2016). Similarly, in rats, when Piezo2 is knocked down in the DRG neurons, the visceromotor pain reflexes resulting from both noxious and innocuous distensions of the colo-rectum were attenuated (Yang et al., 2016). In the cornea, Piezo2 channels are expressed in myelinated, small-diameter Aδ nociceptors, and it is thought that these channels potentially act as mechanical stimuli transducers in the cornea (Alamri et al., 2015; Bron et al., 2014). About 70% of small-diameter myelinated Aδ nociceptors in the bone marrow are positive for Piezo2 (Nencini & Ivanusic, 2017). Therefore, it is suggested that the role of Piezo2 in the bone marrow could also be mechanical stimuli transduction. Electrophysiological studies investigating the afferents that are activated upon the increase in intraosseous pressure identify Aδ nociceptors innervating the bone marrow as key players in sensing noxious mechanical stimuli. In addition, it was shown that responsive afferents express Piezo2 and this could highlight the role of Piezo2 in the transduction of pain signals in diseases that are characterised by high intraosseous pressure (Nencini & Ivanusic, 2017).

In a study using a rat model of CIBP, it was suggested that CIBP recruits the normally silent nociceptive C-fibres. In addition, it was demonstrated that bone afferents work similarly in healthy and CIBP rats. Interestingly, the majority of cells that respond to knee compression in CIBP mice were reported to be “silent” muscle afferents. The technique used to identify these activated neurons was GFP Calmodulin M13 protein 6s (GCaMP6s) imaging. In addition, it was shown that pharmacologically inhibiting Piezo2 decreases the numbers of recruited and activated neurons in response to knee compression (Kucharczyk et al., 2020). These findings do not rule out the participation of bone afferents, and numerous reasons could be postulated. Firstly, the mechanical pressure in this experiment was administered from outside the bone and not from the inside. Secondly, the activation of the bone afferents may require greater pressure than that required to stimulate the nerves in the cutaneous tissues. Therefore, additional research is required to clarify the role of bone marrow sensory neurons in CIBP.

Aside from sensory neurons, another contributing factor to the intraosseous pressure sensation is the mechanotransducing osteocytes. These osteocytes eventually result in bone degradation via mechanisms involving CCL5 and matrix metalloproteinases. As a consequence of the liberated growth factors during

bone degradation, tumour growth is enhanced, eventually leading to more pain (Haroun et al., 2022).

2.1.4.1.3.2. Sprouting and nerve injury

Animal models of CIBP suggest that NGF produced by cancer cells and the stromal cells could be a key factor resulting in the ectopic sprouting of sensory and sympathetic neurons. It was shown that even when cancer cells are unable to produce NGF, ectopic sprouting was still evident, suggesting the important role of the NGF derived from stromal cells. The requirement of NGF-TrkA signalling in bone-innervating neurons for endochondral ossification and vascularisation, as well as bone formation upon mechanical loading, is well established (Tomlinson et al., 2017; Tomlinson et al., 2016). In preclinical models of CIBP, prophylactic antibody-based blocking of NGF prevents ectopic sprouting and neuroma formation (Jimenez-Andrade et al., 2011). It is suggested that even the late blockade of NGF is beneficial in reducing neuromas (Mantyh, 2013) as well as the skeletal and cutaneous pain caused by CIBP (Guedon et al., 2016). In humans, increased innervation density is also observed at sites of active bone remodelling, supporting the importance of neural regulation of skeletal remodelling and pain (Sayilekshmy et al., 2019). More investigations are needed to fully elucidate how neuronal sprouting contributes to hyperalgesia, but one possible explanation could be the accumulation of Na^+ channels at the injured nerve terminals and subsequently causing hyperexcitability and spontaneous firing of these neurons.

2.1.4.2. Central mechanisms of CIBP

At the level of the spinal cord, CIBP modulates synaptic plasticity between the peripheral neurons and second-order neurons, as observed through increased neuronal excitability measured with elevated expression of c-Fos, the internalisation of substance P, the rise in the expression of dynorphin (a pro-nociceptive opioid) and a significant activation and elevation in astrocytes and microglia (Schwei et al., 1999; Yanagisawa et al., 2010). In addition, CIBP has been shown to increase the proportion of the wide dynamic range to nociceptive-specific neurons in the superficial laminae of the dorsal horn in rats (Urch et al., 2003). It was reported that gabapentin can re-establish the typical ratio of wide dynamic range neurons to nociceptive-specific neurons, but long-term use of morphine maintains allodynia and fails to correct the pathophysiological

phenotype of superficial dorsal horn neurons (Urch et al., 2005). Descending modulatory circuits also regulate spinal excitability in CIBP; 5-HT_3 receptor antagonists can diminish the hyperexcitability of lamina I neurons in rodents with CIBP through the blockade of a descending serotonergic facilitatory drive (Donovan-Rodriguez et al., 2006). Other studies report an important role for amplified excitatory neurotransmission that may underlie enhanced spinal cord plasticity in CIBP; spinal glial cells secrete IL-1 that causes hyperalgesia by phosphorylating the NR1 subunit of NMDA receptors (Zhang et al., 2008). Moreover, spinal NR2B expression is increased in CIBP, and its specific inhibition prevents the induction of mechanical and thermal hypersensitivity (Gu et al., 2010). Due to the hypertrophy of astrocytes and the subsequent decline in glutamate reuptake transporters, glutamate concentrations are also elevated in CIBP, which leads to excitotoxicity (Sattler & Tymianski, 2001). Mice with CIBP also exhibit elevated amounts of dynorphin in the dorsal horn (Schwei et al., 1999), which causes long-lasting pain by activating NMDA receptors instead of opioid receptors (Vanderah et al., 1996).

2.2. Aims

A mouse model that involved the injection of Lewis Lung Carcinoma cells into the intramedullary space of the femur of C57BL/6 mice or transgenic mice in the C57BL/6 background was characterised and optimised to serve as a model of CIBP. The characterisation of the model involved the assessment of the skeletal events and whether signs of secondary cutaneous hyperalgesia manifested. The optimization of this model entailed the selection of an optimal number of cancer cells needed to provide robust pain-like behaviour while allowing enough time to assess analgesics.

2.3. Methods

2.3.1. Cell culture

Lewis lung carcinoma (LL/2) cells (from American Type Culture Collection (ATCC)) were cultured in a medium containing 90% Dulbecco's Modified Eagle Medium (DMEM) and 10% foetal bovine serum (FBS) and 0.1% Penicillin/Streptomycin for 14 days before the surgery. DMEM is supplemented with L-glutamine (1%) and glucose (4.5 g/litre). The cells were sub-cultured whenever ~80% confluency was reached, which was done a day before the surgery. On the surgery day, LL/2 cells were harvested by scraping and were

centrifuged at a speed of 1500 rpm for two mins. The supernatant was removed, and the cells were resuspended in a culture medium that contains DMEM to attain various final concentrations: ~2x10^7 cells/ml, 2x10^6 cells/ml, or 2x10^5 cells/ml for the CIBP model optimisation experiments and ~2x10^6 cells/ml for all the remaining studies. The cell counting and viability check were done using the Countess automated cell counter (Thermo Fisher Scientific).

2.3.2. Mice

Mice (males and females) were housed in groups of 2–5 per cage with a 12-hour light/dark cycle and were allowed free access to water and a standard diet. Mice were acclimatised for two weeks before the surgery, and the baseline measurements were taken at the end of these two weeks. All experiments were performed with the approval of personal and project licenses from the United Kingdom Home Office according to guidelines set by the Animals (Scientific Procedures) Act 1986 Amendment Regulations 2012 and guidelines of the Committee for Research and Ethical Issues of IASP.

2.3.3. Surgery

Surgery was carried out on anaesthetised mice. Anaesthesia was achieved using 2-3% isoflurane. The knee area and its surroundings were shaved in both legs of each mouse undergoing surgery, and the shaved area was cleaned using hibiscrub solution. A sterile lacri-lube was applied to the eyes. The reflexes of the mice to pinches in the hind paws were checked to ensure successful anaesthesia. An incision was made in the skin above and lateral to the patella on the left leg. The patella and the lateral retinaculum tendons were loosened to move the patella to the side and expose the distal femoral epiphysis. A 30G needle was used to drill a hole through the femur to permit access to the intramedullary space of the femur. The 30G needle was removed, and a 0.3ml insulin syringe was used to inoculate ~2x10^4 LL/2 cells suspended in DMEM (for the optimisation studies, a range of LL/2 cell numbers was tested). The hole in the distal femur was sealed using bone wax (Johnson & Johnson). To ensure that there was no bleeding, the wound was washed with sterile normal saline. Following that, the patella was re-placed into its original location, and the skin was sutured using 6–0 absorbable vicryl rapid (Ethicon). Lidocaine was applied at the surgery site, and the animals were placed in the recovery chamber and monitored until they recovered.

In all the studies, male and female C57BL/6 mice (or transgenic mice in C57BL/6 background) were used. G power analyses were not done prior to determining the number of mice to include in this study. The choice of the animal number was based on previous experience from animal experiments in our lab.

2.3.4. Behavioural tests

After the surgery, the limb-use score of the mice was checked daily. Any score less than four on the sixth day after the surgery caused the mouse to be sacrificed and excluded from the study. This rule ensured that the observed pain phenotype was only due to the cancer growth and not a complication from the surgery.

2.3.4.1. Limb-use score

The mice housed in the same cage were placed together in a glass box (30 × 45 cm) for at least five minutes. Then each mouse was left in the glass box on its own and was observed for ~4 minutes, and the use of the ipsilateral limb was estimated using the standard limb use scoring system in which: 4 indicates a normal use of the affected limb; 3 denotes slight limping (slight preferential use of the contralateral limb when rearing); 2 indicates clear limping; 1 clear limping, and with a tendency of not using the affected limb; and 0 means there is no use of the affected limb. Reaching a limb-use score of zero was used as an endpoint for the experiment.

2.3.4.2. Static weight-bearing

The scale used for this behavioural test was the Incapacitance Metre (Linton Instrumentation), which has two scales to assess the weight put on each limb. The weight placed on each limb is measured for 3 seconds. The readings for the weight put on the limbs were recorded three times for each mouse, and between the readings, mice were allowed to re-place themselves into the tube. The fraction of the weight put on the ipsilateral paw was determined by the summation of all three readings of the weight put on the ipsilateral paw divided by the summation of all the weight measurements on both paws.

2.3.4.3. Hargreaves' test

The Hargreaves' test was used to measure secondary cutaneous heat hyperalgesia and was performed as previously described by (Hargreaves et al., 1988). In plexiglass containers with a glass base, mice were acclimated for an hour. The chambers were cleansed of urine and faeces prior to testing. Following

that, and until the animal displayed a nocifensive withdrawal reaction, radiant heat was locally administered to the plantar surface of the hind paw. The test was applied three times, and a 15-minute gap was left between each trial. Following that, the average latency was calculated for each mouse. The cut-off duration for the application of radiant heat was 30 seconds.

2.3.4.4. The "up-down" von Frey

The "up-down" von Frey was carried out as described by (Deuis et al., 2017). In this test, secondary cutaneous mechanical sensitivity in the hind paw was assessed by evaluating a 50% withdrawal threshold. Mice were habituated for one hour in darkened enclosures with a wire mesh floor. At the beginning of the test, a certain von Frey filament was applied for three seconds. The application of that filament to the surface of the hind paw resulted in the application of 0.4 grams of weight. In the subsequent trial, a weaker filament was applied if the response was positive, and a stronger filament was applied if the response was negative. To estimate the 50% withdrawal threshold, five filament application trials were done following the first switch in response (from no response to a positive response or vice versa). The formula utilised to estimate the 50% withdrawal threshold was $(10[\chi+\kappa\delta])/10{,}000)$. In this formula, χ represents the log of the last von Frey filament used, δ represents the average variation between filaments used in log units, and κ is a tabular value for the pattern of the responses.

2.3.4.5. The dry ice test

The dry ice test protocol can be found in (Brenner et al., 2012). For this test, dry ice was crushed with a hammer. A 2.5 mL syringe had its top cut off to create the probe's shape. The modified syringe was filled with dry ice powder, and the open end was placed against a smooth surface while pressure was applied to the plunger to flatten the powder into a dense, 1 cm-in-diameter pellet. To evaluate the withdrawal threshold, the end of the syringe was pressed to the glass beneath the hind paw. The distal joints were avoided, and the centre of the hind paw was targeted, making sure that the paw itself was truly touching the glass surface. A stopwatch was used to measure the time taken until the withdrawal. The cut-off point for this point was 30 seconds.

2.3.4.6. Analysis of the median time needed to reach limb-use score zero

The time needed for a mouse to reach zero limb-use score was considered an endpoint, and any mouse that reached this score was sacrificed. Therefore, the time needed to reach this score is considered an indirect pain measure. It is important to note that mice were also sacrificed if the tumour caused the mice to lose 15% of their body weight measured from the day of the surgery.

2.3.5. Micro-computed tomography (µCT)

After each mouse was sacrificed, its femurs, both ipsilateral and contralateral, were dissected. Femurs were then fixed using a 4% paraformaldehyde (PFA) solution for 24 hours. Then, PFA was removed, and femurs were washed using phosphate-buffered saline (PBS). Femurs were then kept in 70% ethanol (v/v) at 4°C until scanned using µCT.

2.3.6. Statistical analyses

The mixed-effects model (RMEL) or the two-way analysis of variance (ANOVA) was used with multiple comparisons to compare the pain-like behaviour between two groups over time. The RMEL was used when data points were missing, followed by posthoc analyses. In all statistical tests, the difference between groups is considered significant when the p-value is <0.05. All statistical analyses were performed using GraphPad Prism 9. Data are presented as mean ± standard error of the mean (SEM). For comparing the time needed to reach limb-use score zero, the Log-rank (Mantel-Cox) and the Gehan-Breslow-Wilcoxon tests were used, and the median duration to reach this limb-use score was compared between groups. Dunnett's test for multiple comparisons was used to compare the mean results after the surgery with the baseline readings. To compare any two groups, the normality of the distribution of the data was tested first using the D'Agostino & Pearson test. Then the t-test was performed when the samples passed the D'Agostino & Pearson test. Statistical significance is expressed as: *p < .05; **p < .01; ***p < .001, ****p < .0001.

2.4. Results

2.4.1. The characterisation of secondary hyperalgesia in the CIBP model

In our lab, a mouse model of CIBP that involves the injection of approximately $2x10^5$ LL/2 cells into the intramedullary space of the femur of C57BL/6 mice was

being used. Mice injected with LL/2 cells were compared to the sham mice that underwent the whole surgery except for the inoculation of the cancer cells. Compared to the sham mice, the cancer group experienced a reduction in the limb-use score and the weight-borne on the ipsilateral paw (Figure 14). The aim here was to test whether forms of secondary cutaneous hyperalgesia can be observed in this model. For this, I conducted the Hargreaves', the dry ice, and the von Frey tests on the paw. These tests were done for both the ipsilateral and the contralateral paws. The time points for conducting these secondary hyperalgesia tests were determined according to the limb-use score. Therefore, these tests were conducted when mice reached limb-use score 3 (mild pain) and limb-use score 1 (severe pain). It is important to note that the von Frey test was not done at limb-use score 3. Results from this study indicated that at advanced stages of the disease (limb-use score 1), significant secondary cutaneous hyperalgesia was seen in the ipsilateral paw but not the contralateral paw, as demonstrated by the reduction in the withdrawal thresholds in the three tests (the Hargreaves' test (Figure 15), the dry ice test (Figure 16), and the von Frey test (Figure 17)).

Mice were followed up until they reached limb-use score zero, and that was considered the humane endpoint for this experiment. Results indicated that the median number of days to reach this limb-use score for the cancer mice was 18 days after the surgery (Figure 18, green).

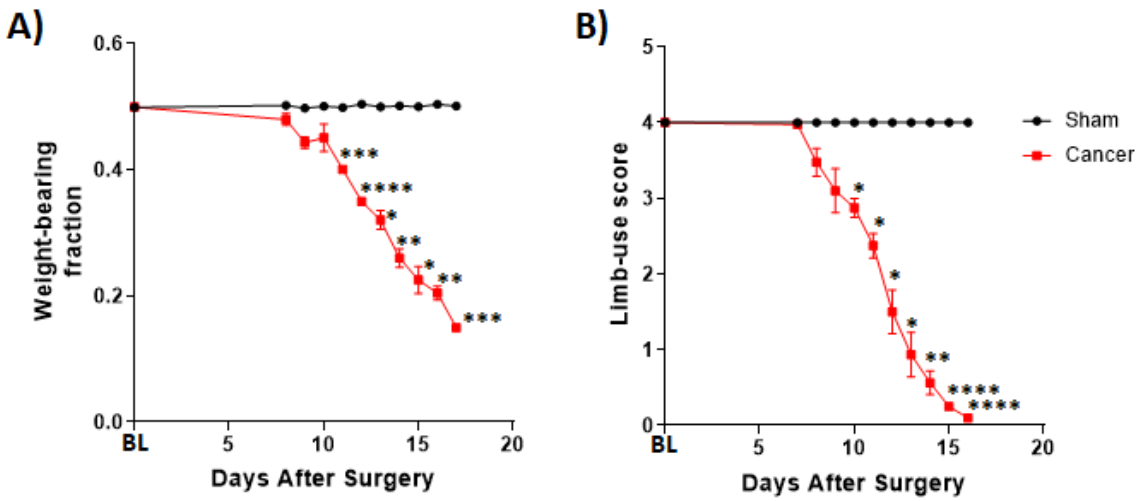

Figure 14: CIBP is associated with a reduction of the weight-borne on the affected limb (A) and its use score (B). *N=5 in the sham group and 4 in the cancer group at the baseline as one mouse was excluded from the cancer group*

because it did not recover fully from surgery. Error bars represent the SEM. The RMEL model indicates that the cancer group has significantly lower limb-use and weight-bearing scores than the sham group over time (p-value <0.0001 in both tests). All mice included in this study were males. The asterisks of significance shown in the figure represent the post hoc analysis results comparing the two groups at each time point.

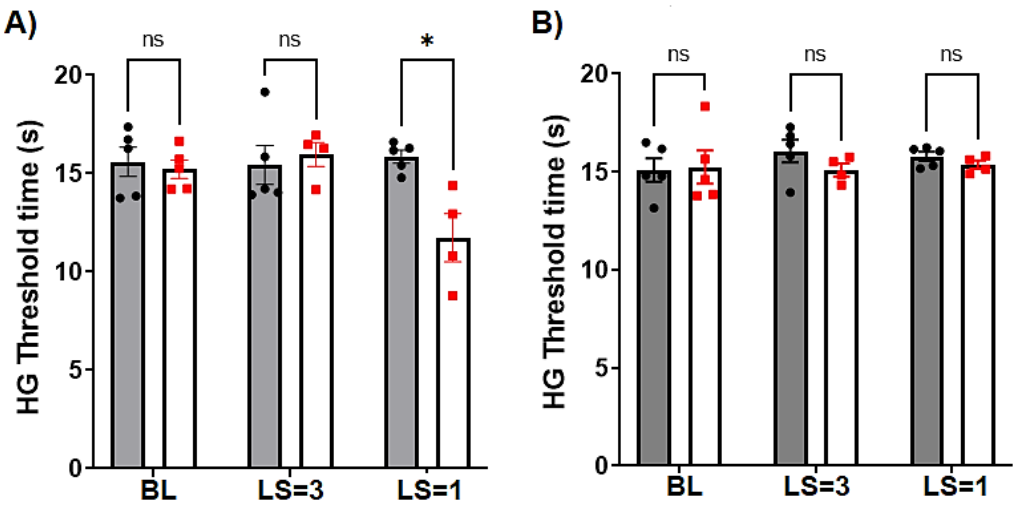

Figure 15: The Hargreaves' test in the paw after the CIBP model involving the intrafemoral inoculation of cancer cells to C57BL/6 mice. *Figure A) shows the results obtained from the ipsilateral paw, while Figure B shows the contralateral paw results. Data indicates that the cancer-bearing mice develop significant secondary heat hyperalgesia at advanced stages of the disease (LS=1), and this hyperalgesia is only detectable in the ipsilateral paw and not the contralateral paw. LS: limb-use score. Statistical analyses were done using the multiple t-tests using GraphPad Prism 9. N=5 at the baseline and n=4 after the surgery because one mouse did not recover from the surgery. All mice included in this study were males.*

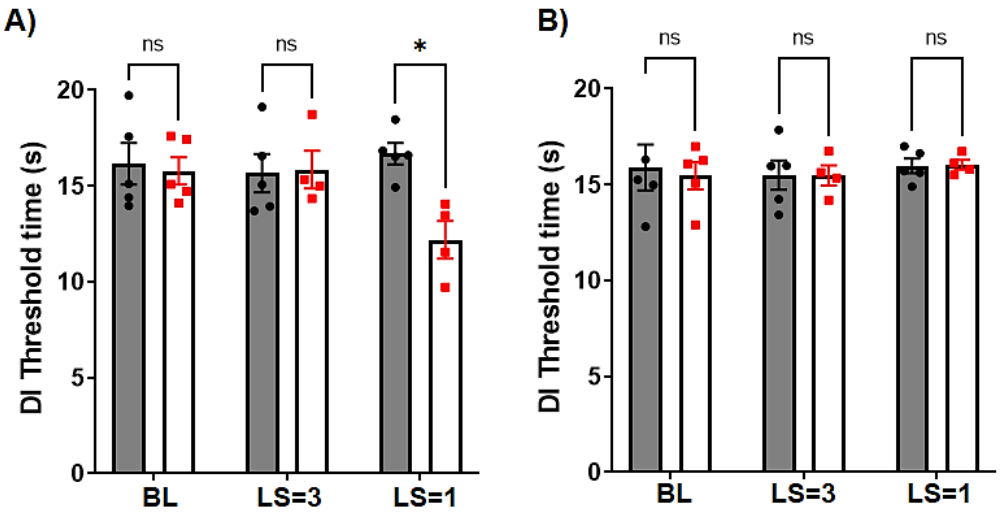

Figure 16: The dry ice test in the paw following the CIBP model in the femur of C57BL/6 mice. *Figure A) shows the results obtained from the ipsilateral paw, while Figure B shows the contralateral paw results. Data indicates that the cancer mice develop significant secondary cold sensitivity at advanced stages of the disease (LS=1), and this hyperalgesia is only detectable in the ipsilateral paw and not the contralateral paw. LS: limb-use score, DI: dry ice. Statistical analyses were done using the multiple t-tests using GraphPad Prism 9. N=5 at the baseline and n=4 after the surgery because one mouse did not recover from the surgery. All mice included in this study were males.*

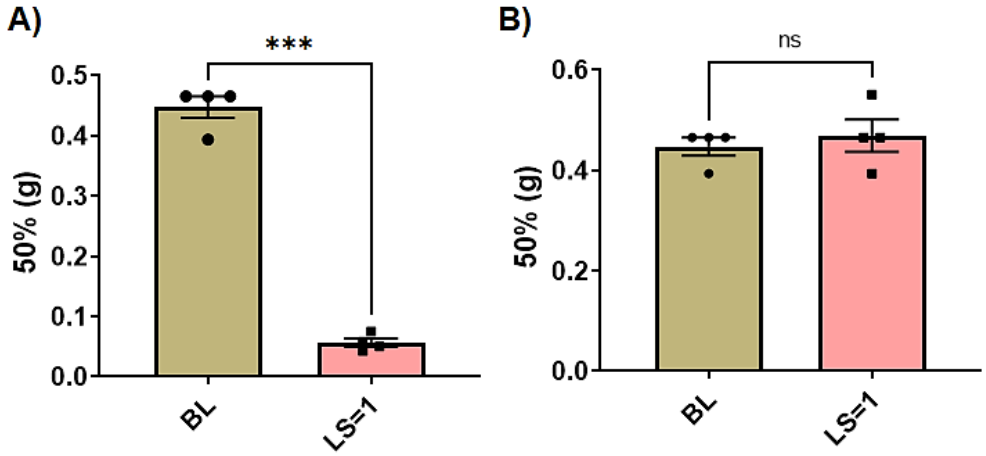

Figure 17: The up-down von Frey test results following the CIBP model in C57BL/6 mice. *Figure A) shows the results obtained from the ipsilateral paw, while Figure B shows the contralateral paw results. Data indicates that mice develop a significant mechanical sensitivity in the ipsilateral paw after inoculating cancer cells in the femur and reaching a limb-use score of one. The contralateral paw remains unaffected. Error bars represent SEM. Statistical analyses were*

done using the paired t-test using GraphPad Prism 9. N=5 at the baseline and n=4 after the surgery because one mouse did not recover from the surgery. All mice included in this study were males.

2.4.2. The optimisation of the CIBP model

Because the median time needed to reach limb-use score zero after the CIBP model that involves the injection of $2x10^5$ LL/2 cells in the intramedullary space of the femur was short (less than 20 days), I attempted to reduce the number of LL/2 cells injected to increase the time needed to reach limb-use score zero and slow down the pain phenotype progression in an attempt to make a model that is more translational of chronic pain conditions. Therefore, two lesser cancer cell numbers were attempted, $2x10^4$ (black, Figure 18) and $2x10^3$ (red, Figure 18), and they were compared to the original cancer cell number (green, figure 18). The reduction of the number of cancer cells injected significantly increased the median time needed to reach limb-use score zero (Figure 18) and showed a dose-dependent reduction in pain phenotype intensity (Figure 19). By referring to the weight-bearing results, it appears that the mean weight-bearing becomes significantly lower than the baseline readings after nine days for the $2x10^5$ cells group (Figure 14A), 13 days for the $2x10^4$ cells group, and 20 days for the $2x10^3$ cells group (Figure 19A). For the $2x10^5$ cells group, the study ended after 18 days post-surgery, which indicated that there was a pain window of 10 days. For the $2x10^4$ cells group, the study ended on the 31st day after the surgery, leaving a pain window of 19 days. For the $2x10^3$ cells group, two mice were still alive at the end of the study, which gives a pain window of more than 21 days, as the study needed to end 40 days after the surgery to satisfy the maximum time permitted by the project licence. The limb-use scoring data indicates that the pain window is nine days for the $2x10^5$ cells group (Figure 14B), 21 days for the $2x10^4$ cells group, and > 23 days for the $2x10^3$ cells group (Figure 19B).

Because decreasing the number of cancer cells injected slowed the speed of the pain phenotype progression, I decided to reduce the number of cancer cells in our subsequent experiments. Between the two lesser cancer cell numbers ($2x10^4$ and $2x10^3$ cells), the use of $2x10^4$ cells resulted in a model that showed no detectable variability between male and female mice (Figure 20); hence, it was selected to be used for the following experiments. µ-CT analyses indicated that

injecting 2x10^4 LL/2 cells into the intramedullary space of the femur of C57BL/6 mice caused a clear bone degradation (Figure 21).

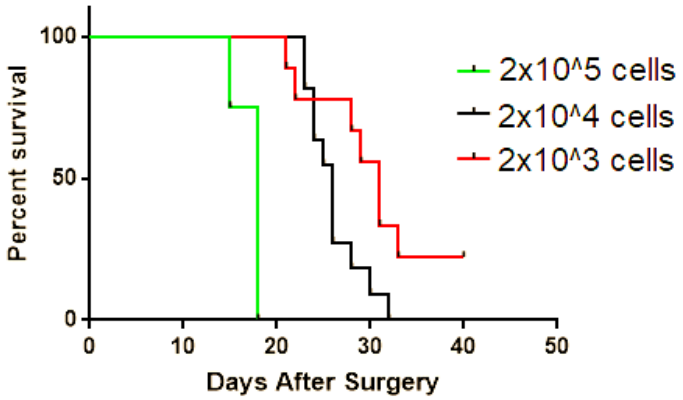

Figure 18: In the CIBP model, the median time needed to reach limb-use score zero of C57BL/6 mice significantly increases as the injected cancer cell number decreases. *After using 2x10^5 cancer cells, the median duration was 18 days after the surgery (n=4, males, green). When the number of cancer cells is reduced to 2x10^4, the median time became 26 days after the surgery (n=11, 5 females and 6 males, black). After the injection of 2x10^3 cancer cells, the median duration was 31 days after the surgery (n=9, 4 females and 5 males, red). The median time needed to reach limb-use score zero in the 2x10^4 cancer cells group was significantly longer compared to the 2x10^5 group (p-value <0.0001). Also, the 2x10^3 cancer cells group spent a significantly longer time to reach limb-use score zero compared to the 2x10^5 group (p-value 0.0003). Similarly, the increase in median time needed to reach limb-use score zero in the 2x10^3 group was significant compared to the 2x10^4 group (p-value <0.05). The analyses were conducted using Log-rank (Mantel-Cox) test and the Gehan-Breslow-Wilcoxon test. Before analysis, one mouse was excluded from each group because of recovery issues.*

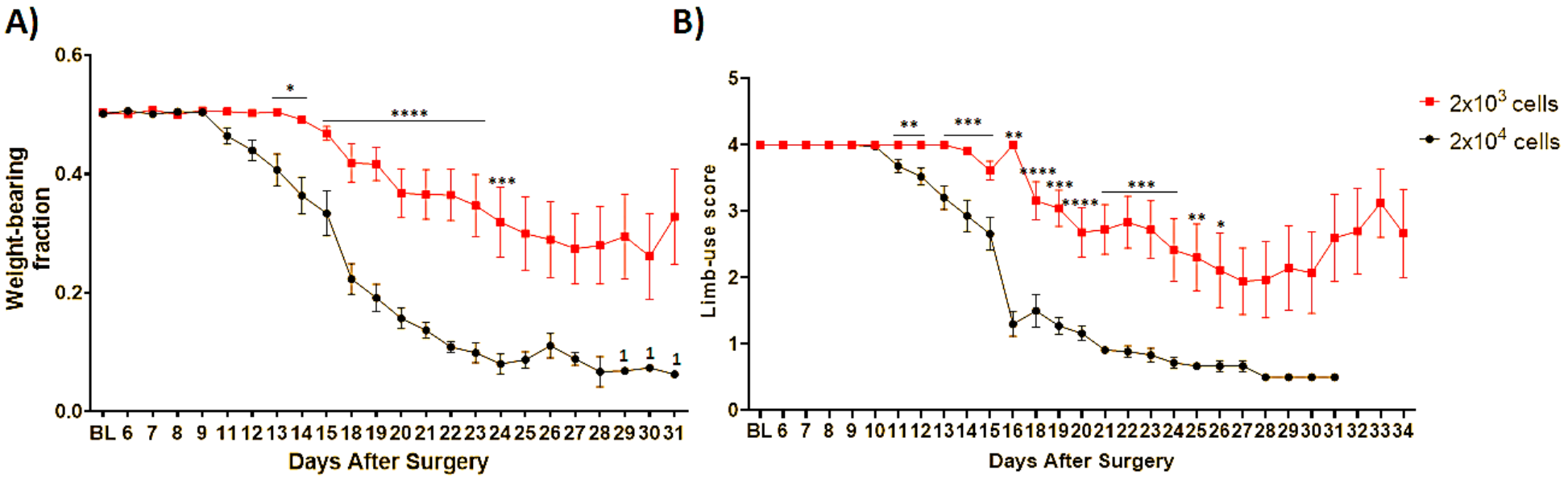

Figure 19: The injection of LL/2 cells into the intramedullary space of the femur of mice caused a significant decline in the weight-borne on the ipsilateral limb (A) and the limb-use score (B), and this decline was dependent on the number of LL/2 cells injected. *(A) The reduction in the weight-bearing became significant (compared to the baseline) on day 13 after the surgery (p-value 0.0048) in the mice that received 2x10^4 cells and after 20 days in the mice that received 2x10^3 cancer cells (p-value 0.0067). Compared to the 2x10^4 group, the 2x10^3 group had a considerably better weight-bearing performance from day 14 after surgery through the completion of the study. (B) The mean limb-use score for the 2x10^4 cancer cells group became significantly lower than the baseline on day 12 (p-value 0.0002). In contrast, it became significantly less than the baseline on day 18 (p-value 0.0384) for the 2x10^3 cancer cells group. The analysis of the weight-bearing results showed that the effect of the cancer cells is statistically significant (p value< 0.0001), with the 2x10^3 group showing higher weight-bearing results than the 2x10^4 group (the mixed-effects model). The comparison of the limb-use score results*

between the $2x10^3$ cells and the $2x10^4$ cells groups (the mixed effects model analysis) showed that reducing the injected cancer cells number improved the limb-use score (p value= 0.0004). At the baselines, n=11 for the $2x10^4$ group and 9 for the $2x10^3$ group (equal mix of sexes). One-way ANOVA (followed by Dunnett's test for multiple comparisons) was used to estimate the time required to cause a significant drop in either the weight-bearing or the limb-use score compared to the baseline after inoculating a specific number of cancer cells in the femur. To compare the two groups at every time point, multiple t-tests were used (indicated by the significance shown in the figure).

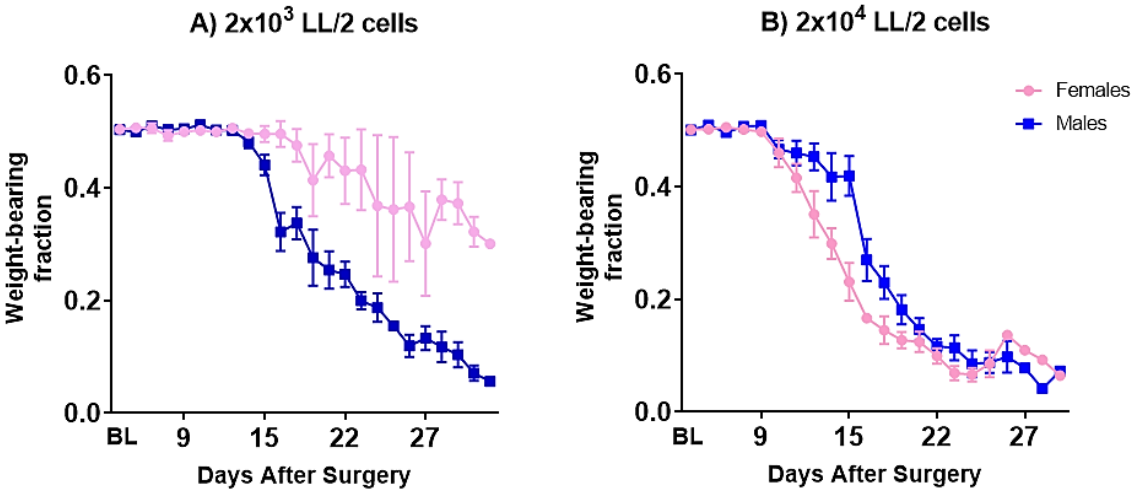

Figure 20: Sex difference in pain-like behaviour was seen after using $2x10^3$ LL/2 cells in the CIBP model (A) but not when $2x10^4$ cells were used (B). *Male and female mice that received the same number of LL/2 cells were compared in their average weight-bearing scores. There was no significant difference between males and females in the group of mice that received $2x10^4$ cells (n=11, (five females and six males)) (p value=0.1219). In contrast, a significant sex difference was seen in the weight-bearing results in the mice that received $2x10^3$ LL/2 cells, with the females showing a significantly milder reduction in the weight-borne on the ipsilateral limb compared to males (n=9, four females and five males) (p-value= 0.0010). The analysis was conducted using the mixed-effects model.*

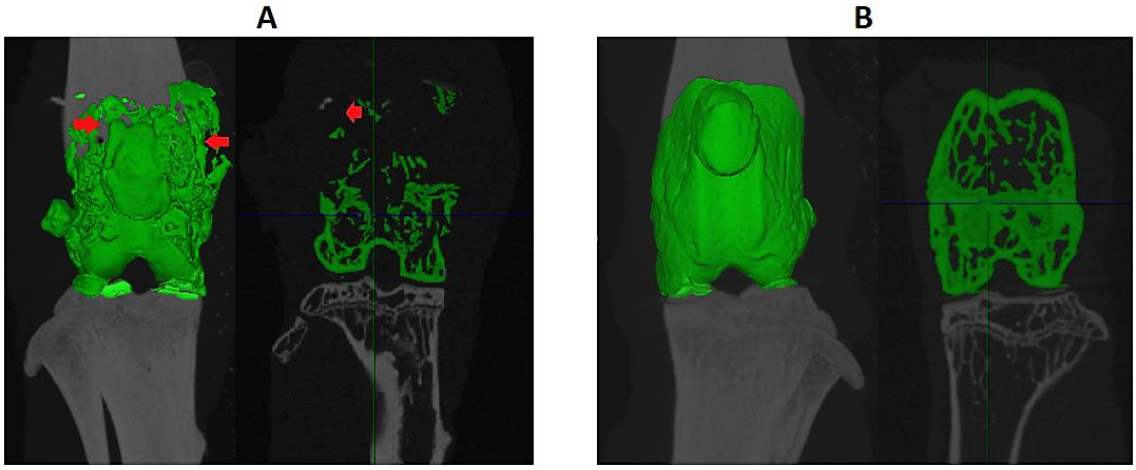

Figure 21: µ-CT imaging showing osteolysis induced by the growth of LL/2 cells in the femurs of C57BL/6 mice. *The tumour growth causes bone degradation in the ipsilateral femur (A), leaving the contralateral femur (B) unaffected. The red arrows in figure A point towards some areas with clear osteolysis (lack of green colour).*

2.5. Discussion

2.5.1. CIBP is associated with enhanced cutaneous sensitivity to heat, cold and mechanical stimulation

The presence of secondary cutaneous hypersensitivity was assessed in a mouse model of CIBP that involves the injection of $2x10^5$ LL/2 cells into the intramedullary space of the femur. With the progression in pain phenotype, there had been an increase in the cutaneous sensitivity in the ipsilateral paw. This had been demonstrated by the reduction in the withdrawal thresholds in the Hargreaves' test, the dry ice test and the von Frey test. This hypersensitivity can be attributed to many factors, including the phosphorylation of voltage and ligand-gated ion channels as a result of the mediators released by the cancer cells and their associated stromal cells.

2.5.2. Sex difference in pain-like behaviour in CIBP

To select an optimal number of cancer cells to be used in our mouse model of CIBP, different quantities of cancer cells were attempted. The fact that men and women could experience pain differently in severity is another intriguing aspect of this research. This is demonstrated by the fact the injection of $2x10^3$ LL/2 cells leads to a significantly milder pain-like behaviour in female mice compared to male mice. While this outcome was consistent with earlier research, which revealed that men experienced more severe post-operative pain than females

(Chia et al., 2002), there are discrepancies with this finding because one study found that women have more severe cancer pain than men (Bartley & Fillingim, 2013) and another found no gender differences in most symptom presentations, the reported outcomes, and radiation response in cancer patients with bone metastases receiving palliative radiotherapy (Chow et al., 2017).

Because clinical data do not highlight striking gender differences in pain among cancer patients, I decided to use $2x10^4$ LL2 cells in all of our subsequent studies because this number of cells did not result in a noticeable sex difference.

2.6. Conclusion

A mouse model of CIBP was optimised. This model involves the injection of ~$2x10^4$ Lewis Lung Carcinoma cells into the intramedullary space of the femur of C57BL/6 mice or transgenic mice in the C57BL/6 background. Mice gradually reduce the use of the affected limb and the weight bearing. Symptoms of secondary cutaneous hyperalgesia in the ipsilateral paw also manifest, as demonstrated by the hypersensitivity in the von Frey test, the Hargreaves' test, and the dry ice test.

3. $Na_V1.7$ channel as a potential analgesic target for cancer-induced bone pain

3.1. Introduction

3.1.1. The rationale for targeting VGSCs in CIBP and $Na_V1.7$ specifically.

Several VGSCs have been shown to be implicated in CIBP. As shown earlier, several pain mediators are released in CIBP, and pathophysiological studies highlighted the role of enhanced expression and/or enhanced conductance of VGSCs as the final pain-causing mechanism for many of those mediators. For example, a study showed that the granulocyte-macrophage colony-stimulating factor could be one of the pain-driving factors following bone cancer, and it was shown that its blockade significantly reduces heat and mechanical hyperalgesia in rat models of CIBP. To understand how the granulocyte-macrophage colony-stimulating factor causes pain, transcriptional profiling and electrophysiological studies were performed on DRG neurons after exposure to the granulocyte-macrophage colony-stimulating factor. Results indicated an upregulation and enhanced conductance of the Na^+ channels $Na_V1.7$, $Na_V1.8$ and $Na_V1.9$, which could at least partly explain the pain phenotype following the injection of the granulocyte-macrophage colony-stimulating factor (Zhang et al., 2019). Moreover, (Qiu et al., 2012) showed that the expression of $Na_V1.8$ and $Na_V1.9$ increases significantly in Sprague-Dawley rats bearing 256 mammary gland carcinoma cells in the intramedullary space of the tibia. PGE2, which is abundantly released in CIBP, was shown to increase $Na_V1.9$ currents (Rush & Waxman, 2004). Similarly, the activity of $Na_V1.8$ channels can be modulated by several inflammatory mediators indirectly via their effects on protein kinases that phosphorylate $Na_V1.8$. For instance, $Na_V1.8$ channels can become phosphorylated in response to several inflammatory mediators like PGE2 and TNFα. As a consequence of the phosphorylation of $Na_V1.8$, the activity of the DRG neurons can be affected through the alteration in the gating characteristics of $Na_V1.8$ (Gold et al., 1998; Jin & Gereau, 2006; Zhou et al., 2002). NGF, which is considered a hallmark of CIBP, was shown to increase the expression of $Na_V1.7$ and $Na_V1.8$ and can allow the opening of these channels to take place at more negative membrane potentials (Gould et al., 2000; Laedermann et al., 2015;

Stamboulian et al., 2010). All of these studies show that VGSCs could play a crucial role in CIBP. Therefore, a significant part of my Ph.D. work focused on VGSCs.

Among the VGSCs that gained considerable interest is $Na_V1.7$. This channel is expressed in almost all DRG neurons but with higher levels in nociceptors (Bennett et al., 2019). $Na_V1.7$ channels are expressed in all parts of the first-order neurons. In the CNS of rodents, besides being expressed in the central terminals of DRG neurons, $Na_V1.7$ is also expressed in several other locations but most notably in the olfactory sensory neurons (Weiss et al., 2011) and magnocellular neurosecretory cells of the supraoptic nucleus (which seems to be linked to vasopressin release) (Black et al., 2013). Recent reports indicate that these channels are also expressed in the projection neurons of humans (Shiers et al., 2023). It was found that painful neuromas from human patients have higher immunoreactivity for $Na_V1.7$ than the nonpainful ones, indicating that $Na_V1.7$ is crucial for nociception (Kretschmer et al., 2002). As mentioned earlier, $Na_V1.7$ produces a TTX-sensitive Na^+ current. Loss of function mutations in the *SCN9A* gene, which encodes for $Na_V1.7$ channels, lead to pain insensitivity in humans and loss of the sense of smell (Cox et al., 2006). In addition, several gain of function mutations in this gene (like *Trp1538Arg* and *Ala1746Gly*) make the channel open at more hyperpolarised potentials than the wild-type $Na_V1.7$ channels, which indicates an enhanced activity of the channel. The mutation *Ala1746Gly* causes early-onset inherited erythromelalgia, while the mutation *Trp1538Arg* causes late-onset erythromelalgia (Bennett & Woods, 2014). Additionally, gain-of-function mutations can also lead to the impairment of the channel inactivation and thereby cause a persistent current that can lead to pain in conditions like paroxysmal extreme pain disorder (Fertleman et al., 2006). Additionally, some conditions where mutations render $Na_V1.7$ channels more active can result in the degeneration of neurons that express this mutant channel. An example of these conditions is small nerve fibre neuropathy (Faber, Hoeijmakers, et al., 2012).

Several animal models were generated to study the role of $Na_V1.7$ in pain sensation. The global $Na_V1.7$ knockout mice die soon after birth, presumably due to the inability to feed (Mohammed A. Nassar et al., 2004). Therefore, several conditional knockout models were generated, and results from these mouse

models have shown that $Na_V1.7$ is a critical player in acute pain sensation and some chronic pain models (Minett et al., 2012; M. A. Nassar et al., 2004). The underlying mechanism by which the deletion of $Na_V1.7$ results in analgesia was studied extensively. It was initially thought that loss of function mutations in $Na_V1.7$ could cause analgesia by preventing action potential propagation, but this appeared not to be the case, as action potentials can be achieved even though suprathreshold stimuli are required for $Na_V1.7$-null neurons (Gingras et al., 2014). The second proposed mechanism is based on the finding that conditional $Na_V1.7$ conditional knockout mice have increased levels of preproenkephalin (*PENK*) mRNA. *PENK* mRNA eventually gives rise to Leu- and Met-enkephalin: both essential components of the endogenous opioids system. Subsequently, it was hypothesised that the increase in enkephalins might play a role in the analgesia seen in $Na_V1.7$ knockout mice and pain insensitivity seen in patients with loss of function mutations (Minett et al., 2015). This mechanism was clinically translated as naloxone injection restored pain sensitivity in pain-insensitive patients whose pain insensitivity occurs due to loss of function mutations in the *SCN9A* gene (Minett et al., 2015). However, recent findings suggest that the upregulation of PENK only happens in C-LTMR and that this does not contribute to analgesia in conditional $Na_V1.7$ knockout mice. One potential reason for the discrepancy between results could be the difference that this group relied on knocking out the expression of $Na_V1.7$ channels in adulthood (Deng et al., 2023), as opposed to congenital knockout mice that previous studies relied on (Minett et al., 2015). In addition, conditional $Na_V1.7$ knockout mice have reduced expression of the serotonin receptor 5HT4, a receptor that has a hyperalgesic effect upon activation (Isensee et al., 2017). Moreover, it was recently shown that conditional $Na_V1.7$ knockout mice have defective neurotransmitter release from the central terminals of DRG neurons in the spinal cord (MacDonald, Sikandar, et al., 2021). Combined, this evidence highlights the role of $Na_V1.7$ in pain sensation. Unfortunately, so far, $Na_V1.7$ blockers have failed in the clinic partly due to selectivity problems (692), and even when selectivity is achieved, maintaining the efficacy seemed challenging as it was insufficient to cause significant analgesia (McDonnell et al., 2018). Accordingly, novel approaches should be employed to target $Na_V1.7$. These include the use of CRISPRi technology, which was shown to result in lasting analgesia in several pain models (Moreno et al., 2021). Also, tools like antisense oligonucleotides to reduce the expression of $Na_V1.7$ channels

have been shown to induce analgesia that lasted for up to four weeks (Mohan et al., 2018). Additionally, approaches that rely on targeting $Na_V1.7$ channels indirectly have also been described, and these include the suppression of CRMP2 SUMOylation to eventually reduce the expression of $Na_V1.7$ channels at the plasma membrane (Cai et al., 2021).

3.1.2. An introduction to the CRISPR-Cas9 system and CRISPRi technology

The Clustered regularly interspaced short palindromic repeat (CRISPR)-Cas system was first discovered in *Escherichia coli* (Ishino et al., 2018). Bacteria use this system to eliminate invading genes incorporated into their genome, such as viral genes; thereby, this method is considered adaptive immunity (Barrangou et al., 2007). There are six types of CRISPR-Cas systems (Koonin et al., 2017; Makarova et al., 2015; Shmakov et al., 2017). From these subtypes, the type II CRISPR system is the one that gained the highest application in gene editing experiments. The Cas type with the broadest practical use is Cas9, with Cas9 from *Streptococcus pyogenes* being the earliest Cas enzyme utilised outside bacterial cells (Jinek et al., 2012). Until now, Cas9 has been the most frequently used Cas. In nature, Cas9 systems require two RNAs: CRISPR RNA (crRNA) (guides Cas9 to its target) and transactivating crRNA (forms a complex with Cas9) (Deltcheva et al., 2011; Gasiunas et al., 2012). Once targeted to the right location of the DNA, Cas9 cuts the DNA double strands generating a blunt end (Garneau et al., 2010). The path for gene therapy was paved after the discovery of this bacterial defence mechanism. In experimental settings, a single guide RNA (sgRNA) is used instead of crRNA and transactivating crRNA (Jinek et al., 2012). The benefit of using one guide RNA is to reduce the off-target effects. The double-strand breaks that Cas9 causes then trigger DNA repair mechanisms which can be put into two main categories: homologous recombination and non-homologous DNA end-joining, with the second mechanism being the dominant pathway in vertebral cells (Sonoda et al., 2006). Non-homologous DNA end-joining causes the incorporation of random nucleotides at the location where the double-strand break occurred, which could result in frameshift mutations (Kramer et al., 1994). Frameshift mutations increase the probability of premature stop codon formation, causing nonsense-mediated decay and eventually leading to loss of function alleles (Chang et al., 1979; Maquat et al., 1981).

Because there are many possible risks associated with the complete loss of a gene, approaches to knockdown the expression of genes can be used as a safer gene targeting tool for therapeutic purposes. To achieve gene knockdown, alternative versions of the Cas9 enzyme were developed, among which is a catalytically inactivated Cas9 (dCas9). The similarity between dCas9 and Cas9 lies in their reliance on a guide RNA for targeting a specific gene, but dCas9 cannot cut the target DNA (Whinn et al., 2019). sgRNA-guided dCas9 enzymes can reduce the transcription of a gene by hindering the binding of RNA polymerase enzyme (Qi et al., 2013). Transcription regulation factors-linked dCas9 have enhanced knockdown efficacy. One example of these transcription regulators is the Kruppel-associated box (KRAB) repressor (Beerli et al., 2000). The approach that uses KRAB-associated dCas9 to knockdown the expression of genes is known as clustered regularly interspaced short palindromic repeat interference (CRISPRi) (Qi et al., 2013). When the fusions of dCas9 and KRAB are targeted to the promoter of a gene, 5' untranslated regions, or the proximal enhancer elements, transcription repression can be achieved (Gilbert et al., 2013) as the binding of dCas9-KRAB diminishes the binding of endogenous transcription factors (Beerli et al., 2000). After the attachment of KRAB domains with the targeted sequences, they recruit the KRAB-associated protein 1 (KAP1) that forms complexes with several epigenetic silencers such as SET domain bifurcated 1, euchromatic histone-lysine N-methyltransferase 2, lysine-specific histone demethylase 1 and the nucleosome remodelling and deacetylase. The euchromatic histone-lysine N-methyltransferases place two or three methyl groups on lysine-9 of histone H3. On the other hand, lysine-specific histone demethylase-1 eliminates histone H3 lysine-4 methylation, while nucleosome remodelling and deacetylase eliminate acetyl groups. These enzymes and histone binding and chaperone proteins make a repressive chromatin state that can quickly expand from the nucleation site of KRAB to affect nearby genes (Groner et al., 2010). The final effect of the KAP1 complex is the recruitment of DNA methyltransferases (DNMTs 3A or 3B) (Quenneville et al., 2012). These DNMTs act in concert with DNMT3L (catalytically inactive) to methylate cytosine at CpG dinucleotides, establishing a permanent repressive state on the adjacent genes (Quenneville et al., 2012). These DNA methyltransferases generally cause highly stable alterations in the methylation status.

In our lab, we thought to employ this technique to knockdown the expression of $Na_V1.7$ channels. Professor Cox designed a dSaCas9-KRAB fusion with a suitable sgRNA to guide the dSaCas9 to the *Scn9a* gene in mice. Supported by the success of the knockdown of $Na_V1.7$ channels in the DRG neurons using an interfering RNA packaged in lentiviral vectors in reducing the pain phenotype in a rat model of CIBP (Pan et al., 2015), I moved forward to employ the CRISPRi technology to knockdown the expression of $Na_V1.7$ channels in our mouse CIBP model. It is important to note that the rat CIBP model that showed the potential analgesic effect of knocking down the expression of $Na_V1.7$ in CIBP involved the injection of Walker 256 breast cancer cells in the tibia of SD female rats. In this model, a significant analgesia phenotype was detected after 24 hours following a single injection of lentivirus (LV). However, this group did not assess whether this analgesia could be maintained for extended periods (Pan et al., 2015). Therefore, I wanted to 1) use a different viral vector (namely recombinant adeno-associated virus for its good safety profile), 2) assess whether analgesia can be achieved, and 3) whether it can be sustained for long periods.

3.1.3. An introduction to recombinant adeno-associated viral vectors and the rationale for choosing them

The fact that viruses naturally can deliver nucleic acids to cells makes them an attractive tool for delivering nucleic acids to cells (Naso et al., 2017). The promising ability of viruses to carry nucleic acids to cells comes with issues like immunogenicity and the possible tendency to cause cancer. These issues represented an obstacle hindering the wide use of viruses clinically. Therefore, in the clinical setting, viruses are mainly used for vaccination and oncolysis (Cotter & Muruve, 2005).

Adeno-associated virus (AAV) is a commonly used vector in gene therapy. The reason behind this naming is that it was first discovered as a contaminant in adenovirus preparations (Hastie & Samulski, 2015; Rose et al., 1966). The simplest way to describe the structure of AAV is to describe it as a protein coat carrying a single-stranded DNA in its inner cavity. The size of the single-stranded DNA is approximately 4800 bases. For AAV to replicate in a cell, it needs a co-infection with another virus, in most cases, an adenovirus. The genome of AAV has two sets of inverted terminal repeats (ITRs), between which three genes are present, namely Rep (Replication), Cap (Capsid), and aap (Assembly). The Rep

gene encodes the proteins needed for the replication and packaging of the viral genome. On the other hand, the Cap gene encodes for the viral capsid proteins, which are needed not only to protect the inner genome but also to bind the target cells and get internalised (Samulski & Muzyczka, 2014). The third gene in the AAV genome, the aap gene, encodes the assembly-activating protein that is needed for the assembly of the capsid proteins (Naumer et al., 2012).

The chief difference between AAV and Recombinant AAV (rAAV) is the lack of Rep proteins in the rAAV. Accordingly, rAAV retains the ability to enter cells and deliver nucleic acids, but they cannot replicate. rAAVs possess a transgene that is flanked by ITR sequences. Following rAAV transduction into a cell, the transgene remains as an episome in the nucleus of the cell, making rAAV attractive from a safety point of view (Choi et al., 2006). Additionally, compared to other viruses, AAV appears to be less immunogenic. This could be attributed to the fact that AAV transduction to antigen-presenting cells (APCs) is not highly efficient (Mays et al., 2014). In a transduced cell, it was shown that AAVs could express their transgenes for a period ranging between 6 and 12 months when used *in vivo* (Berns & Muzyczka, 2017). Because AAV2 was among the early identified serotypes of AAVs, intense work has been done to understand its biology. Therefore, most of the rAAVs use the ITRs of AAV2. Transgenes delivered by rAAV are composed of a suitable promoter, the target gene, and a terminator (Gray et al., 2011).

3.2. Aims

Herein, the role of $Na_V1.7$ channels in CIBP was validated by testing the optimized CIBP model in conditional knockout mice in which this channel is knocked out from sensory neurons. After this initial target validation step, tools to reduce the expression of the *Scn9a* gene were tested as a potential analgesic strategy for CIBP. Herein, I employed the CRISPRi technology to knockdown the expression of this channel. The CRISPRi transgene was delivered to sensory neurons of wild-type C57BL/6 mice using recombinant adeno-associated viral vectors.

3.3. Methods

3.3.1. Surgery

Surgery was done as previously described in section 2.3.3. In all the studies, male and female mice were used. The choice of the animal number was based on previous experience from animal experiments in our lab.

3.3.1.1. $Na_V1.7$ conditional knockout mice in CIBP

Two types of transgenic mice in C57BL/6 background were used in this study (see Table 2). N=9 in the Nav1.7 conditional knockout group (five females and 4 males) and 14 for their littermates (seven males and seven females). The design of these mouse lines and the genotyping protocols can be found below.

3.3.1.1.1. Genotyping

Mouse-ear tissue samples were digested in 30 µl of lysis solution containing Proteinase K for 3 hours at 55°C and after that for 5 minutes at 95°C to render Proteinase K inactive. The samples were vortexed, spun down, and kept at -20 °C. The following ingredients were used in a typical PCR: 10 µl Dreamtaq PCR Mastermix (Thermo Scientific), 7 µl water, 1 µl of every primer (10 µM), and 1 ng of template DNA. Samples were subjected to PCR under conditions designed specifically for each primer set and suitable for Dreamtaq. To segregate bands by size, samples were electrophoretically run on a 1% agarose gel. In 50ml of 1X TAE buffer, 0.5g of agarose (Sigma) was dissolved to create gels (40 mM Tris-acetate, 1 mM EDTA). The gel was set after ethidium bromide (EtBr) (0.5 g/ml) was added. In each gel, 5 µl of a suitable molecular weight marker was run with the samples. A Biodoc System was used to isolate bands that were then seen after samples were run on the gel for 45 minutes at 100 volts. The list of transgenic mice used in this chapter is shown below (Table 2), and the genotyping protocols and PCR products are listed in Table 3.

3.3.1.1.2. Cre recombinase/loxP system

Depending on how they are oriented, the 38 kDa Cre recombinase protein catalyzes the recombination of the DNA sequence flanked between two 34-bp loxP identification sites (Metzger & Feil, 1999). The flanked sequence is removed when the two sites are positioned in the same direction; however, the flanked sequence is inverted whenever the two sites are placed in opposite directions. Two transgenic mouse lines must be used to create a conditional knockout (KO)

mouse: one expresses Cre that is driven by an interest-specific promoter, and the other has loxP sites flanking an area of the target gene. When these two lines are crossed, Cre mediates the excision of the flanking DNA sequence, leading to the deletion of the target gene only in the Cre-expressing animal (such as $Na_V1.8$-Cre). In some cases, the excision of the loxP-flanked sequence can allow the expression of a reporter whose transcription is prevented by a loxP-flanked transcriptional stop region (e.g., rosa-floxstop-tdTomato). Only cells expressing the promoter that causes Cre-expression will produce the reporter protein as a result of Cre-mediated excision of the stop region. The $CreER^{T2}$ system may be used to modulate the timing of Cre recombination (Feil et al., 2009). Here, Cre recombinase has been linked to an estrogen receptor domain that binds tamoxifen; without tamoxifen, the mutant recombinase is confined to the cytoplasm, where it lies dormant. The mutant recombinase is transported to the nucleus when tamoxifen is present, enabling site-specific recombination at the loxP sites and enabling inducible gene deletion or expression (such as fos-$CreER^{T2}$). The $CreER^{T2}$ system will be used in one of the studies reported in Chapter 6. In this chapter, this system was utilised to knockout the expression of the $Na_V1.7$ channels.

Table 2: A summary of the transgenic mice used in this chapter.

Mouse line	Identifier	Citation
$Na_V1.7$ flox	$Scn9a^{tm1.1Jnw}$	(Mohammed A. Nassar et al., 2004)
Advillin Cre	$B6.129P2\text{-}Avil^{tm2(cre)Fawa/J}$	(Zhou et al., 2010)

Table 3: Primers used for PCR to genotype transgenic mice used in this chapter.

PCR product	Forward primer	Reverse Primer
$Na_V1.7$ flox		
$Na_V1.7$ wild-type (382 bp)	CAGAGATTTCTGCATTAGAATTTGTTC	GCAAATCATAATTAATTCATGACACAG
$Na_V1.7$ flox (527 bp)	CAGAGATTTCTGCATTAGAATTTGTTC	GCAAATCATAATTAATTCATGACACAG
		Or
		AGTCTTTGTGGCACACGTTACCTC
$Na_V1.7$ knockout (395 bp)	CAGAGATTTCTGCATTAGAATTTGTTC	GTTCCTCTCTTTGAATGCTGGGCA
Advillin-Cre		
Advillin wild-type (480 bp)	CCCTGTTCACTGTGAGTAGG	AGTATCTGGTAGGTGCTTCCAG
Cre (180 bp)	CCCTGTTCACTGTGAGTAGG	GCGATCCCTGAACATGTCCATC

3.3.1.2. Knocking down the expression of $Na_V1.7$ channels in CIBP

To test the potential analgesia caused by knocking down the expression of $Na_V1.7$ channels, C57BL/6 mice were injected with a recombinant adeno-associated virus (AAV) to knockdown the expression of this channel (or a control virus) eight weeks before they underwent CIBP surgery (n=16 per group). The viruses were injected intrathecally, and the total volume of the injected virus was 5µl per mouse (the titer of the $Na_V1.7$ knockdown virus was 1.95×10^{13} genome copies/µl, while that of the control virus was 1.45×10^{13} genome copies/µl). The rAAV to knockdown the expression of $Na_V1.7$ carried a transgene encoding for a single guide RNA (sgRNA) directed towards the promoter region of the *Scn9a* gene and sequence encoding for dead Cas9 (dSaCas9) enzyme from *Staphylococcus aureus* that is associated with Kruppel-associated box (KRAB) repressor under the control of the advillin promoter, along with a termination

signal. These sequences were flanked by inverted terminal repeats (ITRs). The control virus had the same transgene, but it lacked the sgRNA. It is important to mention that the capsid was obtained from AAV9 for both recombinant viruses. The selection of this serotype was based on the fact that AAV9 is among the least affected AAV serotypes by neutralising antibodies from mice sera (Rapti et al., 2012). Additionally, previous work from our lab and other labs (Weir et al., 2017) indicates that AAV9 transduces DRG neurons successfully. The transgenes in the $Na_V1.7$ knockdown virus can be found in Figure 22. Twenty minutes before the injection of the virus, 200µl of 25% mannitol was injected intravenously, to boost transduction.

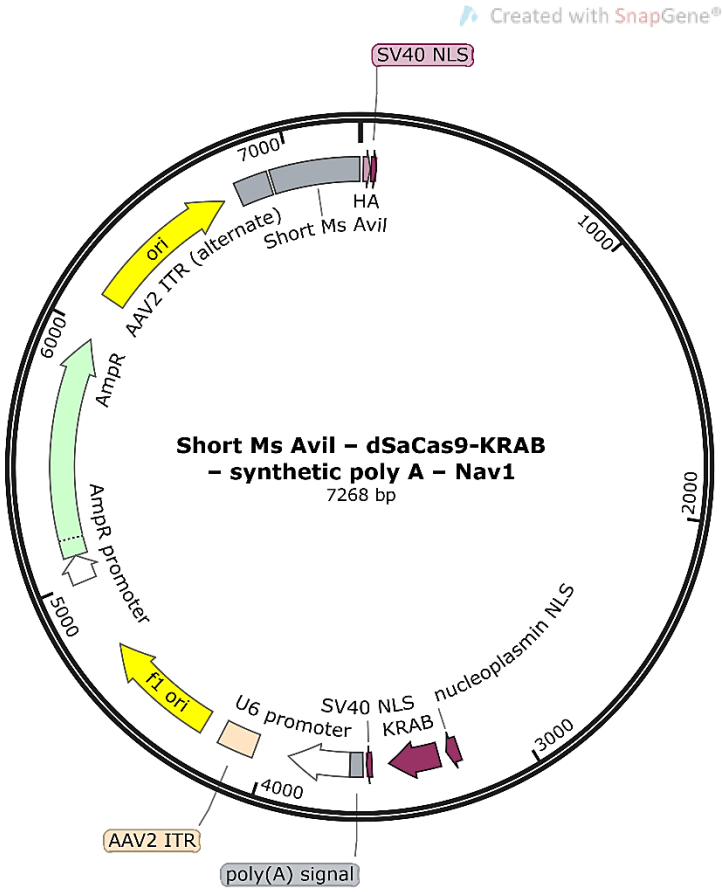

Figure 22: The transgene used to knockdown the expression of the Scn9a gene in DRG neurons of C57BL/6 mice. *KRAB: Kruppel-associated box; AmpR: ampicillin resistance; ITR: inverted terminal repeats.*

3.3.2. Quantitative real-time polymerase chain reaction (qPCR)

3.3.2.1. RNA extraction

In the gene therapy study, when any mouse reached the endpoint (Limb-use score=0 or severe weight loss), it was euthanised by CO_2 asphyxiation followed by cervical dislocation. DRGs located between L2-L4 were extracted, as previous data from our lab suggest that the cell bodies of sensory neurons innervating femurs of C57BL/6 mice are located within these DRGs. The location of the DRGs under study was determined by referring to mouse nerve anatomy (Rigaud et al., 2008). DRGs were then suspended in 1ml TRIzol Reagent (Life Technologies). The DRGs were stored at -80°C until they were used for RNA extraction. On the experiment day, DRGs were homogenised five times for 15 seconds each time. DRGs were placed on ice between each homogenisation round to cool down. The homogeniser used was MINILYS benchtop homogeniser (Peqlab). The PureLink RNA Micro Kit (Invitrogen 12183-016) was used for RNA extraction, and the manufacturer's protocol was followed. The final concentration of RNA was determined using a Nanodrop spectrophotometer (LabTech). The samples were then directly used as templates for synthesising cDNA.

3.3.2.2. cDNA synthesis

SuperScript III First-Strand Synthesis SuperMix for quantitative real-time (qRT)-PCR kit (Invitrogen 11752-050) was used. 166 ng of RNA were used from each sample. RNA was mixed with 1µl oligo dt and 1µl deoxynucleotide triphosphate, and the volume was completed to 10µl using nuclease-free water. The mixture was then incubated in a thermocycler at 65°C for 5 minutes. Then samples were placed on ice for 1 minute. cDNA synthesis mixture was added to the samples in the recommended order. Samples were re-placed in the thermocycler at 50°C for 50 minutes, followed by 85°C for 5 minutes. After that, samples were placed on ice. Then, 1µl of RNaseH was added to each sample, and the mixture was incubated at 37°C for 20 minutes. Samples were stored at -20°C until the day of the qPCR experiment.

3.3.2.3. qRT-PCR

For each sample, a 20µl-mixture shown in Table 4 below was prepared. Each reaction was carried out in triplicate. The final reaction mixtures were placed on a 96-well reaction plate. The Biorad RT-PCR Detection System was used to run the reactions. The protocol used for qPCR was as follows: 50°C for 2 minutes,

95°C for 10 minutes, 95°C for 15 seconds, and 60°C for 1 minute, followed by plate reading. The underlined steps were repeated 40 times. The normalisation of expression levels was done by comparing the expression levels of the test gene to the expression levels of the beta-actin (*Actb*) housekeeping gene *(*a routinely used housekeeping gene). While some evidence suggests that its expression can vary between tissues and may be impacted by certain conditions (Suzuki et al., 2000; Valente et al., 2009), I believe because the same tissue was compared across experiments, it was unlikely that the conclusion of my current study was affected. The results were analysed using the $2^{-\Delta\Delta Ct}$ method (Livak & Schmittgen, 2001).

Table 4: qPCR reaction mixture recipe.

Component	Volume (µl)
2x Taqman master mix	10
***Scn9a* TaqMan probe (Mm07294335_m1) or beta-actin (*Actb)* probe (Mm01205647_g1)**	1
Sample's cDNA	2
Nuclease free water	7

3.3.3. Behavioural tests and statistical analyses

Behavioural tests and statistical analyses were carried out as described in sections 2.3.4 and 2.3.6. Behavioural tests involved survival analysis, weight-bearing and limb-use scoring.

3.4. Results

3.4.1. Conditional $Na_V1.7$ knockout mice show a modest reduction in the pain phenotype associated with CIBP

As shown earlier, loss of function mutations in the *SCN9A* gene encoding for $Na_V1.7$ channels causes congenital insensitivity to pain. It was also shown that conditional knockout mice for this channel in the DRG neurons have high pain thresholds in various sensory tests (MacDonald, Sikandar, et al., 2021). Furthermore, it was demonstrated that several mediators driven from cancer cells and their associated stromal cells sensitise and/or increase the expression of $Na_V1.7$ channels in rodents (Gould et al., 2000; Laedermann et al., 2015; Stamboulian et al., 2010; Zhang et al., 2019). Therefore, the role of this channel in CIBP was tested by assessing whether mice in which this channel is

conditionally knocked-out in the DRG neurons could show a reduction in the pain phenotype caused by bone cancer. To generate conditional $Na_V1.7$ knockout mice in the DRG neurons, heterozygous mice expressing Cre under the control of the advillin promoter and were homozygous floxed for Nav1.7 were crossed with homozygous floxed $Na_V1.7$ mice. The resulting conditional $Na_V1.7$ knockout mice (and Cre-negative littermates) underwent CIBP surgery to inoculate LL/2 cells in their left femurs. The $Na_V1.7$ conditional knockout mice needed a significantly longer time to reach limb-use score zero and showed a slower reduction in the weight-borne on the ipsilateral limb, and better mean limb-use scores (Figure 23) compared to their littermates.

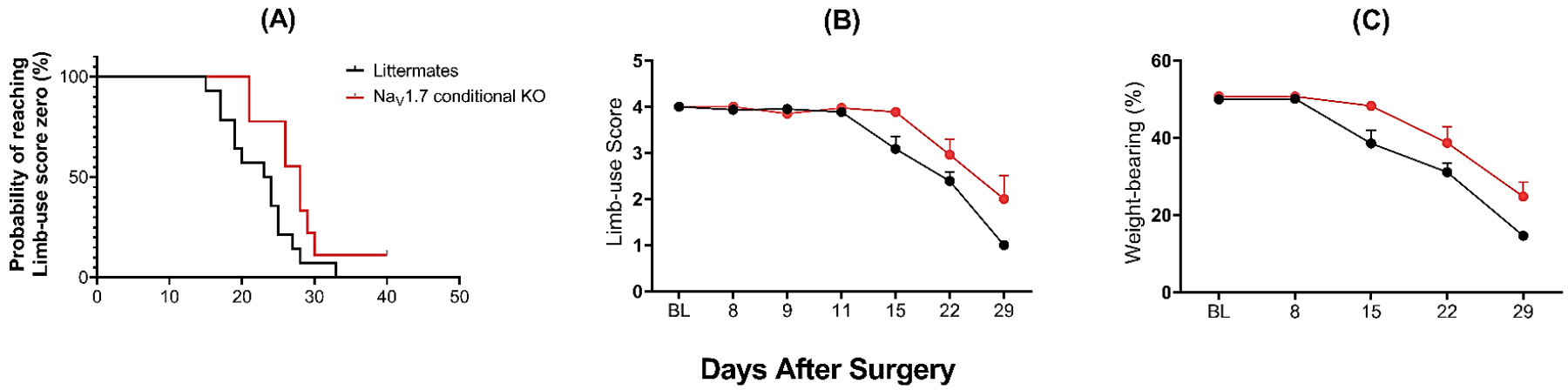

Figure 23: Conditional Na$_V$1.7 knockout mice in the DRGs showed a modest reduction in the pain phenotype associated with CIBP. *A) Analyses of the median time needed to reach limb-use score zero after the CIBP surgery in Na$_V$1.7 conditional knockout mice and their littermates. The median number of days to reach limb-use score zero in the Na$_V$1.7 conditional knockout group was 28 days and 23.5 days in the control group. This difference was statistically significant, according to the Mantel-Cox test (p-value=0.0433) and the Gehan-Breslow-Wilcoxon test (p-value=0.0256). (B) Ipsilateral weight-bearing after the CIBP surgery in Na$_V$1.7 conditional knockout mice and their littermates. The RMEL analysis revealed that the difference between the two groups was statistically significant (p-value=0.0074), with the Na$_V$1.7 conditional knockout mice showing a significantly less reduction in the fraction of weight put on the ipsilateral limb over time compared to their littermates. C) A comparison of the limb-use scores between the conditional Na$_V$1.7 knockout mice and their littermates in the CIBP model. The results indicate that the decline in the use of the affected limb in the conditional Na$_V$1.7 knockout mice was significantly slower than in the control group (the RMEL, p-value=0.0385). Error bars represent SEM. N=9 in the Nav1.7 conditional knockout group (five females and 4 males) and 14 for their littermates (seven males and seven females). No mice were excluded due to recovery issues.*

3.4.2. Recombinant adeno-associated viruses failed to knockdown the expression of $Na_V1.7$ channels and to cause analgesia in a mouse model of CIBP

Because of the well-established association between $Na_V1.7$ channels and pain (5), it was thought to knockdown the expression of this channel by using a rAAV in our mouse model of CIBP. This study was supported by the promising outcomes seen with conditional $Na_V1.7$ knockout mice in CIBP. To test the potential analgesia caused by knocking down the expression of $Na_V1.7$ channels, mice were injected with the recombinant virus (or the control virus) intrathecally. Eight weeks after the injection, the mice underwent CIBP surgery. The knockdown virus carried a transgene encoding for KRAB-associated dSaCas9 as well as a sgRNA directed to the *Scn9a* promoter region to knockdown the expression of the *Scn9a* gene. The transgene of the control virus had no sgRNA. It is important to mention that the capsid was obtained from AAV9 for both recombinant viruses.

The median time needed to reach limb-use score zero after CIBP surgery was 23 days in mice that received an intrathecal injection of the $Na_V1.7$ knockdown virus and 25 days in mice that received an intrathecal injection of the control virus. Statistical analyses, using the Log-rank test for trend and the Gehan-Breslow-Wilcoxon test, showed that the difference in the median time needed to reach limb-use score zero was statistically insignificant (p-value >0.05) (Figure 24A). Statistical analyses using the RMEL model showed that the difference in the virus type did not significantly impact either the weight-bearing or limb-use score results obtained in the CIBP model (Figures 24, B and C). The expression levels of the *Scn9a* gene (normalised to *Actb*) were similar in the L2-L4 DRGs obtained from mice injected with the $Na_V1.7$ knockdown virus and the ones injected with the control virus (Figure 25). The expression levels in the DRG neurons were checked at the end of the study (when mice reached limb-use score zero). This was approximately 11-12 weeks after the virus injection.

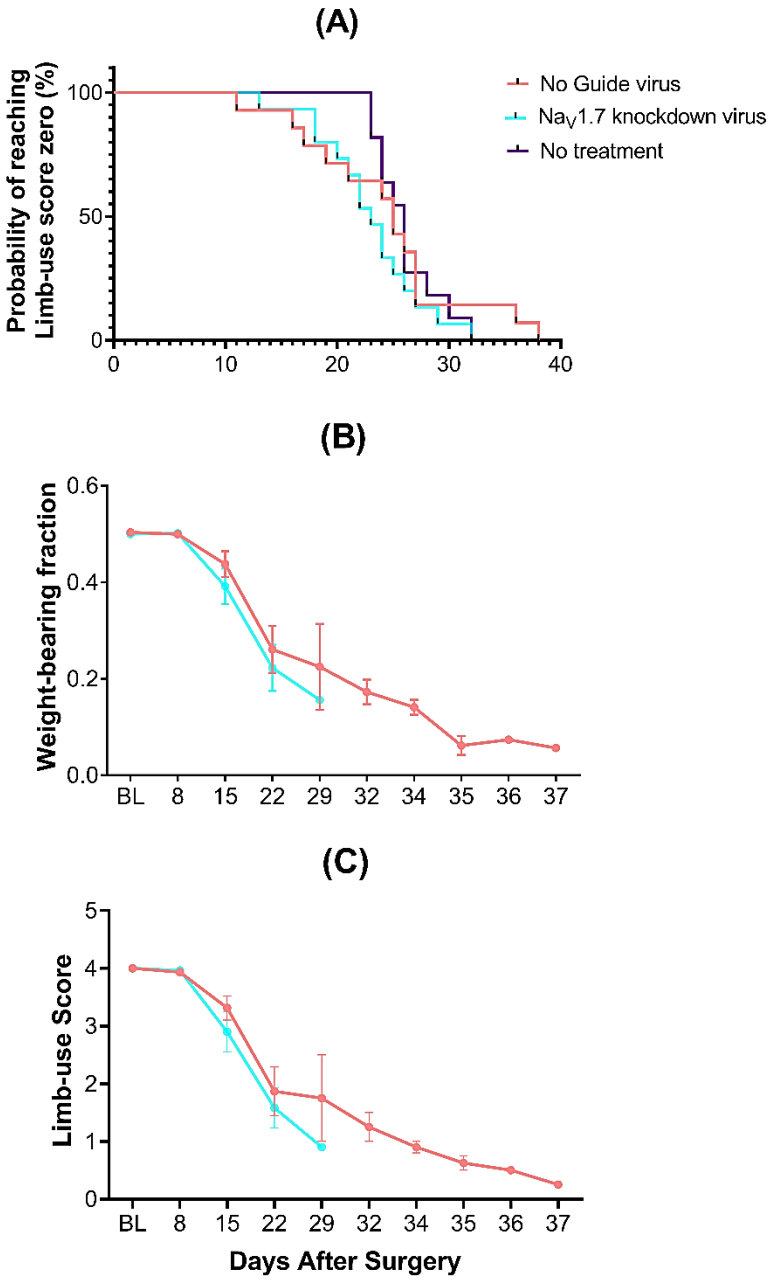

Figure 24: A CRISPRi tool to knockdown the expression of the VGSC $Na_V1.7$ in the DRG neurons failed to reduce pain behaviours in a mouse model of CIBP. *A) A comparison between treatment groups in the time needed to reach limb-use score zero after the CIBP surgery. No significant difference in the median time needed to reach limb-use score zero between the two treatment groups ($Na_V1.7$ knockdown virus or control virus) was detected, with the median time being 23 days in the Scn9a knockdown virus-treated group and 25 days in the control virus-treated group (p-value > 0.25, Log-rank test and Gehan-Breslow-Wilcoxon test). Additionally, the difference in the median time needed to*

reach limb-use score zero in the treated groups was not significantly different from the mice that received no treatment. The RMEL analysis (with Bonferroni post hoc test) showed that there was no statistically significant difference between the two treatment groups in either the weight-bearing (B) or the limb-use score (C), with P-values being > 0.05 for both behavioural tests. Surgery was done on 16 mice for each one of the two treatment groups, but three mice were excluded for limping on day 7 post-surgery (two from the control group and one from the knockdown group). Therefore, the final number of mice was 14 for the control group (seven males and seven females) and 15 for the virus group (seven males and eight females).

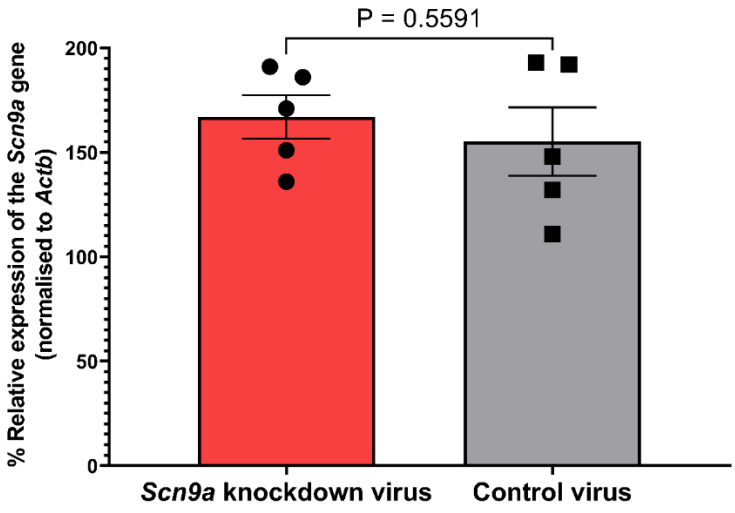

Figure 25: Our designed CRISPRi technology to knockdown the expression of the Scn9a gene in the sensory neurons of C57BL/6 mice failed to cause a significant reduction in the channel expression compared to the control group. *Expression data were normalised to the expression of the housekeeping gene Actb. The statistical test used is the unpaired t-test (P-value 0.5591). n=5 per group. The expression levels were checked at the end of the study (when mice reached limb-use score zero). This was approximately 11-12 weeks after the initial virus injection.*

3.5. Discussion

3.5.1. Validating the role of $Na_V1.7$ channels in CIBP (conditional knockout mice)

In 2014, our lab published a paper in which conditional $Na_V1.7$ knockout mice were tested in the CIBP model (Minett et al., 2014). While the results indicated a tendency of improved limb use in the $Na_V1.7$ conditional knockout ($Na_V1.7^{Wnt1}$) mice compared to their littermates, this difference was not statistically significant. One potential reason for this could be that the CIBP model used was aggressive and did not allow a long enough pain window to assess the difference between the groups. This is because Minett et al. injected $2x10^5$ LL/2 cells into the intramedullary space of the femur, while, here, a tenth of that number was injected. This could have made our model more capable of assessing the analgesic potential of therapeutic targets (Figure 23). With the number of cells injected by Minett et al., this group was only able to observe the mice for 16 days after surgery, while here, mice were observed for up to 40 days. When this refined model was used to compare the pain phenotype between conditional $Na_V1.7$ ($Na_V1.7^{Adv}$) knockout mice to their littermates, modest but significant analgesia was seen in the conditional $Na_V1.7$ knockout group, indicating that $Na_V1.7$ could be playing a role in CIBP (Figure 23). The chief difference between $Na_V1.7^{Wnt1}$ and $Na_V1.7^{Adv}$ is that advillin Cre knocks out $Na_V1.7$ channels from sensory neurons, while Wnt Cre knocks out the channel from sensory neurons as well as sympathetic neurons (Minett et al., 2014).

3.5.2. The assessment of the analgesic potential of knocking down the expression of $Na_V1.7$ channels using CRISPRi technology in CIBP

3.5.2.1. Study design

In this study, knocking down the expression of the *Scn9a* gene was attempted to induce a reduction in the pain-like behaviour in an optimised mouse model of CIBP. An rAAV carrying an ITR-flanked transgene, which provides the instruction for the synthesis of KRAB-associated dSaCas9 (under the control of the advillin promoter), and a sgRNA (under the control of the U6 promoter) was injected intrathecally to knockdown the expression of the *Scn9a* gene in the DRG neurons. The control group for this study received an intrathecal injection of an rAAV whose plasmid has the KRAB-associated dSaCas9 but lacked the sgRNA. The expression of KRAB-associated dSaCas9 was under the control of the

advillin promoter to increase the knockdown specificity (Hasegawa et al., 2007). In addition to the rAAV, each mouse in the study received an intravenous injection of mannitol as it was shown that mannitol increases the transduction of rAAV (Mastakov et al., 2001; Nishimura et al., 1998). The use of hypertonic mannitol to increase the transduction of rAAVs stems from the finding that hypertonic mannitol shrinks the endothelial cells of the capillaries of the brain, enlarging the gaps between these cells transiently and thereby enhancing transduction (Muldoon et al., 1995). Similarly, this shrinkage can occur in non-neuronal cells, which could be preventing the virus from accessing neurons (Nishimura et al., 1998). For all these reasons, mannitol was used in the current study. Approximately eight weeks after the viral injection, mice were subject to CIBP surgery, and behavioural studies followed.

3.5.2.2. Potential reasons for the failure of the Na$_V$1.7 virus

The behavioural results did not significantly differ between the treatment groups (Figure 24). Follow-up experiments showed no significant difference in the expression level of the *Scn9a* gene between the treatment groups (Figure 25). These disappointing outcomes could be attributed to various factors, including reasons related to the immune system, viral capsid-related issues, plasmid design (promoter and insert) and the timing of the CIBP surgery. These reasons will be discussed in the following section.

3.5.2.2.1. The role of the immune system

It is known that adaptive immune responses can be divided into two categories: cell-mediated and humoral immunity. Cell-mediated immunity protects the body from pathogens present intracellularly, while humoral immunity protects the body from extracellular pathogens. A vital element of humoral immunity are antibodies (Pancer & Cooper, 2006). Both of these types of immune responses could have contributed to the lack of efficacy of our rAAV in this study.

3.5.2.2.1.1. The humoral immunity and rAAV efficacy

As mentioned earlier, one significant benefit of using rAAV is that they lack viral genes, which further lessens the likelihood of eliciting immune responses compared to natural AAV (Basner-Tschakarjan & Mingozzi, 2014). Nevertheless, immune responses can still occur against rAAVs as rAAVs still possess capsid proteins, which can be immunogenic. In addition, the protein encoded by the delivered sequence could be immunogenic in some instances.

Humoral immune responses could compromise the efficacy of rAAVs used therapeutically if a previous infection with AAV resulted in transduction to the APCs. APCs could present peptides of the viral capsid to B cells and CD4+ T cells (Ferrand et al., 2015; Sudres et al., 2012). Consequently, memory cells and plasma cells can be generated, leading to the production of antibodies targeting the capsid proteins. The nature of these antibodies differs; they can be neutralising or non-neutralising in nature. Neutralising antibodies are generated to inhibit subsequent infections by AAV, whereas non-neutralising antibodies function through opsonisation, thereby facilitating the elimination of the virus by the spleen (Mays & Wilson, 2011).

Pre-existing immune responses against AAV, especially circulating neutralising antibodies, can have a detrimental impact on the clinical efficacy of AAV used for gene therapy. Unfortunately, these immune responses can be triggered both by systemic delivery as well as local delivery (Ried et al., 2002). It was, for a long time, been thought that neutralising antibodies targeting AAVs affect viral transduction in primate models but not in small animal models used usually in the lab (Jiang et al., 2006; Wang et al., 2010). However, in 2012, Rapti et al. published a study revealing that neutralising antibodies against AAVs are also detected in numerous animal models, both small and large (Rapti et al., 2012). In their study, they showed that mice could also possess neutralising antibodies against AAVs. They found that the number of neutralising antibodies varies with the species of animals and the AAV serotype being studied. The authors' recommendations included the necessity to pre-screen the existence of neutralising antibodies prior to commencing a study involving the injection of AAVs, primarily when large animals are used. They also suggested that neutralising antibody titres greater than ½ should be set as an exclusion criterion. The study's definition for a neutralising titre was the dilution that prevented at least 50% of the transduction compared to the control with no serum. The most relevant piece of information for our study is that neutralising antibodies were also detected in C57BL/6 mice obtained from Charles River. Luckily, AAV9 and AAV2 were the least affected by neutralising antibodies from mice sera. The inhibition of viral transduction was mainly attributed to IgM and not IgG (Rapti et al., 2012). The problem of neutralising antibodies is of great clinical relevance as anti-AAV antibodies are also present in humans. Screening of IgG antibodies from 226

individuals (age range 25-64 years) showed a high prevalence of anti-AAV9 antibodies, with anti-AAV9 antibodies being detected in 47% of the cases when enzyme-linked immunosorbent assay (ELISA) is used for detection (Boutin et al., 2010).

Because of the drastic effects that neutralising antibodies could have on therapeutic outcomes, several preclinical studies focused on finding ways to combat this issue. In an *in vivo* study using immuno-competent mice, a combination of anti-CD4 antibodies and cyclosporine was used to reduce anti-AAV8 antibodies after the administration of an AAV8 vector intravenously. The results from this study showed that there was a twenty-fold decline in the titers of anti-AAV8 antibodies (McIntosh et al., 2012). Another possible solution for the pre-existing capsid-targeting neutralising antibodies is to run screening tests for neutralising antibodies and the variants they target prior to administering an AAV for gene therapy (Akache et al., 2006). Alternatively, AAV evolution technologies that aim to generate neutralising antibody-resistant AAVs could be employed as part of the capsid selection process to reduce the probability of facing issues related to pre-existing anti-capsid neutralising antibodies (Bartel et al., 2012).

3.5.2.2.1.2. The role of cell-mediated immunity in the therapeutic efficacy of rAAVs

It is important not to exclude the possibility of generating an immune response through the transduction of cells other than the APCs. Therefore, a revision of the sequence of events that occur during a natural AAV infection would help identify the points that could lead to such immune responses. These infection events could be summarised as clathrin-mediated uptake of the virus into endosomes (internalisation) (Uhrig et al., 2012), escaping from endosomes, viral transport to the nucleus, followed by the breakdown of the capsid and the release of the transgene (Balakrishnan & Jayandharan, 2014). In many cases, prior to the transport to the nucleus, ubiquitination of the virus can take place in the cytosol. Proteolysis of capsid proteins can serve as a tool for class I major histo-compatibility presentation (Duan et al., 2000). This presentation can result in the formation of capsid-specific CD8+ T cells (Pien et al., 2009). CD8+ T cells are cytotoxic (Zhang & Bevan, 2011) and could, therefore, eliminate the rAAV transduced cells. A study by (Finn et al., 2010) showed that using bortezomib, a

proteasome inhibitor, prevents antigen presentation, which supports the hypothesis that presentation occurs due to proteolysis.

3.5.2.2.2. Empty capsids

One of the main challenges in the manufacturing process of AAVs is the difficulty of delivering the gene sequence of interest to the rAAV capsid. Consequently, the produced viral batch will contain empty viruses. The prevalence of empty viruses in a batch can reach 90% of the total viral particles. To avoid the labour-intensive processes needed to remove empty viruses, higher volumes of viral mixtures are used to compensate for the empty viruses. Unfortunately, this is not always applicable when the injected viral volume cannot exceed a particular limit (Grieger et al., 2016; Hebben, 2018; Hernandez Bort, 2019). One does not exclude the possibility that the presence of a high percentage of empty capsids might have influenced the results observed in this study.

3.5.2.2.3. Vector design

Selecting the optimum capsid

To enter a cell, AAV interacts with carbohydrates on the surface of the to-be-transduced cell. These carbohydrates include heparin sulfate and galactose (Asokan et al., 2012; Wu et al., 2006). As mentioned earlier, AAV9 capsid was used in this study. AAV9 preferentially interacts with galactose on target cells (Bell et al., 2012). This peculiarity enables AAV9 to cross the blood-brain barrier and transduce the CNS neurons (Merkel et al., 2017; H. Zhang et al., 2011). In addition to interactions with carbohydrates, AAVs can form secondary interactions, impacting their specificity to cells. Therefore, these interactions should be considered when choosing the AAV variant for a particular tissue or organ. For example, as AAV9 interacts through galactose and laminin receptors, this justifies its use for the lung, the liver and skeletal muscles (Akache et al., 2006; Gao et al., 2004; Shen et al., 2011). Interestingly, based on the interactions, it is recommended to use AAV1 or AAV5 when neurons are targeted (Naso et al., 2017); therefore, these viral capsids can be used for our future studies.

An alternative, and probably more versatile approach, is to clone novel variants of AAVs and, after testing, identify variants with novel tissue specificities to both enhance transduction into target cells and reduce the off-target effects (Limberis et al., 2009). Similarly, directed evolution and the insertion of random peptides from peptide libraries to the currently existing AAV capsids carry great potential

in producing AAVs with unique cell specificities (Bartel et al., 2012). This method proved effective as it succeeded in generating novel variants of AAVs that possess a high preference for retinal cells (Bartel et al., 2012; Dalkara et al., 2013). Another method used to increase the specificity of AAV variants is to attach large binding proteins into the capsid (Ried et al., 2002). Recently, engineered forms of AAV that can specifically target the peripheral nervous system neurons were developed (Chan et al., 2017), and these capsids proved successful in targeting the DRG neurons that innervate the knee (Chakrabarti et al., 2020).

All these methods are to be considered, as it was shown before that without an exceptionally high blockade of $Na_V1.7$ channels, the upregulation of PENK will not be achieved (Minett et al., 2015), indicating that a high-efficiency knockdown of the *Scn9a* expression could be needed to achieve significant analgesia. These findings emphasise the need to apply all the methods that could favour the transduction of the target cells and prevent the clearance of the rAAV particles.

The packaging capacity of AAV is a significant burden

When designing an rAAV, the genome, including the ITRs, should be less than 5000 bases as larger sizes reduce the yield of the produced viruses and can result in truncating the transgene (Dong et al., 2010). Following the transgene delivery to the nucleus, the single-stranded DNA must be converted to double-stranded DNA before transcription. The formation of the complementary strand is the rate-limiting step in the expression of the transgene (McCarty et al., 2001). To speed up the onset of transgene expression, one could consider using single-stranded DNA that is self-complementary. The main drawback of the use of self-complementary DNA strands is that it reduces the packaging capacity of the rAAV to about 3300 bases (McCarty, 2008; McCarty et al., 2001). One possible solution for this issue is to package the KRAB-dSaCas9 into one AAV virus and package the sgRNA into another AAV. Then both AAVs are used for co-transfection. The merit of this strategy is that it enables the insertion of longer gene sequences. Alternatively, one could attempt to use AAV vectors to deliver the sgRNA only and to use animals that already express dSaCas9 in the desired group of cells/tissue (Lino et al., 2018).

One major issue of the rAAV used in this study is that it had no sequences encoding for fluorescent protein due to the packaging capacity of rAAV; therefore,

qPCR was used to assess the transduction efficacy. Only checking the expression levels of the *Scn9a* gene by qPCR did not allow us to assess if the issue of having inefficient knockdown is because of the KRAB-associated dSaCas9 and/or sgRNA or the lack of viral transduction.

The promoter

To reduce the off-target effects of rAAV, rAAV can be delivered directly to the target organ (e.g. pulmonary delivery (Griesenbach et al., 2015)), or tissue-specific promoters can be used. It is crucial to consider that local delivery cannot entirely eliminate the risk of systemic leakage. The leakage of the virus to the systemic circulation carries many issues, like the high accumulation of rAAV in the liver (Naso et al., 2017).

If the use of tissue-specific promoters is selected as a targeting method, the elements that exist in the natural promoter that lead to acceptable levels of transgene expression without compromising the tissue specificity of the promoter should be identified. Additionally, interactions that could occur between the vector genome and the promoter need to be studied thoroughly. These interactions could, in some instances, alter the activity and/or the specificity of the promoter (Zheng & Baum, 2008). Because all these issues might have occurred in the rAAV used in this study, these points should all be reassessed.

It is generally accepted that in cases where the expression of the target gene needs to occur at high levels, promoters that are strong and constitutively active are chosen (Powell et al., 2015). An example of this class of promoters is the cytomegalovirus (CMV) promoter/enhancer. Like other constitutively active promoters, the CMV promoter lacks tissue specificity, which introduces another issue. Therefore, in studies like ours, when high expression and high specificity are needed, extra attention should be given to promoter choice.

In the current study, two promoters were chosen. The advillin promoter was chosen to control the expression of dSaCas9-KRAB, and the U6 promoter controlled the expression of the sgRNA. U6 belongs to the family of type III RNA polymerase promoters (Mäkinen et al., 2006; Nie et al., 2010). A potential cause for the inadequate knockdown in this study could be the promoter crosstalk, meaning that the presence of these two promoters might have affected their activities *in vivo* (Hampf & Gossen, 2007). In future studies, attempts to enhance the efficacy of promoters should be employed. For example, as studies revealed

that the activity of the U6 promoter could be enhanced by including a CMV enhancer sequence, this approach could be attempted (Ong et al., 2005; Xia et al., 2003). The problem that remains unsolved is the packaging capacity of the AAV vectors that would prevent the incorporation of a CMV enhancer sequence in the current vector.

3.5.2.2.4. Surgery timing

In an unpublished experiment conducted in our lab, an rAAV containing a plasmid that encodes for tandem tomato fluorescent protein under the control of the CMV promoter was used to assess the time at which acceptable levels of transgene expression are achieved after intrathecal injection into C57BL/6 mice. The study showed that the earliest time for achieving good transgene expression levels was eight weeks post-injection. Based on the results from this experiment, the CIBP surgery was conducted approximately eight weeks after the injection of the rAAV virus. The difference in the promoter between the CIBP study (the advillin promoter) and the tandem tomato expression study (the CMV promoter) could contribute to the negative outcomes of the current study. Furthermore, the difference in the protein product between the two studies could alter the optimum time for attaining good expression levels, as the choice of codons can also impact the expression of the target gene. It is known that codon choice highly influences the expression of genes in the bacterial system, but this has also been shown to be true for mammalian cells (Carton et al., 2007). In order to select codons that would allow the highest expression quantities in specific tissues, one can use services to optimise the codon choice (Naso et al., 2017).

In addition to the main three components of the transgene (the promoter, the target gene, and the terminator), the use of additives like post-transcription regulators can have a considerable impact on the gene expression level (Gray & Zolotukhin, 2011). Because of the limited packaging capacity that AAVs offer, sequences encoding for transcription enhancers could not be incorporated into our rAAVs. Even though including such sequences may have increased the expression levels of our transgenes, one needs to note that this still does not ensure that the selected design will function in the desired manner. Therefore, several attempts should be made to select the final construct (Naso et al., 2017).

3.5.3. Future Directions

3.5.3.1. Causing a microdeletion in the Scn9a gene

Even though the use of dCas9 carries many benefits over the use of Cas9, it still has many cons, including the higher sensitivity to changes in sgRNA and the fact that, in many cases, the silencing of a gene is incomplete (Horlbeck et al., 2016; Yeo et al., 2018). An alternative method could be to select a tissue-specific promoter to drive the expression of Cas9 with two guide RNA sequences to cause gene excision (see Figure 26). Unpublished data from our lab revealed that using dual sgRNAs with Cas9 to target two segments of the *Scn9a* gene in mice resulted in a microdeletion in the *Scn9a* gene. This approach succeeded in causing a significant reduction in the pain-like behaviour in the CIBP model in C57BL/6 mice. Even though this method was efficacious in reducing pain-like behaviour, concerns about the irreversibility of gene editing remain compelling.

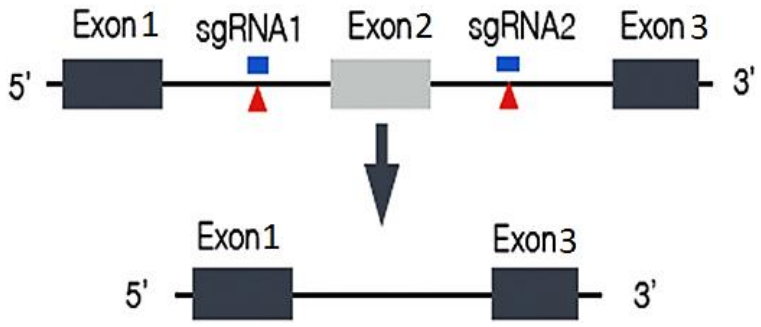

***Figure 26: The use of two single guide RNAs (sgRNAs) for the deletion of a gene**. Adapted from (Spagnuolo & Blenner, 2021).*

3.5.3.2. The simultaneous use of dCas9-KRAB and dCas9-DNMT3A3L

As mentioned earlier, the net effect of KRAB is to recruit DNMTs. When dCas9-KRAB and dCas9-DNMT3A3L were used simultaneously, a profound increase in DNA methylation was obtained (Tarjan et al., 2019). This strategy could be used in future studies to enhance silencing efficiency.

Recently, a heritable novel gene silencing tool was developed and was named CRISPR-off, which has wider potential applications as it does not necessitate the presence of canonical CpG island annotations (Nuñez et al., 2021).

3.5.3.3. Using other KRAB domains from other genes like ZIM3

In the current study, likewise in most CRISPRi studies, the KRAB domain from KOX1 (ZNF10) was used. This broad use of KOX1 KRAB is, presumably,

because it was the first KRAB to be functionally characterised (Margolin et al., 1994). In humans, the number of KRAB domains exceeds 350, and there was shown to be a variation in their transcription repression efficiency and their roles (Margolin et al., 1994; Murphy et al., 2016; Schmitges et al., 2016; Vissing et al., 1995). Alerasool et al. showed that fusing various KRAB domains with dCas9 also results in KRAB-dCas9 fusions with varying transcription repression potencies (Alerasool et al., 2020). It was shown that the interaction of a KRAB domain with Tripartite motif-containing 28 (TRIM28) was, in most cases, a good indication for the expression repression potency of the KRAB domain under study. *ZIM3* KRAB-associated dCas9 was identified as being an extremely potent transcription repressor, with potency exceeding the traditional KOX1 KRAB-associated dCas9 (Alerasool et al., 2020). Interestingly, it was also found that *ZIM3* KRAB-dCas9 had better performance in transcription repression experiments than KOX1-KRAB-methyl CpG binding protein 2 (MeCP2)-dCas9, which was shown before to be superior to the ordinary KOX1 KRAB-Cas9 (Yeo et al., 2018). Therefore, in future experiments, it might be worthwhile to test transcription repression using *ZIM3* KRAB-dCas9.

3.5.3.4. Zinc-Finger-4-KRAB and KRAB-dCas9-dual-gRNA

A recent publication by (Moreno et al., 2021) indicated that effective repression of $Na_V1.7$ channels was achieved in the lumbar DRG neurons in mice following the intrathecal injection of AAVs carrying Zinc-Finger-4-KRAB and KRAB-dCas9-dual-gRNA. They showed that this repression reduced the paclitaxel-induced tactile and cold allodynia until 105 days following the virus injection and about three months after the last injection of paclitaxel. Their results also indicate that the virus maintained high efficacy in preventing the thermal hyperalgesia that follows the intraplantar injection of carrageenan for 308 days. Similar approaches can be applied in CIBP to assess the potential application of these methods as analgesic tools.

3.5.3.5. Changing the route of administration of rAAVs

In our lab, a high transduction efficacy was achieved when rAAVs were administrated by retro-orbital venous sinus injection in adult mice or intraplantar injection in mouse pups. These methods could be tried in the future to knockdown the expression of the *Scn9a* gene in CIBP.

3.6. Conclusion

A mouse model of CIBP was used to assess the applicability of the voltage-gated Na^+ channel, $Na_V1.7$, as an analgesic target for CIBP. Results from these experiments indicated that $Na_V1.7$ plays a role in cancer-induced bone pain and is a potential therapeutic target as conditional $Na_V1.7$ knockout mice in sensory neurons manifested milder pain-like behaviour compared to their littermates. Gene therapy approaches to target the *Scn9a* gene that encodes for $Na_V1.7$ channels were also tested to treat CIBP, with disappointing results indicating that further optimisation is needed.

4. Targeting neuronal subsets in CIBP

4.1. Introduction

Opioids remain the standard of care for moderate-to-severe cancer pain, but they are associated with severe side effects, like tolerance, dependence and respiratory depression. Alternative analgesic methods are therefore needed. However, CIBP is a complex condition involving an inflammatory element, a neuropathic element as well as a cancer-specific element. Accordingly, single molecular targets are unlikely to be sufficient to cause noticeable behavioural changes. Approaches that target neuronal subsets could be beneficial. In this chapter, the role of two neuronal subsets was tested, and these are 1) the $Na_V1.8$-expressing neurons and 2) the μ-opioid receptor-expressing neurons in the spinal cord.

4.1.1. The rationale for targeting $Na_V1.8$ neurons

$Na_V1.8$ is a VGSC encoded by the *SCN10A* gene, and its expression is confined to neurons (Akopian et al., 1996). The role of $Na_V1.8$ in pain has been validated by human genetics, as several gain-of-function mutations have been identified in the *SCN10A* gene in painful small-fibre neuropathy patients (Faber, Lauria, et al., 2012). These mutations include *G1662S* (Han et al., 2014) and *I1706V* (Huang et al., 2013), leading to a significant increase in neuronal activity.

Like $Na_V1.7$ channels, $Na_V1.8$ channels are primarily expressed in nociceptors (Agarwal et al., 2004; Djouhri et al., 2003; L. C. Stirling et al., 2005) and more densely in the free nerve ends (Bennett et al., 2019). These channels are expressed in approximately three-quarters of the DRG neurons, and about 90% of nociceptors express Nav1.8 channels. Not only are these channels expressed in nociceptors, but they are also expressed by a sizable population (40%) of neurons with myelinated Aβ fibres (Shields et al., 2012). $Na_V1.8$ channels are mainly responsible for the upstroke part of the action potential waveform (Blair & Bean, 2002; Renganathan et al., 2001). The inward flow of Na^+ ions through $Na_V1.8$ channels comprises about (58–90%) of the total influx of Na^+ during the rising phase of the action potential (Blair & Bean, 2002; Renganathan et al., 2001). Electrophysiological studies in DRG cultures illustrated that $Na_V1.8$ channels are activated after the activation of other TTX-sensitive channels

(Bennett et al., 2019). NGF seems to play a role in enhancing the expression of $Na_V1.8$ in Trk-A positive peptidergic DRG neurons (Denk et al., 2017). On the other hand, $Na_V1.8$ levels in the non-peptidergic DRG neurons are controlled mainly by glial-derived neurotrophic factor (Cummins et al., 2000; Fjell et al., 1999; Leffler et al., 2002).

Biophysical property studies on $Na_V1.8$ indicate that the currents produced by $Na_V1.8$ are resistant to TTX (Akopian et al., 1996). Three features characterise the fast inactivation of $Na_V1.8$; it is incomplete, occurs at depolarised potentials, and possesses slow kinetics. The effect of incomplete fast inactivation is that it renders the currents produced by $Na_V1.8$ persistent, which explains the observation that $Na_V1.8$ channels are contributors to the ramp currents. The depolarised voltages needed for the inactivation of $Na_V1.8$ (30mV more depolarised than the TTX-sensitive channels in small rat DRG neurons (Elliott & Elliott, 1993)) make these channels retain their active states even at depolarised resting membrane potentials (Huang et al., 2014; Huang et al., 2013). On the other hand, the slow kinetics of the fast inactivation of $Na_V1.8$ allows these channels to remain open for extended periods. It was found that the $Na_V1.8$ inactivation kinetics are approximately ten times slower than that of $Na_V1.7$ channels (Cheng et al., 2008; Huang et al., 2013) and that a depolarising stimulus needs to be applied for 10 seconds to achieve $Na_V1.8$ inactivation. All these properties highlight the importance of $Na_V1.8$ channels in conveying noxious stimuli. It is important to mention that the slow inactivation was found to occur at more polarised potentials at colder temperatures (30°C vs 10°C) for $Na_V1.7$, but the slow inactivation of $Na_V1.8$ remains unaffected (Zhou et al., 2002). Therefore, $Na_V1.8$ plays a vital role in noxious cold sensation and in the sensation of mechanical stimulation at cold temperatures (Zhou et al., 2002). Furthermore, even when fast inactivation is achieved, $Na_V1.8$ channels recover quickly (Choi & Waxman, 2011; Tan et al., 2014). Because the repriming of $Na_V1.8$ channels is quick, these channels can also participate in the currents in the following spikes.

As mentioned above, rodent experiments highlight the importance of targeting $Na_V1.8$ for pain, but it was shown that the effect of $Na_V1.8$ channels on the activity of neurons is higher in humans than in rodents, a fact that encourages scientists to study this channel (Han et al., 2015). Firstly, the activation of the human $Na_V1.8$

occurs at a more hyper-polarised potential compared to the rat $Na_V1.8$. Secondly, fast inactivation happens at more depolarised potentials in humans compared to rat $Na_V1.8$ channels. Thirdly, the kinetics of the fast inactivation is slower in the human $Na_V1.8$ channels (Han et al., 2015). The action potentials produced by human $Na_V1.8$ either in naive human DRGs or in $Na_V1.8$ knockout rat neurons were significantly longer than the rat $Na_V1.8$ channels in patch clamp experiments. Unlike rat DRG neurons, human DRG neurons exhibit more spontaneous firing. Moreover, DRGs expressing human $Na_V1.8$ produce more action potentials upon applying the same stimuli than the DRGs expressing rodent $Na_V1.8$ channels (Han et al., 2015). Of equal importance is the need for careful consideration when translating results related to $Na_V1.8$ channels from rats to humans (Bennett et al., 2019).

For all the observations mentioned above, $Na_V1.8$ is considered a key target for pain research. This channel was shown to play roles in nociception, neuropathic pain, and inflammatory pain. Following the intraplantar injection of carrageenan, $Na_V1.8$ knockout mice develop thermal hyperalgesia later compared to wild-type mice. Additionally, $Na_V1.8$ knockout mice show reduced responses to noxious cold and mechanical stimuli compared to wild-type mice (Akopian et al., 1999). These observations highlight the importance of $Na_V1.8$ in nociception. $Na_V1.8$ also plays an essential role in neuropathic pain, as in saphenous nerve-section neuromas, the neuromas from $Na_V1.8$ knockout mice exhibited a significantly lower spontaneous firing compared to wild-type (Roza et al., 2003). Furthermore, following spinal nerve ligation, $Na_V1.8$ channels redistribute from the injured afferent fibres to the uninjured ones rendering them more active (Gold et al., 2003; Zhang et al., 2004). The redistribution of $Na_V1.8$ channels was also evident in humans after peripheral axotomy (Coward et al., 2000). Additionally, in the STZ diabetes model in rats, the TTX-resistant currents increased in the small-diameter DRG neurons (Hong et al., 2004).

The previous paragraphs highlighted the role of $Na_V1.8$ in pain and how interfering with its function causes significant analgesia in various pain models. Therefore, studies aimed to investigate the role of this VGSC in CIBP were performed where whole-cell current clamp recordings in dissociated DRG neurons from adult rats showed that the current density of $Na_V1.8$ increases significantly in the DRG neurons following CIBP (Liu et al., 2014). This group also

delivered A-803467 (a selective blocker of $Na_V1.8$ at a dose of 150 nmol) via an intrathecal cannula and showed that this treatment alleviated mechanical allodynia when tested using the up-and-down von Frey test. Additionally, the thermal hyperalgesia in the A-803467-treated group was significantly reduced compared to the vehicle-treated group. While it was shown that $Na_V1.8$ is bilaterally downregulated in the DRG neurons in a CIBP model involving the inoculation of Walker 256 breast carcinosarcoma cells in the tibias of rats, further knockdown of $Na_V1.8$ channels by intrathecal injection of antisense oligodeoxynucleotides against $Na_V1.8$ reduced mechanical hyperalgesia and ambulatory-evoked pain in these rats (Miao et al., 2010).

While all these data suggest that $Na_V1.8$ could contribute to CIBP, the ablation of $Na_V1.8$ positive neurons ($Na_V1.8^{DTA}$) did not cause a significant change in the pain-like behaviour of mice with CIBP compared to their littermates (Minett et al., 2014). The behavioural tests used in this study included the weight-bearing and limb-use scoring tests. Here, the role of $Na_V1.8$-positive neurons in CIBP was re-assessed in the optimised CIBP model as it was thought that the short timeframe in the model used by Minett et al. may have hindered the assessment of this approach. Herein, the congenital ablation of $Na_V1.8$ neurons was tested in the optimised CIBP model to validate their involvement in CIBP. After that, chemogenetic tools were used to silence the $Na_V1.8$-positive neurons and were also tested in the CIBP model with positive outcomes.

4.1.2. The rationale for targeting the μ-opioid receptor-expressing neurons

Small doses of morphine are administered intrathecally as part of a successful treatment option for refractory cancer pain. This produces potent analgesic benefits. It is typical practice to provide intrathecal morphine infusion therapy with the help of an implanted intrathecal morphine pump, which is designed for continued usage over an extended period of time. While efficacious, it was also reported that this treatment option affected the day-to-day activities of cancer patients, with side effects like nausea/vomiting and urinary retention being among the most commonly reported (Qin et al., 2020). Moreover, issues like tolerance remain to be a huge obstacle. Therefore, alternative means of targeting the opioid system could be beneficial. In this report, the aim was to assess whether silencing the μ opioid receptor-expressing neurons without the need for opioid agonists can

reduce the pain phenotype associated with CIBP. Herein, the use of modified botulinum compounds to silence the μ-opioid-expressing neurons was attempted as an alternative approach to target the opioid system.

4.1.3. Methods for targeting neuronal subsets

Several ways exist to target neuronal subsets; neuronal subsets can be congenitally ablated (e.g., by diphtheria toxin) or silenced/activated (e.g., by optogenetic or chemogenetic tools). For silencing neurons, two main methods were used; modified botulinum compounds (that inhibit neurotransmitter release by the targeted subset) and chemogenetic tools that rely on the chimeric ion channels (PSAM^4-GlyR). The PSAM^4-GlyR system will be explained in detail in Chapter 6, but this system relies on expressing an ion channel called PSAM^4-GlyR in the desired neuronal subset. Then an agonist is administered (namely varenicline) to render the PSAM^4-GlyR-expressing neurons irresponsive to stimuli.

4.1.3.1. Diphtheria toxin-based neuronal ablation

Specific cell subsets can be conditionally ablated using the diphtheria toxin method (Ivanova et al., 2005). The diphtheria toxin consists of two parts. The cell surface receptor is bound by fragment B, enabling it to enter the phospholipid bilayer and aid in the transfer of the enzymatically active fragment A. Diphtheria toxin fragment A (DTA) inhibits protein synthesis by facilitating the transfer of the nicotinamide adenine dinucleotide's ADP-ribose moiety to elongation factor-2. To activate diphtheria toxin in a specific cell population, two main techniques can be used. Firstly, Cre/loxP, BAC transgenesis, or knockin techniques can be employed to overexpress the diphtheria toxin receptor in particular cell types, thereby making it possible for the toxin to solely work to halt protein synthesis in those cells (Pogorzala et al., 2013). Secondly, fragment A can be expressed in the desired cell type in a Cre-dependent way; because fragment A is already intracellular, the Cre-based expression of this fragment is all that is required to cease protein synthesis and kill the cell (e.g. rosa-floxstop-DTA) (Abrahamsen et al., 2008). This second method was used in this report to ablate the $Na_V1.8$-expressing neurons, and heterozygous rosa-floxstop-DTA mice (C57BL/6 background) were bred with homozygous mice that express Cre in the $Na_V1.8$-positive neurons (C57BL/6 background). Therefore, in some of the offspring, the

$Na_V1.8$-positive neurons were ablated due to the expression of DTA, while in others, the subset remained intact.

4.1.3.2. Modified botulinum compound-based neuronal silencing

Botulinum neurotoxin serotype A is composed of a light-chain zinc endopeptidase as well as a heavy chain that binds to neuronal receptors and promotes light-chain transfer across the endosomal membrane (Montal, 2010). Once incorporated within the cell, the light chain can inhibit neurons for many months by cleaving synaptosomal-associated protein 25 (SNAP25), an important protein for synaptic release (Arsenault et al., 2013; Darios et al., 2010; Ferrari et al., 2011). This suppression is gradually overcome when endopeptidase activity declines (Montal, 2010). Cleaved SNAP25 (cSNAP25) is reported in neurons and not in glial cells, and it seems to be the unique substrate for botulinum protease cleavage (Hepp et al., 1999; Schubert et al., 2011). Maiarù et al. (Maiarù et al., 2018) leveraged a recently established "protein stapling" technique (Arsenault et al., 2013; Ferrari et al., 2011) that enabled the nonchemical linking of recombinantly generated proteins, employing core components of the SNARE (soluble N-ethylmaleimide–sensitive factor attachment protein receptor) complex, to achieve irreversible linking of two distinct peptide segments into a functional unit (Darios et al., 2010). This group used SNARE proteins to bind the light-chain domain of botulinum neurotoxin type A (BOT) to dermorphin, which targets μ-opioid receptor-expressing neurons in the dorsal horn. This construct renders the BOT specific for the μ-opioid receptor-expressing neurons, solving the protein toxicity problems related to botulinum-based compounds. After the binding to the μ-opioid receptors, the construct is internalised due to the presence of the translocation domain in the construct. Subsequently, the protease domain of the toxin is released into the cytoplasm, causing a profound suppression of synaptic release. This group found that the intrathecal injection of 100ng of this construct to mice resulted in a significant reduction in pain-like behaviours following a neuropathic pain model (spinal nerve injury) and an inflammatory pain model (CFA). The ‘analgesia’ was sustained for about three weeks following a single injection of dermorphine-BOT (Derm-BOT) without causing any toxicity (Maiarù et al., 2018). Interestingly, it was found that the intrathecal administration of Derm-BOT in naïve mice did not affect the baseline sensitivity to mechanical stimuli, and the anti-nociceptive effect to mechanical stimuli was only observed

in injury-driven pain states. These results made the authors postulate that the analgesic target for this construct did not depend on the μ-opioid receptor-positive primary afferents but rather the μ-opioid receptor-positive dorsal horn neurons (Maiarù et al., 2018) because, in the dorsal horn, μ-opioid receptors are expressed by interneurons, the central terminals of some of the DRG neurons, and by some second-order neurons (Kemp et al., 1996; Todd, 2017; D. Wang et al., 2018). Derm-BOT was used in this work to silence the μ-opioid receptor-expressing neurons in CIBP.

4.2. Aims

This work aimed to evaluate the role of 1) the $Na_V1.8$-expressing neurons and 2) the μ-opioid receptor-expressing neurons (in the spinal cord) as neuronal subsets that could potentially be contributing to CIBP. The role of the $Na_V1.8$- positive neurons was evaluated by ablating this subset and by silencing it. On the other hand, the role of the μ-opioid receptor-expressing neurons was assessed by silencing this neuronal subset with modified botulinum compounds.

4.3. Methods

Surgery, behavioural tests and statistics were carried out as previously described in section 2.3. For the Derm-BOT study, mice received an intrathecal injection of 100ng of Derm-BOT (or the molar equivalent of the control (unconjugated BOT)) when they reached a limb-use score of 3. As a positive control, some mice received an intrathecal injection of 60ng of morphine when they reached a limb-use score of 3. For silencing the $Na_V1.8$+ neurons, varenicline was administered intraperitoneally at a dose of 0.3 mg/kg and behavioural tests were carried out 30 minutes post-injection. A gap of at least 24 hours was left before each subsequent varenicline injection.

The mouse lines used in this chapter are summarised in Table 5, and the primers used for genotyping and the PCR products are in Table 6. For the Rosa-flex $PSAM^4$-GlyR mouse, see section 6.4.1.3.1.

Table 5: A summary of the transgenic mice used in this chapter

Mouse line	Identifier	Citation
$Na_V1.8$-Cre	Scn10a$^{tm2(cre)Jnw}$	(Mohammed A. Nassar et al., 2004)
Rosa-flox-stop DTA	Gt(ROSA)26Sor$^{tm1(DTA)Jpmb/J}$	(Ivanova et al., 2005)
Rosa-flex PSAM^4-GlyR		In-house

Table 6: Primers used for PCR to genotype transgenic mice used in this chapter.

PCR product	Forward primer	Reverse Primer
$Na_V1.8$-Cre		
$Na_V1.8$ wild-type (258 b.p.)	CAGTGGTCAGGCTGTCACCA	ACAGGCCTTCAAGTCCAACTG
Cre (346 b.p.)	CAGTGGTCAGGCTGTCACCA	AAATGTTGCTGGATAGTTTTTACTGCC
Rosa-flox-stop-DTA		
Wild-type (600 b.p.)	AAAGTCGCTCTGAGTTGTTAT	GGAGCGGGAGAAATGGATATG
DTA (250 b.p.)	AAAGTCGCTCTGAGTTGTTAT	GCGAAGAGTTTGTCCTCAACC

4.4. Results

4.4.1. The diphtheria toxin subunit A-mediated ablation of the $Na_V1.8$ expressing neurons reduced pain-like behaviour in CIBP but did not prevent secondary cutaneous cold sensitivity

To assess whether the $Na_V1.8$-expressing neurons play a role in the pain phenotype associated with CIBP, mice in which $Na_V1.8$ neurons are congenitally ablated were tested in the CIBP model, and different behavioural tests were conducted (like the limb-use scoring, weight-bearing and the dry ice test, see Figures 27 and 28) to compare the mice lacking the $Na_V1.8$-expressing neurons with the control group (mice in which the $Na_V1.8$-expressing neurons remained intact). The comparisons between the two treatment groups highlighted that the decrease in the limb-use score and the weight-bearing was significantly slower in the $Na_V1.8$-DTA group than in the control mice (Figure 27). While the withdrawal latency in the dry ice test had always been longer in the $Na_V1.8^{DTA}$ than their littermates, both groups developed secondary cutaneous cold hypersensitivity in the paw following CIBP in the femur (Figure 28).

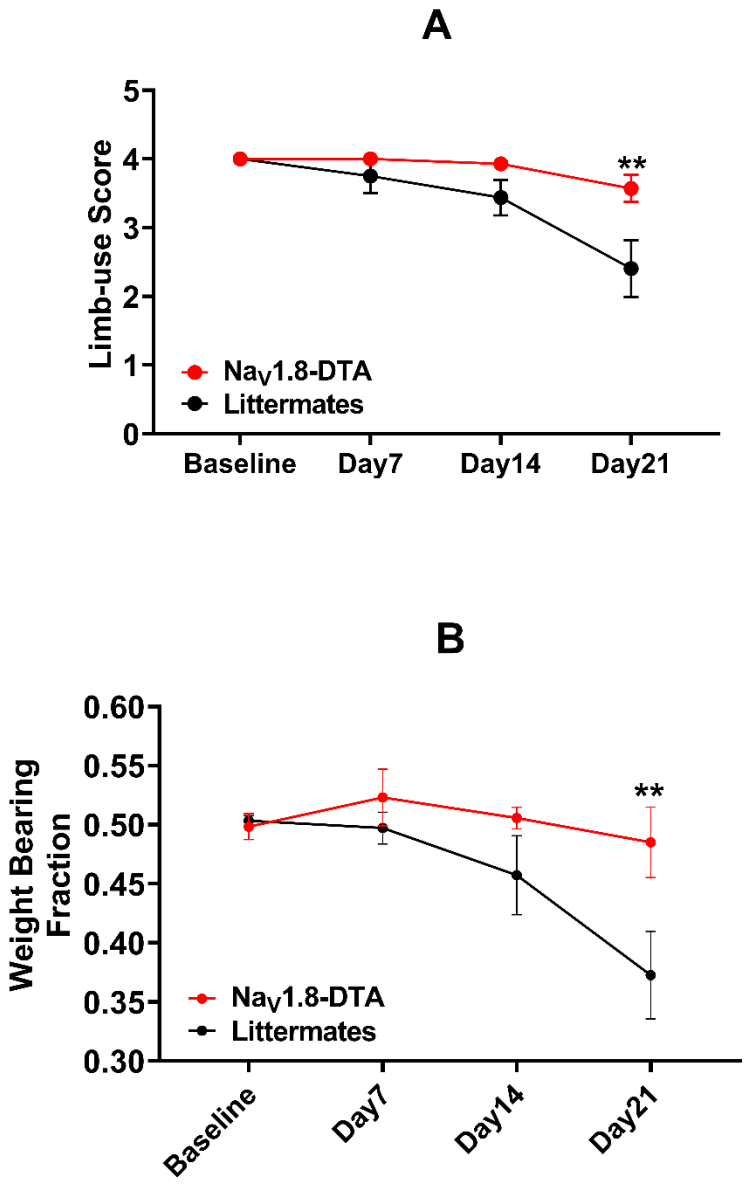

Figure 27: Diphtheria toxin-mediated ablation of Na$_V$1.8-positive nociceptors diminished pain behaviour associated with a mouse model of CIBP. Fifteen mice were used in this study (no mice were excluded for surgical issues). Na$_V$1.8-expressing neurons were ablated in seven mice (Na$_V$1.8-DTA, shown in red, three males and four females), and the remaining were littermates (no ablation of the Na$_V$1.8-positive neurons, shown in black, three males and five females). The limb-use scoring results are shown in Figure A. Additionally, the static weight-bearing behavioural test is illustrated in Figure B.

A) The comparison of the average limb-use score between the two groups over time highlighted a distinct difference between the two groups, with the

Na$_V$1.8-DTA group showing less deterioration in the limb-use (the RMEL analysis, p-value= 0.0615 for the ablation effect and <0.0001 or the time factor). The multiple comparison tests indicated a significant difference in the limb-use score between the two groups on day 21 (adjusted p-value= 0.0017).

B) *The comparison of the average weight-bearing fraction on the affected limb between the two groups over time indicated a distinct difference between them, with an apparent reduced pain-like behaviour displayed by the Na$_V$1.8-DTA group than the control group (the RMEL analysis, p-value= 0.0775 for the column factor and 0.0008 for the time factor (row factor)). The multiple comparisons showed that the DTA group had a significantly higher weight-bearing on day 21 compared to the control group (adjusted p-value= 0.0063).*

DTA: Diphtheria toxin subunit A. Error bars represent the standard error of the mean.

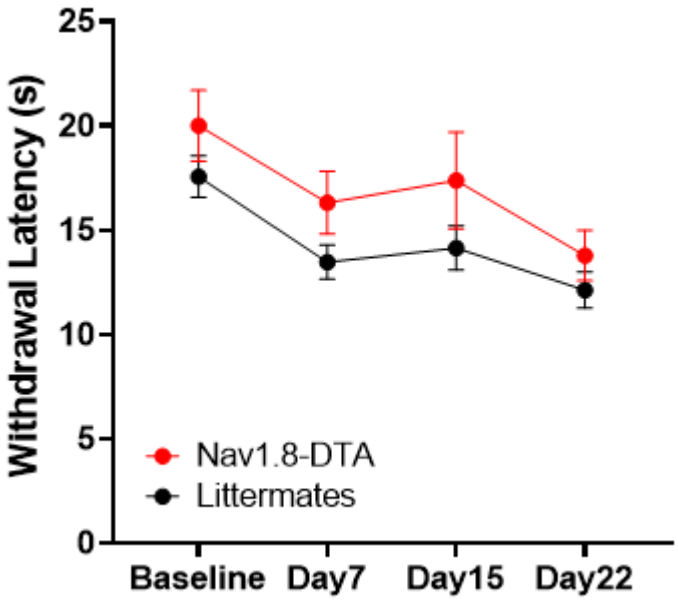

Figure 28: The ablation of the Na$_V$1.8 expressing neurons did not prevent the development of secondary cutaneous cold sensitivity after CIBP. *While the REML analyses indicated that Na$_V$1.8^{DTA} had longer latencies in the dry ice test compared to their littermates over time (p-value= 0.0292), there was no significant difference between the two groups at each time point when analysed using the multiple comparison test. Unlike the Na$_V$1.8^{DTA} group, the drop in the withdrawal latency reached a statistical significance in the littermates group, with*

the average latency time until paw withdrawal being 17.56 s for the littermates in the baseline and 12.12 s on day 22 (p-value= 0.0064, paired t-test). On the other hand, the mean time to withdraw the paw was 20 s in the Na_V1.8-DTA group in the baseline and 13.78 on day 22 (p-value=0.0565, paired t-test). Baseline measurements were taken before the inoculation of the cancer cells into the intramedullary space of the femur. Fifteen mice were used in this study. Na_V1.8-expressing neurons were ablated in seven mice (Na_V1.8-DTA, shown in red, three males and four females), and the remaining were littermates (no ablation of the Na_V1.8-positive neurons, shown in black, three males and five females).

4.4.2. Silencing the Na_V1.8 expressing neurons by chemogenetic tools reduced pain behaviour associated with CIBP

Mice that express the PSAM^4-GlyR channels in the Na_V1.8 expressing neurons were subjected to CIBP surgery. After the surgery, the limb-use scores and the weight-bearing of these mice were assessed. On day seven post-surgery, the use of the affected limb was scored, and no mice were excluded for limping prior to tumour growth. Twelve days after the surgery, mice showed a reduction in limb use as well as the weight-bearing, but the administration of varenicline (0.3 mg/kg, intraperitoneally) significantly increased the mean weight-bearing fraction of these mice (from 0.3751 to 0.4781 by varenicline (p-value= 0.0034)) (Figure 29B). Similarly, on day 15 after the surgery, varenicline injection changed the mean weight-bearing fraction from 0.3035 to 0.3641 (p-value=0.0034) (Figure 29B). Notably, this improved performance was also detected in the limb-use scoring test (p-value=0.0078 on day 12 and 0.01367 on day 15) (Figure 29A). In all these studies, the Wilcoxon matched-pairs signed rank test was used. On the other hand, the intraperitoneal injection of PBS on day 13 after the surgery did

not cause a significant change in either the limb-use score or the weight bearing (Figure 30).

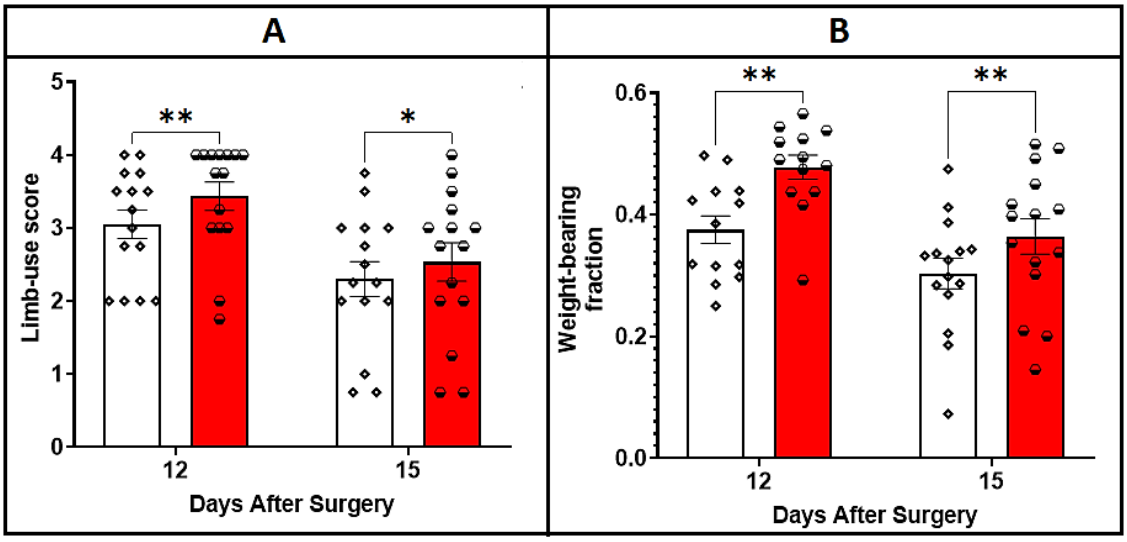

Figure 29: Varenicline partially reversed the reduction in the limb-use score (A) and the weight-bearing (B) in cancer-bearing mice that expressed PSAM^4-GlyR in the Na$_V$1.8-positive neurons. *The white colour shows behavioural results without treatment, while the red colour represents behavioural results after varenicline. Data analysis was done using the Wilcoxon matched-pairs signed rank test. Error bars represent SEM. N=15 (10 females and five males).*

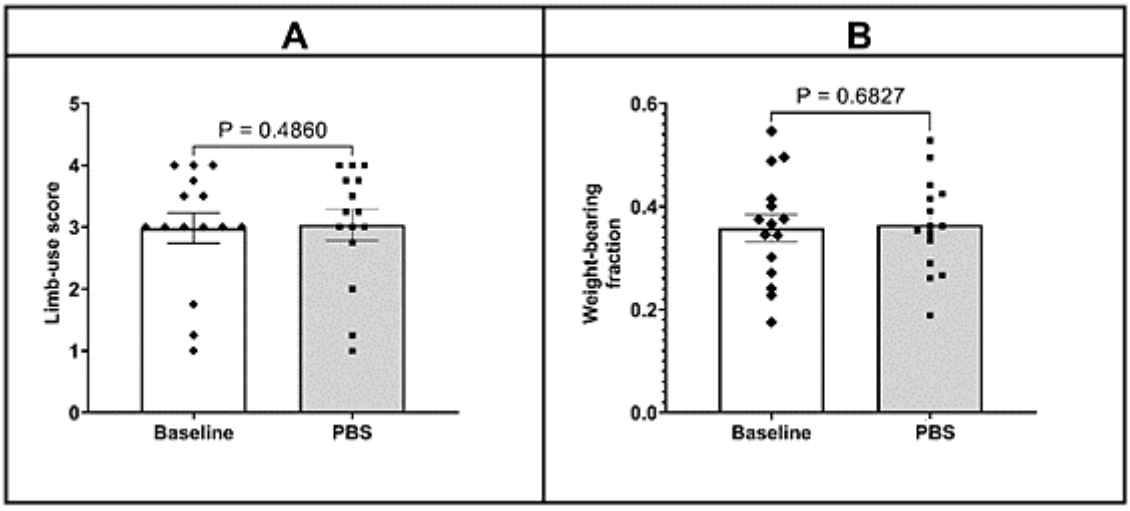

Figure 30: The injection of PBS did not cause a significant change in the limb-use score (A) or the weight-bearing (B) of mice expressing PSAM^4-GlyR in the Nav1.8-positive neurons after CIBP*. p-value=0.4860 (limb-use*

score) and 0.6827 (weight-bearing). Data were analysed using the paired t-test. N=15 (10 females and five males).

4.4.3. Intrathecal Derm-BOT did not cause a significant alteration in the pain-like behaviour after CIBP

For this study, mice underwent the CIBP surgery, and whenever a mouse reached limb-use score 3, it was injected intrathecally with a modified botulinum compound that specifically inhibits the neurotransmission in the μ opioid receptor-expressing neurons (Derm-BOT). The control group for this study involved the use of a botulinum compound that cannot enter the cells, and it was also injected upon reaching limb-use score 3. The comparison between the two treatment groups highlighted no significant difference in the limb-use score, weight-bearing, or the median time needed to reach limb-use score zero (Figure 31). In contrast, the intrathecal injection of morphine improved the limb-use score in mice with CIBP (Figure 32A). The weight bearing was also improved by intrathecal morphine (Figure 32B). It is noteworthy that morphine was administered when mice reached limb-use score 3, which is the same time point used for Derm-BOT administration.

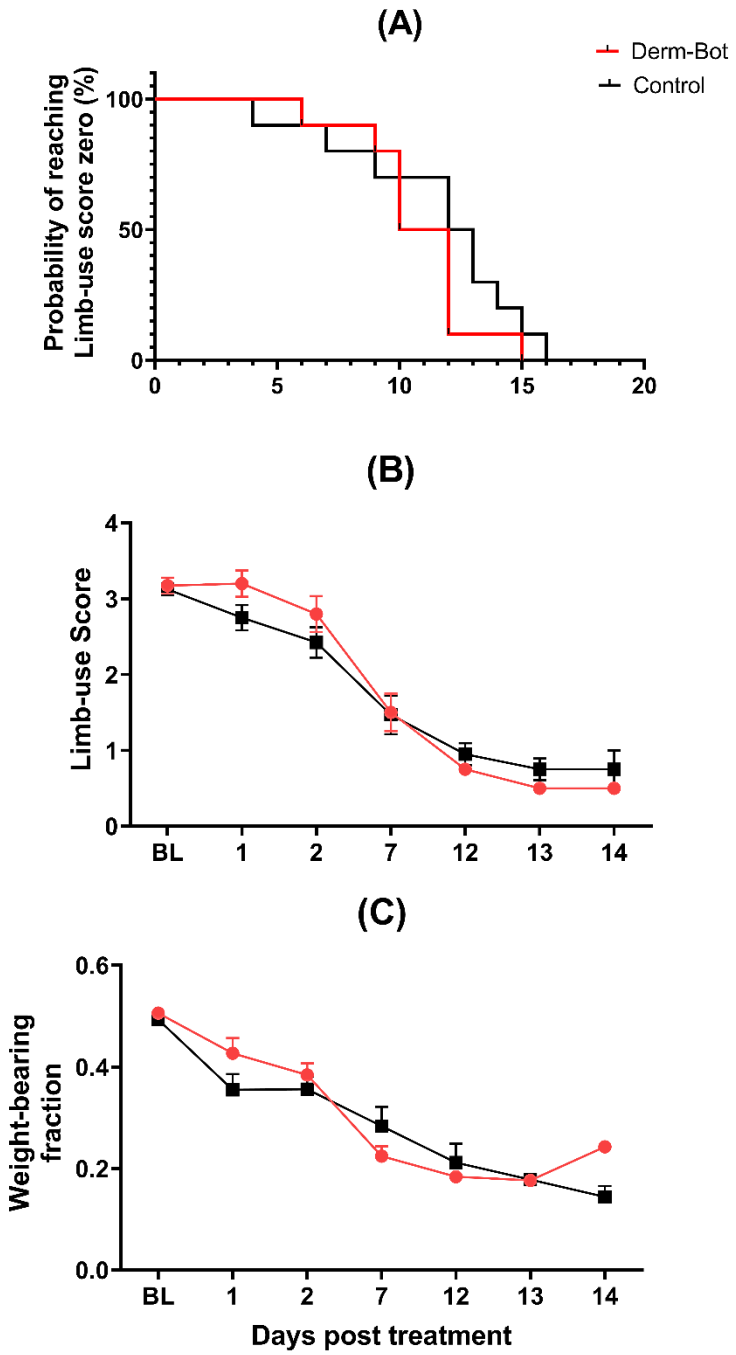

***Figure 31**: **Modified botulinum compounds to silence the μ-opioid receptor-expressing neurons failed to reduce pain-like behaviour in a mouse model of CIBP.** The mice were assessed for recovery from surgery on day 7 after the surgery by measuring the weight-bearing (shown as BL on graph C) and no mice showed signs of limping on that day. After that, the limb use was scored daily using the standard limb-use scoring system. If a mouse reached limb-use score 3 (slight limping), it was injected intrathecally with either 100 ng of Derm-BOT (shown in red) or the molar-equivalent amount of the control (un-conjugated BOT,*

shown in black). Following the intrathecal treatment, several behavioural tests were performed, including the limb-use score (Figure B) and the static weight-bearing (Figure C). A mouse was sacrificed when limb score 0 was reached (Figure A illustrates the time needed to reach limb-score zero after the intrathecal treatment).

A) *The median time needed to reach limb score 0 in the Derm-BOT group was 11 days after the treatment and 12.5 days in the control group. Statistical analyses using the Log-rank (Mantel-Cox) test and the Gehan-Breslow-Wilcoxon test indicated that the difference between the two groups was statistically insignificant (P-values= 0.2545 and 0.3179 for the long-rank and the Gehan-Breslow Wilcoxon tests, respectively).*

B) *The comparison of the average limb-use score between the two treatment groups over time highlighted no significant difference when assessed using the RMEL analyses (the p-value for the treatment effect was 0.7654).*

C) *The comparison of the average weight-bearing fraction on the affected limb between the two treatment groups over time indicated no significant difference between them when assessed using the RMEL analyses (the p-value for the treatment effect was 0.4330).*

Derm-BOT: dermorphine botulinum (a modified botulinum molecule to silence the μ opioid receptor-expressing neurons), BL: baseline (7 days after the surgery), n=10 for each group at the baseline (five males and five females).

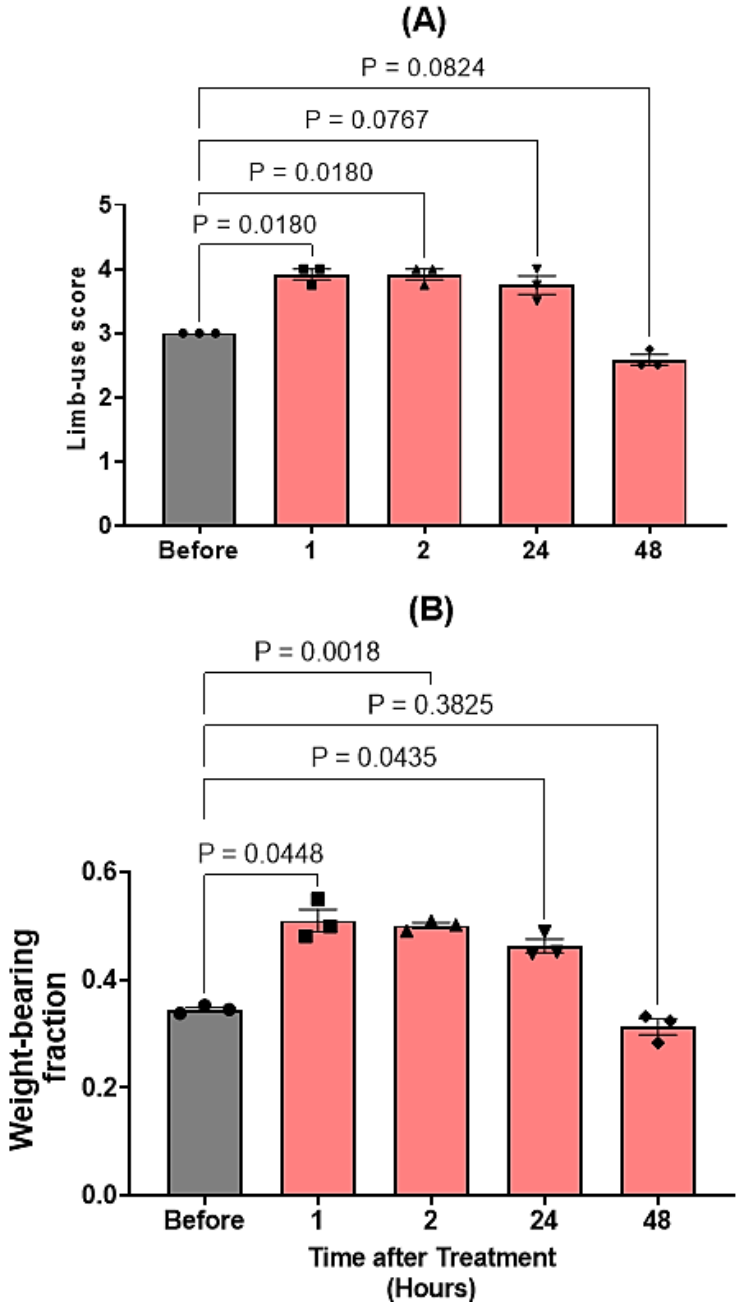

Figure 32: Intrathecal morphine improved limb-use scores (A) and weight-bearing (B) in mice with CIBP. *Morphine was administered intrathecally at a dose of 60ng per mouse when mice reached limb-use score 3. Results were analysed using repeated-measures one-way ANOVA test with multiple comparisons. N=3 (two males and one female). P-values for the one-way ANOVA tests are 0.0034 for the limb-use score test and 0.0061 for the weight-bearing test. The p-values for the multiple comparisons are shown in the figure.*

4.5. Discussion

This chapter aimed to evaluate the role of the μ-opioid receptor-expressing neurons (in the spinal cord) and the $Na_V1.8$-expressing neurons as neuronal subsets that could potentially be contributing to CIBP.

4.5.1. μ-opioid receptor-expressing neurons and CIBP

While the silencing of the μ-opioid receptor-expressing neurons could be a promising analgesic option that lessens problems associated with the intrathecal or systemic administration of opioid agonists (Pope et al., 2016), this approach failed to cause noticeable changes in the pain-like behaviour after CIBP. Problems related to the target itself or the injection technique are unlikely because the intrathecal administration of morphine caused analgesia (Figure 32). Because opioids resulted in a substantial analgesic effect in this work, one should attempt to optimise derm-BOT to be applied in the future for treating CIBP. Firstly, we should stain for c-SNAP25 and co-localise that with μ-opioid receptors. Secondly, and only if c-SNAP25 is detected and co-localised with μ-opioid receptors, the activity of this compound can be tested *in vitro* in cultured μ-opioid receptor-expressing neurons. Thirdly, if the *in vitro* testing gave promising outcomes, different doses of Derm-BOT can be tested *in vivo* using electrophysiological methods to determine a dose that gives a substantial reduction in neuronal activity. After that, the selected dose can be tested in CIBP. Due to time constraints and due to the unavailability of high quantities of Derm-BOT, these experiments were not done in the current report.

4.5.2. $Na_V1.8$-expressing neurons and CIBP

In this work, the role of the $Na_V1.8$-positive neurons in CIBP was evaluated by ablating this subset and by silencing it. The results indicated that the congenital ablation of $Na_V1.8$-expressing neurons, and their silencing, could result in a reduction in pain-like behaviours associated with CIBP, as indicated by the increase in the limb-use score and weight-bearing. Additionally, this work indicates that the ablation of this neuronal subset has little or no favourable effects in secondary cutaneous hyperalgesia that follows CIBP.

4.5.2.1. The congenital ablation of the $Na_V1.8$-expressing neurons in CIBP

4.5.2.1.1. Limb-use and weight-bearing

The current report indicates that the ablation of the $Na_V1.8$-positive neurons improves the limb use and weight-bearing of CIBP mice. These results are different from what had been reported previously. For example, Minett et al. tested the potential analgesic effect of ablating $Na_V1.8$-positive neurons in a mouse model of CIBP and obtained discouraging outcomes (Minett et al., 2014). One possible explanation of the discrepancy between our findings and the published results is the fact that the model used in our report results in a slower decline in the use of the affected limb (and hence a longer time to reach limb-use score zero) when compared to the model used by Minett et al.. Another potential reason for the difference in the outcomes could be the difference in the experimental design between the work by Minett et al. and the work presented here. While the $Na_V1.8^{DTA}$ is similar between the two studies, the littermates are different. In their work, Minett et al. crossed heterozygous $Na_V1.8$Cre mice with homozygous Rosa-flox-stop-DTA, indicating that the littermates were heterozygous Rosa-flox-stop-DTA and lacked the $Na_V1.8$ Cre enzyme. On the other hand, for this work, heterozygous Rosa-flox-stop-DTA mice were crossed with homozygous $Na_V1.8$ Cre mice, entailing that the littermates were $Na_V1.8$ Cre-positive. Thirdly, the degree of ablation of the $Na_V1.8$-expressing neurons might have been different between the two studies. Because Minett et al. did not report data about mRNA levels of $Na_V1.8$ channels or any indication of the degree of neuronal ablation, the comparison between these two studies in this element was hindered.

4.5.2.1.2. Secondary cutaneous cold hypersensitivity

Cold hypersensitivity is seen after several conditions and has been demonstrated to happen after chemotherapeutic treatment. MacDonald et al. showed that cold allodynia that follows the intraplantar injection of oxaliplatin requires silent cold nociceptors that express $Na_V1.8$ channels (MacDonald, Luiz, et al., 2021). They also showed that the ablation of the $Na_V1.8$-positive neurons could lessen this cold allodynia. Also, previous evidence suggests that $Na_V1.8$ channels are linked to cold sensation and that knocking this channel out reduces cold sensitivity (Zhou et al., 2002). For all these reasons, the ablation of the $Na_V1.8$-expressing

neurons was assessed as a tool to reduce the secondary cutaneous cold hypersensitivity associated with CIBP. While the mean withdrawal threshold in the dry ice test had always been higher in the $Na_V1.8$-DTA mice compared to their littermates, both groups showed a degree of secondary cutaneous cold sensitivity after CIBP. Therefore, in my opinion, ablating the $Na_V1.8$-expressing neurons did not prevent the development of secondary cutaneous cold sensitivity after CIBP.

4.5.2.2. Silencing $Na_V1.8$-expressing neurons by chemogenetic tools

Further support to the conclusion that $Na_V1.8$-positive neurons play a role in CIBP is the fact that silencing this neuronal subset by chemogenetic tools improved the use of the cancer-bearing limb as well as the weight-bearing. We, therefore, speculate that these findings could open new doors for finding novel tools for managing CIBP. While delivering chemogenetic tools to the sensory neurons of patients living with CIBP could be a sensible therapeutic option, challenges regarding the safety, cost and applicability of gene therapy tools remain compelling. An alternative way to use the current findings to pave the path for drug discovery would be to check which target/targets in this specific neuronal subset is/are driving this reduction in pain-like behaviour after silencing these neurons. An obvious target would be the $Na_V1.8$ channels themselves. With the current availability of a selective $Na_V1.8$ blocker (Mullard, 2022), this blocker can be tested in CIBP to evaluate its therapeutic applicability for patients living with CIBP.

4.6. Conclusion

This chapter assessed whether the congenital ablation of the $Na_V1.8$-expressing neurons could reduce pain-like behaviour in CIBP, and the results indicated that the diphtheria toxin subunit A-mediated ablation of $Na_V1.8$ neurons ($Na_V1.8^{DTA}$) slowed down the reduction in the limb-use and the weight-bearing after CIBP. While the ablation of this subset in adulthood was not tested here, similar promising results were obtained after silencing the $Na_V1.8$-positive neurons with chemogenetic tools, especially at the early stages of the disease progression. Additionally, the analgesic potential of the modified botulinum compounds that silence the μ-opioid receptor-expressing neurons (Derm-BOT) was assessed in CIBP. While no evidence suggests that MOR+ neurons were silenced by Derm-BOT, our results clearly indicated that Derm-BOT did not cause any noticeable

analgesic effects in our mouse model of CIBP. On the other hand, the intrathecal administration of the μ-opioid receptor agonist, morphine, improved the use of the affected limb as well as the weight-bearing.

5. Dual targeting of NGF and TNFα in CIBP

5.1. Introduction

Drugs to treat pathologies of redundant biological systems often exhibit a high attrition rate in the clinic, mainly because the inhibition of one target can be easily compensated for by other targets (Dyer, 2020). Because the CNS is a redundant system (Mizusaki & O'Donnell, 2021), we, therefore, thought that the simultaneous targeting of several pathways could increase the analgesic efficacy. Additionally, using two compounds at low doses may reduce the off-target effects, leading to safer and more efficacious medications. Also, as shown in section 2.1.4, various interacting mechanisms contribute to CIBP and targeting one mediator may not be ideal for causing noticeable changes in the pain-like behaviour in this model. Therefore, this chapter aims to assess whether targeting two key tumour-derived products could be beneficial for CIBP. The two targets chosen are NGF and TNFα.

5.1.1. The mechanisms of algesia by NGF and TNFα

5.1.1.1. NGF

A critical tumour-derived product in CIBP is NGF, and it can be produced by various types of cancer cells in the bone (e.g., those derived from primary tumours of the breast and prostate). NGF can lead to the sensitisation of sensory neurons directly by increasing the expression of ion channels linked to nociceptive signal transduction and transmission (see Figure 33 for a summary of some of the pain-causing effects of NGF). TrkA, the high-affinity NGF receptor, is expressed in high numbers during the development of neurons (Marmigère & Ernfors, 2007). In adult mice, TrkA expression is almost confined to peptidergic C-fibres and some Aδ-fibres (Averill et al., 1995). NGF seems to have a chief role in multiple pain disorders; for example, NGF is upregulated in cerebrospinal fluid from patients with fibromyalgia (Sarchielli et al., 2007) and synovial fluid samples from arthritis patients (Aloe et al., 1992). What further supports the role of NGF in pain is that NGF or TrkA-null mice are somewhat hypoalgesic (Crowley et al., 1994). Interestingly, humans with mutations in the gene encoding for TrkA have forms of congenital pain insensitivity (Indo et al., 1996). NGF contributes to pain sensation by different mechanisms, including peripheral and central sensitisation. Among the peripheral methods is the ability of NGF to trigger the release of inflammatory mediators (including histamine, serotonin and more NGF) from

immune cells. There is evidence that the production of inflammatory mediators sensitises the surrounding neurons (Kawabata, 2011). Although degranulation of mast cells appears to be the primary cause of the acute effects of NGF administration, this is not the case for bone afferents. Acute effects of NGF on bone afferents appear to be predominantly due to peripheral sensitization (Nencini et al., 2017). Upon the binding of NGF to TrkA expressed on sensory fibres, the complex of NGF and TrkA gets internalised and is retrogradely taken to the soma present in the DRG. Once in the soma, the NGF/TrkA complex alters and/or enhances the expression of many receptors and ion channels implicated in nociception (such as TRPV1, ASIC and VGSCs). The net effect of this enhanced expression is the increase of nociceptor excitability (this is known as peripheral sensitisation). Due to the transcriptional changes caused by NGF/TrkA, neurotransmitters like substance P, CGRP and brain-derived neurotrophic factor are also increased. Accordingly, upon the subsequent stimulation of peptidergic TrkA-positive sensory neurons, the release of peptidergic neurotransmitters at the central terminals is increased. These neuropeptides are released in high quantities along with the excitatory neurotransmitter glutamate, which, under physiological conditions, activates AMPA receptors. The binding of all these peptides to their receptors on the second-order neuron together with glutamate may result in intense depolarisation of the postsynaptic receptors of the second-order neurons. Such strong depolarisations lead to the removal of magnesium ions that block NMDA receptors, allowing glutamate to activate NMDA receptors, which leads to a wind-up effect. As a consequence of the wind-up, the probability of central sensitisation significantly increases, which facilitates the synaptic transmission at the synapses of the dorsal horn and eventually facilitates the transmission of nociceptive signals via the third-order neuron to reach the sensory cortex. Therefore, NGF is implicated not only in peripheral inflammation but also in increasing the excitability of primary afferents by causing various transcriptional changes (Enomoto et al., 2019).

In mouse models of CIBP, the blockade of the interaction between NGF and TrkA by a monoclonal antibody (mAb911, Rinat/Pfizer) successfully reduces CIBP (Jimenez-Andrade et al., 2011; KG et al., 2005). The high-affinity binding between this monoclonal antibody and NGF inhibits the binding of NGF to its receptor,

preventing the downstream effects of TrkA activation. Anti-NGF also reduces the neurochemical markers for peripheral and central sensitisation (Sevcik et al., 2005). It was also shown that bone destruction is reduced in CIBP following the early use of anti-NGF antibody (McCaffrey et al., 2014). Anti-NGF therapy may alleviate hyperalgesia by reestablishing homeostatic μ-opioid receptor expression levels in the DRG, and dorsal horn, as naloxone can antagonise anti-NGF anti-nociceptive effects (Yao et al., 2016). It is important to note that the analgesic effects of anti-NGF antibodies are superior to those of morphine (Sevcik et al., 2005). A humanised form of mAb911 was engineered (named Tanezumab), and it is now being tested in Phase III clinical trials along with opioids for CIBP. The study is a randomised, double-blind, placebo-controlled, multicentre, parallel-group study (Clinical trial NCT02609828). Presently, the clinical trial has ended, and results indicate that subcutaneous tanezumab (20 mg once every 8 weeks) is superior to the placebo in the daily average pain intensity numerical rating score.

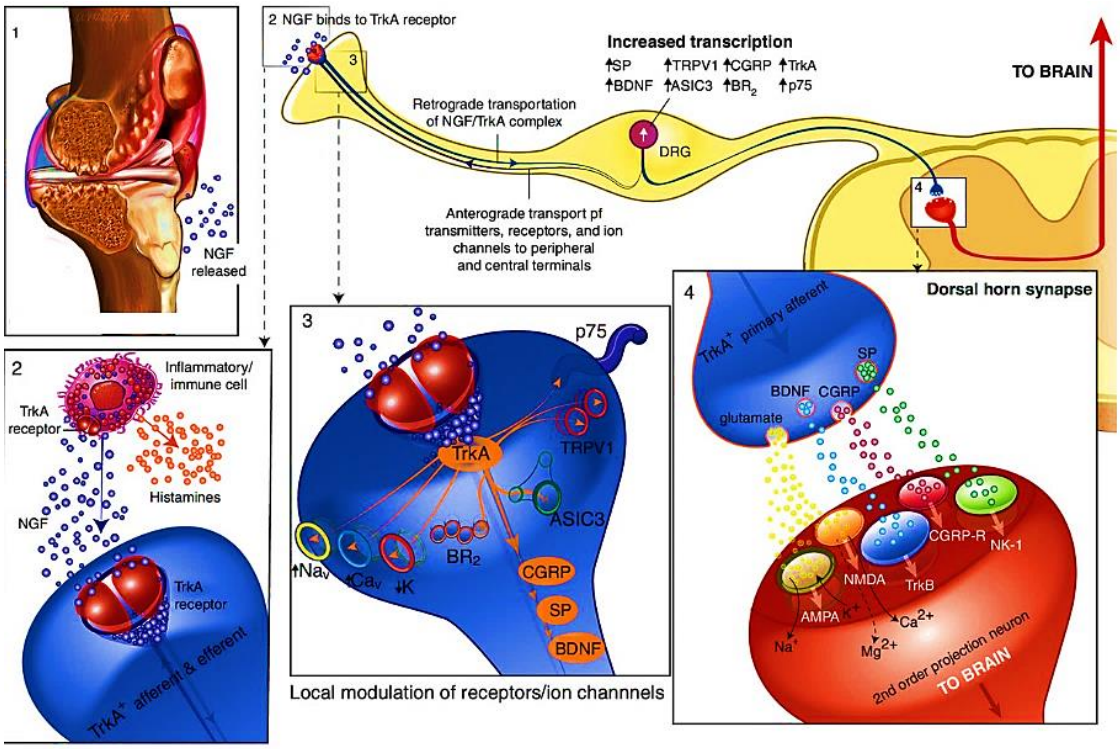

Figure 33: A cartoon showing how the nerve growth factor (NGF) contributes to nociception and neuronal plasticity. *NGF binds TrkA receptors on primary afferents, mast cells, and other immune cells when released peripherally (box 1). NGF promotes the production of inflammatory mediators (including histamine, serotonin (5HT), and additional NGF) when it binds to*

immune cell TrkA receptors (box 2). When NGF binds TrkA on sensory fibres with these receptors, the complex is internalised and retrogradely transported to the DRG soma. Once in the soma, NGF/TrkA complex modifies and/or increases nociception receptors and ion channels (such as TRPV1, ASIC, BR2, Nav, Cav, K and mechanoreceptors). This increased expression leads to peripheral sensitisation of nociceptors (box 3). NGF/TrkA increases SP, CGRP, and BDNF through transcriptional modifications. Upon activation of TrkA-positive peptidergic sensory neurons, central terminals release more peptidergic neurotransmitters, activating peptide receptors (NK1 is activated by SP, CGRP-R is activated by CGRP, and TrkB is activated by BDNF). These peptides are released in high quantities along with the excitatory neurotransmitter glutamate, which activates AMPA receptors. The binding of all these peptides together with glutamate may result in intense depolarisation of the postsynaptic receptors of the second-order neurons located at the dorsal horn of the spinal cord (box 4). Strong depolarisations remove magnesium ions that inhibit NMDA receptors, allowing glutamate to activate them, causing wind up. The wind-up increases the possibility of central sensitisation, which enhances synaptic transmission at the dorsal horn synapses and nociceptive signal transmission via the third-order neuron to the sensory cortex. NGF causes transcriptional alterations that increase primary afferent excitability and peripheral inflammation. Abbreviations: 5-HT (5-hydroxytryptamine), AMPA (α-amino-3-hydroxy-5-methyl-4-isoxazole propionic acid), ASIC (acid-sensing ion channel), BDNF (brain-derived neurotrophic factor), BR2 (bradykinin receptor 2), Cav (voltage-gated Ca^{2+} channel), CGRP (calcitonin gene-related peptide), CGRP-R (calcitonin gene-related peptide receptor), DRG (dorsal root ganglia), K (delayed-rectifier K^{+} channel), Nav (voltage-gated Na^{+} channel), NMDA (glutamatergic N-methyl-D-aspartate), NGF (nerve growth factor), NK-1 (neurokinin 1 receptor), p75 (neurotrophin receptor), SP (substance P), trkA (tropomyosin receptor kinase A), TrkB (tropomyosin receptor kinase B) and TRPV1 (transient receptor potential vanilloid 1). Adapted from (Enomoto et al., 2019).

5.1.1.2. TNFα

Several changes occur in the microenvironment as the tumour grows. Chemotaxis of immune cells (including macrophages, leukocytes, and thrombocytes) and the release of inflammatory mediators such as cytokines are

among these alterations (Alexander et al., 1998). TNFα is one of the cytokines contributing to pain in bone cancer models. TNFα contributes to pain sensation by acting on both peripheral and central nervous systems. Regarding peripheral effects, intraplantar, intradermal, endoneurial, or intramuscular injections of TNFα cause heat hyperalgesia and mechanical allodynia (L. Zhang et al., 2011). In addition, TNFα affects several ion channels like VGSCs (increases TTX-resistant sodium currents) and K^+ channels (diminishes outward K^+ currents) (Czeschik et al., 2008) and results in the spontaneous firing of primary sensory neurons. In conjunction with its peripheral effects, TNFα seems to have central effects since it can enhance synaptic transmission and cause hyperexcitability of dorsal horn neurons. Multiple observations highlight the central role of TNFα in pain. Firstly, in many chronic pain syndromes, TNFα is elevated in the spinal cord's glial cells. Secondly, injecting TNFα intrathecally generates thermal hyperalgesia and mechanical allodynia. Thirdly, chronic pain can be diminished following the intrathecal injection of the inhibitor of TNFα, etanercept. Fourthly, experiments on spinal cord slices showed that when TNFα is perfused, the spontaneously-generated excitatory postsynaptic currents were increased, and also, the currents due to the activation of NMDA receptors in lamina II neurons were amplified. Furthermore, TNFα released during inflammation increases the GluR1 AMPA receptor trafficking within the spinal cord dorsal horn (Haroun et al., 2022). TNFR1 and TNFR2 are the two primary receptors for TNFα (Gough & Myles, 2020). It was discovered that these two receptors play essential roles in inflammatory pain disorders, with TNFR1 contributing to all phases of pain and TNFR2 just to the early phase. These results were achieved using knockout mice that were injected intraplantarly with formalin, complete Freund's adjuvant, or TNFα (L. Zhang et al., 2011). When it comes to their effects on bone cells, TNFR1 and TNFR2 have opposite effects on osteoclast formation and function, with TNFR1 being a positive regulator of osteoclast function while TNFR2 is an inhibitor. Despite the fact that TNFα binds TNFR2 with higher affinity than TNFR1, TNFR1 is considered the chief receptor for TNFα signalling in the vast majority of cells. Thus, more work has been done to decode the signalling pathways that TNFR1 activates, while TNFR2 has received less interest. The mechanism by which TNFR2 inhibits osteoclastogenesis needs to be investigated especially because TNFR2 activates NF-κB; one of the most potent transcriptional factors

needed for the formation, activation and survival of osteoclasts (Franzoso et al., 1997; Jimi et al., 1998; Miyazaki et al., 2000).

In CIBP, TNFα contributes to heat hyperalgesia. In general, tumour growth induces heat hyperalgesia and mechanical allodynia, which correspond strongly with the extent of bone damage (see section 2.4.1). The data indicate that TNFα plays a major role in heat hyperalgesia in these mice. The TNF inhibitor, etanercept, appears to inhibit the initiation of heat hyperalgesia rather than reverse it. *In vitro* experiments also validated the reduction in heat sensitivity of nociceptive fibres following etanercept administration. TNFα considerably raised the heat response magnitudes of a large proportion (42%) of C fibres in less than 10 minutes after its addition to sensory neurons derived from healthy mice *in vitro*. The mechanisms underpinning TNFα's function in heat hyperalgesia include sensitising and raising the number of TRPV1 channels on nociceptor membranes. The sensitisation of TRPV1 channels was validated *in vitro*, as the currents obtained from heat-sensitive neurons rose significantly after TNFα application, and their activation threshold decreased from 43° without TNFα to 41°C after TNFα. SB203580 and BIM1 inhibited the effects of TNFα on the heat stimulation of sensory neurons *in vitro*, suggesting that the TNFα-induced sensitisation of TRPV1 channels in sensory neurons is mediated by a mechanism that requires p38 MAP kinase/PKC pathways. PKC is capable of phosphorylating TRPV1 channels, and so altering their activity (Bhave et al., 2002; Tominaga et al., 1998). On the other hand, there are phosphorylation sites within the intracellular domains of TRPV1 channels that do not represent reaction sites for PKC, PKA (protein kinase A), or CaMKII (Ca^{2+}/calmodulin-dependent protein kinase II). These intracellular locations may be the targets that p38 MAP kinases react against. The speed with which TNFα increases the sensitivity of sensory neurons highlights the significance of the TRPV1 sensitisation mechanism, as the timeframe is too short to be explained by transcriptional or translational modifications of the channel but rather by a post-translational enhancement of the already-present TRPV1 channels. The administration of TNFα (10 ng/ml) for 1 and 2 hours increases the surface expression of TRPV1 channels via a post-transcriptional mechanism, which is another mechanism of action of TNFα on TRPV1 on DRG neurons. In multiple models of inflammatory pain, it has been demonstrated that TRPV1 expression increases via a post-

transcriptional mechanism (Chuang et al., 2001; Davis et al., 2000; Ji et al., 2002). Importantly, TNFα mediates its effects in heat hyperalgesia in bone cancer models via TNFR2. In addition, mouse models of fibrosarcoma showed that TNFα contributes to mechanical hypersensitivity in these mice. It was also shown that the use of a soluble receptor of TNFα attenuated mechanical hyperalgesia. The soluble receptors prevent the interaction between the surface receptors of TNFα and TNFα (Wacnik et al., 2005).

TNFα could therefore be an important contributing factor to bone pain. Inhibiting the effects of TNFα could be achieved by using mAbs against it, or alternatively, the soluble TNFR1 could be targeted instead of targeting TNFα directly (Feige et al., 2000; Romas et al., 2002).

5.2. Aims

Because of their contribution to CIBP, NGF and TNF represented attractive targets for CIBP. Backed by the potential repurposing of bispecific antibodies that target these two mediators simultaneously, this work aimed to assess whether the dual inhibition of these mediators could reduce pain-like behaviours associated with CIBP as well as signs of secondary cutaneous hyperalgesia. For this, MEDI-578 was used to inhibit NGF, and etanercept, which can also bind TNFβ, was used to inhibit TNFα.

5.3. Methods

The CIBP surgery, behavioural tests, and statistical analyses were carried out as previously described in section 2.3. Drugs (etanercept (10mg/kg), MEDI-578 (3mg/kg), control antibody (NIP-228 (Isotype control antibody for MEDI-578)), or PBS were administered intraperitoneally ten days after the surgery. For the qPCR experiments, the TaqMan probe for TNFα (ThremoFisher, catalogue number 4331182) was used with the same reaction mixture ratios shown in section 3.3.2. All mice included in this study were wild-type C57BL/6 (8-10 weeks old on the surgery day), and the total number of mice included in this study was 52 mice (Control antibody (n=10, five males and five females), PBS (n=13, six males and seven females), MEDI578 (n=13 six females and seven males), etanercept (n=13 six males and seven females), and the combination (n=13 six females and seven males)). The mice were purchased from Charles River. The doses of MEDI578 and NIP-228 were chosen as these doses gave positive results in a previous

study from our lab (Ter Heegde et al., 2019), while the dose of etanercept was chosen because previously a total amount of ~15 mg/kg of etanercept was reported in a mouse model of CIBP (Yang et al., 2017).

5.3.1. DRG sections preparation and staining

The lumbar DRGs (L2-L4) were extracted and placed in 4% paraformaldehyde (Sigma-Aldrich) dissolved in 0.1M phosphate-buffered saline (PBS) (pH = 7.4) (overnight at 4 C°). The solution was then removed, and the DRGs were kept overnight in 30% w/v sucrose in 0.1M PBS at 4°C. following that, the DRGs were removed from the sucrose solution and were inserted in moulds containing O.C.T. embedding compound (Tissue-Tek®, Sakura) and left on dry ice, then stored at -80°C until sectioning. The whole DRG was sectioned at 11µm thickness and was collected on electrostatically charged slides (Superfrost® Plus, Thermo-Scientific). Slides were permitted to dry at room temperature and then stored at -80°C till needed. The sections were then washed using 1x PBS (three times, for five minutes each at room temperature). Then the sections were permeabilised using 1% Tween in 1xPBS (for 1 hour at room temperature). Following that, the sections were washed using 1xPBS for 5 minutes at room temperature. The non-specific binding was blocked by the application of a blocking buffer at 4°C overnight. The blocking buffer was prepared using 5% w/v milk powder (Sigma) in 1% tween 20 in 1xPBS. Then the sections were incubated in the diluted primary antibody solution dissolved in blocking buffer (overnight at 4°C). The primary antibody against ATF3 was Rabbit anti-ATF3 (1:500; Santa Cruz Biotechnology, USA, sc-188). The sections were then washed using 0.1% tween 20 in 1x PBS (three times, 10 minutes each, at room temperature). The sections were then incubated in a solution of the blocking buffer that contained the secondary antibody and DAPI (1: 5000, Invitrogen, D3571). The secondary antibody was donkey anti-rabbit 488 (1:1000, ThermoFisher, A-21206).

The slides were kept in the dark (overnight at 4°C). The slides were then washed three times (5 minutes each at room temperature). They were allowed to dry before the mounting medium was added). Images were then acquired using a Leica confocal microscope. Cells were deemed ATF3 positive when the signal was ≥ four times the background signal.

5.4. Results

5.4.1. The simultaneous inhibition of NGF and TNFα increased the median time needed to reach limb-use score zero after CIBP

As NGF and TNFα play essential roles in CIBP, the aim was to investigate whether blocking these two tumour-derived products could reduce the pain phenotype in our mouse model of CIBP (Figure 34). Etanercept and MEDI-578 were used to inhibit TNFα and NGF, respectively. The synergy between MEDI-578 and Etanercept was evident as the combination was the only treatment option that resulted in a significant increase in median time needed to reach limb-use score zero after CIBP, compared to the control group (Figure 34A), with the median time needed to reach limb-use score zero in the control group being 22 days after the surgery and 27 days in the combination-treated group. The median time needed to reach limb-use score zero in the etanercept-treated group was 23 days after the surgery, while that of the MEDI-578-treated group was 25 days.

5.4.2. Inhibiting NGF and/or TNFα slowed down the reduction of the use of the cancer-bearing limb and the weight bearing

The administration of Etanercept (a protein that inhibits TNF) and/or MEDI-578 (anti-NGF) reduced the pain-like behaviours associated with CIBP (weight-bearing (Figure 34B) and limb-use score (Figure 34C)) compared to the control group. The co-administration of MEDI-578 and Etanercept always resulted in a more profound reduction in the pain phenotype compared to each treatment separately. This improvement was statistically significant compared to Etanercept alone (p-value= 0.0070, RMEL for the weight-bearing test in the period between day 8 to day 22 after the surgery, Figure 34B).

5.4.3. Secondary cutaneous heat hypersensitivity is prevented by the co-administration of MEDI-578 and Etanercept

The administration of Etanercept (a protein that inhibits TNF) and/or MEDI-578 (anti-NGF) reduced secondary cutaneous heat sensitivity (Figure 34D) significantly compared to the control group when tested using the Hargreaves' test. The combination treatment reduced the secondary cutaneous heat sensitivity to the extent that it reached statistical significance compared to Etanercept alone (Figure 34D) (p-value= 0.0097, RMEL (day8-day22 after surgery)). While the performance of MEDI-578 was impressive, it was still less effective than the combination treatment, as there had been a consistent trend of

improved performance in the group treated with the combination. The superiority of the combination treatment compared to the use of MEDI578 alone was convincing in the Hargreaves' test, with the RMEL analysis showing a p-value of 0.0263 when the two groups are compared after the CIBP surgery (day 8-day22) (Figure 34D).

5.4.4. The administration of MEDI-578 and/or Etanercept did not cause a significant change in the mRNA levels of TNFα in the spinal cord

Because previous reports from a mouse model of CIBP indicated that etanercept reduces the mRNA levels of TNFα in the spinal cord (Yang et al., 2017), this was measured in the current study. While the mRNA levels of TNFα in the spinal cord were less in the mice treated with etanercept and anti-NGF compared to the control group, this difference was not significantly significant (p-value=0.7111, multiple comparisons after the one-way ANOVA test) (Figure 35).

5.4.5. The co-administration of MEDI-578 and Etanercept reduced the expression of the neuronal injury marker ATF3 in the ipsilateral DRG neurons after CIBP

Previous reports from a mouse model of CIBP indicated that anti-NGF antibodies reduce the expression of ATF3 in the ipsilateral DRG neurons of cancer-bearing mice; we, therefore, thought to assess the ATF3 levels in the ipsilateral DRG neurons in our current study (Sevcik et al., 2005). The combination treatment reduced the expression of the neuronal injury marker ATF3 in the ipsilateral DRG neurons (L2-L4) of mice after CIBP, while the use of either etanercept or MEDI-578 separately did not significantly alter the ATF3 levels compared to the control group (Figure 36).

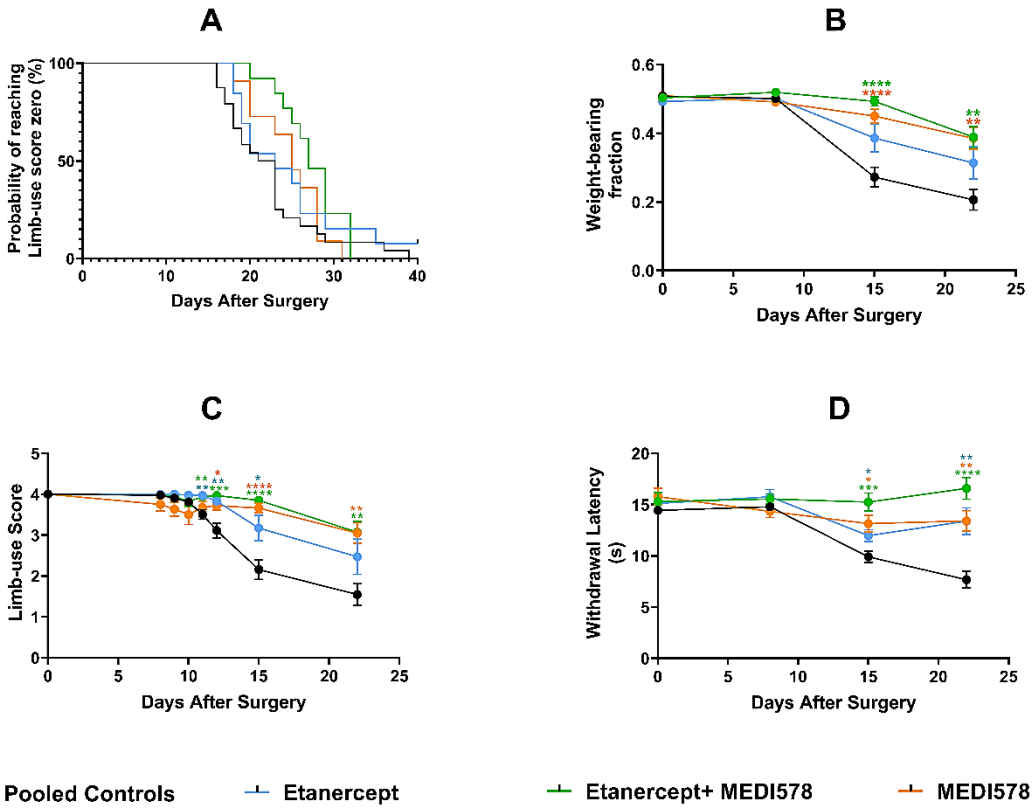

Figure 34: The dual inhibition of NGF and TNF reduced heat hypersensitivity and pain-like behaviours associated with CIBP. A) An analysis of the time needed to reach limb-use score zero after the CIBP surgery. *The median time needed to reach limb-use score zero for the mice that received anti-NGF (MEDI578) + Etanercept (a protein that inhibits the binding of TNF to its receptors) was 27 days, which was significantly longer than the control group (Gehan-Breslow-Wilcoxon test (p-value= 0.0026) and Log-rank Mantel-Cox test (p-value= 0.0357). The median time needed to reach limb-use score zero for the control group was 22 days after the surgery.* ***B) Antagonising NGF, TNF or both slowed down the reduction in the weight put on the ipsilateral limb after CIBP.*** *Compared to the control group, the etanercept-treated group had significantly higher mean weight-bearing results (the RMEL, p-value=0.0095). Similarly, the mice treated with MEDI578 showed a significantly less drop in the weight-bearing (the RMEL, p-value=0.0002). The combination of MEDI578 and Etanercept also had a higher fraction of weight put on the ipsilateral limb compared to the controls (p-value=<0.0001). Mice treated with the combination of Etanercept and MEDI578 had a statistically significant higher weight-bearing performance than the ones treated with Etanercept alone (p-value=0.0049, the RMEL), but not compared to the mice treated with MEDI578*

alone (p-value= 0.1886). ***C) Blocking NGF, TNF, or both slowed down the reduction in the limb-use score associated with CIBP.*** *Compared to the control group, the etanercept-treated group had a significantly higher mean limb-use score (the RMEL, p-value=0.0029). Similarly, the mice treated with MEDI-578 showed significantly less drop in the use of the affected limb (the RMEL, p-value=0.0275). The combination of MEDI578 and Etanercept also had better use of the affected limb compared to the controls (p-value=0.0002). Mice treated with Etanercept, and MEDI578 did not significantly improve the limb-use score statistically compared to those treated with MEDI578 alone (p-value=0.1691, the mixed-effects model) or Etanercept alone (p-value= 0.1298).* ***D) The concurrent application of MEDI-578 and Etanercept prevented the development of secondary cutaneous heat hyperalgesia associated with CIBP.*** *The application of MEDI578 significantly diminished heat hyperalgesia associated with CIBP compared to the control group (p-value=0.0007). Similarly, Etanercept significantly lessened heat hyperalgesia associated with CIBP compared to the control group (p-value=0.0003). The simultaneous application of MEDI-578 and Etanercept prevented the development of secondary cutaneous heat hyperalgesia entirely and had a significantly improved effect compared to Etanercept alone (p-value= 0.0097) and MEDI578 alone (p-value=0.0263). To compare the combination with etanercept or MEDI-578, the RMEL was conducted for the period between day 8 and day 22 after the surgery.*

The asterisks of significance shown in the figure represent the post hoc analysis results comparing each treatment with the control group at each time point. n=13 in each group at the baseline (except for the control group (n=23)). Doses: Etanercept (10mg/kg) and MEDI-578 (3mg/kg). The drugs were injected intraperitoneally on day ten post-surgery. Control antibody (n=10, five males and five females), PBS (n=13, six males and seven females), MEDI578 (n=13, six females and seven males), etanercept (n=13, six males and seven females), and the combination (n=13 six females and seven males). In this study, no mice were excluded due to limping issues on day 7 post-surgery.

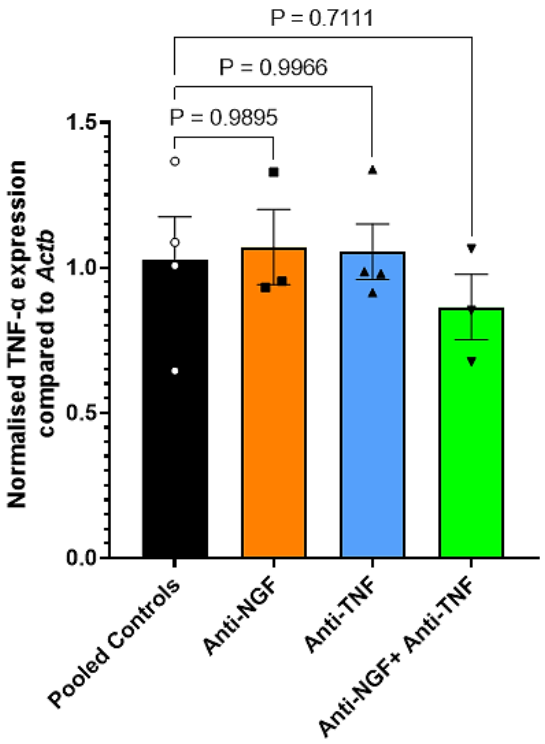

Figure 35: No significant difference was detected in the mRNA levels of TNFα in the spinal cord (L2-L4) between mice treated with anti-NGF, anti-TNF or their combination. *(p-value= P=0.6860, Ordinary one-way ANOVA with multiple comparisons (p-values for the multiple comparisons are shown in the figure)). N=4 for the control group and the anti-TNF groups and 3 for the other groups.*

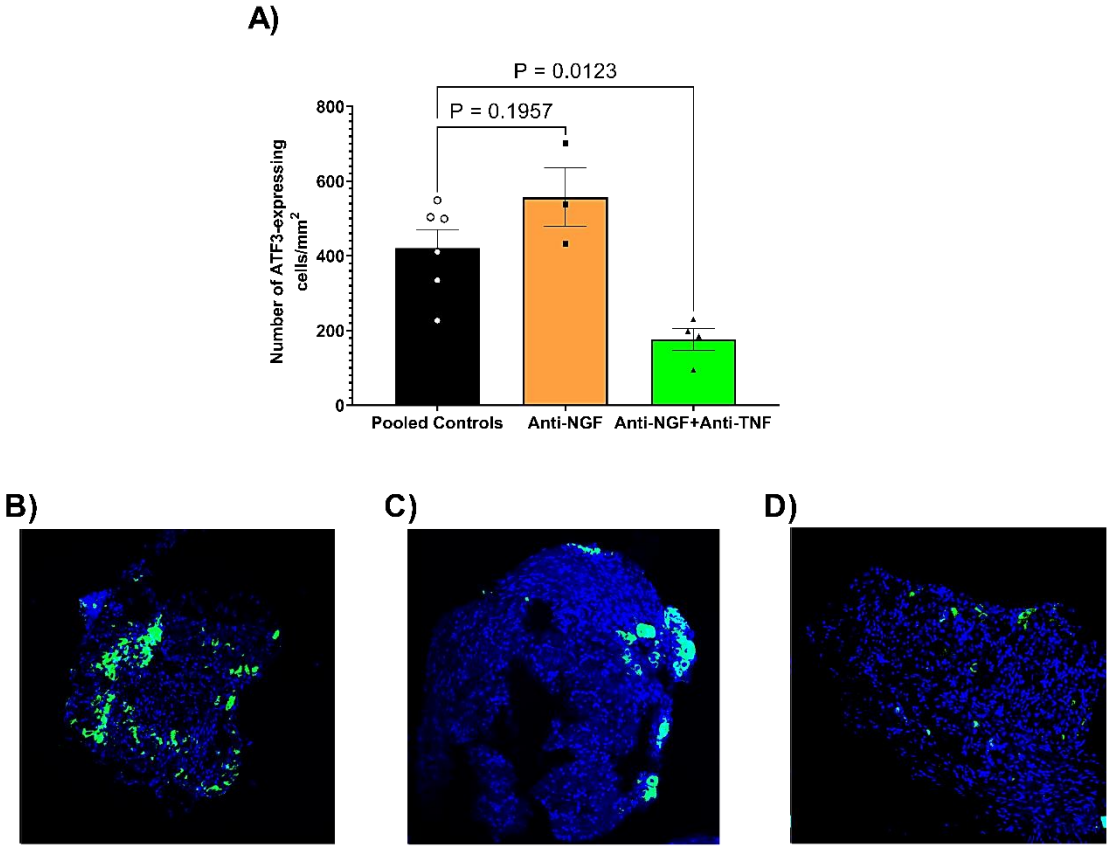

Figure 36: The simultaneous treatment with etanercept (anti-TNF) and MEDI-578 (anti-NGF) reduced the expression of ATF3 in the ipsilateral DRG neurons (L2-L4) of mice after CIBP in the femur when tested using immunostaining.

A) A comparison of the number of ATF3+ DRG neurons between different treatment groups. Statistical analyses were done using the one-way ANOVA test with multiple comparisons. ATF3: Activating Transcription Factor 3, and it is a marker of amputated sensory neurons. N=5 for the control group, n= 4 for the anti-NGF+ anti-TNF group and 3 for the anti-NGF group.

B-D) Representative DRG sections from control (B), anti-NGF-treated (C), and anti-NGF and etanercept-treated (D) mice. Blue colour represents DAPI while green colour represents ATF3.

5.5. Discussion

This chapter aimed to evaluate whether the simultaneous targeting of NGF and TNFα could be a potential analgesic tool for CIBP. The hypothesis behind the inhibition of NGF is backed up by previous findings, which indicate that in CIBP, inhibiting NGF actions reduces neuromas (Mantyh et al., 2010), prevents central sensitisation (Sevcik et al., 2005), and reduces the NGF-mediated neurotransmitters and ion channel expression elevation. Also, this target is validated by human genetics as loss of function mutations in the receptor TrkA are linked to pain insensitivity, mainly because this mutation leads to neurodegeneration of TrkA-positive neurons (Franco et al., 2016). On the other hand, inhibiting the binding of TNF to its receptor carries countless benefits in CIBP (Yang et al., 2017), like the prevention of secondary cutaneous heat and mechanical sensitivity.

While the results from this study fit with the published literature in terms of the promising behavioural outcomes in CIBP following the administration of either etanercept or anti-NGF antibodies, the follow-up studies showed different results. Firstly, it was previously reported that anti-NGF antibodies reduce ATF3 expression in the ipsilateral DRG neurons in CIBP (Sevcik et al., 2005). But the results from my experiments did not show a reduction of ATF3 expression in the anti-NGF-treated mice. Secondly, anti-TNF was shown to reduce the mRNA levels of TNFα in the spinal cord (Yang et al., 2017), but I did not detect any significant reduction in the TNFα expression following the treatment with etanercept. One possible reason for the difference in the study outcomes could be that in these previous studies, the authors reported multiple dosing of anti-NGF or etanercept, but here, mice were treated only once. Also, in the studies by Yang et al. and Sevcik et al., the tissue samples (i.e., the DRGs or the spinal cord) were collected on day 14 after the surgery. Herein, the samples were collected at the end of the study (when the mice reached limb-use score zero). Because the median time needed to reach limb-use score zero in the etanercept and the anti-NGF groups was 23 days and 25 days, respectively, this indicates that I collected the samples after a significantly longer time compared to the previous reports. This delayed sampling may have contributed to the differences observed in the expression analysis results.

To the best of my knowledge, this is the first study that assessed the analgesic efficacy of targeting NGF and TNF simultaneously. Results indicated that this combination, unlike targeting a sole mediator (i.e., TNF or NGF), significantly increased the time needed to reach limb-use score zero after the CIBP surgery in C57BL/6 mice. These results indicate that mice treated with etanercept and MEDI-578 concurrently demonstrated significantly less pain-like behaviour. Also, the combination-treated mice had considerably less secondary cutaneous heat hypersensitivity compared to those treated with MEDI-578 or etanercept alone.

5.6. Conclusion

The simultaneous use of etanercept to inhibit the tumour necrosis factor and the use of monoclonal antibodies against the nerve growth factor (MEDI-578) resulted in an impressive reduction in the pain phenotype associated with CIBP and prevented the development of secondary cutaneous heat hyperalgesia. The analgesic potential of the combination of etanercept and MEDI-578 was convincingly superior to the use of each one of the two treatment options separately.

A bispecific antibody, named MEDI7352, that targets NGF and TNF is currently being clinically tested to treat painful osteoarthritis of the Knee (ClinicalTrials.gov Identifier: NCT04675034). Given the good preclinical results of the dual targeting approach in CIBP, MEDI7352 could be repurposed from osteoarthritis to help patients living with CIBP.

6. Chemogenetic tools for pain research

6.1. Introduction

The term ‘chemogenetics’ refers to the use of chemical compounds to control engineered proteins (Roth, 2016; Sternson & Roth, 2014). In a chemogenetic tool, two key characteristics are needed (Atasoy & Sternson, 2018). Firstly, a receptor that is not active in the absence of the drug molecule. Secondly, the drug molecule should only act on the chemogenetic receptors and should lack any off-target effects.

The earliest chemogenetic tools used were the receptor activated solely by synthetic ligands (RSSALs) (Coward et al., 1998). Among the most important RSSALs is the receptor based on the structure of kappa opioid receptors, which belong to the GPCR superfamily. The synthetic ligand used for these RSSALs is spiradoline (Zhao et al., 2003). The main issue with those was that they were not of great applicability in the field of neuroscience. Because the ligand is active on kappa opioid receptors, which are expressed in many neuronal populations, the agonist use could alter the activity of some neurons that lack the engineered receptors (Sternson & Roth, 2014). In addition, RSSALs suffered from the problem of constitutive activity (Hsiao et al., 2008). To understand the concept of constitutive activity, one should understand the states in which GPCRs exist. GPCRs are found in equilibrium between two states: a ground state and an active state. Usually, the active state is stabilised by agonists, both partial and full. However, in the case of constitutive activity, the active conformation is found even without an agonist. The active state can then promote the formation of a signalling complex that leads to the activation of the downstream effector system of the GPCRs (Seifert & Wenzel-Seifert, 2002). As the main aim of using chemogenetics is to have complete control of the activity by applying the drug, constitutive activity appears as the main problem with a patient potentially being put at risk by the lack of temporal control, which makes the chemogenetics tool irreversible. Even though more RSSALs were developed (Gao et al., 2006; Kristiansen et al., 2000), and they were based on various receptors, they still did not have great popularity in the field of neuroscience due to the low potency (Kristiansen et al., 2000) and/or modest signalling (Airan et al., 2009).

The second revolutionary step in the field of chemogenetics started with the discovery of the designer receptor exclusively activated by designer drugs (DREADDs) technology (Alexander et al., 2009). DREADDs are engineered proteins that can be activated by clozapine N-oxide (CNO). All the first-generation DREADDs are based on muscarinic acetylcholine receptors (AChRs). The ligand-binding domain (LBD) was engineered to abolish the responsiveness to ACh, the natural ligand, and make the receptors respond only to CNO (Thompson et al., 2018). There are three main DREADDs with applications in the field of neuroscience, and these are hM3Dq, hM4Di, and GsD. hM3Dq DREADDs rely on engineered human muscarinic acetylcholine receptors type 3, which are coupled to Gαq, which results in increasing the intracellular Ca^{2+} concentration. This DREADD has been shown to activate neurons both *in vitro* and *in vivo (Kong et al., 2012; Sasaki et al., 2011)*. The mechanism of the enhanced firing can, in part, be explained by the reduction of the M-current (a type of K^+ current) (Brown & Adams, 1980), which is sensitive to phosphatidylinositol 4,5-bisphosphate (PIP2) (Zhang et al., 2003). The function of those M-currents is to diminish neuronal excitability (Hille, 1992). This K^+ current reduction occurs because CNO treatment of hM3D-expressing cells converts phosphatidylinositol 4,5-bisphosphate (PIP2) to inositol trisphosphate (IP3) (Atasoy & Sternson, 2018). In addition, IP3 releases Ca^{2+} from internal stores (Luyten et al., 2017). Such internal Ca^{2+}release can activate the Na^+/Ca^{2+} exchanger (Blaustein & Lederer, 1999), which is electrogenic and can result in a depolarising inward current upon rises in intracellular Ca^{2+} concentration (Lee & Boden, 1997; Niggli & Lederer, 1993). Activation of dopamine neurons in the periaqueductal grey/dorsal raphe was also attempted using the hM3Dq/CNO system, and anti-nociceptive effects were evident (C. Li et al., 2016).

The hM4Di DREADDs are Gi-coupled. The application of CNO to hM4Di-expressing neurons results in hyperpolarisation through the activation of inwardly rectifying K^+ channel activation (Armbruster et al., 2007). hM4Di was extensively used in the pain field; for example, to silence TRPV1-expressing sensory neurons, a single CNO dose greatly elevated the pain threshold of these mice and reduced their excitability, resulting in analgesia lasting up to 3 hours. Notably, CNO-independent effects were detected, such as significant changes in Na^+ current, enhanced $Na_V1.7$ expression, and diminished voltage-gated Ca^{2+}

channel conductance. In addition, endogenous Gi-coupled signalling was impaired in hM4Di-expressing neurons (Atasoy & Sternson, 2018).

The third important DREADD in the field of neuroscience is the chimeric GsD (rM3Ds) which is coupled to Gαs that increases the intracellular concentration of cyclic adenosine monophosphate (cAMP) upon the binding of CNO. The increase in cAMP modulates the activity of neurons (Brancaccio et al., 2013; Farrell et al., 2013). The DREADD technology was revolutionary, and it carried several advantages. Regarding the ligand, CNO is orally active and possesses a long duration of action, no specialised devices are needed for the administration of CNO, and it has good bioavailability (Sternson & Roth, 2014). However, the DREADD technology suffered from various issues. It was shown that CNO could be metabolised to form clozapine in guinea pigs and humans (Jann et al., 1994), which could cause fatal agranulocytosis (Mijovic & MacCabe, 2020) and is also an active drug in the brain (Kitagawa et al., 2021). Another concern is related to the fact that the DREADDs technology relies on the use of engineered GPCRs. The use of GPCRs adds an intervening step between the effector and the receptor activation, the G protein. The presence of an intermediate step makes the process more complicated than just the ligand binding as the receptor activation does not directly mean that the desired effect can occur (Magnus et al., 2019). To avoid this issue, particularly when it comes to controlling neuronal activities, the use of ligand-gated ion channels (LGICs) is favourable as they provide direct control of neuronal activity without the involvement of a G protein (Magnus et al., 2019).

6.2. Ligand-gated ion channels (LGICs) to control neuronal activity

There are three main methods used to control neuronal activity using unmodified LGICs. The first and the most classical method relies on the over-expression of certain ion channels to cause the final desired effect, but this approach caused toxicity in many cases (Sutherland et al., 1999). One example of this technique is the over-expression of inward rectifier K^+ channels to eventually suppress neuronal excitability (Ehrengruber et al., 1997). Not only does this method result in toxic effects, but it can also activate compensatory mechanisms (Sternson & Roth, 2014). The second technique relies on expressing the desired nonessential mammalian LGICs in specific cell populations in a global knockout system. These LGICs can then be controlled by a wide range of ligands leading to neuronal

silencing or activation. Global knockout systems are used to not activate the endogenous channels. One example of the application of this strategy involves the expression of TRPV1 channels in specific cell populations and the use of capsaicin to activate the TRPV1-expressing neurons (Zemelman et al., 2003). The third approach relies on expressing invertebrate ion channels in vertebrate cells. This technique is useful as the activation of the invertebrate ion channels is distinct when compared to the mammalian LGICs (Sternson & Roth, 2014). A classic example of the use of invertebrate LGICs to control neuronal activity is the use of glutamate-gated chloride channels (from *Caenorhabditis elegans*) with their ligand to silence neurons (Slimko et al., 2002). The anthelmintic drug ivermectin can activate these channels. Because these channels do not exist in vertebrates, they became an attractive candidate for use in controlling specific cell populations. A potential issue of those channels is their responsiveness to glutamate (which is present endogenously), but this issue can be diminished by a single-point mutation (Y182F) in the binding pocket of glutamate (Li et al., 2002). While this modification enhanced the applicability of this chemogenetic tool for *in vivo* neuronal silencing, problems related to the ligand (ivermectin) remained unsolved as ivermectin is highly lipophilic, a property that leads to its accumulation in the adipose tissue, limiting the systemic availability and making the side effects control more challenging (McKellar et al., 1992). Ivermectin-activated chloride channels were tested as means to silence the DRG neurons in *in vivo* models of chronic pain (Weir et al., 2017). Even though the results were promising, concerns about ivermectin lipophilicity and the potential immunogenicity of these LGICs represent a significant obstacle.

More recently, another branch of chemogenetic tools to manipulate neuronal activity was introduced. These novel tools are based on chimeric ion channels, which were created through genetic engineering as well as chemical engineering of selective interactions between ion channels and their agonists (Magnus et al., 2011). By introducing this technique, several limitations related to the classical LGICs-based chemogenetic tools were overcome, including the poor characterisation of invertebrate channels and the laborious process of knocking out endogenous mammalian ion channel genes (Sternson & Roth, 2014).

The idea stemmed from the discovery that the extracellular LBD of the α7 nicotinic acetylcholine receptor (α7nAChR) acts as an independent actuator module when

transplanted onto the ion pore domain (IPD) of another member of the enormous Cys-loop ion channels family (see Figure 37). Therefore, splicing the LBD of α7 nAChR to the serotonin receptor type 3 (5HT3a) IPD gives rise to a channel whose pharmacology is identical to α7 nAChRs, but its conductance properties are from the 5HT3 ion channels (Eiselé et al., 1993). By splicing the α7 nAChR LBD to the chloride-selective glycine receptor (GlyR) IPD, an ACh-gated chloride channel (α7-GlyR) can be created (Grutter et al., 2005). This modular feature provides a solid foundation for optimising functional properties. Furthermore, because α7nAChR LBDs can self-assemble leading to homomeric pentamers formation, chimeric LGICs based on them can also self-assemble without the need for other cofactors. The main issue with using these chimeric ion channels arises when cell-type–selective perturbation methods are needed as α7 nAChR is expressed endogenously by several neuron subsets, resulting in off-target effects. As previously stated, this issue has generally been addressed by simply removing the endogenous allele, that typically necessitates costly and time-consuming mouse breeding methods. A more straightforward solution was used for chimeric channels based on the extracellular LBD of the α7 nAChR, and that relied on engineering the ligand-recognising region of the LBD using a “bump-hole” strategy to reduce the responsiveness to the endogenous ligand and enhance the responsiveness to other chemical compounds, which should not activate the un-modified channels (Sternson & Roth, 2014). The engineered LGIC is called PSAM (pharmacologically selective actuator module), and the small molecule used to activate these engineered channels is called PSEM (pharmacologically selective effector molecule).

There are various combinations of PSAMs and PSEMs. PSAMs were spliced to IPDs from many Cys-loop LGIC family members, including 5HT3, glycine, GABA receptor type C, and nAChRs. Since the IPD governs ionic conductance characteristics, PSAM-IPD chimeric channels stimulated with the corresponding PSEMs allowed for pharmacological control of ionic conductance for nonspecific

cations, chloride ions, or Ca^{2+} (Magnus et al., 2011). The PSAM-PSEM concept is explained in Figure 38.

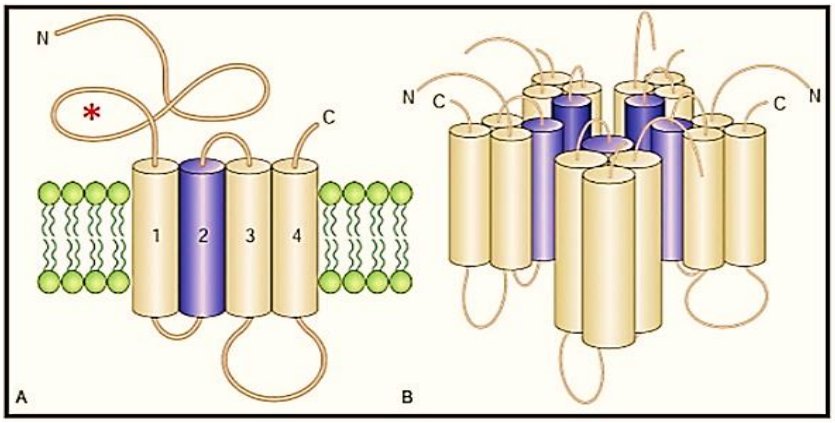

Figure 37: The structure of cys-loop ion channels. *Cys-loop ion channels are pentameric proteins, with each protein formed of a single polypeptide that crosses the plasma membrane four times (M1-M4). Besides the segment within the plasma membrane, there is also an intracellular segment and an extracellular segment. The term "cys-loop" originated from the fact that each of the proteins has a disulphide bond between two cysteine residues in the extracellular domain (shown by the red asterisk). Modified from (Macdonald & Botzolakis, 2010).*

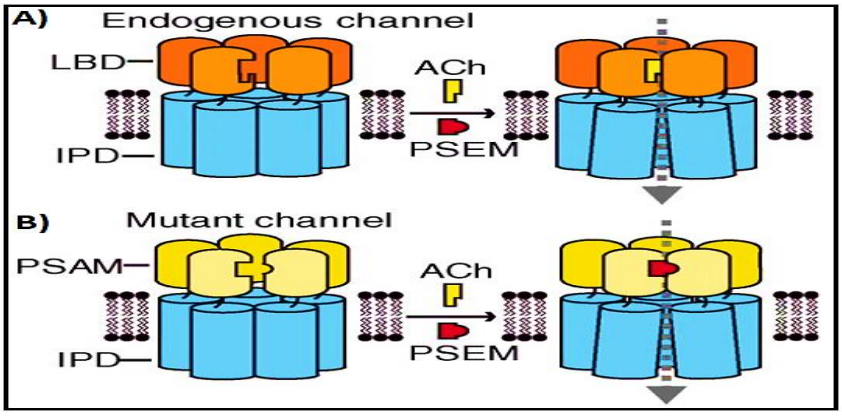

Figure 38: Engineered ligand-gated ion channels based on the structure of the cys-loop ion channels. *When the LBD from a member of the cys-loop ion channel (e.g., α7 nAChR, orange) is transplanted onto the IPD from another member of the cys-loop ion channel (blue), a chimeric channel is created, and its pharmacology is identical to the α7 nAChR (responsive to ACh but irresponsive to PSEM), while its ion specificity resembles that of an ion channel from which the IPD was driven (A). However, when modifications are introduced in the LBD to abolish the responsiveness to ACh and enhance the responsiveness to PSEM,*

the LBD is named PSAM (B). LBD: ligand-binding domain, nAChR: nicotinic acetylcholine receptors, IPD: ion-pore domain, Ach: acetylcholine, PSEM: pharmacologically selective effector molecule, PSAM: pharmacologically selective actuator module. Adapted from (Magnus et al., 2011).

In 2019, Magnus et al. published a novel PSAM, which they named PSAM^4. This PSAM relies on a triple mutant LBD of α7 nAChR (Magnus et al., 2019). They spliced this PSAM^4 onto the IPD of 5HT3 receptors for neuronal activation and onto the IPD of glycine receptors (GlyR) for neuronal silencing. The modifications introduced into the α7 nAChR are L131G, Q139L and Y217F. With these mutations, PSAM^4 became almost irresponsive to Ach, with the potency of ACh on PSAM^4 being 13 times lower than its potency on α7nAChR (EC50 (the concentration needed to achieve 50% of the maximum effect) of ACh at PSAM^4 is 83 ± 20 μM). This EC50 is almost 100,000-fold greater than basal mouse brain ACh concentration, which is ~0.9 nM (Uutela et al., 2005). It is also important to note that the EC50 of ACh on PSAM^4 is also much higher than the concentrations of ACh in the brain during transient rises, which do not typically exceed 2μM (Parikh et al., 2007). One PSEM that can activate PSAM^4 is varenicline, a smoking-cessation drug (Magnus et al., 2019). Sternson's group showed that the application of varenicline to PSAM^4 with the IPD from glycine receptors (PSAM^4-GlyR) resulted in neuronal silencing *ex-vivo* (see Figure 39) and *in vivo* (see Figure 40). The neuronal silencing efficiency after the application of varenicline to PSAM^4-GlyR expressing neurons and the reversibility of the silencing made this system attractive for silencing the DRG neurons as a potential analgesic tool for chronic pain conditions. Similarly, as the application of varenicline to PSAM^4-5HT3-expressing neurons was shown to activate these neurons, this method was tested to activate pain-suppressing neurons. The pain-suppressing neurons targeted here were the recently identified neuronal subset in the central amygdala of mice that were shown to drive, at least in part, the analgesic effect of general anaesthetics (Hua et al., 2020). Hua et al. demonstrated that upon exposure to general anaesthetics, certain neurons in the central amygdala of mice are activated, as demonstrated by the expression of c-Fos (a marker of neuronal activation). This group hypothesised that the activation of these neurons could be responsible for the analgesic effect of general anaesthetics. To test this hypothesis, Hua et al. assessed whether the activation of these general-

anaesthetic-activated neurons in the central amygdala (CeAGA) by optogenetic tools could cause an analgesic effect, and their results indicated that there was a significant elevation in the withdrawal threshold in different sensory tests upon the activation of these neurons (Hua et al., 2020) (See Figure *41*). This group also showed that the optogenetics-based activation of the CeAGA had an analgesic effect in inflammatory pain models as well as neuropathic models (Hua et al., 2020).

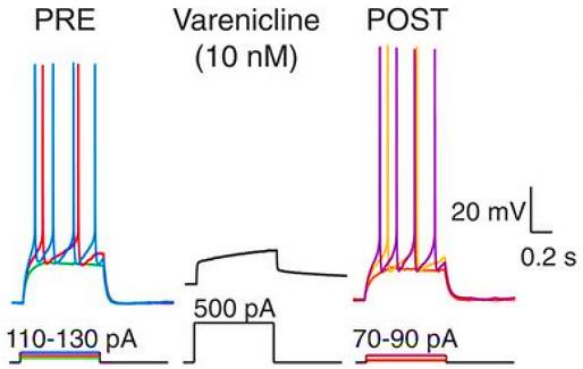

Figure 39: Varenicline silences PSAM^4-GlyR expressing cortical neurons ex-vivo. *Whole-cell current-clamp electrophysiological recordings show that the ability of PSAM^4-GlyR expressing cortical neurons to generate action potentials was strongly suppressed upon the application of varenicline (10nM) and was restored after varenicline washout. Obtained from (Magnus et al., 2019).*

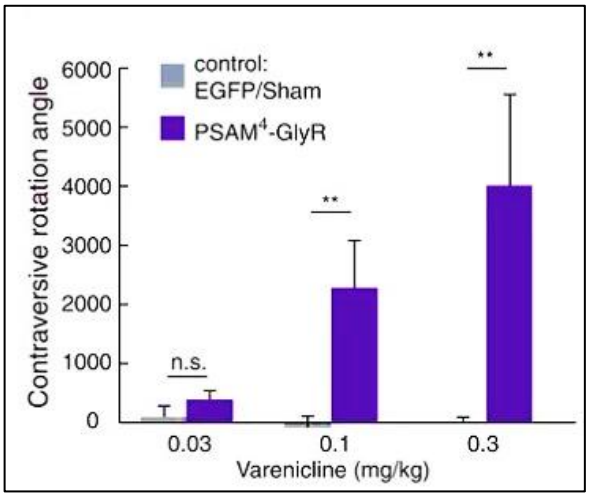

Figure 40: Varenicline silences PSAM^4-GlyR expressing GABAergic neurons in vivo as demonstrated by the behavioural changes. *Unilateral targeting using viral vectors to induce the expression of PSAM^4-GlyR in the GABAergic neurons that express Slc32a1 (vesicular GABA transporter) in substantia nigra reticulata caused contraversive motion in the mice that express*

*these receptors upon the application of varenicline, and the angle of the contraversive movement was increasing in a dose-dependent manner in PSAM^4-GlyR-expressing mice (n=9 mice) but not sham-operated or EGFP- expressing mice (n=6 mice). Results are expressed as Mean±SEM, **P < 0.01 (Mann-Whitney U test). EGFP: enhanced green fluorescence protein. Obtained from (Magnus et al., 2019).*

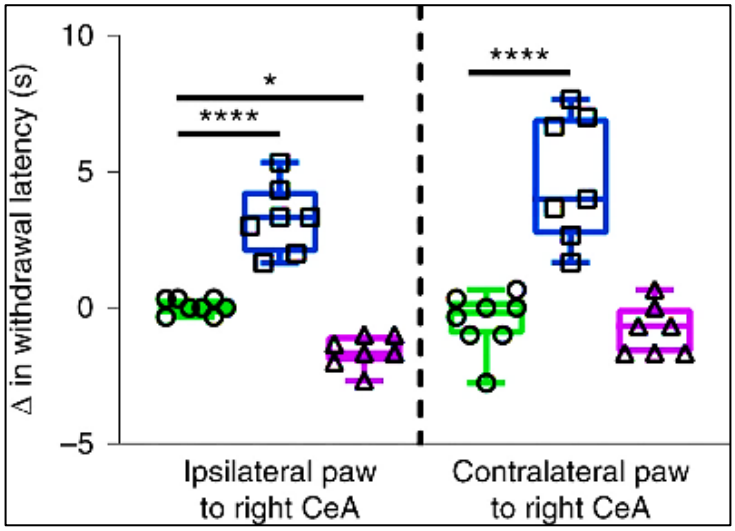

Figure 41: Optogenetic activation of the right CeAGA increases withdrawal latency in the dry ice test ipsilaterally and contralaterally while optogenetic-based silencing of the CeAGA diminishes withdrawal latency in the ipsilateral paw but not the contralateral paw. *n = 8 in the control group (negative for channelrhodopsin, green) and 7 for each of the channelrhodopsin (blue) and Archaerhodopsin 3.0 groups (purple). Channelrhodopsin is an optogenetic neuronal activator, while archaerhodopsin 3.0 is an optogenetic silencer. Statistical analyses were done using the two-way ANOVA test; ****P < 0.0001, *P < 0.05; F2,38 = 71.37). Data are mean ± s.e.m. Obtained from (Hua et al., 2020).*

6.3. Aims and work outline

The aim of this work was to explore the applicability of the varenicline/PSAM^4-GlyR system in silencing DRG neurons using 1) plasmids, 2) recombinant adeno-associated viruses, and 3) mouse lines that express PSAM^4-GlyR in certain DRG neuronal subsets. Additionally, chemogenetic tools were tested to activate the general-anaesthetic-activated neurons in the central amygdala (CeAGA). To achieve this goal, the CeAGA neurons were activated by exposing mice to

general anaesthetics. For these experiments, two different mouse lines were subjected to general anaesthetics, and these mouse lines are characterised by their ability to express Cre enzyme selectively in activated neurons (mechanisms will be explained later in section 6.6.2.1). In these mice, Cre-dependent transgenes can be delivered to the activated neurons using viral vectors, and these viruses can be directly injected into the central amygdala of mice. The first mouse line is called Fos-2A-TVA and in this one, hM3Dq was expressed in a Cre-dependent manner in activated neurons. In this mouse line, C21 was used to activate the hM3Dq receptors and to assess whether analgesia could be detected. The second mouse line is the CreER^{T2} mouse line that expresses the Cre enzyme in activated neurons. In this mouse line, the PSAM^{4}-5HT3 receptors were expressed, and varenicline was used to activate the chemogenetic receptors.

6.4. Methods

6.4.1. PSAM^{4}-GlyR for silencing the DRG neurons as a potential analgesic tool

6.4.1.1. Plasmids

6.4.1.1.1. Making CMV PSAM^{4}-GlyR WPRE BGH pA plasmid

The plasmid A (Vectorbuilder) (see the sequence in **appendix 1** and map in Figure 42) was subjected to restriction digestion using the two restriction enzymes: XbaI and AccI (New England Biolabs (NEB)) in the cutsmart buffer. The restriction digestion reaction mixture was incubated at 37°C for 16 hours. Then the reaction products were run on a gel (1% agarose in 1x Tris-acetate-EDTA (TAE) buffer). The reaction gave rise to two bands: 3755 bp and 2074 bp. The band corresponding to 3755 bp was extracted using the Qiagen gel extraction kit following the manufacturer's protocol. The extracted 3755 bp band will be named 'Cut vector' as it contained the backbone with inverted terminal repeats (ITRs). The Woodchuck hepatitis virus posttranscriptional regulatory element (WPRE) sequence and Bovine growth hormone polyadenylation signal (BGH pA) were present in this sequence. See Figure 42.

6.4.1.1.1.1. Polymerase Chain Reaction (PCR)

To produce a CMV-driven PSAM^{4}-GlyR WPRE BGH pA sequence, the CMV promoter sequence and the PSAM^{4}-GlyR sequences needed to be amplified from

other vectors to enable their cloning into the 'cut vector' sequence via Gibson cloning (Kalva et al., 2018). For amplifying the CMV promoter sequence, plasmid A was used as a template. The PCR protocol was 95°C 3mins, 98°C 20 secs, 55-60°C annealing gradient for 30 secs, 72°C (1min/1kb), cycles from step 2 were repeated 34 times, 72°C for 5 mins, incubation at 12C°). The forward primer used for this PCR was (TCACTAGGGGTTCCTTCTAGGTATAGAAAAGTTGTAGTTATTAAT), and the reverse primer was (TACAAACTTGGATCTGACGGTTTCACTAGGGGTTCCTTCTAG). These two primers allowed the addition of appropriate 20-bp overhangs (underlined) on each side of the CMV promoter fragment to permit the use of the TakaraBio In-fusion kit for cloning, which necessitates the presence of at least 15 bp overhangs on each side. To amplify the PSAM^4-GlyR, the plasmid 119739 (Addgene) was used as a template (see the sequence in **appendix 2**), and the same PCR protocol was followed. However, with the annealing gradient being between 65 and 72°C instead of 55-60°C. In this reaction, the forward primer was (CCGTCAGATCCAAGTTTGTAGGGCTAGCGCCACCATGCGCT), and the reverse primer was (TGTACAAGAAAGCTGGGTCTCCGCTTACTGGTTGTGTACGTC). All PCR reactions were carried out using the KAPA-HiFi enzyme (Roche). The reaction products were run on a gel (1% agarose in TAE). Then, the desired bands were extracted: 633 bp for the first reaction and 1354 bp for the second reaction. For the rest of the report, the 633bp fragment will be named the CMV fragment, and the 1354 bp will be named the PSAM^4-GlyR fragment. The gel extraction was carried out using the Qiagen gel extraction kit following the manufacturer's protocol.

6.4.1.1.1.2. Gibson Cloning using Takara Bio In-fusion kit

The in-fusion reaction using the HD in-fusion kit (Takara Bio) was carried out using 100ng of the cut vector, 33.3 ng of the CMV fragment, and 72 ng of the PSAM^4-GlyR fragment. 1.5µl of the reaction mixture was transformed into Stbl3 cells (ThermoFisher) (40 secs at 42C° followed by 2 mins in ice). The recovery of Stbl3 cells was achieved by adding 200µl of SOC medium, and the bacterial cells were incubated at 37°C for 1 hour. The suspension was then poured onto an LB agar (with ampicillin 100µg/ml) plate and was incubated at 37°C overnight. After

16 hours, several colonies were present, and one of them was picked and grown in 5ml of LB ampicillin broth for 6 hours. Then, the 5ml medium was transferred into a 200ml LB ampicillin broth flask and left shaking at 220 RPM at 37°C overnight. Following that, the DNA was extracted using the Qiagen Maxiprep kit following the manufacturer's protocol. The resulting DNA was sent for sequencing (Source Bioscience) using the following primers: (GTCGGGTTTCGCCACCTCTGAC, CTGGCTGACCGCCCAACGACC, GATGTACTGCCAAGTAGGAAAGTC, CGTAACAACTCCGCCCCATTGAC, GTCAATTCTTCAGGCCACTGCCTG, TAATATGGACGCCGCTCCAGCTAG, ATTGGATCATCTACAAGATTGTGCG, ACAACACCACGGAATTGTCAGTG, CTATGTTGCTCCTTTTACGCTATG, GTCTTCGCCTTCGCCCTCAGAC, GGTGGGGTGGGGCAGGACAG, AAAGCGAAAGGAGCGGGCGCTAAG). The resulting plasmid was named CMV PSAM^4-GlyR WPRE BGH pA (the sequence can be found in **appendix 3**). See Figure 42.

6.4.1.1.2. Adding sequences encoding for fluorescent labels (AcGFP1 (Aequorea coerulescens GFP) or mCherry) to the CMV PSAM^4-GlyR WPRE BGH pA plasmid

The CMV PSAM^4-GlyR WPRE BGH pA plasmid was subjected to an overnight restriction digestion reaction using BsaI-HF v2 (NEB). The restriction reaction products were run on a gel, and the linearised vector (5686 bp) was extracted as described above. A gene fragment corresponding to IRES-AcGFP1 was synthesised by Integrated DNA Technologies (IDT), and appropriate 15 bp overhangs on each side were also incorporated in the fragment to allow successful cloning into the linearised CMV PSAM^4-GlyR WPRE BGH pA plasmid. The in-fusion reaction was carried out using 100ng of the vector with 47.7ng of the gene fragment IRES AcGFP1 to form CMV PSAM^4-GlyR IRES AcGFP1 WPRE BGH pA (see the plasmid map in Figure 44). A similar approach was used to clone IRES-mCherry into the linearised vector. 100 ng of cut vector was used with a 3:1 insert-to-vector molar ratio with IRES mCherry to generate the final plasmid CMV PSAM^4-GlyR IRES mCherry WPRE BGH pA (see Figure 42). IRES stands for internal ribosome entry site, and it is used to allow the translation of an independent protein sequence encoded in the same plasmid without the need to add another promoter.

To sequence CMV PSAM^4-GlyR IRES AcGFP1 WPRE BGH pA, the following primers were used: (GTCGGGTTTCGCCACCTCTGAC, CTGGCTGACCGCCCAACGACC, GATGTACTGCCAAGTAGGAAAGTC, CGTAACAACTCCGCCCCATTGAC, GTCAATTCTTCAGGCCACTGCCTG, TAATATGGACGCCGCTCCAGCTAG, ATTGGATCATCTACAAGATTGTGCG, CTGGCCGAAGCCGCTTGGAATAAG, CCTCGGTACACATGCTTTACATGTG, TGGTGAATCGCATCGAGCTGACCG, ACAACACCACGGAATTGTCAGTG, CTATGTTGCTCCTTTTACGCTATG, GTCTTCGCCTTCGCCCTCAGAC, GGTGGGGTGGGGCAGGACAG, AAAGCGAAAGGAGCGGGCGCTAAG).

To sequence CMV PSAM^4-GlyR IRES mCherry WPRE BGH pA, the same primers of CMV PSAM^4-GlyR IRES AcGFP1 WPRE BGH pA were used except for the replacement of TGGTGAATCGCATCGAGCTGACCG by TGGGACATCCTGTCCCCTCAGTTC. The sequences of the gene fragments synthesised by IDT can be found in **appendix 4**. The resulting plasmids can be found in **appendix 5**.

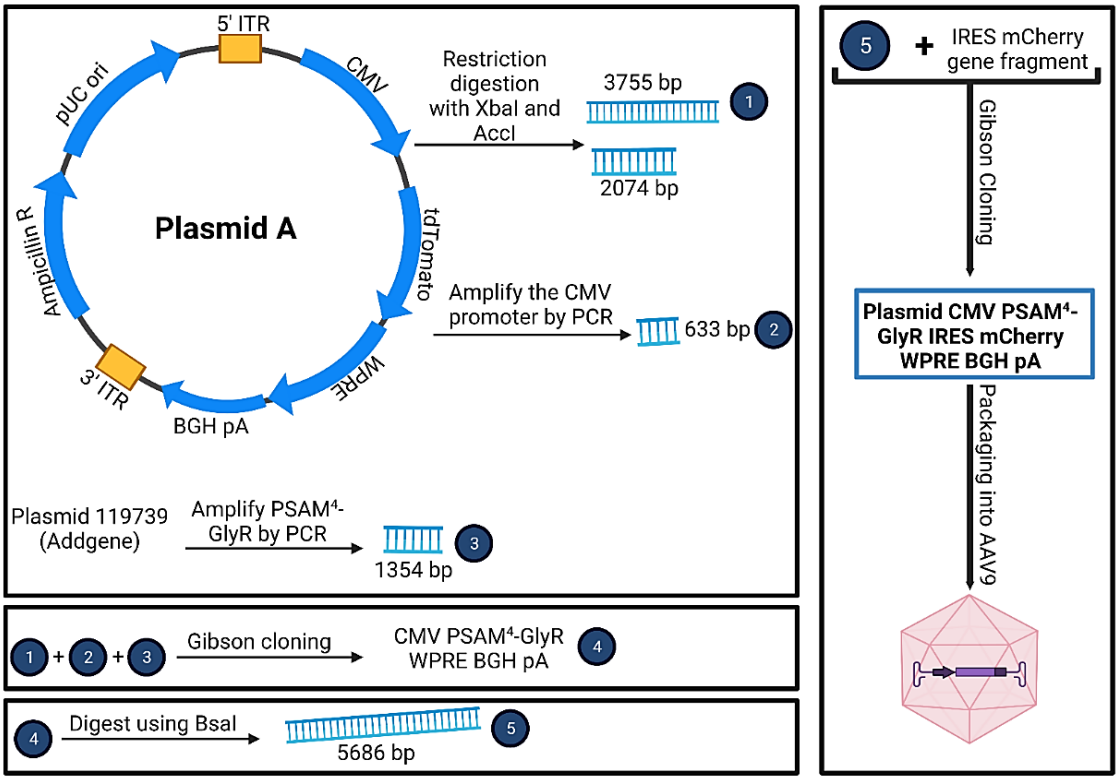

Figure 42: Cloning protocol for plasmid CMV PSAM^4-GlyR IRES mCherry WPRE BGH pA*. ITR: inverted terminal repeats, WPRE: Woodchuck hepatitis virus posttranscriptional regulatory element sequence, BGH pA: Bovine growth hormone polyadenylation signal, CMV: cytomegalovirus promoter sequence,*

IRES: Internal Ribosome Entry Site, PCR: polymerase chain reaction, Ampicillin R: ampicillin resistance.

6.4.1.1.3. Primary DRG culture to test plasmids encoding for PSAM^4-GlyR

Primary cultures of DRG neurons were prepared from C57BL/6 mice expressing GFP Calmodulin M13 protein 3 (GCaMP3) under the control of the *Pirt* promoter for Ca^{2+} imaging experiments. This promoter allows the expression of GCaMP3 in most nociceptive DRG neurons (Kim et al., 2008). The GCaMP3 mouse line was kindly provided by Prof. Xinzhong Dong (John Hopkins University, Baltimore, MD) (Kim et al., 2014). The Lonza Amaxa P3 primary cell 4D-Nucleofector X kit was used for transfection. The plasmid/rAAV CMV PSAM^4-GlyR IRES mCherry WPRE BGH pA was used for Ca^{2+} imaging experiments.

For each experiment, an adult C57BL/6 mouse was sacrificed by inhalation of a rising CO_2 concentration followed by cervical dislocation to confirm death. DRGs were dissected from the entire length of the spinal column. During dissection, DRGs were placed in a 35mm dish containing HBSS buffer, and the dish was always placed on ice. After the dissection, DRGs were digested in a pre-equilibrated enzyme mix for 45 minutes at 37˚C with 5% CO2. The composition of the enzyme mix was Hanks' balanced salt solution containing collagenase (type XI; 5 mg/ml), dispase (10 mg/ml), HEPES (5 mM) and glucose (10 mM). DRGs were then gently centrifuged for 5 minutes at 300 revolutions per minute; the supernatant was discarded and replaced with 1 ml of warmed Dulbecco's modified Eagle's medium (DMEM), supplemented with L-glutamine (1%), glucose (4.5 g/litre), Na^+ pyruvate (110 mg/litre) and 10% fetal bovine serum (FBS). Then, DRGs were triturated mechanically using three fire-polished glass Pasteur pipettes of progressively decreasing inner diameter. The triturated DRGs were then centrifuged at 300 revolutions per minute for eight minutes, and the supernatant was discarded.

When plasmids were used, the cells were resuspended in P3 buffer from the Amaxa P3 primary cell 4D-Nucleofector X kit and the plasmid of interest was added to the mixture. Following that, the electroporation protocol was followed according to the manufacturer's recommended protocol. After the electroporation, a warmed RPMI medium (Thermofisher) was added to the cells, and the cells were left at room temperature for 5 minutes. The DRGs were then

centrifuged for 5 minutes at 300 revolutions per minute. To remove the excess plasmid and the excess P3 solution, the supernatant was discarded, and the cells were resuspended in the needed volume of DMEM, supplemented with L-glutamine (1%), glucose (4.5 g/litre), Na^+ pyruvate (110 mg/litre), nerve growth factor (50 ng/ml) and 10% fetal bovine serum (FBS). Finally, cells were plated onto 9 mm glass coverslips coated with poly-L-lysine (1 mg/ml) and laminin (1 mg/ml). Cells were incubated at 37˚C in 5% CO_2. Ca^{2+} imaging experiments were carried out after 48-72 hours post-dissociation and electroporation.

6.4.1.1.4. Ca^{2+} imaging experiments

In Ca^{2+} imaging experiments, the changes in GCaMP3 fluorescence in $PSAM^4$-GlyR mCherry expressing DRG neurons were recorded over time.

(i) To test whether there is a significant difference in Ca^{2+} responses between $PSAM^4$-GlyR positive neurons and $PSAM^4$-GlyR negative neurons to veratridine (30µM), artificial cerebrospinal fluid (ACSF) was applied for 30 seconds, followed by veratridine (30µM in ACSF) for 30 seconds, then ACSF for 30 seconds. See Figure 46A.

(ii) To assess the response of transfected and non-transfected cells to Ach, the protocol involved applying ACSF (30 seconds), ACh (30µM, 1 minute), followed by ACSF application (30 seconds). See Figure 46B.

(iii) To investigate the impact of varenicline (20nM) on non-transfected cells, ACSF was applied for 30 seconds, followed by varenicline (20nM) for 1 minute, and then ACSF (30 seconds). See Figure 46C.

(iv) To test the ability of varenicline (20nM) to silence the $PSAM^4$-GlyR-expressing DRG neurons, the protocol was ACSF for 30 seconds, veratridine (30µM) for 10 seconds, followed by ACSF for 30 seconds, then varenicline (20nM) was applied for 5 minutes, and then a solution containing veratridine (30µM) and varenicline (20nM) was applied for 10 seconds to re-assess the response to veratridine (see Figure 47).

6.4.1.2. Recombinant AAVs encoding for $PSAM^4$-GlyR

6.4.1.2.1. Ca^{2+} imaging experiments

6.4.1.2.1.1. *In vitro* Ca^{2+} imaging

DRGs were cultured as shown previously. When an rAAV (CMV $PSAM^4$-GlyR IRES mCherry WPRE BGH pA, Vector builder) was used, 4 coverslips were

placed in a 35 mm^3 dish, and the dish was filled with the culture medium (described above). 5µl of the virus ($1x10^{13}$ genome copies/µl) was added to the dish, and then the dish was incubated at 37˚C in 5% CO_2. The *in vitro* viral transduction was tested and was shown to induce a high transduction efficiency (Figure 48) and good silencing upon the application of varenicline (see Figure 51). For the silencing testing experiments, the protocol involved applying ACSF for 30 seconds, veratridine (30µM) for 10 seconds, followed by ACSF for 30 seconds, then varenicline (20nM) was applied for 5 minutes, and then a solution containing veratridine (30µM) and varenicline (20nM) was applied for 10 seconds to re-assess the response to veratridine.

6.4.1.2.1.2. *In vivo* Ca^{2+} imaging

6.4.1.2.1.2.1. Choosing the best injection route

For the *in vivo* testing, two injection routes were tested; intrathecal in adult mice and intraplantar injections in mouse pups. All the mice used in these experiments expressed GCaMP3 under the control of the *Pirt* promoter. For intrathecal injections, mice were injected with 5µl of the rAAV ($1x10^{13}$ genome copies/µl), and the transduction efficiency was tested after eight weeks by extracting the DRGs (Figure 50). For the intraplantar injection in pups, six C57BL/6 mouse pups (3 males and three females, P5) were placed on ice for anaesthesia and then injected intraplantarly with the virus (CMV $PSAM^4$-GlyR IRES mCherry WPRE BGH pA) using a Hamilton syringe. The volume injected in each paw was 5µl ($1x10^{13}$ genome copies/µl). One mouse was sacrificed (as described above) 10 weeks after the injection to assess the viral transduction efficiency. L2-L5 DRGs were extracted as previously described. The DRGs were prepared for sectioning as previously described in section 5.3.1. After sectioning, slides were covered and left to set at room temperature for 15 minutes. Then they were washed twice with phosphate-buffered saline (PBS) and were left to dry again at room temperature for 30 minutes. Vectashield (Vector laboratories) mounting media was placed on the sections, followed by a coverslip (24x60mm), and then imaged using a Leica SP8 confocal microscope (Figures 49 and 50). Because the intraplantar injection in pups resulted in high transduction (Figure 49), mice injected through this route were used for *in vivo* Ca^{2+} imaging and behavioural tests after they reached adulthood.

6.4.1.2.1.2.2. Acquisition

Ketamine (100 mg/kg), xylazine (15 mg/kg), and acepromazine (2.5 mg/kg) were used to anesthetise adult mice expressing GCaMP3. Intramuscular injections of anaesthetics were administered into the hindlimb on the opposite side of the DRG utilised for imaging. Every 20 to 30 minutes, the animal received a new dosage. The pedal response in each of the four paws was watched in order to gauge the depth of anaesthesia. As further signs of profound anaesthesia, absent whisker movement and a constant respiratory rate were employed. Only once the pedal reflex was completely gone in all four limbs, whisker movement was gone, and respiration was calm the procedure was started. Using a heated pad, the animals were kept at a constant body temperature of 37°C (VetTech). All surgical equipment was heat-sterilised using a bead steriliser. At spinal level L3-5, a lateral laminectomy was done. In order to expose the spinal column, the skin was longitudinally incised. Using microdissection scissors and an OmniDrill 35, the vertebra's transverse and superior articular processes were eliminated. Using microdissection forceps, the dura mater and arachnoid membranes were meticulously dissected to reveal the sensory neuron cell bodies in the ipsilateral DRG. The vertebral column (L1), rostral to the laminectomy, was clamped using a specially constructed clamp to hold the animal in place. Sterilised orthodontic sponges were used to stop bleeding. To reduce breathing-related disturbance, the animal's trunk was slightly raised. To preserve tissue integrity during the process, artificial cerebrospinal fluid [120 mM NaCl, 3 mM KCl, 1.1 mM CaCl2, 10 mM glucose, 0.6 mM NaH2PO4, 0.8 mM MgSO4, 1.8 mM NaHCO3 (pH 7.4 with NaOH)] was perfused over the exposed DRG or the DRG was separated by covering with silicone elastomer. Using a Leica SP8 confocal microscope, images were acquired. A 10x dry, 0.4-NA objective with a 2.2 mm working distance and a 0.75–3x optical zoom was utilised to magnify the images. A 488 nm laser line was used to ignite GCaMP3 (1–15% of maximal laser power). A 552 nm laser line operating at 1–15% of maximal laser power was used to stimulate mCherry. The emitted light's filtering and collecting were adjusted to increase yield and reduce cross-talk (Leica Dye 164 Finer, LasX software, Leica). A hybrid detector with 100% gain was used to find GCaMP and a photomultiplier tube was used to find mCherry (500-600V gain). At a frame rate of 1.55 Hz, a bidirectional scan speed of 800 Hz, and a pixel dwell time of 2.44 µs, 512 × 512-pixel pictures were recorded. The left hind paw was subjected to various types of stimuli ipsilateral

to the exposed DRG. Using a Pasteur pipette, the paw was subjected to water heated to 55°C. The DRG exposure was done by Dr Ana Luiz, and the remaining steps were done by Rayan Haroun.

6.4.1.2.1.2.3. Analysis

The Leica LasX software was used to quantify the Ca^{2+} signal over time, as indicated by the mean pixel intensity over time. Excessive Z movement in stacks was disregarded for analysis. Stacks from DRGs with abnormal blood flow or surgical injury were also disregarded. Using the free hand tool, regions of interest (ROI) were manually formed all around cells that appeared to be reacting. ROIs covered the whole cell, not just the cytoplasm. A variety of characteristics, including a distinctive cell shape, the presence of a dark nucleus possessing less GCaMP signal, an elevation in fluorescence after sensory stimulation, the lack of unstable fluorescence alterations not tied to stimulation, suggestive of non-sensory activity, as well as the absence of a continuous high GCaMP signal, suggestive of cell death or injury, were necessary for manually identifying responsive cells. It was easier to distinguish between neighbouring cells and avoid fluorescence signal overlap when there was no GCaMP3 signal in the satellite glial cells that surrounded and divided nearby DRG somata.

6.4.1.2.2. Behavioural tests on mice injected with rAAV

6.4.1.2.2.1. Sensory tests

Behavioural tests included the Hargreaves' test, the up-down von Frey test, and the dry ice test (Figure 52 A-C), and these tests were done as previously described in section 2.3.4.

6.4.1.2.2.2. Motor coordination

To test motor abilities, the rotarod test was carried out as previously described by (L. Caroline Stirling et al., 2005) (Figure 52D).

6.4.1.2.2.3. Inflammatory pain

Mice were injected with 20µl of a 500 µM solution of PGE2 intraplantarly. 40 minutes After the injection, mice underwent the Hargreaves' test (Figure 54A).

6.4.1.2.2.4. Chemotherapy-induced cold allodynia

Mice were injected with 80µg (dissolved in 5% glucose solution and the total volume injected was 40µl) of oxaliplatin intraplantarly as previously described by

(MacDonald, Luiz, et al., 2021), and after approximately 4 hours mice underwent the dry ice test (Figure 54B).

6.4.1.3. Mouse lines expressing PSAM^4-GlyR in a Cre dependent manner

6.4.1.3.1. Breeding strategy

The Rosa26 FLEx PSAM^4-GlyR IRES tdTomato mouse line encodes for PSAM^4-GlyR in a Cre-dependent manner (Cyagen). Upon crossing a Rosa26 FLEx PSAM^4-GlyR IRES tdTomato mouse with a homozygous mouse that expresses Cre enzyme in a subset of neurons, the resulting offspring will express PSAM^4-GlyR and the fluorescent protein tdTomato in that specific neuronal subset. For genotyping, three primers were used (TCCACTGCAAGTAGTGATCGGTCC, GGCAACGTGCTGGTTATTGTG and GCATCTGACTTCTGGCTAATAAAG). When the mouse has a FLEx PSAM^4-GlyR IRES tdTomato (i.e. no Cre activity) allele, a 537bp band was seen. But when there was Cre activity (i.e. PSAM^4-GlyR and tdTomato are produced), one band with either 358bp or 356bp size was seen. Figure 43 shows the breeding strategies for this mouse line.

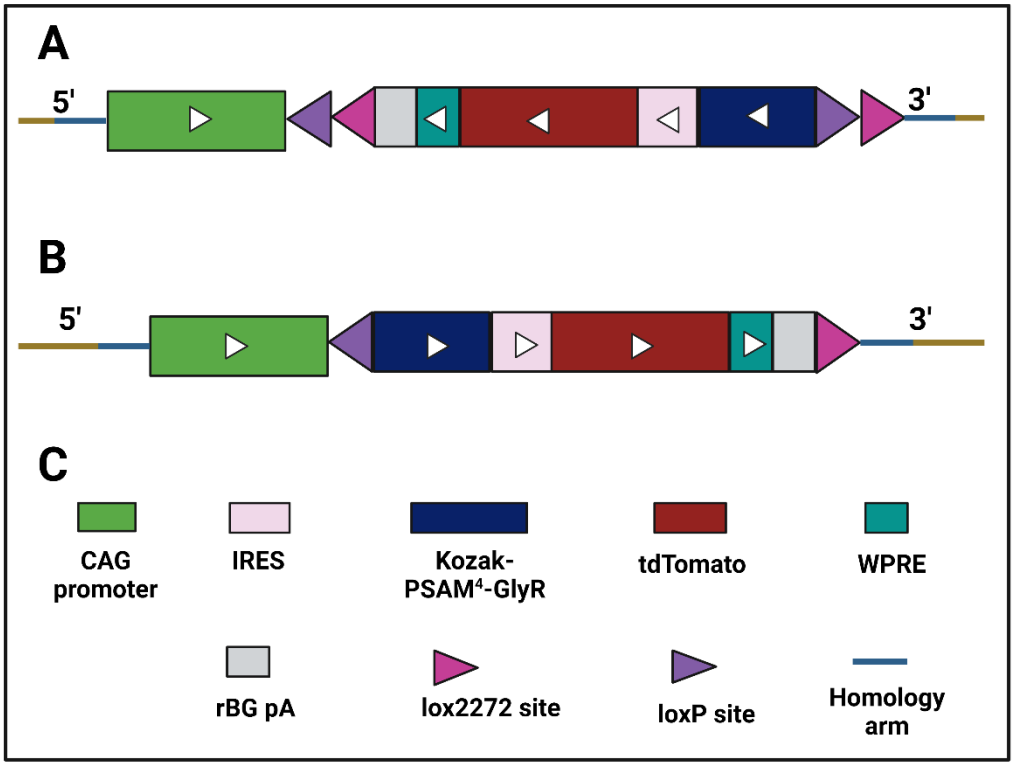

Figure 43: The breeding strategy to produce Rosa26 FLEx PSAM^4-GlyR IRES tdTomato and the products after Cre-based recombination. *A) shows the knockin allele without Cre activity. B) the knockin allele after Cre*

recombination (PSAM^4-GlyR and tdTomato will be produced), and C) the key for the figure.

6.4.1.3.2. Chronic constriction injury of the sciatic nerve

A longitudinal skin incision was made at the level of the right femur after the right thigh region had been shaved and the skin had been cleaned with hibiscrub. The muscular fibres were separated with forceps to make it possible to visualize the sciatic nerve. Following that, three 5-0 silk sutures were loosely tied around the sciatic nerve's diameter to enable the generation of nerve injury. The skin was sutured to close the surgery site using a 6-0 Vicril suture. Importantly, surgical operations were only carried out when mice were fully anaesthetized using isoflurane (2–3%).

Following that, lidocaine was applied topically at the surgery site. Animals were then kept in a warm area until fully recovered. Behaviour analyses were conducted during the second and third weeks after the operation. This model was shown to induce mechanical, heat, and cold hypersensitivity (Labuz et al., 2016; Minett et al., 2014). For the sham-operated mice, the same steps were followed except for the sciatic nerve ligation.

6.4.1.3.3. Behavioural tests on mice expressing PSAM^4-GlyR in the Na$_V$1.8-positive neurons

Heterozygous Rosa26 FLEx PSAM^4-GlyR IRES tdTomato mice were bred with homozygous mice that express Cre in the Na$_V$1.8-positive neurons. Ear biopsies were taken from the resulting litters, and mice that had both the Cre band (see the Na$_V$1.8 Cre mouse in section 4.3) and the FLEx PSAM^4-GlyR IRES tdTomato band were used for behavioural tests. These behavioural tests included the Randall-Selitto test, the acetone evaporative test, the von Frey test, the Hargreaves' test, and the dry ice test. The latter three tests were done as described previously in section 2.3.4.

6.4.1.3.3.1. Randall-Selitto test

The Randall-Selitto test for noxious mechanical sensation was done by applying mechanical pressure on the tail as previously described by (Abrahamsen et al., 2008; MacDonald, Sikandar, et al., 2021). In a transparent plastic tube, animals were restrained. The mouse's tail was pressed using a 3 mm^2 blunt probe until the rodent displayed a nocifensive response, like retracting its tail or vocalising.

The pressure was increasing over time. Over the course of three trials, the pressure needed to elicit nocifensive behaviour was averaged. The maximum limit permitted was 500 g.

6.4.1.3.3.2. Acetone evaporative test

Mice were positioned in plastic chambers on a metal mesh platform. A drop (about 20 µl) of acetone was applied to the plantar surface of the ipsilateral hind paw. After the acetone application, and for 1 minute, the duration of nocifensive behaviour was counted in seconds. Nocifensive behaviours included licking, flinching, and lifting. The measurements were repeated three times with a 10-minute gap to determine a mean value for the duration of nocifensive behaviour.

6.4.1.3.4. Immunohistochemistry on DRG neurons

To check the expression of PSAM4-GlyR in the $Na_V1.8$+ neurons, DRGs were fixed and sectioned as previously described. To image tdTomato, rabbit anti-red fluorescent protein (anti-RFP) antibody was used (Rockland, 600-401-379, 1:500), and the secondary antibody was Alexa Fluor 647 anti-rabbit (Jackson ImmunoResearch, 711-605-152, 1:500). To image peripherin, mouse anti-peripherin antibody was used (Sigma-Aldrich, P5117, 1:8000), and the secondary antibody was goat anti-mouse IgG conjugated Alexa 488 (life technologies, A11001, 1:1000).

6.4.1.4. Statistical analyses

To compare between two groups, the D'Agostino & Pearson test was used first. When the data had a normal distribution, the t-test was used for comparison. If the data is not normal, a non-parametric test is used. To compare two groups over time, the two-way ANOVA test was used, followed by multiple comparisons. Statistical analyses were conducted using GraphPad Prism 9. Statistical significance is expressed as: * $p < 0.05$; ** $p < 0.01$; *** $p < 0.001$, **** $p < 0.0001$.

6.4.2. Chemogenetic tools for neuronal activation as a potential analgesic tool

6.4.2.1. PSAM^4-5HT3

6.4.2.1.1. Plasmids

6.4.2.1.1.1. Cloning protocol to produce a CMV-driven FLEx PSAM^4-5HT3 plasmid

Plasmid CMV PSAM^4-GlyR IRES AcGFP1 WPRE BGH pA was subject to a restriction digestion reaction using NheI-HF and BsaI-HF v2 enzymes in the cutsmart buffer. The reaction was left overnight at 37°C. The reaction products were run on a gel and then visualised under UV light. Two main products were formed, and they were distinguished by their band size. The bands obtained were: 4381bp (the backbone) and 2635bp (PSAM^4-GlyR IRES AcGFP1). The 4381bp band was extracted. After the extraction of the backbone, the DNA was used for a restriction digestion reaction using the SacI-HF enzyme in the cutsmart buffer to excise the WPRE sequence. This reaction gave rise to two bands: 3731bp (extracted) and 650bp (discarded). The following step involved the addition of a FLEx PSAM^4-GlyR IRES mEGFP sequence to the 3731bp backbone. To add FLEx PSAM^4-GlyR IRES mEGFP, this sequence was amplified from plasmid 119741 (Addgene) using the forward primer ATCCAAGTTTGTAGGGCTAGgcgccccccataacttcgt and the reverse primer ACAGTCGAGGCTGATCAGCGtcgagggacataacttcgtata. These primers enabled the amplification of the FLEx PSAM^4-GlyR IRES mEGFP sequence while adding 20-bp overhang sequences on each side to enable the use of Gibson cloning-based kits for the subsequent cloning step. A gradient PCR protocol was carried out, as shown in section 6.4.1.1.1.1, and the resulting PCR product (3018bp) was extracted. After that, an infusion reaction between the PCR product and the cut vector was performed to produce CMV FLEx PSAM^4-GlyR IRES mEGFP plasmid (6713bp). This plasmid was then digested using SpeI-HF and NotI-HF enzymes in the cutsmart buffer to replace the PSAM^4-GlyR sequence with a PSAM^4-5HT3 sequence. The restriction digestion resulted in two products (5380bp and 1333bp). The 5380bp band was extracted and was used for an in-fusion reaction with a synthesized DNA fragment (IDT Technologies) that has the PSAM^4-5HT3 sequence along with appropriate 15-bp overhang sequences on each side. After conducting the Gibson cloning protocol, the resulting plasmid was CMV FLEx

PSAM^4-5HT3 IRES mEGFP (6813 bp). The sequence of this plasmid was checked using the following primers: CTGGCCGAAGCCGCTTGGAATAAG, CACTGCAAGTAGTGATCGGTCCAG, TATCTTCATTGTACGGCTGGTACAT, CACGATGATAATATGGCCACAACC, GGTGGGGTGGGGCAGGACAG, GTAAGCGGCAGGGTCGGAACAG, GTCAATTCTTCAGGCCACTGCCTG, CCCTTGTTGAATACGCTTAGGAG, GTGGAAAGAGTCAAATGGCTCTCC, GTCCAGGAGCGCACCATCTTCTTC, AAAGCACTAAATCGGAACCCTAAAG, GTCGGGTTTCGCCACCTCTGAC, CTGGCTGACCGCCCAACGACC, CGTAACAACTCCGCCCCATTGAC, AAAGCGAAAGGAGCGGGCGCTAAG, and GATGTACTGCCAAGTAGGAAAGTC. See Figure 44 for the cloning protocol for plasmid CMV FLEx PSAM^4-5HT3 IRES mEGFP.

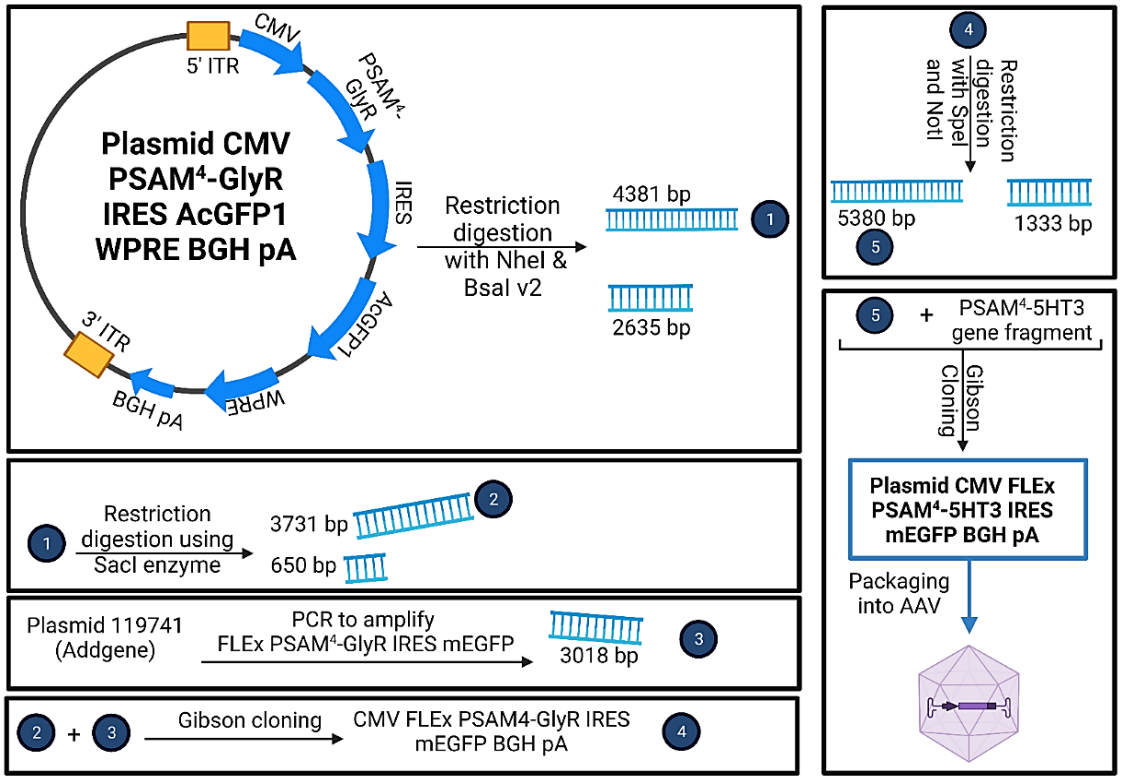

Figure 44: Cloning protocol for plasmid CMV FLEx PSAM^4-5HT3 IRES mEGFP BGH pA. *ITR: inverted terminal repeats, BGH pA: Bovine growth hormone polyadenylation signal, CMV: cytomegalovirus promoter sequence, IRES: Internal Ribosome Entry Sites, PCR: polymerase chain reaction, mEGFP: modified enhanced green fluorescence protein.*

6.4.2.1.1.2. *In vitro* Ca^{2+} imaging for the FLEx $PSAM^4$-5HT3 plasmid

For the *in vitro* Ca^{2+} imaging experiments, a modified version of the CMV FLEx $PSAM^4$-5HT3 IRES mEGFP was made to replace the fluorescent protein with mCherry. To clone this plasmid, CMV FLEx $PSAM^4$-5HT3 IRES mEGFP was subjected to restriction digestion using the restriction enzymes BlpI and BamHI-HF in cutsmart buffer. This reaction resulted in two bands 6189 bp (extracted) and 624 bp (discarded). The extracted band was used in a Gibson cloning reaction along with a gene fragment corresponding to mCherry (synthesised by IDT, see appendix **6**) to generate CMV FLEx $PSAM^4$-5HT3 IRES mCherry.

A primary DRG culture from GCaMP3 mice was prepared, as described in section 6.4.1.1.3. These GCaMP3-expressing DRG neurons were subjected to electroporation to introduce two plasmids. The first causes the expression of a Cre enzyme under the control of the advillin promoter. The second plasmid is a CMV FLEx $PSAM^4$-5HT3 IRES mCherry. 1µg was used from each plasmid. The electroporation technique is described in section 6.4.1.1.3. As a result of co-transfection, the DRG neurons would express the $PSAM^4$-5HT3 LGIC and the fluorescent protein; mCherry. The Ca^{2+} imaging experiment was conducted by applying ACSF for 30 seconds. This was followed by applying varenicline (20nM) for 60 seconds to activate $PSAM^4$-5HT3 receptors. Then, the varenicline was washed out by applying ACSF for 60 seconds. Data were analysed using the standard Ca^{2+} imaging analysis protocol described above.

6.4.2.1.2. rAAV encoding FLEx $PSAM^4$-5HT3

6.4.2.1.2.1. Making rAAV for CMV FLEx $PSAM^4$-5HT3

With the promising *in vitro* data for chemogenetics-based neuronal activation, CMV FLEx $PSAM^4$-5HT3 IRES mEGFP was packaged into an rAAV vector to enable the testing of this virus *in vivo*. The packaging was done at the Massachusetts Institute of Technology (MIT) by Andrew Harrahill with my assistance.

HEK293T cells were cultured using DMEM (10% FBS) for three days. On day 3, five 15 cm tissue culture plates of HEK293T were prepared, with $2.7x10^7$ cells/plate. The plates were incubated in a cell culture incubator at 37°C with 5% CO_2. On the fourth day, the culture medium was aspirated, and 18 mL of culture

medium (DMEM, 10% FBS) was added to each plate. The plates were then kept in a cell culture incubator for one hour. A mixture containing 5.7 µg of plasmid DNA, 22.8 µg of the AAV capsid (AAV-2/1), and 11.45 µg of AAV helper 1 was prepared. Then the volume of this mixture was completed to 1ml using DMEM (without FBS). Another mixture containing 120 µg of 25K PEI (1 µg/µl, PEI MAX (Polysciences)) in 880µl of DMEM was prepared. The PEI-containing mixture was added to the DNA-containing mixture, and the two solutions were mixed and vortexed for 10 seconds. Then the mixture was left to stand for 15 minutes. 2 ml of PEI+DNA mixture was added to each 15 cm plate dropwise and was incubated in a cell culture incubator overnight. On the fifth day, the culture medium was aspirated from the plates and replaced with 20ml (5% FBS in DMEM). Then the cells were kept in the cell culture incubator overnight. On the seventh day, the cells were collected from the plates by pipetting up and down, and the cell mixture was spun down at 10,000g (8080 rpm) for 10 min at 4 °C. The supernatant was collected (solution 1). The cell palette was suspended in 10 ml of DPBS, and the mixture was centrifuged at 1500 g for 10 min at room temperature. The DPBS supernatant was collected and added to the supernatant of the cell (solution 1). The resulting mixture will be named mixture 2. Five ml PEG stock solution (average molecular weight 8,000, (Millipore-Sigma)) was added to mixture 2 from each cell plate (mixture 3). The cell pellet and mixture 3 were kept on ice for 1 hour. Mixture 3 was spun at 10,000 g (8080 rpm) for 30 minutes at 4°C. The supernatant was discarded, and the virus pellet was resuspended with 7 mL SAN digestion buffer (no enzyme). The virus suspension was added to the cell pellet and was stored at -80°C overnight (mixture 4). On day eight, 1 µL nuclease enzyme (250 U/µL) was added to mixture 4, and the mixture was shaken and incubated in a 37°C water bath for 1 hour. To purify the resulting AAV, the protocol by (Challis et al., 2019) was followed. An 18-gauge needle was used to collect 5ml of the virus layer. The needle was then replaced with a 0.22-micron filter. 5 mL DPBS + F-68 (Pluronic™ F-68 Non-ionic Surfactant (Fisher)) buffer was added to the syringe, and then the solution was pushed through the 0.22-micron filter. The filter tube was spun at 4000x g for 20 min at 4°C. The bottom solution was discarded, 14 ml of F-68 was added, and the mixture was spun again for 10 minutes. The last step was repeated three times. On the last spin, the mixture was spun until only ~150 µL remained. The virus solution was transferred to a Protein LoBind Tube. The filter was washed with DPBS + F-68. The amount

of DPBS + F-68 was chosen so that it can bring the total volume to ~150 uL. On the ninth day, the titre was quantified using the ddPCR Titration of AAV Vectors protocol by Addgene (Addgene, 2022).

6.4.2.1.2.2. Injecting CMV FLEx PSAM^4-5HT3 IRES mEGFP in the central amygdala of CreER^{T2} mice (+ targeted recombination in active populations (TRAPing))

The Institutional Animal Care and Use Committee at the Massachusetts Institute of Technology gave its approval for all experimental protocols. For this experiment, six adult CreER^{T2} mice were used (3 males and 3 females). These mice were anaesthetised until deep anaesthesia was obtained. Following that, mice underwent a stereotaxic surgery to inject 200nl of the CMV FLEx PSAM^4-5HT3 IRES mEGFP virus into the right central amygdala. The mouse undergoing surgery was injected subcutaneously with meloxicam (5mg/kg) and was moved to a stereotaxic frame (David Kopf Instruments). Following that, the scalp was shaved, and an incision was made to expose the skull. Thereafter, tiny craniotomies were made over the CeA. According to bregma, the following CeA coordinates were used: ML = 2.86±0.02 mm, AP = 1.22±0.05 mm, and DV = 4.25±0.03 mm. 200nl of the CMV FLEx PSAM^4-5HT3 IRES mEGFP virus was injected in the right CeA, and the virus injection rate was 50nl/min. The needle was removed 30 mins after the end of the injection, the incision was sutured, and mice were then monitored until they recovered. After the end of the surgery, mice were treated with a subcutaneous injection of buprenorphine (0.5mg/kg) and they were also treated with meloxicam (5mg/kg) 24 hours after the surgery. 8-9 days after the viral injection, mice were singly housed. 10-11 days after the viral injection, mice were anesthetised at 1.5% isoflurane and 0.8 oxygen for 90 mins while placed on a heating pad. Following that, each mouse received an intraperitoneal injection of 4-hydroxy tamoxifen (4-OHT) (50mg/kg). After the injection, mice were placed back in the isoflurane (1.2-1.25%) and were left for 3 hours. The behavioural tests (mainly the Hargreaves' test) were carried out approximately 10 days after 4OHT injection.

6.4.2.1.2.3. Checking the expression of PSAM^4-5HT3 in the central amygdala

At the end of the study, mice were transcardially perfused, and the brain was then extracted and kept in a 4% cold PFA solution overnight at 4° C. Then the PFA solution was replaced with 30% sucrose in PBS, and the brains were kept at 4°C overnight. Following that, the brains were dried and kept in an O.C.T. compound that was fast-frozen using dry ice. Following that, the brains were stored at −80 °C until sectioning. The brains were then sectioned at a thickness of 80µm. After acquiring brain slices, the slices were imaged using a laser scanning confocal microscope (Zeiss 700). Entire brain slices were imaged at ×5 resolution, while the whole CeA was imaged at ×10 resolution using a z stack of about 30 µm.

6.4.2.2. hM3Dq

6.4.2.2.1. Injecting the CANE virus in combination with hM3Dq viruses to capture CeAGA neurons

Adult Fos-2A-dsTVA mice (3 females and 2 males) aged 9-10 weeks old were placed in single cages for at least one day prior to being exposed to 1.5% isoflurane (0.8 ml O_2) for 2 hours. To keep the mice warm, a heating mat (at 37° C) was used during the isoflurane exposure. Also, the eyes were lubricated with an eye ointment. This two-hour isoflurane exposure was done to induce c-fos expression in the CeAGA. Capturing Activated Neural Ensembles (CANE)-LV-Cre and Cre-dependent AAV were combined (1:1 volume ratio). The Cre-dependent AAV, in this case, was pAAV-hSyn-DIO-hM3D(Gq)-mCherry (addgene 44361-AAV1, titre 2.2x10^{13} GC/ml, LOT v127505). For effective viral diffusion, a total of one 1000nl was administered unilaterally at the right amygdala at a rate of 50 nl/min, followed by a 20-minute waiting period. Following that, the needle was removed. The incision was sutured. Mice were then injected subcutaneously with buprenorphine (0.5 mg/kg). The mice were monitored until they recovered. Twenty-four hours after surgery, mice were given meloxicam again (5mg/kg) and were monitored closely for 3 days after the surgery. Then behavioural tests were conducted 3 weeks after the surgery. These behavioural tests included the Hargreaves' test, the dry ice test, the von Frey test, the intraplantar injection of PGE2 and the intraplantar injection of oxaliplatin. All behavioural tests were performed as described in section 6.4.1.2.2.

6.4.2.2.2. Immunohistochemistry of brain slices and imaging (hM3Dq virus-injected mice)

To identify CeAGA neurons, animals were anaesthetized with isoflurane (1.5%) for 2 hours. Following that, mice were transcardially perfused with PBS (pH 7.4) and then with 4% cold PFA fixation solution. The brain was then extracted and kept in a 4% cold PFA solution overnight at 4°C. Then the solution was replaced with 30% sucrose in PBS, and the brains were kept at 4°C overnight. Following that, the brains were dried and kept in an O.C.T. compound that was fast-frozen using dry ice. The brains were stored at −80°C until sectioning at a thickness of 80µm, and the sections were stained following the standard immunofluorescence protocol. For the Fos expression analysis, the primary antibody used was goat anti-Fos (Santa Cruz Biotechnology, sc520g, 1:300), and the secondary antibody was Alexa Fluor 488 donkey anti-goat (Jackson ImmunoResearch, 705-545-147, 1:500). To image the mCherry, rabbit anti-RFP antibody was used (Rockland, 600-401-379, 1:500), and the secondary antibody was Alexa Fluor 647 anti-rabbit (Jackson ImmunoResearch, 711-605-152, 1:500).

Brain slices were imaged using a laser scanning confocal microscope (Zeiss 700). Entire brain slices were imaged at ×5 resolution, while the whole CeA was imaged at ×10 resolution using a z stack of about 30 µm.

6.5. Results

6.5.1. PSAM^4-GlyR for neuronal silencing

6.5.1.1. Plasmids

As mentioned in the methods section, after cloning CMV PSAM^4-GlyR WPRE BGH pA, sequences encoding for fluorescent proteins were added into this plasmid, as this could make the assessment of the viral transduction more straightforward. Vectors that comprise two different genes of interest are named bicistronic vectors, and there are many ways to produce them. Using a second promoter in the same vector is perhaps the most direct way for coexpression. In this case, the vector should comprise two independent expression cassettes with a separate promoter for each gene in the two-promoter scheme. The main limitation of this method is that it may not be suitable for vectors with limited packaging capacity. This approach was avoided because the packaging capacity is a significant element to consider when dealing with rAAV vectors. Strategies that allow for one promoter include the use of an internal ribosome entry site

(IRES) or a Peptide 2A (P2A) sequence (Chan et al., 2011). P2A sequences are sandwiched between the two target genes and cause ribosomal "skipping" during translation, resulting in a missing peptide bond and effectively separating the two proteins. One of the pros of this strategy is the small size of the P2A sequence (just 19 amino acids). Unfortunately, employing P2A is not free from challenges. Two significant challenges need to be considered when P2A is used for co-expression. Firstly, as a result of the cleavage, both genes retain a portion of the P2A sequence. This may have an impact on the proteins' functioning or targeting. Second, the efficiency of expression is determined by cleavage efficiency, which is influenced by the downstream gene. If cleavage fails, a fusion protein with reduced or no function will be produced unless the genes can be produced as a polyprotein. On the other hand, the IRES strategy is used to take advantage of a virus's natural capacity to express multiple genes from within a stretch of mRNA (cap-independent translation), with the IRES linkage allowing the translation of a protein downstream of the IRES. To allow the expression of two independent proteins simultaneously and stay within the packaging capacity offered by the AAV virus and to avoid the potential cleavage issues caused by the P2A strategy, the IRES strategy was selected.

For the IRES strategy, a suitable fluorescent protein needed to be selected. For Ca^{2+} imaging experiments, mice expressing the Ca^{2+} sensor GCaMP3 were used. As GCaMP3 has a green fluorescence, a different type of fluorescence (e.g., red) was needed to enable the detection of each protein using a different wavelength. Within the options of the red fluorescent proteins available, mCherry was selected as it is a small protein whose sequence can be easily incorporated into an rAAV vector. Another plasmid with a green fluorescent protein was cloned for electrophysiological recording experiments. After cloning CMV PSAM^4-GlyR IRES mCherry WPRE BGH pA and CMV PSAM^4-GlyR IRES AcGFP1 WPRE BGH pA, the expression of the PSAM^4-GlyR and the fluorescent proteins was checked in primary DRG cultures (see Figure 45). Results indicated that plasmids encoding for PSAM^4-GlyR and mCherry or AcGFP1 were successfully cloned, and they allowed the expression of transgenes in DRG cultures following electroporation. The percentage of cells showing mCherry signal ranged between 5% and 10% of the total number of cells expressing GCaMP3 following

electroporation of cells with plasmid vectors to express PSAM^4-GlyR and mCherry.

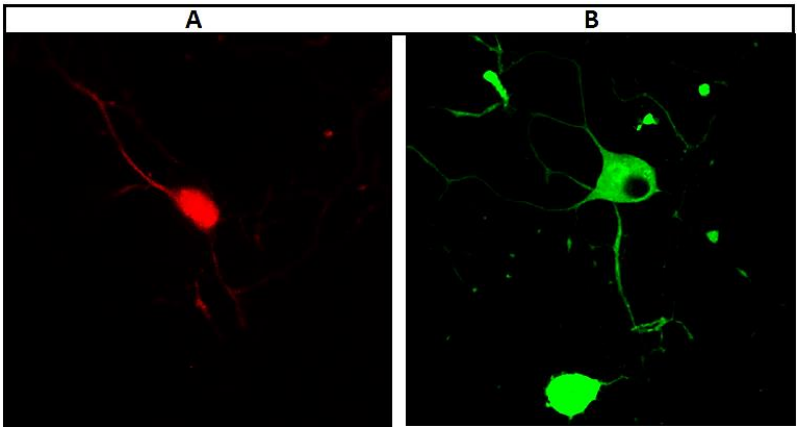

Figure 45: The expression of the PSAM^4-GlyR using the plasmids CMV PSAM^4-GlyR IRES mCherry WPRE BGH pA (A) and CMV PSAM^4-GlyR IRES AcGFP1 WPRE BGH pA (B) in primary DRG cultures from C57BL/6 mice. *The images were obtained 2 days after electroporation using Amaxa P3 primary cell 4D-Nucleofector X kit. Images were acquired using a Leica SP8 confocal microscope (25× water immersion, 0.95-N.A. objective).*

6.5.1.1.1. Assessing the criteria of PSAM^4-GlyR as a chemogenetic tool

A good chemogenetic tool should have a receptor that does not affect the cell in the absence of the ligand and a ligand that does not affect the cells that do not express the chemogenetic receptor. To assess the former criterion, two experiments were conducted. The first involved comparing Ca^{2+} responses to the activating agent veratridine (a sodium channel agonist that causes the subsequent activation of voltage-gated calcium channels leading to higher intracellular Ca^{2+} and increased GCaMP signals (Mohammed et al., 2017)) (30µM) between transfected and non-transfected DRG neurons from C57BL/6 mice using GCaMP3 imaging. The results revealed no significant difference in the intensity of Ca^{2+} response (dF/F_0) between transfected cells and the non-transfected ones (see Figure 46A). For the Ca^{2+} imaging experiments, veratridine was chosen as an activating agent because the resulting increase in the Ca^{2+} signal driven by veratridine application is not a direct effect of veratridine action but rather an indirect effect due to cell activation. The second experiment involved assessing whether the expression of the chemogenetic receptor PSAM^4-GlyR

alters the response of PSAM^4-GlyR expressing cells to ACh compared to PSAM^4-GlyR negative neurons. This experiment was done to assess whether, in the absence of an exogenous ligand, the receptor will be activated by ACh (the endogenous ligand of nAChRs). The results revealed that the mean response to ACh (30µM) was not significantly different between the transfected cells and the non-transfected cells (unpaired t-test, p-value=0.4768, see Figure 46B). Together these results indicated that the expression of the PSAM^4-GlyR LGICs did not perturb the cell. Regarding varenicline, potential off-target effects of 20nM varenicline were assessed by applying the drug (20nM in ACSF) to non-transfected cells, and no significant changes in the Ca^{2+} signal were detected (Mann-Whitney test, p-value=0.3593, see Figure 46C).

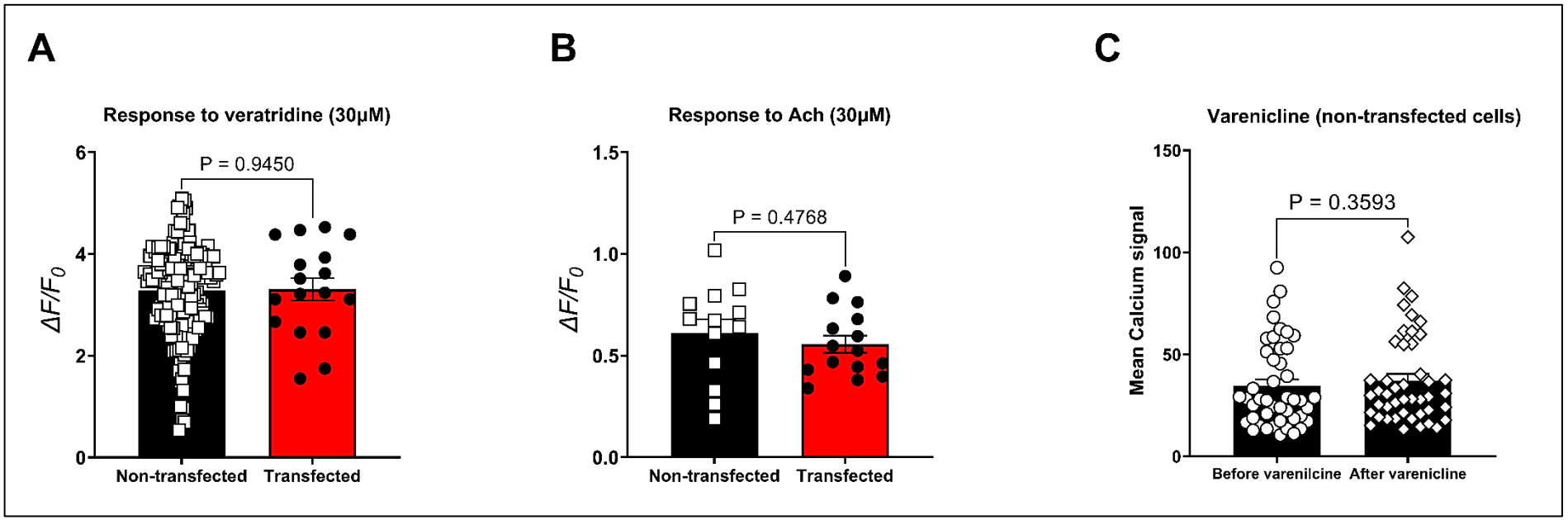

Figure 46: PSAM^4-GlyR (+ varenicline) system is a suitable tool to study DRG neurons.

A) The expression of the PSAM^4-GlyR LGIC did not cause a significant change in the Ca^{2+} responses to veratridine (30µM). *The responses were assessed using Ca^{2+} imaging on DRG cultures from C57BL/6 mice expressing the Ca^{2+} sensor GCaMP3 under the control of the Pirt promoter. Statistical analysis was done using the unpaired t-test (p-value=0.9450)—n=17 for the transfected group and 181 for the non-transfected.*

B) PSAM^4-GlyR-expressing DRG neurons showed a similar response to acetylcholine (30μM) compared to the non-transfected cells. *The responses were assessed using Ca^{2+} imaging on DRG cultures from C57BL/6 mice expressing the Ca^{2+} sensor GCaMP3 under the control of the Pirt promoter. Statistical analysis was done using the unpaired t-test (p-value=0.4768)—n=15 for transfected cells and 13 for non-transfected cells.*

C) The application of varenicline (20nM) did not significantly change the mean Ca^{2+} signal in non-transfected cells. *The responses were assessed using Ca^{2+} imaging on DRG cultures from C57BL/6 mice expressing the Ca^{2+} sensor GCaMP3 under the control of the Pirt promoter. Statistical analysis was done using the Mann-Whitney test (p-value= 0.3593)—n=45.*

Error bars represent the standard error of the mean. Transfected cells are cells that express PSAM^4-GlyR (as indicated by mCherry positivity) and non-transfected cells are cells that lack mCherry signal.

6.5.1.1.2. Testing the ability of varenicline (20nM) to silence PSAM^4-GlyR expressing DRG neurons

To assess whether applying varenicline 20 (nM) silences the PSAM^4-GlyR expressing DRG neurons, PSAM^4-GlyR was expressed in primary DRG cultures from mice that express GCaMP3 under the control of the *Pirt* promoter using plasmid vectors. Varenicline (20nm) was applied for 5 minutes. Then DRG neurons were activated using veratridine (30µM). Results indicated that PSAM^4-GlyR-expressing DRG neurons responded significantly less than the non-transfected cells, with the mean Ca^{2+} response ($\Delta F/F0$) being 1.9 in the non-transfected group and 0.37 in the transfected group (Figure 47). The data on (Figure 47) was generated from DRG cultures prepared from more than five mice expressing GCaMP3 under the control of the *Pirt* promoter, With these promising results, the plasmid was packaged into AAV9 vectors to enable further testing.

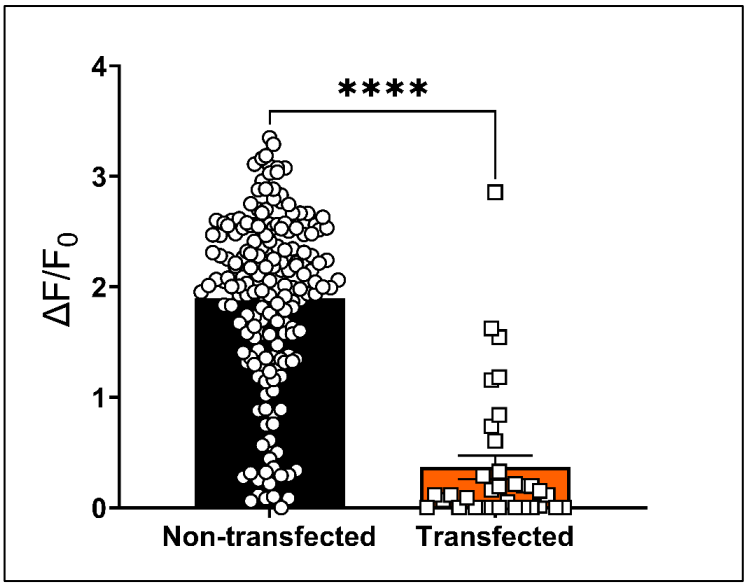

Figure 47: The application of varenicline silenced the veratridine-evoked Ca^{2+} responses in PSAM^4-GlyR+ DRG neurons in vitro. *Varenicline (20nM) was applied for 5 minutes followed by the application of Veratridine 30µM+ varenicline (20nM) for 10 seconds. The comparison of the veratridine evoked increase in the Ca^{2+} signal revealed the PSAM^4-GlyR+ DRG neurons (transfected, red column) responded significantly less than the PSAM^4-GlyR- DRG neurons (non-transfected, black column). Statistical analyses were done using the Mann-Whitney test (p-value <0.0001). n-189 for the non-transfected*

cells and 35 for the transfected cells. Error bars represent the standard error of the mean.

6.5.1.2. Recombinant viruses encoding for PSAM^4-GlyR

6.5.1.2.1. Assessing the viral transduction efficiency *in vitro* and *in vivo*

With the successful results obtained by the plasmid CMV PSAM^4-GlyR IRES mCherry WPRE BGH pA in Ca^{2+} imaging experiments, this plasmid was sent for packaging into an rAAV vector (Vector Builder, AAV9 capsid). 5µl of the virus mixture (10^{13} genome copy number/µl) was used in primary DRG cultures from C57BL/6 mice that express GCaMP3 under the control of the *Pirt* promoter. Seven days after *in vitro* transduction, it was found that the rAAV had transduced more than 90% of the cells (see Figure 48). The *in vivo* transduction efficiency was checked 10 weeks after the intraplantar injections of 5µl of the virus in each paw in mouse pups (P2-P5) (see Figure 49) or 8 weeks after the intrathecal injection of 5µl of the virus to adult mice (6-8 weeks) (Figure 50). After intraplantar injection, more than 70% of the GCaMP3+ neurons were mCherry-positive, while less than 20% colocalization was seen after intrathecal injection. Therefore, intraplantar injection was used for subsequent studies.

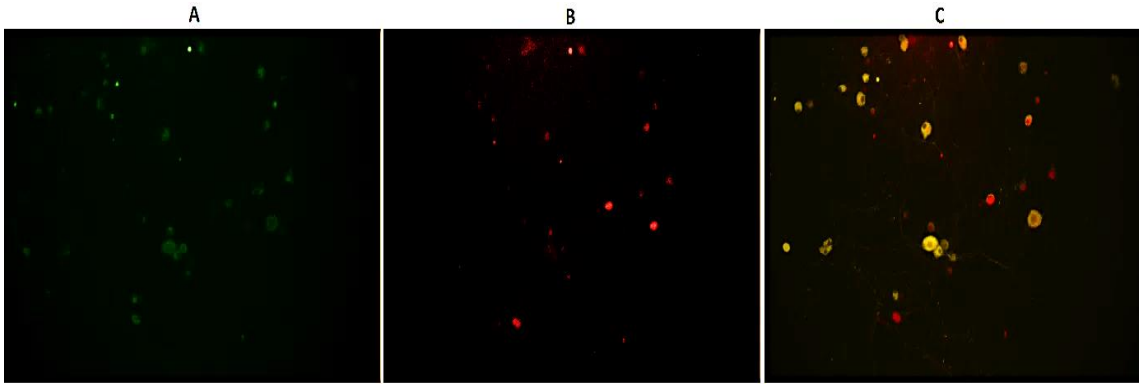

Figure 48: The expression of PSAM^4-GlyR following the use of rAAV vector carrying PSAM^4-GlyR. *The rAAV resulted in high transduction efficacy. A: GCaMP3 expressing DRG neurons; B: PSAM^4-GlyR expressing DRG neurons; C: a merged picture showing that more than two-thirds of the DRG neurons expressed both PSAM^4-GlyR and GCaMP3. A CCD camera was used to obtain these images.*

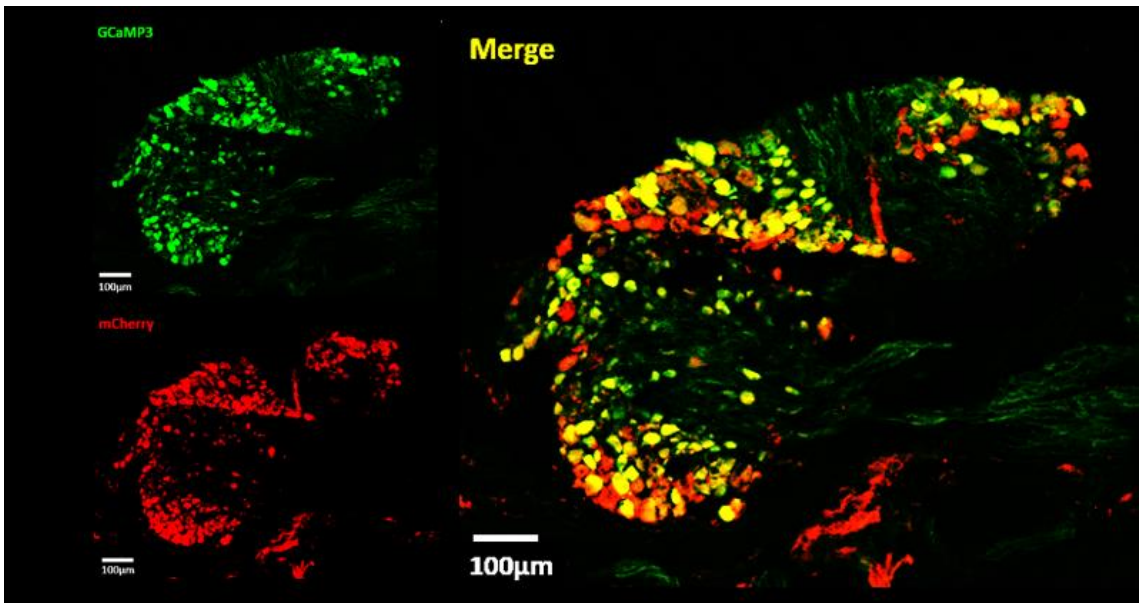

Figure 49: The expression of PSAM^4-GlyR 10 weeks after injecting an rAAV carrying PSAM^4-GlyR and mCherry transgenes into mouse pups that express the Ca^{2+} sensor GCaMP3 under the control of the Pirt promoter. *The injection was done intraplantarly on day 5 after birth. The green colour represents DRG neurons expressing GCaMP3, the red colour DRG neurons expressing PSAM^4-GlyR, yellow colour represents DRG neurons co-expressing GCaMP3 and PSAM^4-GlyR.*

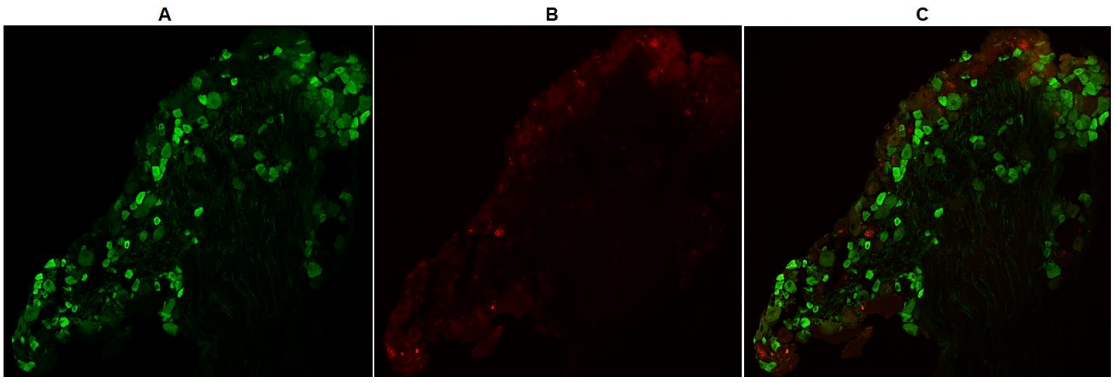

Figure 50: The expression of PSAM^4-GlyR 8 weeks after injecting an rAAV carrying PSAM^4-GlyR and mCherry (under the control of the CMV promoter) intrathecally into adult mice that express the Ca^{2+} sensor GCaMP3 under the control of the Pirt promoter. *A: DRG neurons expressing GCaMP3, B: DRG neurons expressing PSAM^4-GlyR, C: a merged picture (A and B).*

6.5.1.2.2. Assessing whether varenicline application silences Ca^{2+} responses to veratridine in DRG neurons expressing $PSAM^4$-GlyR as a result of *in vitro* viral transduction

A rAAV carrying $PSAM^4$-GlyR and mCherry was used in primary DRG cultures from mice that express GCaMP3. Veratridine was used to activate these cells and varenicline was shown to silence the responses of DRG neurons that express $PSAM^4$-GlyR to the veratridine (Figure 51). Results from these experiments indicated that varenicline silenced the responses of more than 80% of DRG neurons that expressed $PSAM^4$-GlyR to veratridine activation and lowered the mean response intensity in the remaining 20% of cells by more than 70%. Varenicline did not significantly affect the veratridine-evoked responses in non-transduced cells (Figure 51). The baseline responses to veratridine were similar between transduced and non-transduced cells, showing that the expression of the receptor is not sufficient to alter the behaviour of the cell (Figure 51). These results aligned with the plasmid results.

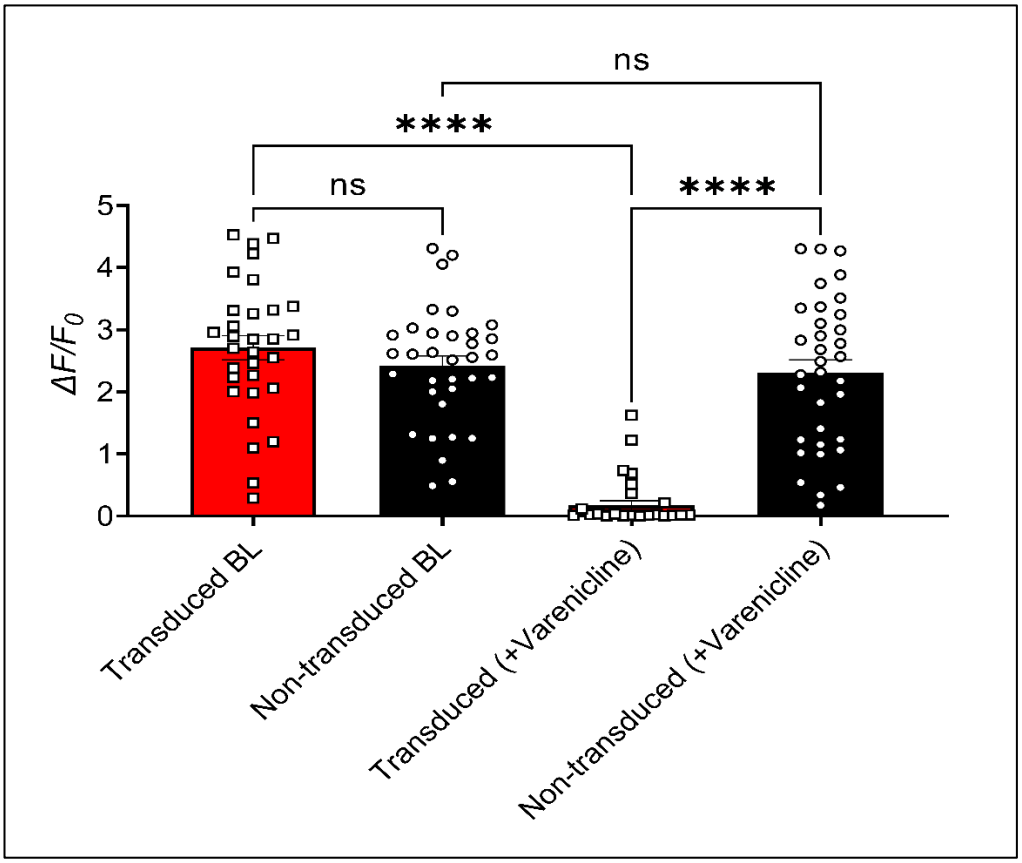

Figure 51: Varenicline (20nM) silenced the responses of $PSAM^4$-GlyR expressing DRG neurons to veratridine (30μM) following rAAV vector-based transfection. *There was no significant difference in the first response to*

veratridine (30μM) between transfected and non-transfected cells (unpaired t-test, p-value= 0.4268), but after the exposure to varenicline (20nM) for 5 minutes, the transfected cells responded to veratridine (30μM) significantly less than the non-transfected cells and significantly less than their responses in the baseline. On the other hand, there was no significant difference between the baseline responses of the non-transfected cells before and after varenicline (p-value= 0.9572). Transfected cells are the DRG neurons expressing PSAM^4-GlyR. Data were analysed using the two-way ANOVA test with Tukey's multiple-comparisons test. Tukey's multiple comparisons test results are shown on the graph. n=31 for the transfected and 33 for the non-transfected.

6.5.1.2.3. Assessing whether varenicline injection elevates pain threshold in mice expressing PSAM^4-GlyR in the DRG neurons and whether this is driven by DRG silencing

6.5.1.2.3.1. Sensory and motor co-ordination tests

The injection of varenicline (0.3mg/kg) rendered the withdrawal latency/thresholds of mice expressing PSAM^4-GlyR significantly longer/higher than the control group (expressing PSAM^4-GlyR but injected with PBS instead of varenicline) in sensory tests. The viral injection was conducted intraplantarly in mouse pups (P2-P5) and behavioural tests were done 10-12 weeks after the administration of AAV9 carrying PSAM^4-GlyR. The behavioural tests included the Hargreaves' test, the von Frey test, and the dry ice test (see Figure 52 (A-C), respectively). These behavioural tests were carried out 30 minutes after the drug injection. In the Hargreaves' test, the mean withdrawal latency was 23.10 seconds for the varenicline-treated mice, while it was 14.11 seconds for the PBS-treated group (Figure 52A). Similarly, PSAM^4-GlyR activation elevated the withdrawal latency in the dry ice test to become 21.07 in the varenicline group, while the PBS-treated group was 12.03 seconds (Figure 52B) (p-value <0.0001, unpaired t-test). Importantly, varenicline almost doubled the mean withdrawal threshold in the von Frey test compared to the control group (0.67 grams vs. 1.32 grams), indicating an impairment of the innocuous touch sensation (Figure 52C). To assess whether the administration of varenicline to PSAM^4-GlyR-expressing mice caused any noticeable impairment in motor abilities, the rotarod test was

done, and mice treated with varenicline were compared to mice treated with PBS. No significant difference was detected between the two groups (Figure 52D).

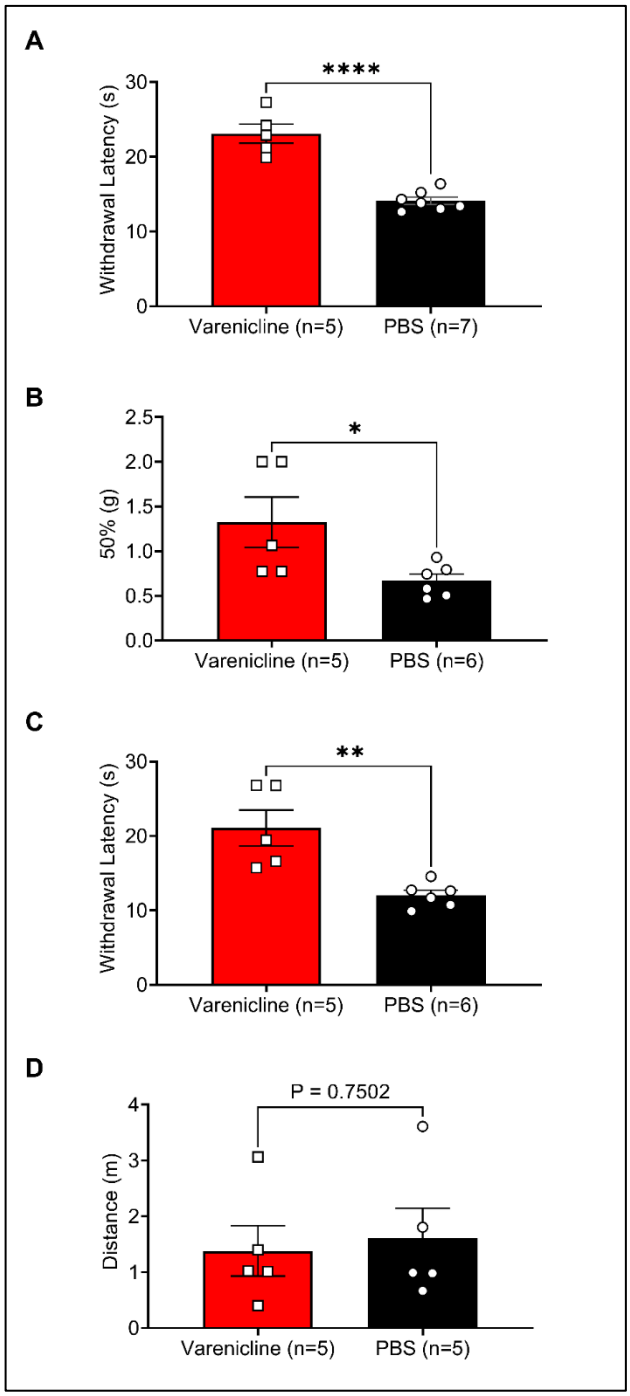

Figure 52: Varenicline application increased the withdrawal thresholds of mice expressing PSAM^4-GlyR compared to their controls in various sensory tests (Hargreaves' test, the Up-down von Frey test, and the dry ice test) without impairing motor coordination. *Both groups express PSAM^4-GlyR. Statistical analyses were done using the unpaired t-test (p-value= <0.0001 (Hargreaves' test (A)), 0.0373 (von Frey (B)), and 0.0035 (the dry ice test (C))).*

On the other hand, the administration of varenicline to PSAM^4-GlyR expressing mice did not significantly alter their motor abilities compared to the controls without varenicline (D). The varenicline dose was (0.3 mg/kg), and the behavioural tests were done 30 minutes after the intraperitoneal varenicline or PBS injection. Error bars represent the standard error of the mean. PBS: phosphate-buffered saline.

6.5.1.2.3.2. *In vivo* Ca^{2+} imaging to validate the increase in withdrawal thresholds

In vivo, Ca^{2+} imaging was used to examine whether activating PSAM^4-GlyR with varenicline could silence DRG neurons *in vivo* after AAV9-based transgene delivery (Figure 53). The *in vivo* imaging experiments indicated that there was a significant reduction in the number of cells responding to the application of 55°C water to the paw in the ipsilateral L4 DRG neurons 30 minutes after the intraperitoneal administration of varenicline (0.3 mg/kg) to PSAM^4-GlyR expressing mice (Figure 53 (A)) as indicated by the significant reduction in the number of heat responding cells per mm^2 in the superficial layer of L4 DRG. These results indicate that approximately 80% of the heat-responding cells were silenced in the varenicline-treated group. Figures 53B and 53C show the average peak intensity trace of the cells before the application of varenicline (baseline response) compared to the silenced neurons after varenicline administration (B) or the cells that remained responsive after varenicline (C). For the peak intensity analysis, 147 cells were analyzed, and two-thirds of them were silenced (98 cells) after varenicline administration (shown in Figure 53 B). Figure 53 (D-F) shows examples of representative *in vivo* Ca^{2+} imaging experiments.

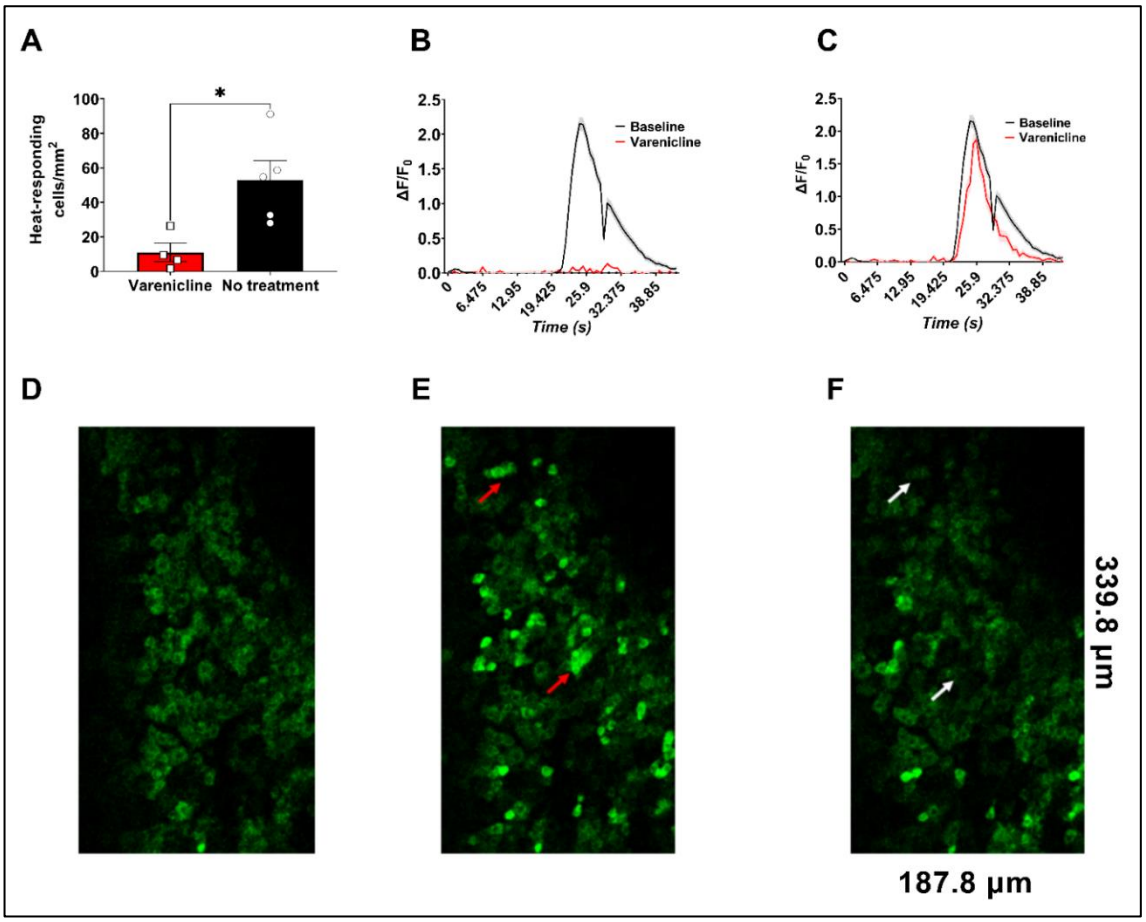

Figure 53: Varenicline reduced the Ca^{2+} responses of the DRG neurons responding to the application of 55°C water to the ipsilateral hind paw of mice expressing the Ca^{2+} sensor GCaMP3 under the control of the Pirt promoter and $PSAM^4$-GlyR following rAAV9 vector-based transduction.

A) The number of DRG neurons per mm^2 (in L4) responding to hot water (55°C) in the paw was reduced significantly after the intraperitoneal administration of varenicline to $PSAM^4$-GlyR expressing mice (p-value= 0.0175 (un-paired t-test, n=5 mice in the control group and four mice in the treatment group)).

B) Plot showing the mean response amplitude before (black trace) and after varenicline administration in the silenced neurons (n = 98 cells for the varenicline-treated group and 147 for the baseline). Cells were recorded from three mice.

C) Plot showing the mean response amplitude before (black trace) and after varenicline administration in the silencing-resistant neurons (n = 49 cells for the varenicline-treated group and 147 for the baseline). Cells were recorded from three mice. The number of cells recorded from each mouse was similar.

D) represents the basal Ca^{2+} signal in L4 (no stimulation) in mice expressing GCaMP3 and PSAM^4-GlyR. E) shows the increase in the Ca^{2+} signal in the ipsilateral DRG after the application of 55°C water to the ipsilateral paw (no treatment). Red arrows point towards representative heat-responding cells. F) shows the response of the same DRG to the application of 55°C water to the paw 30 minutes after the mouse received an intraperitoneal injection of varenicline (0.3 mg/kg) (The white arrows point toward the cells that previously responded to heat before varenicline application).

Data are presented as mean±SEM.

6.5.1.2.3.3. The efficacy of the PSAM^4-GlyR (+varenicline) system in inflammatory and neuropathic pain models

Following initial validation steps, the PSAM^4-GlyR (+ varenicline) system was tested in a reversible inflammatory model involving the intraplantar injection of PGE2. Previous studies suggested that the proinflammatory actions of PGE2 involve the activation of the protein kinases A and C, which results in heat hyperalgesia (Sachs et al., 2009) as these kinases sensitize many receptors and ion channels, like TRPV1 (Kawabata, 2011). The PSAM^4-GlyR (+varenicline) system showed good efficacy in reducing signs of heat hypersensitivity that usually follow PGE2 injection when tested using the Hargreaves' test (Figure 54A). While mice treated with varenicline still exhibited signs of heat hyperalgesia, this hyperalgesia was significantly less than the ones treated with PBS, with the mean withdrawal latency in the Hargreaves' test in the varenicline-treated mice being almost triple that of the PBS-treated group (6.69 seconds vs 2.62 seconds) (unpaired t-test, p-value=0.0249, Figure 54A).

PSAM^4-GlyR expressing mice were injected with the chemotherapeutic agent oxaliplatin intraplantarly. Oxaliplatin is known to induce cold allodynia (demonstrated by the reduction in the withdrawal latency in the dry ice test). This allodynia was reversed in the PSAM^4-GlyR-expressing mice treated with

varenicline compared to the ones treated with PBS (Figure 54B) (unpaired t-test, p-value= 0.0209).

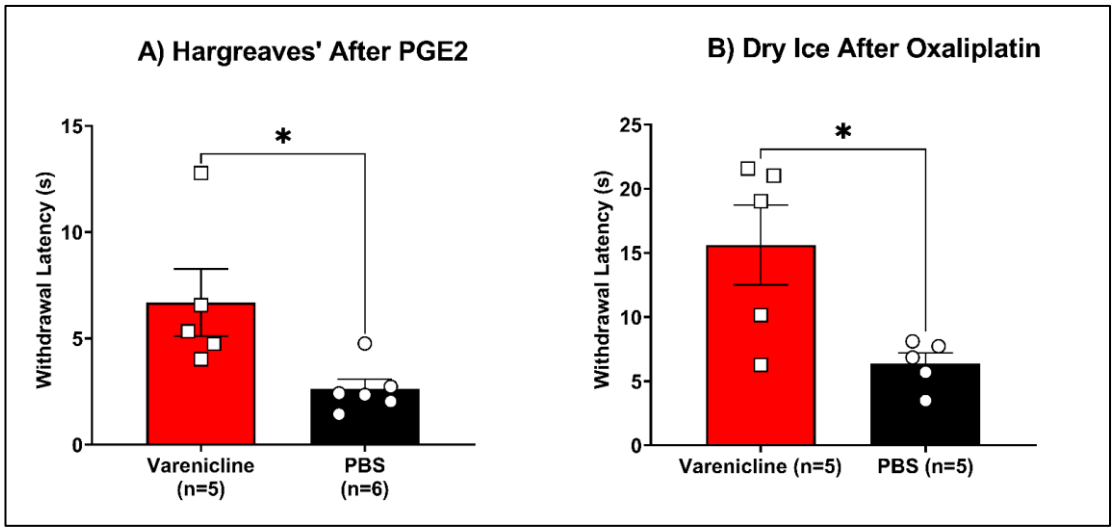

Figure 54: the administration of varenicline to mice expressing PSAM^4-GlyR in the DRG neurons reduced heat hyperalgesia following the intraplantar injection of PGE2 and cold allodynia induced by oxaliplatin. *A) PGE2 (500 µM, total volume 20 µl) was injected intraplantarly, and after 10 minutes, either varenicline or PBS was injected intraperitoneally. After 40 minutes of the PGE2 injection, the Hargreaves' test was performed. The varenicline-treated mice had significantly less heat hyperalgesia following the intraplantar injection of PGE2 compared to the PBS-treated group (p-value= 0.0249, unpaired t-test). B) The administration of varenicline to mice expressing PSAM^4-GlyR in the DRG neurons abolished the cold allodynia driven by the intraplantar injection of 80µg oxaliplatin (p-value= 0.0209 (the unpaired t-test)). The dry ice test was done after 4.5 hours of the intraplantar injection of oxaliplatin (80µg) and 30 minutes after the varenicline injection. Error bars represent SEM.*

6.5.1.3. PSAM^4-GlyR transgenic knockin mouse line

6.5.1.3.1. Assessing the expression of PSAM^4-GlyR after crossing the Rosa26 FLEx PSAM^4-GlyR IRES tdTomato with Na$_V$1.8 Cre mouse line.

The Rosa26 FLEx PSAM^4-GlyR IRES tdTomato mouse line encodes for PSAM^4-GlyR in a Cre-dependent manner. Upon crossing a Rosa26 FLEx PSAM^4-GlyR IRES tdTomato mouse with a homozygous mouse that expresses the Cre enzyme in a subset of neurons, the resulting offspring will express PSAM^4-GlyR

and the fluorescent protein tdTomato in that specific neuronal subset. Once varenicline is administered to these mice, that neuronal subset will be silenced, allowing us to study the effects of this subset without having the compensatory alteration seen with the congenital neuronal ablation or gene knockout approaches.

To achieve this, heterozygous Rosa26 FLEx PSAM^4-GlyR IRES tdTomato mice were crossed with homozygous Na$_V$1.8 Cre mice. Figures 55 (A-C) show how PSAM^4-GlyR (and tdTomato) are expressed in the Na$_V$1.8-positive neurons after this crossing.

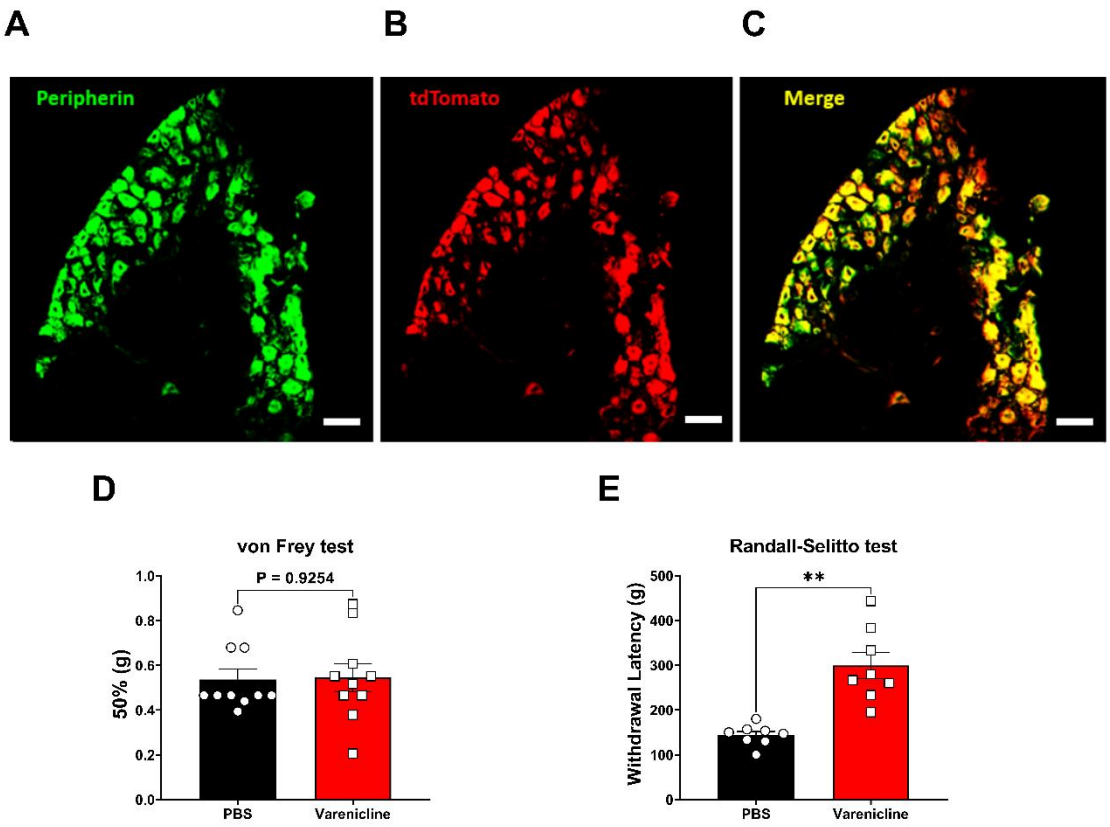

Figure 55: Varenicline treatment to mice that express PSAM^4-GlyR in the Na$_V$1.8 expressing neurons elevated their withdrawal thresholds in the Randall-Selitto test without impairing innocuous touch sensation.

Figures (A-C) show the expression of PSAM^4-GlyR in the DRGs from mice carrying a Rosa26-FLEx-PSAM^4-GlyR-IRES-tdTomato allele and expressing Cre enzyme in the Na$_V$1.8-positive neurons. A: peripherin expressing DRG neurons; B: PSAM^4-GlyR expressing DRG neurons (as demonstrated by tdTomato

expression); C: a merged picture of A and B showing the co-expression of peripherin and PSAM^4-GlyR. Images were obtained using a Leica SP8 confocal microscope. The scale bars represent 50µm. n=8 for the Randall-Selitto test and n=10 for the von Frey test.

Figure (D) shows how the systemic administration of varenicline caused no significant alteration in the withdrawal thresholds of the mice expressing PSAM4-GlyR in the NaV1.8-positive neurons in the von Frey test (p-value=0.9254, paired t-test)) and Figure (E) shows the Randall Selitto test results (p-value= 0.0011, paired t-test). Error bars represent SEM.

6.5.1.3.2. Evaluating whether varenicline could alter the mechanical withdrawal thresholds in mice expressing PSAM^4-GlyR in the Na$_V$1.8 positive neurons.

6.5.1.3.2.1. The up-down von Frey test

Ten mice expressing PSAM^4-GlyR in the Na$_V$1.8 positive neurons were intraperitoneally injected with either varenicline (0.3 mg/kg) or PBS. Following that, the up-down von Frey test was conducted. The results indicated that there was no significant difference in the mean withdrawal threshold between the readings obtained after varenicline compared to the readings of the same mice after PBS (p-value= 0.9254, the paired t-test) (Figure 55D). This data aligns with what has been previously reported from mice in which the Na$_V$1.8+ neurons are ablated (Abrahamsen et al., 2008). This is considered an advantage over viruses that do not restrict the expression of PSAM^4-GlyR to a specific neuronal subtype.

6.5.1.3.2.2. The Randall-Selitto test

Because it was previously shown that the DTA-mediated ablation of the Na$_V$1.8-positive neurons significantly increases the withdrawal threshold in the Randall-Selitto test (Abrahamsen et al., 2008), this test was performed in varenicline-treated mice expressing PSAM^4-GlyR in the Na$_V$1.8-expressing neurons, and they were compared with test results when treated with PBS. In this test, mechanical pressure was applied to the tail until vocalisation or withdrawal occurred. Results indicate that varenicline treatment to mice expressing PSAM^4-GlyR in the Na$_V$1.8+ neurons doubled their withdrawal thresholds in the Randall-Selitto test (143.75 g after PBS treatment and 299.38 g after varenicline treatment, p-value= 0.0011, paired t-test) (Figure 55E).

Following these tests, mice that express PSAM^4-GlyR in the Na$_V$1.8-expressing neurons were tested in the CIBP model. Results can be found in section 4.4.2. Results indicated that these mice increased the use of the affected limb after the administration of varenicline, highlighting the role of this neuronal subtype in CIBP.

6.5.1.3.3. Evaluating whether the administration of varenicline to mice expressing PSAM^4-GlyR in the Na$_V$1.8 positive neurons could reduce neuropathic pain.

Mice that express the PSAM^4-GlyR channels in the Na$_V$1.8-expressing neurons were subjected to chronic constriction injury surgery of the sciatic nerve. After the surgery, mice demonstrated signs of increased mechanical, heat, and cold hypersensitivity (Figure 56, black). Then these mice received an intraperitoneal injection of varenicline (0.3 mg/kg), and the results showed that varenicline, compared to PBS treatment, reversed signs of mechanical (Figure 56A, red vs. black, two-way ANOVA, p-value=<0.0001), heat (Figure 56B, red vs. black, two-way ANOVA, p-value=<0.0001) and cold hypersensitivity ((Figure 56C, dry ice test, red vs. black, two-way ANOVA, p-value=<0.0001) (Figure 56D, acetone test, red vs. black, one-way ANOVA test with Tukey's test, p-value=0.0009)).

Injured mice that express PSAM^4-GlyR in the Na$_V$1.8 positive neurons treated with varenicline were also compared with sham mice, and the difference in the von Frey (two-way ANOVA, p-value= 0.4278), Hargreaves' (two-way ANOVA, p-value= 0.4626), dry ice (two-way ANOVA, p-value= 0.5148) and acetone tests (one-way ANOVA test with Tukey's test, p-value=0.8554) was statistically insignificant between these two groups in all these tests (Figure 56, red vs. blue). However, in the absence of varenicline, there was dramatic sensitization of sensory neurons (Figure 56, black vs. blue (p-value <0.0001 for the von Frey and the dry ice tests (two-way ANOVA), 0.0064 (for the Hargreaves' test, two-way ANOVA), and 0.0059 (for the acetone test, one-way ANOVA with Tukey's test)).

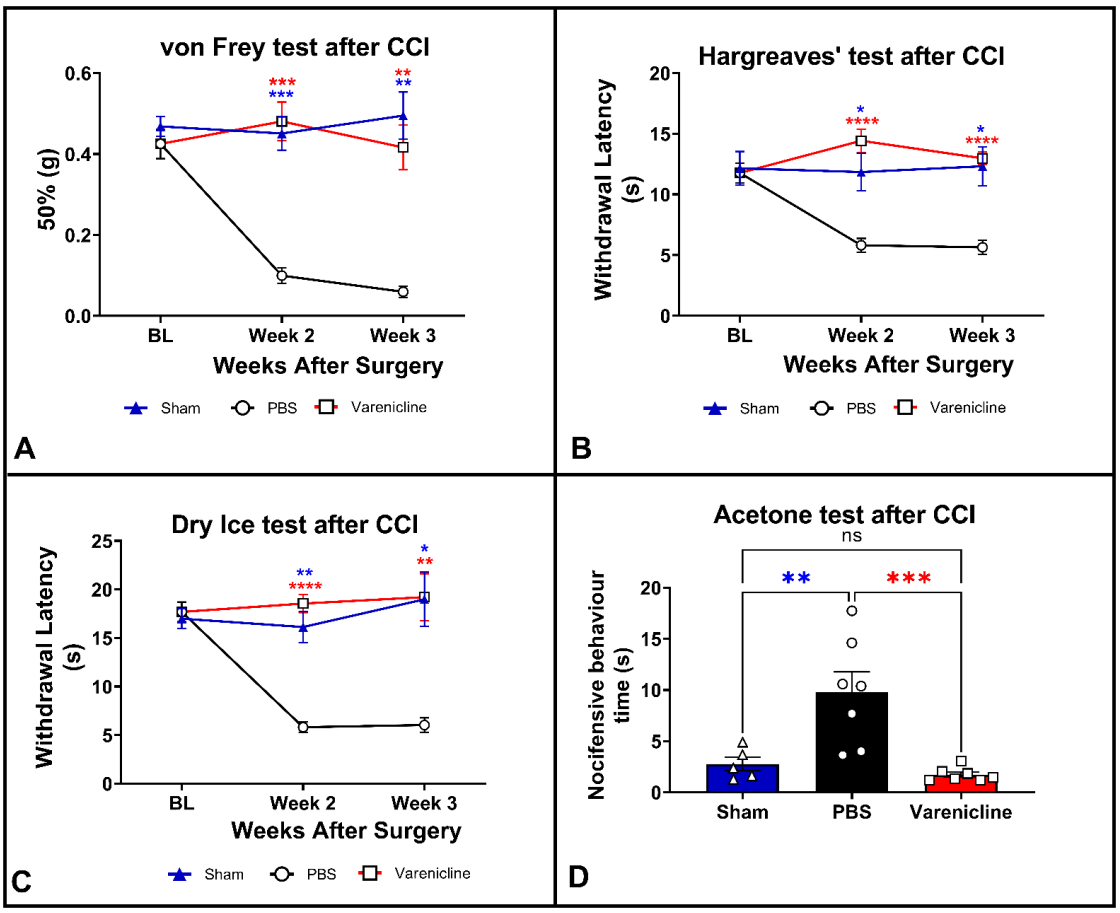

Figure 56: The systemic injection of varenicline in mice expressing PSAM^4-GlyR in Na$_V$1.8-positive neurons reversed mechanical, thermal, and cold sensitivity caused by the chronic constriction injury of the right sciatic nerve. *Each mouse received either PBS or varenicline and the behavioural tests were carried out 30 minutes after drug administration. 24 hours after that, and within the same week, each mouse received the other treatment, and the behavioural tests were repeated. In graphs (A-D), mice with ligated sciatic nerves (and treated with either varenicline (red) or PBS (black)) are compared with sham mice in which the sciatic nerve was exposed but not ligated (blue). Figure A shows the up-down von Frey test results for mechanical sensitivity. Figure B illustrates the Hargreaves' test results (heat sensitivity). Figure C shows the dry ice test results (cold sensitivity). Figure D shows the acetone test results on week 3 after the chronic constriction injury of the sciatic (affective responses to cold). For Figures A-C, data were analysed using the two-way ANOVA with Tukey's multiple-comparisons test, but for Figure D, the one-way ANOVA test with Tukey's multiple-comparisons test was employed. n=7 for mice expressing PSAM^4-GlyR in the Na$_V$1.8+ neurons (three males and four females), and for the*

sham group, n=5 mice (four males and one female). The asterisks of significance shown in the Figure represent Tukey's multiple-comparisons test results comparing the varenicline-treated group (red asterisks) or the sham group (blue asterisks) with the PBS-treated group at each time point. Varenicline was used at a dose of (0.3mg/kg) and was injected intraperitoneally. Error bars represent SEM.

6.5.2. Chemogenetic tools for neuronal activation

6.5.2.1. in vitro assessment of PSAM^4-5HT3 (and varenicline) for neuronal activation

The CMV FLEx PSAM^4-5HT3 IRES mCherry BGH pA plasmid was used for Ca^{2+} imaging experiments. When DRG neurons were co-transfected with Advillin Cre and CMV FLEx PSAM^4-5HT3 IRES mCherry BGH pA plasmids, they expressed PSAM^4-5HT3 LGIC and the fluorescent protein; mCherry. When varenicline binds to PSAM^4-5HT3 expressing DRG neurons, an increase in GCaMP3 fluorescence is observed as a result of the activation. Figure 57A summarises a set of quantitative experimental data indicating the efficacy of PSAM^4-5HT3 in activating DRG neurons upon the application of varenicline (20nM), with the mean response intensity being 1.17 in the transfected cells and 0.20 in the non-transfected cells. Figure 57B shows how varenicline (20nM) application increased the GCaMP3 fluorescence in PSAM^4-5HT3 expressing DRG neurons. It is important to note that the DRG neurons that were transfected with only one of the two plasmids should not show a mCherry signal, so they were regarded as un-transfected cells and were used as controls.

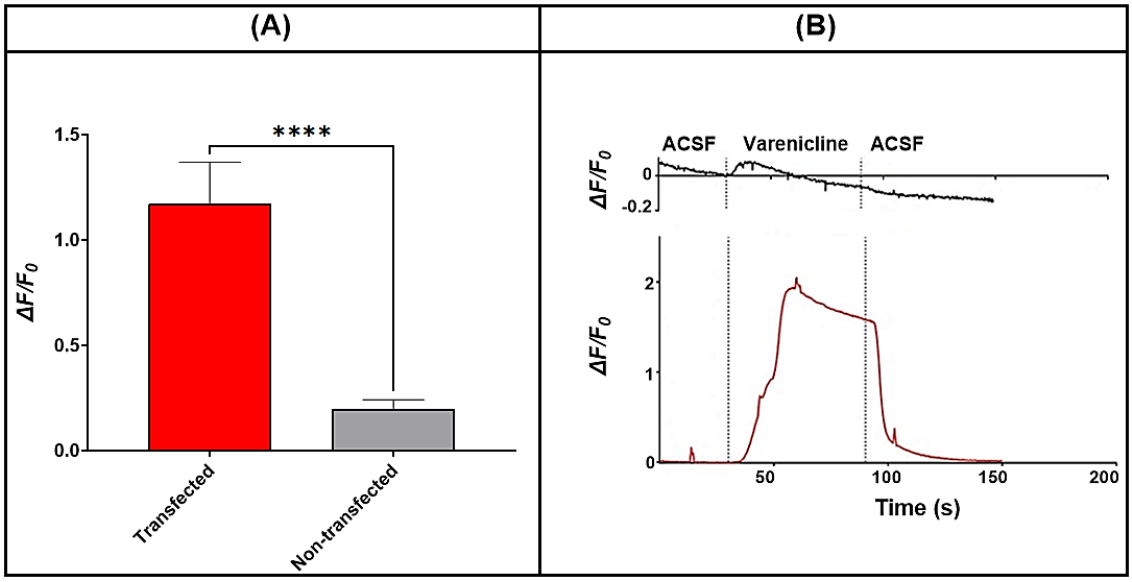

Figure 57: In vitro Ca^{2+} imaging revealed that varenicline (20nM) activated $PSAM^4$-5HT3 expressing DRG neurons, as demonstrated by the increase in the peak Ca^{2+} response (ΔF/F0). *(A) A comparison of the change in ΔF/F0 in response to varenicline (20nM) between $PSAM^4$-5HT3 expressing DRG neurons (n=57, red) and DRG neurons lacking $PSAM^4$-5HT3 (n=50, grey). The application of varenicline (20nM) caused a significant rise in ΔF/F0 in $PSAM^4$-5HT3 expressing DRG neurons compared to $PSAM^4$-5HT3 negative DRG neurons (P-value < 0.0001, Mann Whitney test using GraphPad prism 9). Data are presented as mean ± SEM. (B) Representative traces of ΔF/F0 evoked by the application of varenicline (20nM) on $PSAM^4$-5HT3 positive DRG neurons (red trace) and non-transfected ($PSAM^4$-5HT3 negative) DRG neurons (black traces). The figure shows that varenicline (20nM) activated $PSAM^4$-5HT3 expressing DRG neurons. The experiment was conducted by applying ACSF for 30 seconds. This was followed by applying varenicline (20nM) for 60 seconds to activate $PSAM^4$-5HT3 receptors. Then, the varenicline was washed out by applying ACSF for 60 seconds. S; seconds, ACSF; artificial cerebrospinal fluid.*

6.5.2.2. The activation of the central amygdala by chemogenetic tools

Having obtained promising preliminary *in vitro* data, the next intended step was to activate the CeAGA neurons *in vivo*. Two chemogenetic-based activation techniques were used. The first one relied on the expression of hM3Dq in the CeAGA and the administration of C21 for activation. The second relied on $PSAM^4$-5HT3 and varenicline for neuronal activation. Two different transgenic mouse lines were used. For the DREADDs experiments, the Capturing Activated Neural Ensembles (CANE) technique for labelling activated neurons was used. This method necessitates the use of Fos-2A-dsTVA mice. For the $PSAM^4$-5HT3 experiments, the targeted recombination in active populations (TRAP) technique for labelling activated neurons was used. The TRAP technique uses $CreER^{T2}$ mice. Both strategies rely on expressing transgenes in activated neuronal populations. The differences between these two mouse lines in capturing activated neurons will be discussed later in this chapter (see section 6.6.2.1). It is important to mention that the expression of these chemogenetic receptors was targeted to the right CeAGA only.

6.5.2.2.1. hM3Dq and C21 to activate the right CeAGA in Fos-2A-dsTVA mice

The expression of hM3Dq was induced in the right central amygdala of Fos-2A-dsTVA mice by the co-administration of CANE Cre LV together with the Cre-dependent virus pAAV-hSyn-DIO-hM3D(Gq)-mCherry. Because the CANE virus that carries sequences encoding for Cre enzyme can only transduce activated neurons that express c-fos, mice were exposed to isoflurane for 90 minutes to induce Fos expression in the CeAGA neurons, thereby enabling the entrance of the CANE Cre virus to allow the Cre enzyme to be expressed. Once the Cre enzyme is present and active, hM3Dq and mCherry transgenes will be expressed. After the stereotaxic injection of the CANE Cre LV and pAAV-hSyn-DIO-hM3D(Gq)-mCherry rAAV, mice were given 3 weeks before any behavioural tests were conducted to ensure that the chemogenetic receptors were expressed at good levels.

To test whether the CeAGA neurons could be activated by chemogenetic tools, mice were treated with C21 to activate the hM3Dq receptors and to assess whether any analgesia could be detected. Results indicated that the intraperitoneal administration of 0.3 mg/kg of C21 to mice expressing hM3Dq receptors in the right CeAGA neurons elevated their withdrawal thresholds in various sensory tests (see Figure 58), and this elevation was dependent on the dose of C21. The mean withdrawal latency in the Hargreaves' test increased dose-dependently from 5.7 seconds with PBS to 6.82 when mice were treated with 0.3 mg/kg of C21 and 8.88 seconds when treated with 3 mg/kg of C21 (Figure 58A). Similarly, C21 (0.3 mg/kg) increased the mean withdrawal latency of mice that express HM3Dq in the CeAGA from 5.11 seconds to 7.52 seconds in the dry ice test (Figure 58B). Additionally, the withdrawal threshold increased from 0.46 g in the von Frey test to 1.18g (Figure 58C). It is important to note that even though hM3Dq receptors are expressed in the right central amygdala, the elevation of the withdrawal thresholds was seen on both the ipsilateral and the contralateral paws. Additionally, the heat hyperalgesia induced by the intraplantar injection of PGE2 was significantly lowered after the injection of C21 in the mice expressing hM3Dq in the right CeAGA (see Figure 59A). On the other hand, C21 did not significantly alter mechanical or cold sensitivity caused by PGE2 in mice expressing hM3Dq in the CeAGA (Figures 59 B and C). Furthermore, while the

activation of the hM3Dq DREADDs system in the central amygdala diminished the cold allodynia driven by the intraplantar injection of the chemotherapeutic agent oxaliplatin, this effect failed to reach a statistical significance (Figure 60).

After these behavioural tests, mice were sacrificed and perfused to check the expression of the fluorescent protein mCherry in the brain. To ensure that only general-anaesthetics-activated neurons were captured, mice were subject to isoflurane for 90 minutes prior to sacrificing them to assess whether the expression of the chemogenetic receptor was in the same neurons that possessed Fos expression. As figure 61 indicates, a good co-localisation (>90%) between mCherry and c-fos expression was seen.

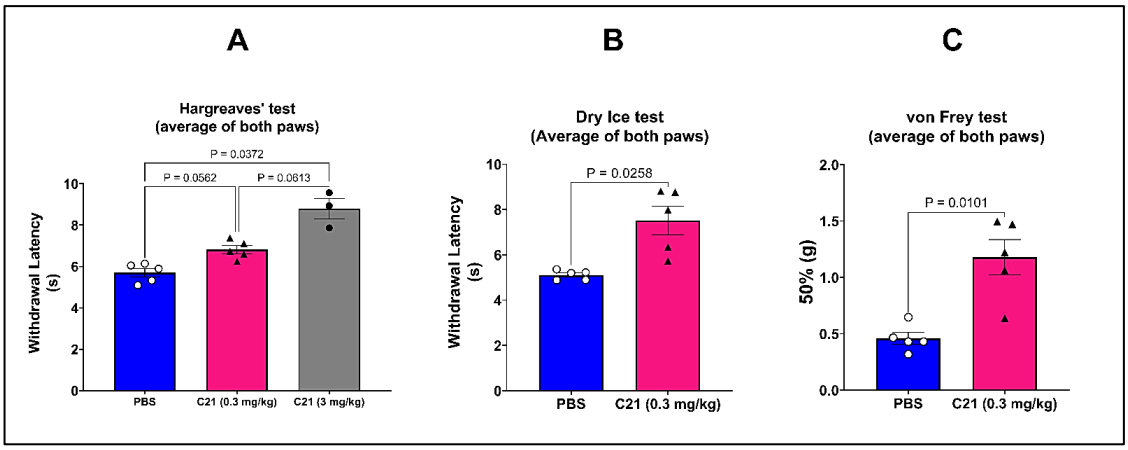

Figure 58: The systemic application of C21 (0.3 mg/kg) to mice expressing hM3Dq receptors in the right CeAGA neurons elevated their withdrawal thresholds when tested using the Hargreaves' (A), the dry ice (B), and the von Frey (C) tests. *The von Frey test was done 30 mins after the drug injection (p-value= 0.0101), the Hargreaves' test was done after 1 hour after the drug injection, and the dry ice test was done 90 mins after the drug injection (p-value= 0.0258). PBS and C21 were injected intraperitoneally. N=5 (three females and 2 males). Data were analysed using the paired t-test for the von Frey test and the dry ice test, and the RMEL analysis with Tukey's test for the Hargreaves' test.*

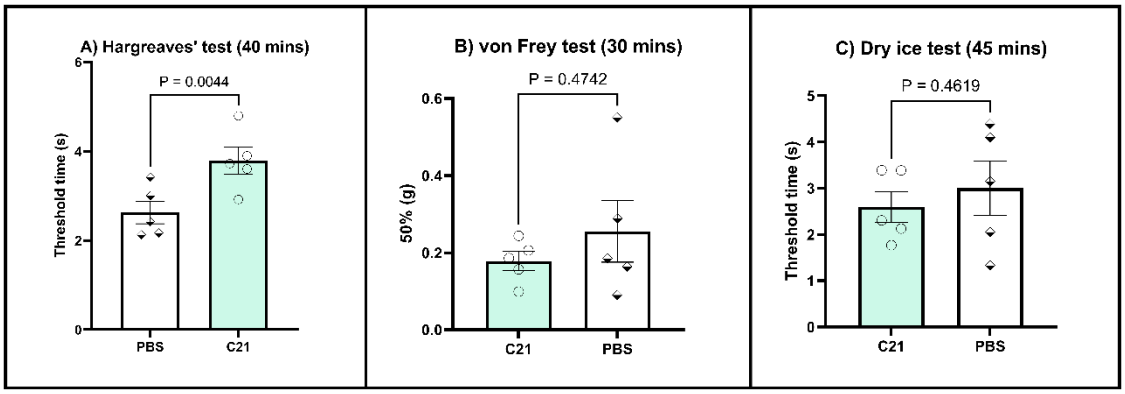

Figure 59: The systemic administration of C21 to mice expressing hM3Dq in the right central amygdala lessened heat hyperalgesia induced by the intraplantar injection of PGE2 without causing a significant reduction in mechanical and cold sensitivity induced by PGE2. *PGE2 (500 µM, total volume 20 µl) was injected into the right paw, and 5 minutes after injecting PGE2, 0.3 (mg/kg) of C21 was injected intraperitoneally. A) 40 minutes after C21 administration, the Hargreaves' test was conducted. B) 30 minutes after C21 injection, the von Frey test was conducted on the ipsilateral paw. C) the dry ice test was done 45 minutes after C21 administration. Data were analysed using the paired t-test and are presented as mean±SEM. N=5 (three females and two males).*

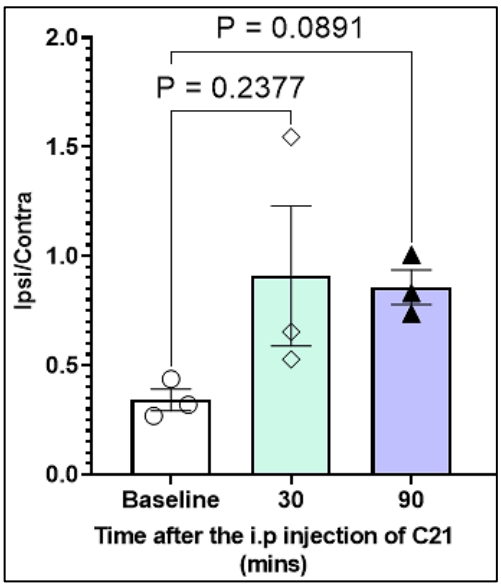

Figure 60: The effect of the intraperitoneal injection of C21 on oxaliplatin-induced cold allodynia in mice expressing hM3Dq in the right central

amygdala. *The cold allodynia was tested using the dry ice test on the two hind paws. Oxaliplatin (80µg) was injected into the right paw and behavioural tests started 4 hours after the oxaliplatin injection. Because oxaliplatin was injected into the right paw, the y-axis shows the withdrawal latency of the right paw (ipsilateral paw) compared to the left paw (contralateral paw). N=3 (females). Statistical analyses were done using the one-way ANOVA test (p-value= 0.2142) followed by Holm-Sidak's multiple comparisons (p-values are shown in the figure). C21 was injected intraperitoneally (0.3 mg/kg).*

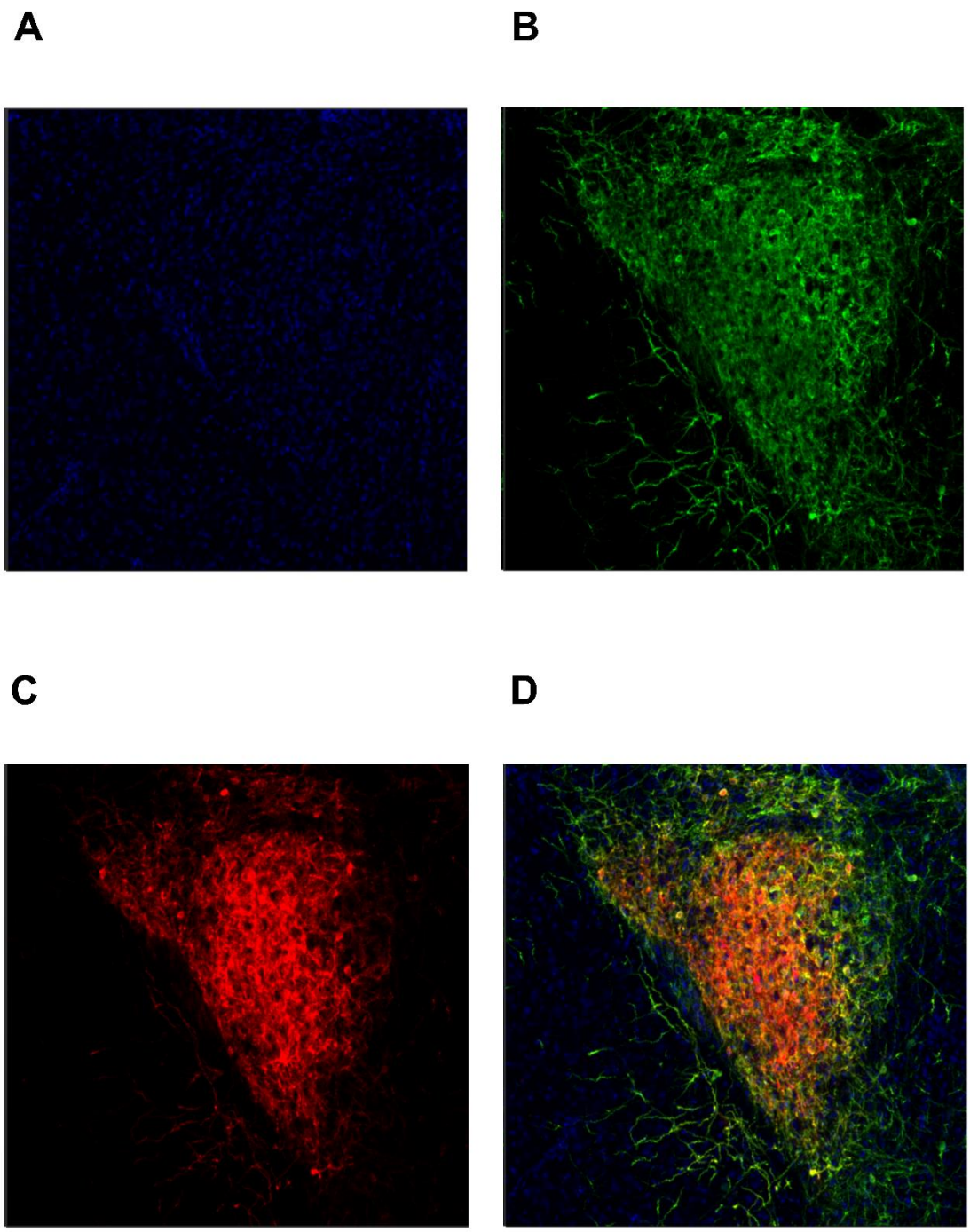

Figure 61: mCherry expression colocalised with the c-fos expression in the right central amygdala of Fos-2A-dsTVA mice co-injected with pAAV-hSyn-DIO-hM3D(Gq)-mCherry and CANE Cre after the exposure to 1.5 hours of isoflurane. *DAPI is shown in blue (A), C-fos is shown in green (B), mCherry is shown in red (C), and Figure (D) shows a merged picture of A, B, and C.*

6.5.2.2.2. PSAM^4-5HT3 and varenicline in CreER^{T2} mice

To assess the analgesic potential of activating CeAGA neurons by the PSAM^4-5HT3 (+varenicline) system, the TRAP technique for labelling activated neurons was employed. As mentioned earlier, this technique necessitates the use of CreER^{T2} mice. In these mice, the expression of PSAM^4-5HT3 was induced by injecting the CMV FLEx PSAM^4-5HT3 IRES mEGFP, and after several days, mice were exposed to isoflurane to enable fos expression in the CeAGA. Fos expression results in the expression of Cre enzyme in these neurons (which have already been transduced with the CMV FLEx PSAM^4-5HT3 IRES mEGFP virus). To render the expressed Cre enzyme active, 4OHT was intraperitoneally injected after the isoflurane exposure. Because the Cre activity in this mouse line is both inducible and activity-dependent, isoflurane exposure and 4OHT injection should enable the expression of PSAM^4-5HT3 (as well as mEGFP) in the CeAGA. Ten days later, the Hargreaves' test was carried out on these mice with and without varenicline administration, and a small increase in the withdrawal thresholds was detected after varenicline (Figure 62). Unfortunately, no significant mEGFP signal was seen after the brains of the mice under study were extracted, sliced and imaged (Figure 63).

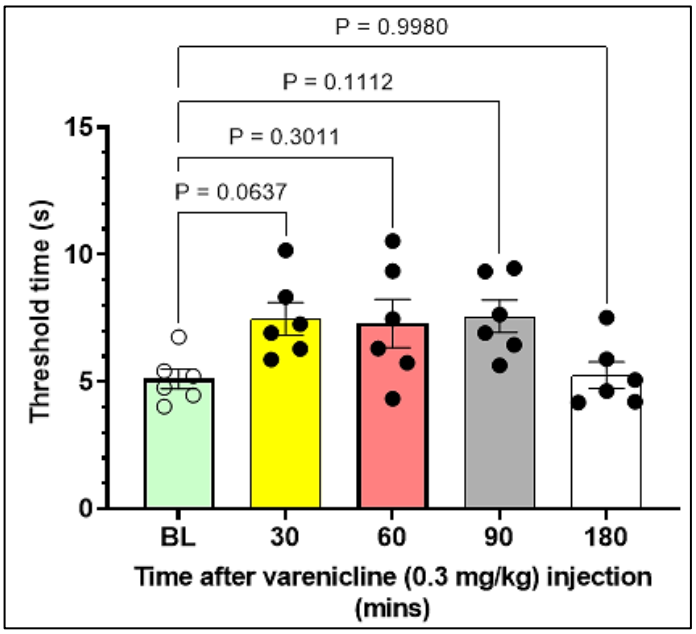

Figure 62: The Hargreaves' test in varenicline-treated CreER^{T2} mice injected with a rAAV to induce the expression of PSAM^4-5HT3 in the right CeAGA. *The test was done on the right paw on day 10 after one round of TRAPing. The analyses were done using the one-way ANOVA test (p-value= 0.0292) followed*

by Dunnett's test for multiple comparisons (p-values are shown in the figure). N=6 (three males and three females).

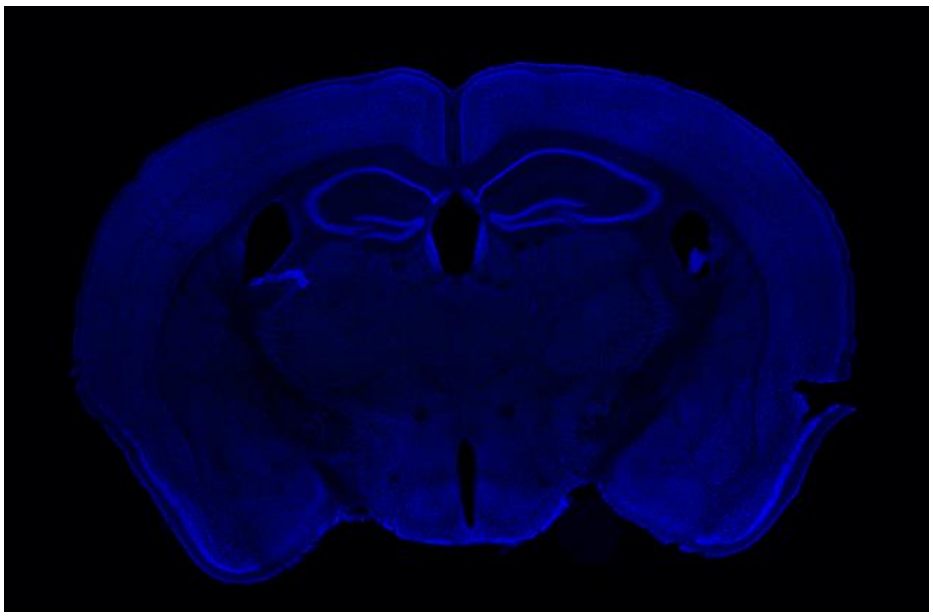

Figure 63: No mEGFP signal was detected in the central amygdala of CreER^{T2} mice following the induction of Cre expression in the CeAGA by exposing mice to general anaesthetics and the injection of 4OHT. *The absence of the mEGFP signal could indicate a no/ low expression of PSAM^4-5HT3 in the central amygdala.*

6.6. Discussion

In this chapter, the use of the engineered LGICs PSAM^4-GlyR and PSAM^4-5HT3 with the smoking cessation drug varenicline was attempted as a potential analgesic tool. The former was tested for silencing the DRG neurons, while the latter was tested for activating the CeAGA. The efficacy of the PSAM^4-GlyR (+varenicline) system in silencing DRG neurons was tested using 1) plasmids, 2) recombinant AAV carrying the PSAM^4-GlyR transgene, and 3) transgenic mice that express PSAM^4-GlyR in a Cre dependent manner. For this mouse line, Na$_V$1.8 Cre was used to investigate the role of Na$_V$1.8+ neurons in chronic pain conditions. The second part of the work focused on the application of PSAM^4-5HT3 (+ varenicline) or hM3Dq (+ C21) to activate the CeAGA neurons in mice. Results highlight that these chemogenetic systems can be useful in causing an analgesic effect that can be reversed upon ligand washout.

6.6.1. Silencing the DRG neurons using PSAM^4-GlyR and varenicline

6.6.1.1. Chemogenetic tools are attractive to silence the DRG neurons.

Several options exist to silence a neuron, including the use of the CRISPR Cas9 system to delete genes encoding for ion channels required for neuronal activation, such as VGSCs. However, CRISPR Cas9 system-based gene editing carries some disadvantages, the most important of which is the permanent change in the genome which can occur either at the site of action or at off-target sites. The permanent nature of gene editing caused by the CRISPR Cas9 system makes controlling potential side effects extremely challenging (Ledford, 2020). CRISPR interference can be an attractive alternative, but in complex conditions targeting one gene may not be sufficient, as indicated in Chapter 3. An alternative option to the CRISPR Cas9 system could be the use of optogenetic tools that are known to be highly efficient for controlling neuronal activity. However, the high degree of invasiveness severely limits *in vivo* optogenetics. To allow light delivery *in vivo*, optogenetic tools necessitate an optical fibre implantation in many cases. Deep brain implants also involve the aspiration of the tissue over the target site. Chemogenetics, therefore, represent a viable option as it is efficient, significantly less invasive, reversible, and extremely specific. Chemogenetics, when combined with an intersectional approach, can also be applied for cell-type and projection-specific dissection (Lee et al., 2020).

6.6.1.2. PSAM^4-GlyR based chemogenetic tools; promises and concerns.

6.6.1.2.1. PSAM^4-GlyR effectively silences CNS neurons

PSAM^4-GlyR is a chemogenetic receptor with an LBD formed from a triple mutant LBD from α7nAChR and an IPD from a glycine receptor. This chimeric channel, upon activation, shows conductance properties similar to glycine receptors which are chloride-selective. Glycine is one of the primary components in the CNS that mediate rapid inhibitory neurotransmission. While GABA acts on the rostral part of the CNS by interacting with $GABA_A$ receptors, glycine-mediated transmission acts on the caudal part (brain stem and spinal cord). Early experiments by (Curtis & Watkins, 1960) and (Werman et al., 1967) showed that glycine diminishes action potential firing by the spinal cord neurons. This is thought to occur because once activated, glycine-gated ion channels (GlyRs) lead to postsynaptic

hyperpolarisation triggered by chloride input or a shunt effect defined by a decrease in membrane resistance following increased chloride conductance (Van den Eynden et al., 2009).

In order to understand how glycine-gated ion channels cause hyperpolarisation in the CNS neurons, we need to understand the central governors of Cl^- ion homeostasis in neurons. In neurons, there are two key determinants of the intracellular concentration of chloride ions, and these are Na^+-K^+-$2Cl^–$ cotransporter 1 (NKCC1) and K^+-$Cl^–$ cotransporter 2 (KCC2) (Ben-Ari et al., 2012). The former transporter allows two Cl^- ions to enter the cell, along with a K^+ and a Na^+. On the other hand, the KCC2 transporter allows a Cl^- ion to leave the cell. Both transporters do not consume energy to exert their action as they are driven by the chemical gradients of Na^+ (high in the extracellular space) and K^+ (high in the intracellular solution) (Wilke et al., 2020). The NKCC1 transporter causes a depolarised shift in the reversal potential of Cl^- ions, while KCC2 results in a negative shift in the reversal potential of Cl^-. The low concentration of Cl^- ions in the mature CNS neurons renders the opening of Cl^- channels as hyperpolarising as the channels allow the Cl^- ions to enter the cell from the extracellular space.

These pieces of information explain why the expression of the LGIC, $PSAM^4$-GlyR and the application of varenicline silenced the GABAergic neurons in the substantia nigra (as shown in Figure 40). Because, like all the CNS neurons, these GABAergic neurons possess a low intracellular Cl^- concentration, the opening of $PSAM^4$-GlyR LGICs causes a hyperpolarisation in their membrane potential. When the membrane potential is hyperpolarised, a greater than usual stimulus is needed to activate those neurons (i.e., they are silenced). If similar silencing is achieved in the DRG neurons, the overall effect would be beneficial in chronic pain conditions as it could inhibit nociceptive signal transmission from the periphery to the spinal cord.

6.6.1.2.2. Concerns about applying $PSAM^4$-GlyR to silence the DRG neurons

As mentioned earlier, a vital determinant of the silencing effect of $PSAM^4$-GlyR in the CNS neurons is the low intracellular Cl^- ions concentration. When considering the application of $PSAM^4$-GlyR in silencing the DRG neurons, differences between the DRG neurons and the CNS neurons in Cl^- ions concentration need

to be considered carefully. Dramatic differences exist between these neuronal types, with the intracellular concentration of Cl^- in the DRG neurons being higher than the equilibrium potential in those neurons, indicating that the opening of Cl^- channels leads to depolarisation in the membrane potential of the DRG neurons (unlike the mature CNS neurons). One possible explanation for this fact could be that DRG neurons have extremely low levels of the KCC2 transporter, if present at all. Instead of KCC2, DRG neurons express KCC1 and KCC3 (Lucas et al., 2012). The latter two transporters are activated by swelling, and they do not highly impact the intracellular Cl^- concentration under physiological conditions (Gamba, 2005). The poor expression of KCC2 could partly explain why DRG neurons have a high intracellular Cl^- ion concentration compared to CNS neurons. Another factor that could contribute to the high intracellular Cl^- concentration in DRG neurons could be the Na^+-independent chloride-bicarbonate exchanger (Pfeffer et al., 2009), which is expressed in more than half of the peptidergic neurons and about a third of the non-peptidergic DRG neurons (Barragán-Iglesias et al., 2014). This exchanger removes bicarbonate from the intracellular space and exchanges it with a Cl^- ion, further enhancing the concentration of the intracellular Cl^- ions. These observations highlight the fact that the intracellular chloride ion concentration is high, and several studies attempted to measure the concentration of chloride ions in the DRG neurons, and it was found to be 23.6 mM (Alvarez-Leefmans et al., 1988) and 53 mM (Gallagher et al., 1978) in the frog DRGs and the cat DRG neurons respectively. To estimate how high these readings are compared to the CNS neurons, studies revealed that the intracellular concentration of chloride ions in the neocortical pyramidal neurons of rats is 3.73 ± 0.35 mM (P18–P28 neurons) (DeFazio et al., 2000). Even though some reports reveal that even the DRG neurons undergo a slight decrease in the intracellular concentration of Cl^- ions after birth, it was shown that this is not due to an increase in the expression of the KCC2 over time (Mao et al., 2012). However, these same reports indicated that even after this Cl^- concentration reduction, this concentration is still higher than the equilibrium concentration of Cl^- ions in all the subsets of DRG neurons, confirming that the opening of Cl^- channels will lead to egress of Cl^- ions from the intracellular space to the extracellular space. Because the intracellular concentration of Cl^- ions in the DRG neurons remains high, targeting chloride ions in the DRG neurons has long been hindered by the fear that the opening of Cl^- channels could lead to depolarisation and result in

activating the neurons rather than silencing them. In addition, the enhanced Cl^- ion accumulation in the DRG neurons has been linked to various pain states (Morales-Aza et al., 2004). It is thought that this enhanced accumulation leads to excessive Cl^- ion efflux upon the opening of Cl^- channels (like $GABA_A$ receptors) (Price et al., 2009). For instance, the application of inflammatory mediators increases NKCC1 expression with elevated phosphorylation while significantly reducing KCC2 expression, implying increased excitatory Cl^- current in sensory neurons and leading to inflammatory hyperalgesia (Funk et al., 2008). Arthritis was also associated with altered KCC2 and NKCC1 expression (Morales-Aza et al., 2004). In a visceral hyperalgesia model, intracolonic capsaicin treatment increased NKCC1 phosphorylation and trafficking (Galan & Cervero, 2005). Collectively, to modulate neuronal excitabilities, the activities of NKCC1 and KCC2 are closely regulated through alterations in their expression or function, which aids in developing and maintaining persistent pain states (Wood, 2020). In addition, Cl^- build-up is modulated by alterations in cotransporter expression or functional activities through phosphorylation and membrane trafficking (Price et al., 2009) (see Figure 64B). Combined, these observations enhanced the avoidance of Cl^- ion targeting within the DRG neurons for pain modulation.

6.6.1.3. Potential mechanisms for varenicline silencing of PSAM^4-GlyR-positive DRG neurons

As the results section shows, the opening of PSAM^4-GlyR LGICs silenced the responses of the DRG neurons to veratridine (30µM). These results, although desired, could, to some extent, be considered unexpected.

Even though one would expect an enhancement of the neuronal firing upon depolarised shifts in the membrane potential, several researchers found that the outward movement of Cl^- ions can have either an inhibitory or stimulatory effect on the cell (see Figure 64). Herein, the mechanisms by which Cl^- ions egress can have an inhibitory effect on DRG neurons will be explained, and these include two main mechanisms: depolarisation block and shunting inhibition (Kaila et al., 2014).

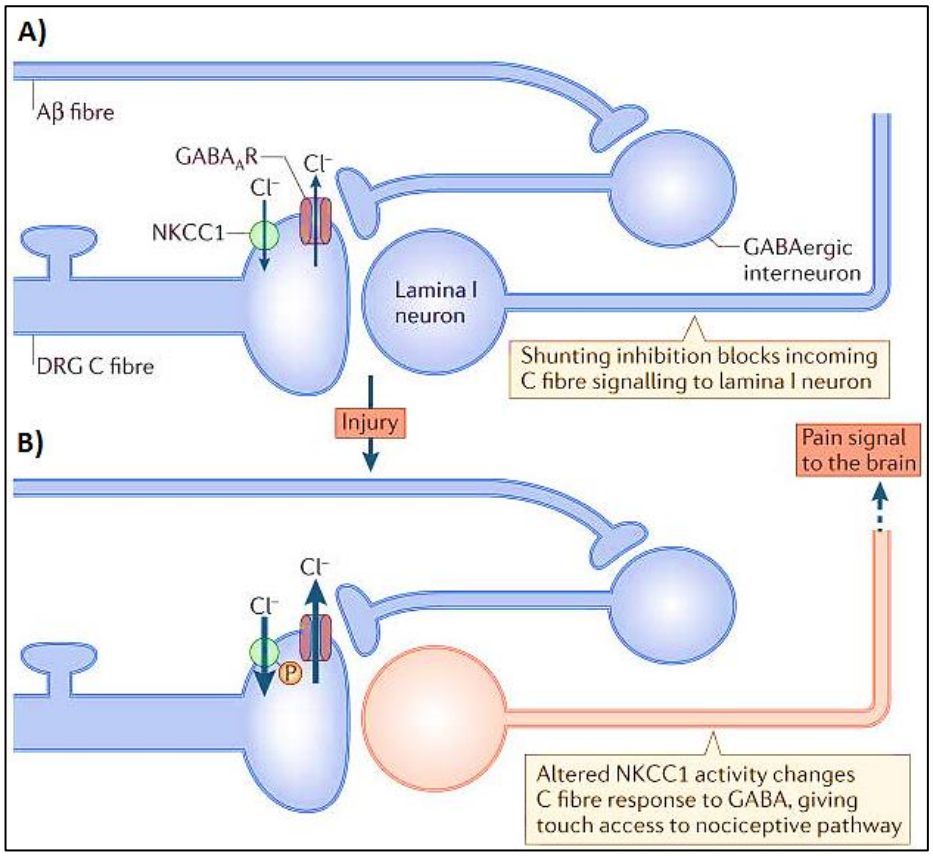

Figure 64: Cl^- efflux in the DRG neurons can have an excitatory or an inhibitory effect on the activity of the neuron. *A) under physiological conditions, the activation of the Aβ fibres leads to the activation of GABAergic interneurons in the spinal cord. These interneurons synapse with C fibres. Upon activation of GABAergic interneurons, they release GABA, which activates $GABA_A$ receptors on the presynaptic terminals of C fibres. This causes Cl^- ions to leave from the intracellular space to the extracellular space of the C fibres, which, in turn, inactivates VGSCs leading to inhibition of C-fibre-mediated activation of nociceptive specific (NS) neurons in the spinal cord, which means that no pain signal is generated after an innocuous touch. B) In certain pathological conditions, the phosphorylation of the NKCC1 transporters expressed in C fibres increases significantly, resulting in a significant increase in the intracellular concentration of Cl^- ions. When this is the situation, the activation of GABAergic interneurons by Aβ fibres, and the subsequent activation of $GABA_A$ receptors expressed on the presynaptic terminals of C fibres, results in a great outward Cl^- current, which increase the probability of release of neurotransmitters from these presynaptic terminals leading to the activation of NS neurons. The overall effect of this process is the generation of pain signals after a fine touch, a phenomenon known as allodynia. It is important to note that not only does the*

injury change the phosphorylation state of the NKCC1 receptors, but it also reduces the expression of the KCC2 receptors, which also enhances the intracellular concentration of Cl^- ions. Therefore, it was thought that gene therapy approaches aiming to deliver KCC2 receptors could have a beneficial effect on allodynia seen after nerve injury. The reduction in the expression of KCC2 is seen in many conditions like inflammation (Price et al., 2009), opioid-induced hyperalgesia (Ferrini et al., 2013), and spinal cord injury (Jean-Xavier et al., 2006). Adapted from (Kaila et al., 2014).

6.6.1.3.1. Depolarisation block

Depolarisation block mainly occurs as a result of the slight depolarisation that the opening of Cl^- channels causes. This depolarisation leads to the inactivation of the VGSCs and/or voltage-gated Ca^{2+} channels. These mechanisms can then inhibit action potential propagation or neurotransmitter release depending on the location at which depolarisation occurs within the DRG neuron.

6.6.1.3.1.1. Activation of Cl^- channels at the soma

The inhibitory effect caused by the Cl-driven depolarisation can partly be explained by the unique structure of the DRG neurons, which influences the net effect of ion movements across the plasma membrane. The morphology of the primary sensory neurons is pseudo-unipolar, indicating that the neuron has a single axon that splits into two projections; the first is the central projection heading to the CNS (it synapses with the second-order neurons at the dorsal horn of the spinal cord) and the second is the peripheral projection that innervates the peripheral tissue (Takahashi & Ninomiya, 1987). For instance, (Du et al., 2017) showed that the mechanism of action that renders intraganglionic GABA one of the approaches leading to nociceptive transmission reduction is that it causes the opening of chloride channels in the soma of DRG neurons. Because it is thought that the intracellular concentration of Cl^- ions in the DRG neurons is higher than the equilibrium potential of Cl^- ions, Cl^- ions leave the cell upon the opening of Cl^- channels leading to depolarisation in the soma of the DRG neurons and leads to depolarisation in the T-junction. Upon depolarisation, VGSCs open, and then they shift to the inactivated state (Dib-Hajj et al., 2009). Therefore, when a stimulus in the periphery succeeds in generating action potential firing, the action potential propagates across the axon of the DRG neurons and finally reaches the T junction. Once there, the action potential will not propagate further when VGSCs

are unavailable for opening (because they will be acquiring their inactive state). This process is known as depolarisation block. These effects were seen after the activation of $GABA_A$ receptors, which belong to the cys-loop LGICs (Goetz et al., 2007).

6.6.1.3.1.2. Activation of ligand-gated Cl^- channels at the central terminals of DRG neurons

As shown in Figure 64A, the activation of $GABA_A$ channels expressed at the central terminals of C fibres inhibits the activation of nociceptive-specific projection neurons after innocuous touch at physiological conditions. This is thought to occur because innocuous touch activates Aβ fibres which then activate GABAergic interneurons, releasing GABA. Upon the binding of GABA to $GABA_A$ receptors on the central terminals of C fibres, Cl^- ions leave the cell, which, in turn, inactivates voltage-gated Ca^{2+} channels leading to inhibition of C-fibre-mediated activation of nociceptive specific neurons in the spinal cord because of the inhibition of neurotransmitter release.

6.6.1.3.2. Shunting inhibition

Shunting inhibition entails that the opening of ion channels diminishes the transmembrane resistance by lessening the amplitude of excitatory postsynaptic potentials (Paulus & Rothwell, 2016). Shunting inhibition is especially effective at removing depolarising current brought in by nearby excitatory synapses (Furman, 1965). It was shown that shunting inhibition explains the silencing effect seen after the opening of glutamate-gated chloride channels in the DRG neurons (Weir et al., 2017).

Combined, depolarisation block and shunting inhibition can explain the inhibitory effect of Cl^- ion egress on the electrical activity of the DRG neurons under normal conditions. However, it is important to note that the same outward movement of Cl^- ions from the intracellular space upon the opening of Cl^- channels can be excitatory (Figure 64B). But when the degree of depolarisation is high, or the speed of the Cl^- ion exit is high, neuronal activation becomes evident (Kaila et al., 2014). This explanation reveals that the speed of Cl^- egress is crucial in determining the overall effect on neuronal excitability and that slow depolarisations favour neuronal silencing.

6.6.1.3.3. PSAM^4-GlyR LGICs have a slow opening kinetics

(Grutter et al., 2005) showed how the opening kinetics of chimeric channels made with the LBD of α7 nAChRs and the IPD of-GlyR possess slow opening kinetics. Current clamp experiments showed that even at saturating ACh concentrations (1mM), applications for more than 1 s were required to achieve a steady-state response with channel chimaeras made by LBD from α nAChR and IPD from glycine receptors. This slow activation distinguished this chimeric channel from other LGICs, which activate in less than a millisecond. These slow kinetics of the chimeric channel came as a surprise as both of the parent LGICs (nAChRs and GlyRs) have fast opening kinetics. To understand the reasons behind the slow kinetics, (Grutter et al., 2005) built a molecular model of the chimeric channel α7nAChR-GlyR. According to the model, the Cys-loop from the ECD enters the extracellular face of the IPD near the four M1-M4 helices. By comparing the sequence of the cys loop of the αnAChR and that of the GlyR, it appears that some residues in the Cys-loop differ between nAChR and GlyR. Accordingly, it was speculated that the bonds between Cys-loop residues from α7 LBD and IPD residues from-GlyR in the α7/Gly chimaera might not be ideal, resulting in a weak coupling between the two domains. To test this hypothesis, (Grutter et al., 2005) substituted the α7 Cys-loop from chicks with the α1-GlyR Cys-loop from humans as they are structurally homologous. This replacement built a new chimaera that possessed a greater activation rate when subject to saturating concentrations of ACh. These results highlighted the critical role of the Cys-loop in the activation rates of these chimaeras. The further analysis helped Grutter et al. identify two amino acid residues from the GlyR Cys-loop, which are needed for fast activation. Combined, these pieces of information indicate that the chimeric channel α7nAChR-GlyR has slow opening kinetics. This chimeric channel α7nAChR-GlyR was used as a starting point to build PSAM^4-GlyR. The key difference between PSAM^4-GlyR and α7nAChR-GlyR is the three mutations in the ligand-recognition domain. As explained earlier, the speed by which depolarisation occurs plays a key role in determining whether the overall effect is excitatory or inhibitory. Having shown that the opening kinetics of PSAM^4-GlyR is slow, this observation could indicate that the depolarisation may not be speedy, and therefore, this enhances the possibility of neuronal silencing and, indeed, this is the effect that PSAM^4-GlyR opening exerted in the DRG neurons (see the Results section). In general, slow depolarisations lead to what is named closed-state inactivation of the

VGSCs, which means that voltage-gated channels shift to this inactivation when the outer mouth of the channel is closed. This could, at least partly, explain how the opening of PSAM^4-GlyR LGICs silenced the responses of the DRG neurons to veratridine (30µM).

6.6.1.4. Mouse line expressing PSAM^4-GlyR in a Cre-dependent manner and the role of Na$_V$1.8+ neurons

Viral transduction studies have an intrinsic variability. We, therefore, designed a mouse line that expresses PSAM^4-GlyR receptors in a Cre-dependent manner to allow the expression of the PSAM^4-GlyR in specific neuronal subsets to enable detailed mechanistic studies. For the mouse line, the flip-excision (FLEx) switch was used. For this, our transgene of interest (PSAM^4-GlyR IRES tdTomato) was inverted and flanked by two antiparallel loxP-type recombination sites. These sites first undergo coding sequence inversion, and then two sites are excised, leaving one of each orthogonal recombination site with an orientation that prevents it from engaging in further recombination. Even though some approaches rely on a single pair of LoxP sites that are arranged in an antiparallel orientation to achieve the inversion of the coding sequence and subsequent cell-specific expression, this technique was adopted as the inversion alone is unstable and results in a mixture of reverse and forward configurations, and that could lower the expression levels of the transgene of interest (Atasoy et al., 2008). The use of the CAG promoter and the ability to unlock the PSAM^4-GlyR in any neuronal cell with the use of either the appropriate Cre or the local injection of viruses carrying Cre as a transgene makes this mouse line a valuable research tool that could be applied to any area of research in the neuroscience field.

The established role of Na$_V$1.8 in mouse pain has recently been validated by human genetics, as several gain-of-function mutations have been identified in the *SCN10A* gene that encodes for Na$_V$1.8 in painful small-fibre neuropathy patients (Faber, Lauria, et al., 2012). These mutations include *G1662S* (Han et al., 2014) and *I1706V* (Huang et al., 2013), leading to a significant increase in neuronal activity. Na$_V$1.8 channels are primarily expressed in nociceptors (Agarwal et al., 2004; Djouhri et al., 2003; L. C. Stirling et al., 2005). The inward flow of Na^+ through Na$_V$1.8 channels comprises about (58–90%) of the total influx of Na^+ during the rising phase of the action potential (Blair & Bean, 2002; Renganathan et al., 2001). Additionally, the conditional ablation of Na$_V$1.8+ neurons affects

noxious mechanical sensation without impacting innocuous mechanical sensation (Abrahamsen et al., 2008). $Na_V1.8$ thus represents a key target for pain research. We, therefore, selected the $Na_V1.8+$ subset of sensory neurons to assess whether an analgesic effect could be seen after silencing these neurons. The role of $Na_V1.8+$ neurons was explored in CIBP and neuropathic pain. These models were selected because these conditions are hard to treat. Regarding neuropathic pain, estimates suggest that the prevalence of neuropathic pain in the general population ranges from 3% to 17%. The majority of neuropathic pain medications on the market have a moderate level of effectiveness and have side effects that restrict their use (Cavalli et al., 2019). The problem of neuropathic pain becomes clear when we look at the statistics, which reveal that only one-third of people with persistent neuropathic pain, including shingles or diabetic neuropathy, obtain pain reduction with pregabalin (Derry et al., 2019). We, therefore, examined CIBP and neuropathic pain models. Our results indicated that the administration of varenicline diminished signs of hypersensitivity (cold, thermal, and mechanical) after sciatic nerve injury in $PSAM^4$-GlyR-expressing mice (Figure 56), without affecting innocuous mechanical sensation (Figure 55B). These results align with previous findings suggesting the involvement of these neurons in neuropathic pain (Roza et al., 2003). This work also supports published data suggesting that the ablation of $Na_V1.8+$ neurons does not impact innocuous touch sensation (Abrahamsen et al., 2008). The pressing need to find novel analgesics for neuropathic pain and the positive outcomes obtained by silencing the $Na_V1.8+$ neurons encourage the application of chemogenetic tools for patients living with these conditions if effective viral targeting can be established. In addition, these findings highlight the role of this neuronal subset in neuropathic pain, paving the path to identifying targets within this subset for future clinical application.

6.6.2. Chemogenetic-based activation of the general anaesthetics-activated neurons in the central amygdala (CeAGA)

6.6.2.1. Techniques for labelling activated neurons

For labelling the neurons activated by general anaesthetics, several methods could have been employed. Herein, I applied two techniques: The TRAP technique and the Capturing Activated Neural Ensembles (CANE) technology. Both of these techniques relied on Fos expression by activated neurons in the

CNS. Fos is an immediately early gene (IEG) and has, for a long time, been utilised as a good marker for neuronal activation in response to various sensory events and in various behaviours (Morgan & Curran, 1989). Technologies that can identify if similar or distinct ensembles of neurons are activated and subsequently express Fos in various settings would be a useful means of understanding the role of these neurons in a specific behaviour through manipulating the activity of specific neuronal subsets and monitoring the effects of this manipulation on the overall behaviour.

6.6.2.1.1. TRAP technique

This technique relies on disrupting the endogenous Fos gene by the null allele Fos-CreER^{T2}. This allows the expression of the CreER^{T2} enzyme in activated neurons. Moreover, tamoxifen or 4-hydroxy tamoxifen (4OHT) are needed to stimulate CreER^{T2} to enable it to cause recombination (Denny et al., 2014; Guenthner et al., 2013).

6.6.2.1.2. CANE technology

Fan Wang's group developed an interesting technique for temporally and precisely capturing Fos+ neurons, and they named it "CANE", which stands for capturing activated neuronal ensembles using engineered mice and viruses. This group developed a lock-and-key technique utilising a genetically engineered mouse line as well as pseudotyped viruses in order to attain the anatomical and temporal specificity needed to capture the neurons that express Fos in response to certain behaviours. This group engineered a knockin mouse line (Fos-2A-dsTVA) in which the Fos expression also initiates the expression of a destabilised TVA (dsTVA) receptor, and 2A is a self-processing peptide that permits the co-translation of Fos and dsTVA (de Felipe et al., 2006). TVA is an avian-specific receptor that is not naturally found in the mouse genome (Barnard et al., 2006; Barnard & Young, 2003). The construction of the dsTVA happens through fusing the C terminal of the TVA receptor with a "PEST" sequence which targets the protein for degradation (Li et al., 1998). The design of this knockin mouse line expects that the freely behaving Fos-2A-dsTVA mouse, like other mouse lines, will express Fos after neuronal activation, but in this line, Fos expression will be accompanied by the expression of dsTVA within a time frame resembling that needed for expressing Fos itself. Because TVA possesses a high specificity for the Avian sarcoma and leukosis virus (EnvA) envelope protein

(Barnard & Young, 2003), viruses that express EnvA on their surfaces transduce the Fos-expressing cells effectively. Accordingly, in order to preferentially transduce these recently activated neurons, pseudotyped viruses possessing an EnvA-coat can be delivered into the brain of Fos-2A-dsTVA mice shortly after the time supposed to cause the co-expression of dsTVA and Fos (Figure 65). Data from the Wang lab indicates that 1.5-2 hours after the desired behaviour is when a good Fos staining is observed. Among the viruses that can be pseudotyped are the LVs and deficient monosynaptic rabies viruses and this would allow the test of the potential short-time predisposition of Fos/dsTVA expressing neurons to viral infection. The main advantage of LVs is the lack of toxicity, which could be beneficial when stable transgene expression is desired. On the other hand, the monosynaptic rabies viruses (Callaway, 2008; Wickersham et al., 2007) could be useful when the study aims to explore the neurons sending inputs to these Fos/dsTVA positive neurons.

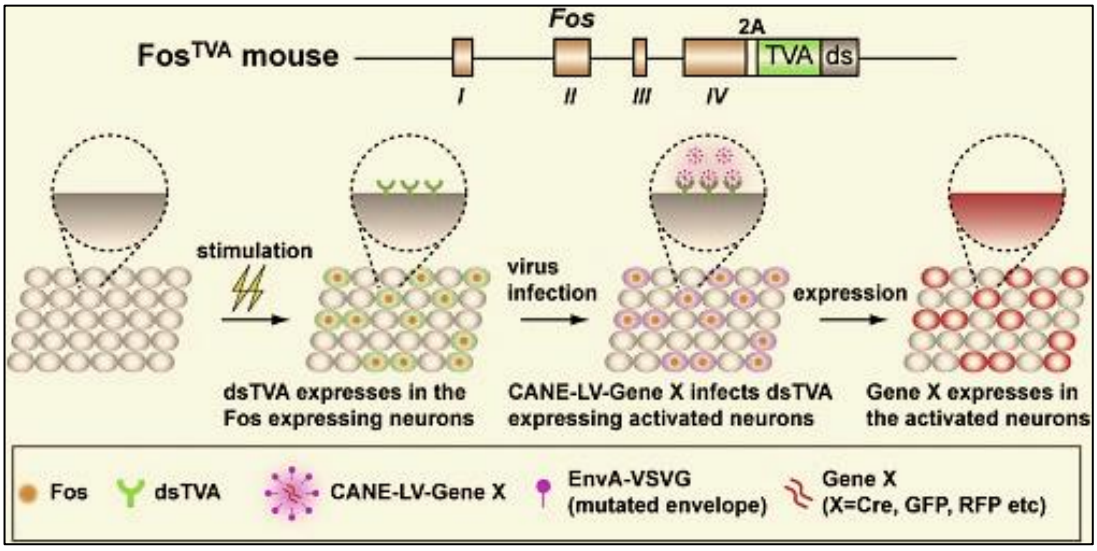

Figure 65: A schematic representation of the CANE technology for labelling Fos+ neurons. *The mice used in this technology are named Fos-2A-dsTVA mice as their neurons not only express Fos upon activation, but they concomitantly express a destabilised TVA (dsTVA). Therefore, the transient presence of dsTVA on the surface of activated neurons enables the transduction of pseudotyped viruses expressing the Avian sarcoma and leukosis virus (EnvA) envelope protein. These viruses can be used as vectors of various transgenes (Gene x) that can then be selectively expressed by the activated neurons in the behaviour under study; obtained from (Sakurai et al., 2016).*

There are many similarities between these two techniques. Firstly, they both relied on the Fos expression (TRAP can use Arc too). Secondly, the mouse lines used in both techniques are Cre-dependent. Thirdly, they both necessitate the use of a Cre-dependent AAV. While similar in many aspects, distinctions exist between these techniques. CANE requires Fos-2A-dsTVA knock-in mouse, while TRAP requires a CreER^{T2} mouse. The facilitator/the vehicle employed to capture/label the IEG-expressing neurons is CANE LV for CANE technology and tamoxifen/4OHT for TRAP. Moreover, capturing starts at the same time as Fos expression in the CANE technology (as dsTVA is expressed at approximately the same time as Fos expression), while the onset varies in the TRAP technology, and it can range between zero and six hours following the drug injection and lasts until the drug is fully metabolised (can last for 24 hours). Table 7 summarises the pros and cons of the CANE technology and the TRAP technology for labelling activated neurons.

Table 7: The pros and cons of the TRAP and CANE technologies for labelling activated neurons in vivo (Sakurai et al., 2016).

	CANE	TRAP
Pros	- Good temporal resolution. - Can tag the majority of activated neurons in the brain. - Can label not only the activated neurons but also neurons that send inputs to those activated neurons.	Permits systemic labelling of activated neurons.
Cons	- Stereotaxic injection is needed, which makes systemic injection not achievable. - The injection process needs to be gentle to avoid inducing Fos expression by brain damage. - If the perturbation of neuronal activity needs to occur within a few days after tagging, CANE may not be suitable as it needs time to achieve a high level of expression of the transgene. - Requires the application of anaesthetics and surgery, which could interfere with certain behaviours that are sensitive to these.	- The endogenous expression of Fos/Arc is affected by CreER. - Tamoxifen can continue to label neurons for extended periods beyond the behaviour under study. - The fact that CreER^{T2} is only expressed transiently can make the labelling incomplete since administering tamoxifen one time typically only activates a portion of CreER enzymes. - The fact that CreER^{T2} could be mosaically activated could make the labelling random and makes correlating it to the behaviour under study challenging. - Possibility of background labelling due to the spontaneous activation of CreER^{T2}.

6.6.2.2. The rationale for targeting the central amygdala for pain suppression

In 2020, Professor Fan Wang's lab published a paper in which a novel pain-reducing set of neurons was identified in the central amygdala of mice and that this set of neurons accounts, at least in part, for the analgesia produced by general anaesthetics (Hua et al., 2020). They identified that this set of neurons is activated by general anaesthetics. When activated by optogenetic tools, a significant analgesic effect is seen in mice. Therefore, this work attempted to activate these neurons using chemogenetic tools to produce a longer-lasting analgesic effect.

When the CeAGA neurons were captured using the CANE technology and were labelled with hM3Dq, a good labelling specificity was seen in the central amygdala, characterised by a high co-localisation with Fos expression. Furthermore, the administration of C21 to mice expressing hM3Dq in the CeAGA resulted in good analgesia (in sensory tests, neuropathic and inflammatory models) that lasted for more than 90 mins.

Surprisingly, while the use of modified LGICs is promising, PSAM^4-5HT3 (+varenicline) did not give a good analgesic effect in the central amygdala. These disappointing results could be because of (1) the quality of the rAAV, (2) the difference in the labelling technique as in the PSAM^4-5HT3 studies, CreER^{T2} mice were used instead of the CANE technique used for the hM3Dq. Therefore, in the future, the CANE technology can be used to induce PSAM^4-5HT3 expression in the CeAGA to enable a better comparison between the DREADDs and the modified LGICs-based technologies for activating the CeAGA.

6.6.2.3. Potential reasons for the failure of the PSAM^4-5HT3-based CeAGA activation

Many reasons may have accounted for the failure of the activation of the CeAGA neurons by PSAM^4-5HT3 and varenicline. These could be related to the rAAV (discussed in Chapter 3) or to the cons related to the TRAP technique in general (see Table 7 above). In the future, the CANE technology can be used to assess the ability of PSAM^4-5HT3 (+ varenicline) to activate the CeAGA and cause noticeable behavioural changes.

6.7. Conclusion

In this chapter, the use of the engineered LGICs PSAM^4-GlyR and PSAM^4-5HT3 with the smoking cessation drug varenicline was attempted as a potential tool. The former was tested for silencing the DRG neurons, while the latter was tested for activating the CeAGA.

***V*alidating the PSAM^4-GlyR system for silencing the DRG neurons:**

- Plasmids encoding for PSAM^4-GlyR were successfully cloned, and various fluorescent protein labels were added, namely mCherry and AcGFP1.
- GCaMP3 imaging indicated that the engineered channel expression does not affect the cell significantly in the absence of varenicline. GCaMP3 imaging also indicated that the drug varenicline (20nM) does not significantly alter the mean Ca^{2+} signal in the non-transfected cells. Combined, these two findings indicate that PSAM^4-GlyR, in conjunction with varenicline, represent an excellent method that could be applied for silencing the DRG neurons as they satisfy the criteria of a good chemogenetic tool.
- The application of varenicline (20nM) significantly reduced the Ca^{2+} responses to veratridine in the transfected cells (PSAM^4-GlyR positive cells) compared to the non-transfected cells. These two observations show that the opening of PSAM^4-GlyR silences the DRG neurons.
- It is proposed that this silencing caused by PSAM^4-GlyR opening occurs because of the ability of the depolarising Cl- currents to inactivate the voltage-gated channels needed for action potential propagation and potentially due to shunting inhibition.
- The expression of PSAM^4-GlyR *in vivo* using viral vectors, followed by the application of varenicline, resulted in increased pain thresholds in the Hargreaves' test, the dry ice test, and the up-down von Frey test.
- Genetically encoded PSAM^4-GlyR in the DRG neurons, in combination with varenicline, elevates pain thresholds.

Assessing the ability of the PSAM^4-5HT3 system to activate the CeAGA neurons

- hM3Dq can be expressed selectively in the CeAGA neurons after exposing the Fos-2A-dsTVA mice to isoflurane (1.5%) for 90 minutes.

- The injection of C21 to Fos-2A-dsTVA mice expressing hM3Dq in the CeAGA elevates their pain thresholds.
- Immunohistochemical studies showed that when viral vectors carrying a Cre-dependent hM3Dq are injected together with a CANE-Cre virus into the central amygdala of Fos-2A-dsTVA mice that are pre-exposed to 1.5% isoflurane, the expression of the hM3Dq receptor colocalised with the c-fos expression, confirming the c-fos-dependency of the CANE system.
- Plasmids encoding for PSAM^{4}-5HT3 were successfully cloned, and rAAV was successfully produced. Notably, the plasmid and the virus are Cre-dependent.
- Further optimisation aiming to increase the viral transduction is needed to assess the ability of varenicline to elevate the pain thresholds of CreER^{T2} mice expressing PSAM^{4}-5HT3 in the central amygdala.

7. General conclusion

Chronic pain remains a huge global problem. This thesis investigated two main topics. The first is the preclinical evaluation of various analgesic modalities for cancer-induced bone pain (CIBP). The second involved the potential application of chemogenetic tools for pain research.

Chapters 2, 3, 4 and 5 summarised the work related to CIBP. Here, a mouse model of CIBP was optimised. This model involves the injection of ~$2x10^4$ Lewis Lung Carcinoma cells into the intramedullary space of the femur of C57BL/6 mice or transgenic mice in the C57BL/6 background. Mice gradually reduce the use of the affected limb and the weight bearing. Symptoms of secondary cutaneous hyperalgesia also manifest, as demonstrated by the hypersensitivity in the von Frey test, the Hargreaves' test, and the dry ice test. In this model, three potential analgesic modalities were assessed during my PhD work, and they can be broadly divided into three categories: (1) targeting the voltage-gated Na^+ channels $Na_V1.7$; (2) approaches to target neuronal subsets (namely the μ-opioid receptor-expressing neurons and the sensory neurons that express $Na_V1.8$ channels), and finally (3) the dual targeting of two of the tumour-derived products (nerve growth factor and tumour necrosis factor). Results from these experiments indicated that $Na_V1.7$ plays a role in pain associated with CIBP and that the congenital deletion of the $Na_V1.8$ expressing neurons reduced pain behaviour associated with CIBP. Moreover, the use of etanercept to inhibit tumour necrosis factor and the use of monoclonal antibodies against nerve growth factor resulted in an impressive reduction in the pain phenotype associated with CIBP and prevented the development of secondary cutaneous heat hyperalgesia. As analgesics available on the market resulted in promising preclinical outcomes in CIBP, this work could open the door for re-purposing these analgesics for patients living with CIBP.

The second half of my work (Chapter 6) focused on chemogenetic tools, with a special focus on modified ligand-gated ion channels. This work showed that expressing $PSAM^4$-GlyR in the DRG neurons and the agonism with varenicline silences the DRG neurons and elevates the withdrawal thresholds of mice in various tests. Therefore, these results show that while targeting chloride currents has, for a long time, been avoided in the DRG neurons, it could be a good analgesic option. Additionally, chemogenetic-based activation of certain neurons

in the central amygdala was also shown to increase pain thresholds. Therefore, these chemogenetic techniques represent promising research tools for future studies investigating the effects of manipulating neuronal subsets.

All in all, the work presented here reinforces the conclusion that single molecular targets often fail to effectively treat complex pain conditions due to the intricate nature of such conditions, where multiple pathways and mechanisms contribute to the overall experience of pain. This is because pain is a multifaceted phenomenon, involving a complex interplay of neural, immune, and psychological factors, making it challenging to address adequately with a single target. Additionally, chronic pain often involves both peripheral and central sensitization, necessitating a more comprehensive approach targeting various pathways simultaneously. Furthermore, neuroplasticity plays a significant role in chronic pain conditions, and a single molecular target is unlikely to fully address the rewiring of neural circuits that contribute to persistent pain experiences. While targeting single molecules by drugs like opioids may provide temporary relief, problems like tolerance, dependency, and potential side effects limit their long-term use. What further limits the efficacy of single molecular targets is the heterogeneity of pain conditions among individuals, as what works for one person may not be effective for another. Therefore, holistic approaches, such as multimodal therapies combining medications, physical therapy, and psychological interventions, offer a more effective approach to addressing the complexities of pain. With a growing understanding of the multifaceted nature of pain, it becomes evident that a more comprehensive and personalised approach is crucial to effectively manage complex pain conditions and improve patients' quality of life.

Herein, a good example of a single molecular target was presented (anti-NGF). Its efficacy perhaps stems from the fact that targeting this target affects multiple downstream pathways and targets, but it still was not free from problems as it did not treat all the pain/injury aspects assessed here (such as ATF3 expression). On the other hand, neuronal silencing using chemogenetic tools proved effective, but challenges related to the use of viral vectors and their cost remain compelling when we think about therapeutic application especially when a specific neuronal subset is to be targeted. Similarly, while the use of anti-NGF in combination with etanercept showed impressive results, polypharmacy may not be ideal given the

challenges related to patient compliance. While the use of bispecific antibodies that target the two targets simultaneously looks promising, we still need to consider the cost of manufacturing and marketing large biologics when it comes to clinical application. Therefore, while basic experimental research is beneficial in suggesting new targets, a multidisciplinary team is needed to assess the applicability of these targets in real life, where therapeutic efficacy may not be the only problem.

8. Supplementary data

Appendix 1

cctgcaggcagctgcgcgctcgctcgctcactgaggccgcccgggcaaagcccgggcgtcgggcgacctt
tggtcgcccggcctcagtgagcgagcgagcgcgcagagagggagtggccaactccatcactaggggttcc
ttctagacaactttgtatagaaaagttgtagttattaatagtaatcaattacggggtcattagttcatag
cccatatatggagttccgcgttacataacttacggtaaatggcccgcctggctgaccgcccaacgacccc
cgcccattgacgtcaataatgacgtatgttcccatagtaacgccaatagggactttccattgacgtcaat
gggtggagtatttacggtaaactgcccacttggcagtacatcaagtgtatcatatgccaagtacgccccc
tattgacgtcaatgacggtaaatggcccgcctggcattatgcccagtacatgaccttatgggactttcct
acttggcagtacatctacgtattagtcatcgctattaccatggtgatgcggttttggcagtacatcaatg
ggcgtggatagcggtttgactcacggggatttccaagtctccaccccattgacgtcaatgggagtttgtt
ttggcaccaaaatcaacgggactttccaaaatgtcgtaacaactccgccccattgacgcaaatgggcggt
aggcgtgtacggtgggaggtctatataagcagagctggtttagtgaaccgtcagatccaagtttgtacaa
aaaagcaggctgccaccatggtgagcaagggcgaggaggtcatcaaagagttcatgcgcttcaaggtgcg
catggagggctccatgaacggccacgagttcgagatcgagggcgagggcgagggccgcccctacgagggc
acccagaccgccaagctgaaggtgaccaagggcggccccctgcccttcgcctgggacatcctgtccccc
agttcatgtacggctccaaggcgtacgtgaagcaccccgccgacatccccgattacaagaagctgtcctt
ccccgagggcttcaagtgggagcgcgtgatgaacttcgaggacggcggtctggtgaccgtgacccaggac
tcctccctgcaggacggcacgctgatctacaaggtgaagatgcgcggcaccaacttcccccccgacggcc
ccgtaatgcagaagaagaccatgggctgggaggcctccaccgagcgcctgtacccccgcgacggcgtgct
gaagggcgagatccaccaggccctgaagctgaaggacggcggccactacctggtggagttcaagaccatc
tacatggccaagaagcccgtgcaactgcccggctactactacgtggacaccaagctggacatcacctccc
acaacgaggactacaccatcgtggaacagtacgagcgctccgagggccgccaccacctgttcctggggca
tggcaccggcagcaccggcagcggcagctccggcaccgcctcctccgaggacaacaacatggccgtcatc
aaagagttcatgcgcttcaaggtgcgcatggagggctccatgaacggccacgagttcgagatcgagggcg
agggcgagggccgcccctacgagggcacccagaccgccaagctgaaggtgaccaagggcggccccctgcc
cttcgcctgggacatcctgtccccccagttcatgtacggctccaaggcgtacgtgaagcaccccgccgac
atccccgattacaagaagctgtccttccccgagggcttcaagtgggagcgcgtgatgaacttcgaggacg
gcggtctggtgaccgtgacccaggactcctccctgcaggacggcacgctgatctacaaggtgaagatgcg
cggcaccaacttcccccccgacggccccgtaatgcagaagaagaccatgggctgggaggcctccaccgag
cgcctgtacccccgcgacggcgtgctgaagggcgagatccaccaggccctgaagctgaaggacggcggcc
actacctggtggagttcaagaccatctacatggccaagaagcccgtgcaactgcccggctactactacgt
ggacaccaagctggacatcacctcccacaacgaggactacaccatcgtggaacagtacgagcgctccgag
ggccgccaccacctgttcctgtacggcatggacgagctgtacaagtagacccagctttcttgtacaaagt
gggaattccgataatcaacctctggattacaaaatttgtgaaagattgactggtattcttaactatgttg
ctccttttacgctatgtggatacgctgctttaatgcctttgtatcatgctattgcttcccgtatggcttt
cattttctcctccttgtataaatcctggttgctgtctctttatgaggagttgtggcccgttgtcaggcaa
cgtggcgtggtgtgcactgtgtttgctgacgcaacccccactggttggggcattgccaccacctgtcagc
tcctttccgggactttcgctttcccctccctattgccacggcggaactcatcgccgcctgccttgcccg
ctgctggacaggggctcggctgttgggcactgacaattccgtggtgttgtcggggaagctgacgtccttt
ccatggctgctcgcctgtgttgccacctggattctgcgcgggacgtccttctgctacgtcccttcggccc

tcaatccagcggaccttccttcccgcggcctgctgccggctctgcggcctcttccgcgtcttcgccttcg
ccctcagacgagtcggatctccctttgggccgcctccccgcatcgggaattcctagagctcgctgatcag
cctcgactgtgccttctagttgccagccatctgttgtttgcccctcccccgtgccttccttgaccctgga
aggtgccactcccactgtcctttcctaataaaatgaggaaattgcatcgcattgtctgagtaggtgtcat
tctattctgggggggtggggtggggcaggacagcaaggggaggattgggaagagaatagcaggcatgctg
gggagggccgcaggaacccctagtgatggagttggccactccctctctgcgcgctcgctcgctcactgag
gccgggcgaccaaaggtcgcccgacgcccgggctttgcccgggcggcctcagtgagcgagcgagcgcgca
gctgcctgcaggggcgcctgatgcggtattttctccttacgcatctgtgcggtatttcacaccgcatacg
tcaaagcaaccatagtacgcgccctgtagcggcgcattaagcgcggcgggggtggtggttacgcgcagcg
tgaccgctacacttgccagcgccttagcgcccgctcctttcgctttcttcccttcctttctcgccacgtt
cgccggctttccccgtcaagctctaaatcgggggctccctttagggttccgatttagtgctttacggcac
ctcgaccccaaaaaacttgatttgggtgatggttcacgtagtgggccatcgccctgatagacggtttttc
gccctttgacgttggagtccacgttctttaatagtggactcttgttccaaactggaacaacactcaactc
tatctcgggctattcttttgatttataagggattttgccgatttcggtctattggttaaaaaatgagctg
atttaacaaaaatttaacgcgaattttaacaaaatattaacgtttacaattttatggtgcactctcagta
caatctgctctgatgccgcatagttaagccagccccgacacccgccaacacccgctgacgcgccctgacg
ggcttgtctgctcccggcatccgcttacagacaagctgtgaccgtctccgggagctgcatgtgtcagagg
ttttcaccgtcatcaccgaaacgcgcgagacgaaagggcctcgtgatacgcctatttttataggttaatg
tcatgataataatggtttcttagacgtcaggtggcacttttcggggaaatgtgcgcggaacccctatttg
tttatttttctaaatacattcaaatatgtatccgctcatgagacaataaccctgataaatgcttcaataa
tattgaaaaaggaagagtatgagtattcaacatttccgtgtcgcccttattccctttttgcggcatttt
gccttcctgtttttgctcacccagaaacgctggtgaaagtaaaagatgctgaagatcagttgggtgcacg
agtgggttacatcgaactggatctcaacagcggtaagatccttgagagttttcgccccgaagaacgtttt
ccaatgatgagcacttttaaagttctgctatgtggcgcggtattatcccgtattgacgccgggcaagagc
aactcggtcgccgcatacactattctcagaatgacttggttgagtactcaccagtcacagaaaagcatct
tacggatggcatgacagtaagagaattatgcagtgctgccataaccatgagtgataacactgcggccaac
ttacttctgacaacgatcggaggaccgaaggagctaaccgcttttttgcacaacatgggggatcatgtaa
ctcgccttgatcgttgggaaccggagctgaatgaagccataccaaacgacgagcgtgacaccacgatgcc
tgtagcaatggcaacaacgttgcgcaaactattaactggcgaactacttactctagcttcccggcaacaa
ttaatagactggatggaggcggataaagttgcaggaccacttctgcgctcggcccttccggctggctggt
ttattgctgataaatctggagccggtgagcgtggaagccgcggtatcattgcagcactggggccagatgg
taagccctcccgtatcgtagttatctacacgacggggagtcaggcaactatggatgaacgaaatagacag
atcgctgagataggtgcctcactgattaagcattggtaactgtcagaccaagtttactcatatatacttt
agattgatttaaaacttcatttttaatttaaaaggatctaggtgaagatccttttgataatctcatgac
caaaatcccttaacgtgagttttcgttccactgagcgtcagaccccgtagaaaagatcaaaggatcttct
tgagatccttttttttctgcgcgtaatctgctgcttgcaaacaaaaaaaccaccgctaccagcggtggttt
gtttgccggatcaagagctaccaactctttttccgaaggtaactggcttcagcagagcgcagataccaaa
tactgttcttctagtgtagccgtagttaggccaccacttcaagaactctgtagcaccgcctacatacctc
gctctgctaatcctgttaccagtggctgctgccagtggcgataagtcgtgtcttaccgggttggactcaa
gacgatagttaccggataaggcgcagcggtcgggctgaacgggggttcgtgcacacagcccagcttgga
gcgaacgacctacaccgaactgagatacctacagcgtgagctatgagaaagcgccacgcttcccgaaggg
agaaaggcggacaggtatccggtaagcggcagggtcggaacaggagagcgcacgagggagcttccagggg

gaaacgcctggtatctttatagtcctgtcgggtttcgccacctctgacttgagcgtcgatttttgtgatg
ctcgtcaggggggcggagcctatggaaaaacgccagcaacgcggccttttacggttcctggccttttgc
tggccttttgctcacatgt

Appendix 2

Plasmid 119739

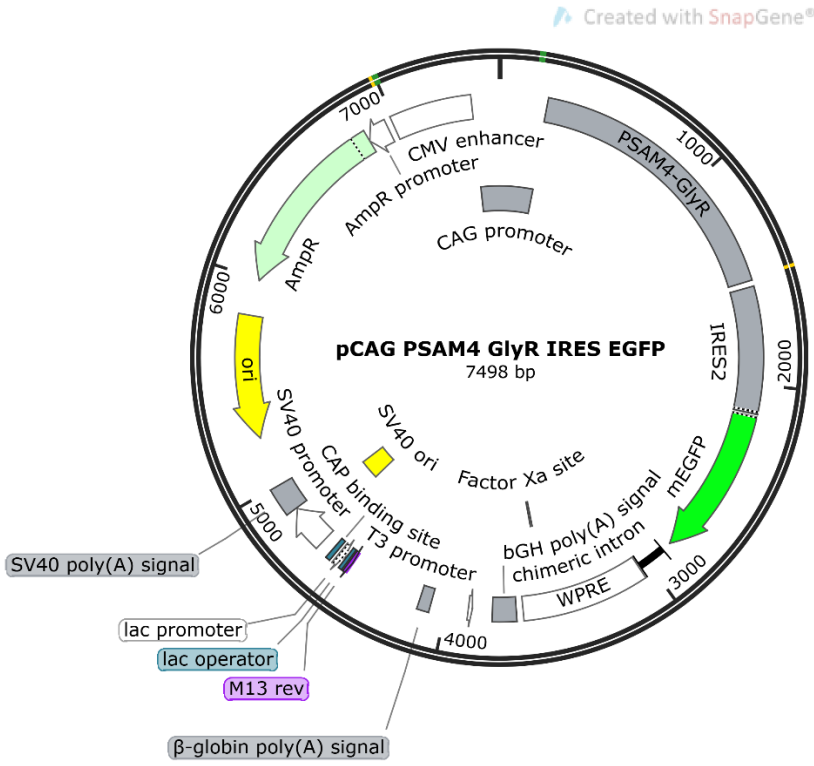

ggggacggctgccttcgggggggacggggcagggcggggttcggcttctggcgtgtgaccggcggctcta
gagcctctgctaaccatgttcatgccttcttcttttttcctacagctcctgggcaacgtgctggttattgt
gctgtctcatcattttggcaaagaattcggtaccgcgggcccggcgcgccagctggatatctccggaccc
gggctagcgccaccatgcgctgttctccaggcggcgtgtggctcgccctggctgcttcccttctgcacgt
tagcctgcagggtgagttccagcgcaaactgtataaggagcttgttaagaattataacccccctggagcgg
ccggtcgcaaatgattcccagccactgacagtgtacttcagcctctccttgctgcagatcatggacgtgg
atgaaaagaaccaggtgctgaccactaatatttggttgcagatgtcctggaccgatcactacttgcagtg
gaatgtgagcgaatacccaggtgtaaagactgtaagattccctgacggccaaatctggaaaccagatatc
ctgctgtacaacagcgcagacgaaaggtttgatgcaacatttcacaccaacgtgggagtcaattcttcag
gccactgcctgtacctgccccctggaatcttcaagtcctcatgctatatcgacgtccgctggtttccctt
cgacgtccagcactgcaaactcaaattcgggagctggagctacggcggatggagcctggatctgcaaatg
caggaggctgacatctctggttacatcccgaatggggagtgggaccttgtgggaatccccggtaaaagaa
gcgagcgattttatgaatgctgcaaagagcccttcccagatgtcaccttcacagtgaccatgcggagacg
catgggttattatctgatccaaatgtatatcccaagcttgcttatagtgattttgtcatggatctccttc
tggattaatatggacgccgctccagctagggtcggactgggcatcaccacagtgctgacaatgactactc
agagctcaggcagccgagccagcttgcccaaggtttcttacgtgaaggccatcgatatctggatggctgt
ctgccttctgtttgtcttcagcgcactgctggaatacgccgctgtcaattttgtgtctcgacagcataaa
gagctgttgcggttcagaagaaaacgacgccaccacaaagaggatgaggcaggagaaggacgcttcaact

ttagcgcctatggtatgggacctgcttgcctccaggctaaagacggaatttccgtgaagggagccaacaa
tagcaacacaaccaacccacccccctgctccatctaagagcccggaggaaatgcgcaaactctttattcag
agagcgaaaaagatcgacaaaatctcccggatcggattccccatggctttcctgattttcaacatgtttt
attggatcatctacaagattgtgcgaagggaggacgtacacaaccagtaagcggccgcaattcccccccgc
ccccccccccctctccctcccccccccctaacgttactggccgaagccgcttggaataaggccggtgtg
cgtttgtctatatgttattttccaccatattgccgtcttttggcaatgtgagggcccggaaacctggccc
tgtcttcttgacgagcattcctaggggtctttcccctctcgccaaaggaatgcaaggtctgttgaatgtc
gtgaaggaagcagttcctctggaagcttcttgaagacaaacaacgtctgtagcgacccctttgcaggcagc
ggaaccccccacctggcgacaggtgcctctgcggccaaaagccacgtgtataagatacacctgcaaaggc
ggcacaaccccagtgccacgttgtgagttggatagttgtggaaagagtcaaatggctctcctaagcgtat
tcaacaaggggctgaaggatgcccagaaggtaccccattgtatgggatctgatctggggcctcggtgcac
atgctttacatgtgtttagtcgaggttaaaaaaacgtctaggccccccgaaccacggggacgtggttttc
ctttgaaaaacacgatgataatatggccacaaccatgggggatccggtgagcaagggcgaggagctgttc
accggggtggtgcccatcctggtcgagctggacggcgacgtaaacggccacaagttcagcgtgtccggcg
agggcgagggcgatgccacctacggcaagctgaccctgaagttcatctgcaccaccggcaagctgcccgt
gccctggcccaccctcgtgaccaccctgacctacggcgtgcagtgcttcagccgctaccccgaccacatg
aagcagcacgacttcttcaagtccgccatgcccgaaggctacgtccaggagcgcaccatcttcttcaagg
acgacggcaactacaagacccgcgccgaggtgaagttcgagggcgacaccctggtgaaccgcatcgagct
gaagggcatcgacttcaaggaggacggcaacatcctggggcacaagctggagtacaactacaacagccac
aacgtctatatcatggccgacaagcagaagaacggcatcaaggtgaacttcaagatccgccacaacatcg
aggacggcagcgtgcagctcgccgaccactaccagcagaacaccccatcggcgacggccccgtgctgct
gcccgacaaccactacctgagcacccagtccaagctgagcaaagaccccaacgagaagcgcgatcacatg
gtcctgctggagttcgtgaccgccgccgggatcactctcggcatggacgagctgtacaagtaatctagag
tcgaggtaccgatgaatagctaaggtcgaggccgcaggtaagtatcaaggttacaagacaggtttaagga
gaccaatagaaactgggcttgtcgagacagagaagactcttgcgtttctgataggcacctattggtctta
ctgacatccactttgcctttctctccacaggtgtcgacaatcaacctctggattacaaaatttgtgaaag
attgactggtattcttaactatgttgctccttttacgctatgtggatacgctgctttaatgcctttgtat
catgctattgcttcccgtatggctttcattttctcctccttgtataaatcctggttgctgtctctttatg
aggagttgtggcccgttgtcaggcaacgtggcgtggtgtgcactgtgtttgctgacgcaacccccactgg
ttggggcattgccaccacctgtcagctcctttccgggactttcgctttccccctccctattgccacggcg
gaactcatcgccgcctgccttgcccgctgctggacaggggctcggctgttgggcactgacaattccgtgg
tgttgtcggggaagctgacgtcctttccatggctgctcgcctgtgttgccacctggattctgcgcgggac
gtccttctgctacgtcccttcggccctcaatccagcggaccttccttcccgcggcctgctgccggctctg
cggcctcttccgcgtcttcgccttcgccctcagacgagtcggatctccctttgggccgcctccccgcctg
gaattcgagctcggtacgatcagcctcgactgtgccttctagttgccagccatctgttgtttgcccctcc
cccgtgccttccttgaccctggaaggtgccactcccactgtcctttcctaataaaatgaggaaattgcat
cgcattgtctgagtaggtgtcattctattctgggggggtggggtggggcaggacagcaaggggaggattg
ggaagacaatagcccagcttttgttccctttagtgagggttaattgcgcgcttggcgtaatcatggtcat
agcckaattcactcctcaggtgcaggctgcctatcagaaggtggtggctggtgtggccaatgccctggct
cacaaataccactgagatcttttcccctctgccaaaaattatggggacatcatgaagccccttgagcatc
tgacttctggctaataaaggaaatttattttcattgcaatagtgtgttggaatttttgtgtctctcact
cggaaggacatatgggagggcaaatcatttaaaacatcagaatgagtatttggtttagagtttggcaaca

tatgcccatatgctggctgccatgaacaaaggttggctataaagaggtcatcagtatatgaaacagcccc
ctgctgtccattccttattccatagaaaagccttgacttgaggttagatttttttatattttgttttgt
gttatttttttctttaacatccctaaaatttttccttacatgttttactagccagattttttcctcctctcc
tgactactcccagtcatagctgtccctcttctcttatggagatccctcgacctgcagcccaagcttggcg
taatcatggtcatagctgtttcctgtgtgaaattgttatccgctcacaattccacacaacatacgagccg
gaagcataaagtgtaaagcctggggtgcctaatgagtgagctaactcacattaattgcgttgcgctcact
gcccgctttccagtcgggaaacctgtcgtgccagcggatccgcatctcaattagtcagcaaccatagtcc
cgcccctaactccgcccatcccgcccctaactccgcccagttccgcccattctccgccccatggctgact
aatttttttttatttatgcagaggccgaggccgcctcggcctctgagctattccagaagtagtgaggaggc
ttttttggaggcctaggcttttgcaaaaagctaacttgtttattgcagcttataatggttacaaataaag
caatagcatcacaaatttcacaaataaagcatttttttcactgcattctagttgtggtttgtccaaactc
atcaatgtatcttatcatgtctggatccgctgcattaatgaatcggccaacgcgcggggagaggcggttt
gcgtattgggcgctcttccgcttcctcgctcactgactcgctgcgctcggtcgttcggctgcggcgagcg
gtatcagctcactcaaaggcggtaatacggttatccacagaatcaggggataacgcaggaaagaacatgt
gagcaaaaggccagcaaaaggccaggaaccgtaaaaaggccgcgttgctggcgtttttccataggctccg
ccccccctgacgagcatcacaaaaatcgacgctcaagtcagaggtggcgaaacccgacaggactataaaga
taccaggcgtttcccccctggaagctccctcgtgcgctctcctgttccgaccctgccgcttaccggatacc
tgtccgcctttctcccttcgggaagcgtggcgctttctcatagctcacgctgtaggtatctcagttcggt
gtaggtcgttcgctccaagctgggctgtgtgcacgaaccccccgttcagcccgaccgctgcgccttatcc
ggtaactatcgtcttgagtccaacccggtaagacacgacttatcgccactggcagcagccactggtaaca
ggattagcagagcgaggtatgtaggcggtgctacagagttcttgaagtggtggcctaactacggctacac
tagaagaacagtatttggtatctgcgctctgctgaagccagttaccttcggaaaaagagttggtagctct
tgatccggcaaacaaaccaccgctggtagcggtggtttttttgtttgcaagcagcagattacgcgcagaa
aaaaaggatctcaagaagatcctttgatcttttctacggggtctgacgctcagtggaacgaaaactcacg
ttaagggattttggtcatgagattatcaaaaaggatcttcacctagatccttttaaattaaaaatgaagt
tttaaatcaatctaaagtatatatgagtaaacttggtctgacagttaccaatgcttaatcagtgaggcac
ctatctcagcgatctgtctatttcgttcatccatagttgcctgactccccgtcgtgtagataactacgat
acgggagggcttaccatctggccccagtgctgcaatgataccgcgagacccacgctcaccggctccagat
ttatcagcaataaaccagccagccggaagggccgagcgcagaagtggtcctgcaactttatccgcctcca
tccagtctattaattgttgccgggaagctagagtaagtagttcgccagttaatagtttgcgcaacgttgt
tgccattgctacaggcatcgtggtgtcacgctcgtcgtttggtatggcttcattcagctccggttcccaa
cgatcaaggcgagttacatgatcccccatgttgtgcaaaaaagcggttagctccttcggtcctccgatcg
ttgtcagaagtaagttggccgcagtgttatcactcatggttatggcagcactgcataattctcttactgt
catgccatccgtaagatgcttttctgtgactggtgagtactcaaccaagtcattctgagaatagtgtatg
cggcgaccgagttgctcttgcccggcgtcaatacgggataataccgcgccacatagcagaactttaaaag
tgctcatcattggaaaacgttcttcggggcgaaaactctcaaggatcttaccgctgttgagatccagttc
gatgtaacccactcgtgcacccaactgatcttcagcatcttttactttcaccagcgtttctgggtgagca
aaaacaggaaggcaaaatgccgcaaaaaagggaataagggcgacacggaaatgttgaatactcatactct
tccttttcaatattattgaagcatttatcagggttattgtctcatgagcggatacatatttgaatgtat
ttagaaaaataaacaaataggggttccgcgcacatttccccgaaaagtgccacctggtcgacattgatta
ttgactagttattaatagtaatcaattacggggtcattagttcatagcccatatatggagttccgcgtta
cataacttacggtaaatggcccgcctggctgaccgcccaacgacccccgcccattgacgtcaataatgac

gtatgttcccatagtaacgccaatagggactttccattgacgtcaatgggtggagtatttacggtaaact
gcccacttggcagtacatcaagtgtatcatatgccaagtacgcccctattgacgtcaatgacggtaaat
ggcccgcctggcattatgcccagtacatgaccttatgggactttcctacttggcagtacatctacgtatt
agtcatcgctattaccatggtcgaggtgagccccacgttctgcttcactctccccatctcccccccctcc
ccacccccaattttgtatttatttatttttttaattattttgtgcagcgatgggggcgggggggggggggg
cgcgcgcc

Appendix 3

CMV PSAM^4-GlyR WPRE BGH pA

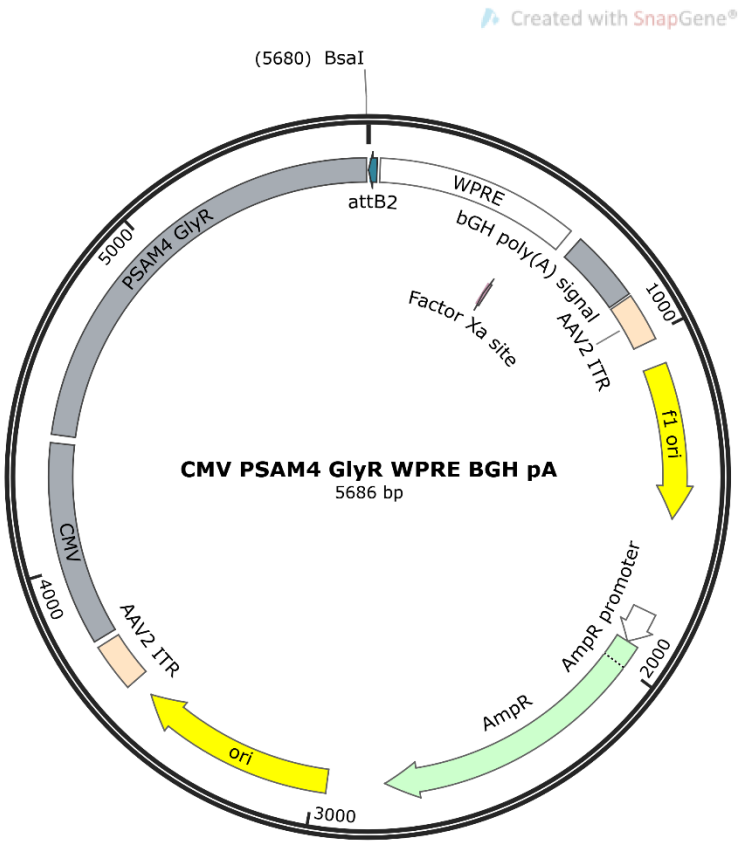

agacccagctttcttgtacaaagtgggaattccgataatcaacctctggattacaaaatttgtgaaagat
tgactggtattcttaactatgttgctccttttacgctatgtggatacgctgctttaatgcctttgtatca
tgctattgcttcccgtatggctttcattttctcctccttgtataaatcctggttgctgtctctttatgag
gagttgtggcccgttgtcaggcaacgtggcgtggtgtgcactgtgtttgctgacgcaacccccactggtt
ggggcattgccaccacctgtcagctcctttccgggactttcgctttcccctccctattgccacggcgga
actcatcgccgcctgccttgcccgctgctggacaggggctcggctgttgggcactgacaattccgtggtg
ttgtcggggaagctgacgtcctttccatggctgctcgcctgtgttgccacctggattctgcgcgggacgt
ccttctgctacgtcccttcggccctcaatccagcggaccttccttcccgcggcctgctgccggctctgcg
gcctcttccgcgtcttcgccttcgccctcagacgagtcggatctccctttgggccgcctccccgcatcgg
gaattcctagagctcgctgatcagcctcgactgtgccttctagttgccagccatctgttgtttgcccctc
ccccgtgccttccttgaccctggaaggtgccactcccactgtcctttcctaataaaatgaggaaattgca
tcgcattgtctgagtaggtgtcattctattctgggggggtggggtggggcaggacagcaagggggaggatt
gggaagagaatagcaggcatgctggggagggccgcaggaacccctagtgatggagttggccactccctct

ctgcgcgctcgctcgctcactgaggccgggcgaccaaaggtcgcccgacgcccgggctttgcccgggcgg
cctcagtgagcgagcgagcgcgcagctgcctgcaggggcgcctgatgcggtattttctccttacgcatct
gtgcggtatttcacaccgcatacgtcaaagcaaccatagtacgcgccctgtagcggcgcattaagcgcgg
cgggggtggtggttacgcgcagcgtgaccgctacacttgccagcgccttagcgcccgctcctttcgcttt
cttcccttcctttctcgccacgttcgccggctttccccgtcaagctctaaatcgggggctccctttaggg
ttccgatttagtgctttacggcacctcgaccccaaaaaacttgatttgggtgatggttcacgtagtgggc
catcgccctgatagacggtttttcgccctttgacgttggagtccacgttctttaatagtggactcttgtt
ccaaactggaacaacactcaactctatctcgggctattcttttgatttataagggattttgccgatttcg
gtctattggttaaaaaatgagctgatttaacaaaaatttaacgcgaattttaacaaaatattaacgttta
caattttatggtgcactctcagtacaatctgctctgatgccgcatagttaagccagccccgacacccgcc
aacacccgctgacgcgccctgacgggcttgtctgctcccggcatccgcttacagacaagctgtgaccgtc
tccgggagctgcatgtgtcagaggttttcaccgtcatcaccgaaacgcgcgagacgaaagggcctcgtga
tacgcctatttttataggttaatgtcatgataataatggtttcttagacgtcaggtggcacttttcgggg
aaatgtgcgcggaacccctatttgtttatttttctaaatacattcaaatatgtatccgctcatgagacaa
taaccctgataaatgcttcaataatattgaaaaaggaagagtatgagtattcaacatttccgtgtcgccc
ttattccctttttgcggcattttgccttcctgtttttgctcacccagaaacgctggtgaaagtaaaaga
tgctgaagatcagttgggtgcacgagtgggttacatcgaactggatctcaacagcggtaagatccttgag
agttttcgccccgaagaacgttttccaatgatgagcacttttaaagttctgctatgtggcgcggtattat
cccgtattgacgccgggcaagagcaactcggtcgccgcatacactattctcagaatgacttggttgagta
ctcaccagtcacagaaaagcatcttacggatggcatgacagtaagagaattatgcagtgctgccataacc
atgagtgataacactgcggccaacttacttctgacaacgatcggaggaccgaaggagctaaccgcttttt
tgcacaacatgggggatcatgtaactcgccttgatcgttgggaaccggagctgaatgaagccataccaaa
cgacgagcgtgacaccacgatgcctgtagcaatggcaacaacgttgcgcaaactattaactggcgaacta
cttactctagcttcccggcaacaattaatagactggatggaggcggataaagttgcaggaccacttctgc
gctcggcccttccggctggctggtttattgctgataaatctggagccggtgagcgtggaagccgcggtat
cattgcagcactggggccagatggtaagccctcccgtatcgtagttatctacacgacggggagtcaggca
actatggatgaacgaaatagacagatcgctgagataggtgcctcactgattaagcattggtaactgtcag
accaagtttactcatatatactttagattgatttaaaacttcatttttaatttaaaaggatctaggtgaa
gatccttttgataatctcatgaccaaaatcccttaacgtgagttttcgttccactgagcgtcagacccc
gtagaaaagatcaaaggatcttcttgagatccttttttctgcgcgtaatctgctgcttgcaaacaaaaa
aaccaccgctaccagcggtggtttgtttgccggatcaagagctaccaactctttttccgaaggtaactgg
cttcagcagagcgcagataccaaatactgttcttctagtgtagccgtagttaggccaccacttcaagaac
tctgtagcaccgcctacatacctcgctctgctaatcctgttaccagtggctgctgccagtggcgataagt
cgtgtcttaccgggttggactcaagacgatagttaccggataaggcgcagcggtcgggctgaacgggggg
ttcgtgcacacagcccagcttggagcgaacgacctacaccgaactgagatacctacagcgtgagctatga
gaaagcgccacgcttcccgaagggagaaaggcggacaggtatccggtaagcggcagggtcggaacaggag
agcgcacgagggagcttccagggggaaacgcctggtatctttatagtcctgtcgggtttcgccacctctg
acttgagcgtcgatttttgtgatgctcgtcaggggggcggagcctatggaaaaacgccagcaacgcggcc
tttttacggttcctggccttttgctggccttttgctcacatgtcctgcaggcagctgcgcgctcgctcgc
tcactgaggccgcccgggcaaagcccgggcgtcgggcgacctttggtcgcccggcctcagtgagcgagcg
agcgcgcagagagggagtggccaactccatcactagggggttccttctaggtatagaaaagttgtagttat
taatagtaatcaattacggggtcattagttcatagcccatatatggagttccgcgttacataacttacgg

taaatggcccgcctggctgaccgcccaacgacccccgcccattgacgtcaataatgacgtatgttcccat
agtaacgccaatagggactttccattgacgtcaatgggtggagtatttacggtaaactgcccacttggca
gtacatcaagtgtatcatatgccaagtacgccccctattgacgtcaatgacggtaaatggcccgcctggc
attatgcccagtacatgaccttatgggactttcctacttggcagtacatctacgtattagtcatcgctat
taccatggtgatgcggttttggcagtacatcaatgggcgtggatagcggtttgactcacggggatttcca
agtctccaccccattgacgtcaatgggagtttgttttggcaccaaaatcaacgggactttccaaaatgtc
gtaacaactccgccccattgacgcaaatgggcggtaggcgtgtacggtgggaggtctatataagcagagc
tggtttagtgaaccgtcagatccaagtttgtagggctagcgccaccatgcgctgttctccaggcggcgtg
tggctcgccctggctgcttcccttctgcacgttagcctgcagggtgagttccagcgcaaactgtataagg
agcttgttaagaattataacccccctggagcggccggtcgcaaatgattcccagccactgacagtgtactt
cagcctctccttgctgcagatcatggacgtggatgaaaagaaccaggtgctgaccactaatatttggttg
cagatgtcctggaccgatcactacttgcagtggaatgtgagcgaatacccaggtgtaaagactgtaagat
tccctgacggccaaatctggaaaccagatatcctgctgtacaacagcgcagacgaaaggtttgatgcaac
atttcacaccaacgtgggagtcaattcttcaggccactgcctgtacctgcccccctggaatcttcaagtcc
tcatgctatatcgacgtccgctggtttcccttcgacgtccagcactgcaaactcaaattcgggagctgga
gctacggcggatggagcctggatctgcaaatgcaggaggctgacatctctggttacatcccgaatgggga
gtgggaccttgtgggaatccccggtaaaagaagcgagcgattttatgaatgctgcaaagagcccttccca
gatgtcaccttcacagtgaccatgcggagacgcatgggttattatctgatccaaatgtatatcccaagct
tgcttatagtgattttgtcatggatctccttctggattaatatggacgccgctccagctagggtcggact
gggcatcaccacagtgctgacaatgactactcagagctcaggcagccgagccagcttgcccaaggtttct
tacgtgaaggccatcgatatctggatggctgtctgccttctgtttgtcttcagcgcactgctggaatacg
ccgctgtcaattttgtgtctcgacagcataaagagctgttgcggttcagaagaaaacgacgccaccacaa
agaggatgaggcaggagaaggacgcttcaactttagcgcctatggtatgggacctgcttgcctccaggct
aaagacggaatttccgtgaagggagccaacaatagcaacacaaccaacccacccccctgctccatctaaga
gcccggaggaaatgcgcaaactctttattcagagagcgaaaaagatcgacaaaatctcccggatcggatt
ccccatggctttcctgattttcaacatgttttattggatcatctacaagattgtgcgaagggaggacgta
cacaaccagtaagcgg

Appendix 4

PS IRES AcGFP1

acacaaccagtaagcctttcttgtacaaagtgggcccctctccctcccccccccctaacgttactggccg
aagccgcttggaataaggccggtgtgcgtttgtctatatgttattttccaccatattgccgtcttttggc
aatgtgagggcccggaaacctggccctgtcttcttgacgagcattcctaggggtctttcccctctcgcca
aaggaatgcaaggtctgttgaatgtcgtgaaggaagcagttcctctggaagcttcttgaagacaaacaac
gtctgtagcgacccttgcaggcagcggaacccccacctggcgacaggtgcctctgcggccaaaagcca
cgtgtataagatacacctgcaaaggcggcacaaccccagtgccacgttgtgagttggatagttgtggaaa
gagtcaaatggctctcctcaagcgtattcaacaaggggctgaaggatgcccagaaggtaccccattgtat
gggatctgatctggggcctcggtacacatgctttacatgtgtttagtcgaggttaaaaaaacgtctaggc
cccccgaaccacggggacgtggttttcctttgaaaaacacgatgataatatggccacaaccatggtgagc
aagggcgccgagctgttcaccggcatcgtgcccatcctgatcgagctgaatggcgatgtgaatggccaca
agttcagcgtgagcggcgagggcgagggcgatgccacctacggcaagctgaccctgaagttcatctgcac
caccggcaagctgcctgtgccctggcccaccctggtgaccaccctgagctacggcgtgcagtgcttctca

cgctaccccgatcacatgaagcagcacgacttcttcaagagcgccatgcctgagggctacatccaggagc
gcaccatcttcttcgaggatgacggcaactacaagtcgcgcgccgaggtgaagttcgagggcgataccct
ggtgaatcgcatcgagctgaccggcaccgatttcaaggaggatggcaacatcctgggcaataagatggag
tacaactacaacgcccacaatgtgtacatcatgaccgacaaggccaagaatggcatcaaggtgaacttca
agatccgccacaacatcgaggatggcagcgtgcagctggccgaccactaccagcagaatacccccatcgg
cgatggccctgtgctgctgcccgataaccactacctgtccacccagagcgccctgtccaaggaccccaac
gagaagcgcgatcacatgatctacttcggcttcgtgaccgccgccgccatcacccacggcatggatgagc
tgtacaagtgaaagcggagacccagc

PS IRES mCherry

acacaaccagtaagcctttcttgtacaaagtggcccctctccctccccccccccctaacgttactggccga
agccgcttggaataaggccggtgtgcgtttgtctatatgttattttccaccatattgccgtcttttggca
atgtgagggcccggaaacctggccctgtcttcttgacgagcattcctaggggtctttcccctctcgccaa
aggaatgcaaggtctgttgaatgtcgtgaaggaagcagttcctctggaagcttcttgaagacaaacaacg
tctgtagcgacccttgcaggcagcggaacccccacctggcgacaggtgcctctgcggccaaaagccac
gtgtataagatacacctgcaaaggcggcacaaccccagtgccacgttgtgagttggatagttgtggaaag
agtcaaatggctctcctcaagcgtattcaacaaggggctgaaggatgcccagaaggtaccccattgtatg
ggatctgatctggggcctcggtacacatgctttacatgtgtttagtcgaggttaaaaaaacgtctaggcc
ccccgaaccacggggacgtggttttcctttgaaaaacacgatgataatatggccacaaccatggtgagca
agggcgaggaggataacatggccatcatcaaggagttcatgcgcttcaaggtgcacatggagggctccgt
gaacggccacgagttcgagatcgagggcgagggcgagggccgcccctacgagggcacccagaccgccaag
ctgaaggtgaccaagggtggcccccctgcccttcgcctgggacatcctgtcccctcagttcatgtacggct
ccaaggcctacgtgaagcaccccgccgacatccccgactacttgaagctgtccttccccgagggcttcaa
gtgggagcgcgtgatgaacttcgaggacggcggcgtggtgaccgtgacccaggactcctccctgcaggac
ggcgagttcatctacaaggtgaagctgcgcggcaccaacttcccctccgacggccccgtaatgcagaaga
agaccatgggctgggaggcctcctccgagcggatgtaccccgaggacggcgccctgaagggcgagatcaa
gcagaggctgaagctgaaggacggcggccactacgacgctgaggtcaagaccacctacaaggccaagaag
cccgtgcagctgcccggcgcctacaacgtcaacatcaagttggacatcacctcccacaacgaggactaca
ccatcgtggaacagtacgaacgcgccgagggccgccactccaccggcggcatggacgagctgtacaagta
aaagcggagacccagc

Appendix 5

CMV PSAM^4-GlyR IRES AcGFP1 WPRE BGH pA

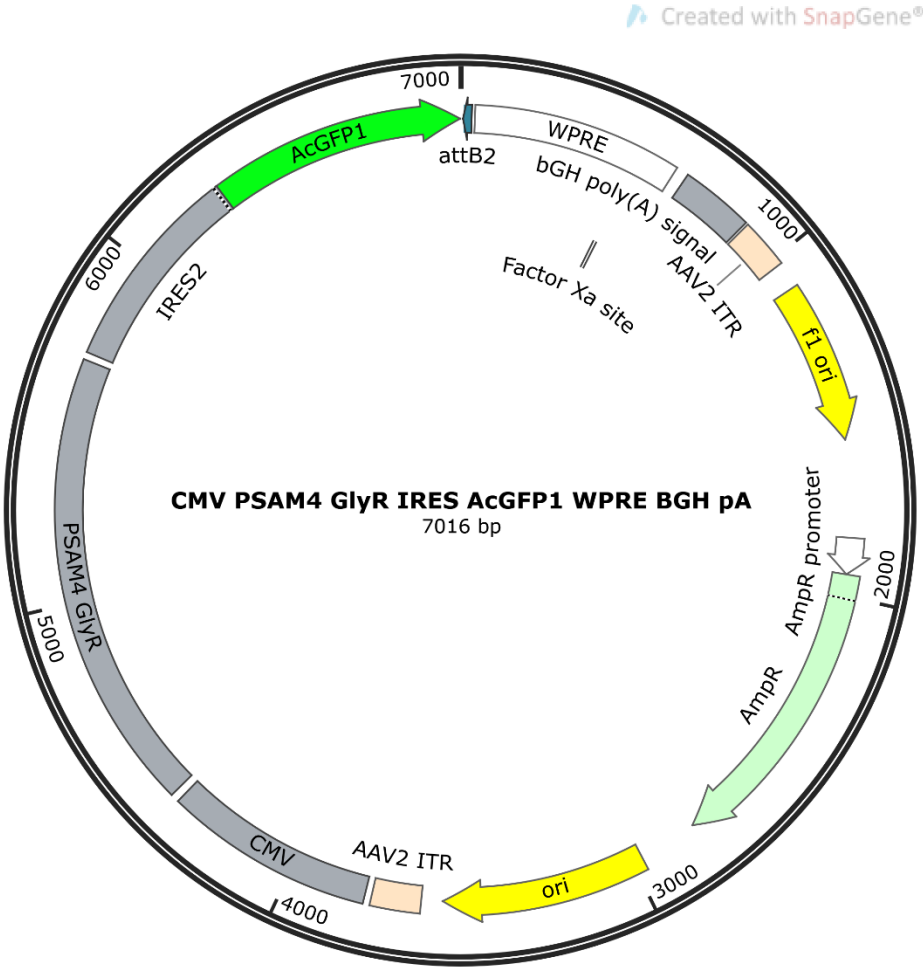

aagcggagacccagctttcttgtacaaagtgggaattccgataatcaacctctggattacaaaatttgtg
aaagattgactggtattcttaactatgttgctccttttacgctatgtggatacgctgctttaatgccttt
gtatcatgctattgcttcccgtatggctttcattttctcctccttgtataaatcctggttgctgtctctt
tatgaggagttgtggcccgttgtcaggcaacgtggcgtggtgtgcactgtgtttgctgacgcaacccccca
ctggttggggcattgccaccacctgtcagctcctttccgggactttcgctttccccctccctattgccac
ggcggaactcatcgccgcctgccttgcccgctgctggacaggggctcggctgttgggcactgacaattcc
gtggtgttgtcggggaagctgacgtcctttccatggctgctcgcctgtgttgccacctggattctgcgcg
ggacgtccttctgctacgtcccttcggccctcaatccagcggaccttccttcccgcggcctgctgccggc
tctgcggcctcttccgcgtcttcgccttcgccctcagacgagtcggatctccctttgggccgcctccccg
catcgggaattcctagagctcgctgatcagcctcgactgtgccttctagttgccagccatctgttgtttg
cccctcccccgtgccttccttgaccctggaaggtgccactcccactgtcctttcctaataaaatgaggaa
attgcatcgcattgtctgagtaggtgtcattctattctgggggtggggtggggcaggacagcaaggggg
aggattgggaagagaatagcaggcatgctggggagggccgcaggaacccctagtgatggagttggccact
ccctctctgcgcgctcgctcgctcactgaggccgggcgaccaaaggtcgcccgacgcccgggctttgccc
gggcggcctcagtgagcgagcgagcgcgcagctgcctgcaggggcgcctgatgcggtattttctccttac
gcatctgtgcggtatttcacaccgcatacgtcaaagcaaccatagtacgcgccctgtagcggcgcattaa

gcgcggcgggggtggtggttacgcgcagcgtgaccgctacacttgccagcgccttagcgcccgctccttt
cgctttcttcccttcctttctcgccacgttcgccggctttccccgtcaagctctaaatcgggggctccct
ttagggttccgatttagtgctttacggcacctcgaccccaaaaaacttgatttgggtgatggttcacgta
gtgggccatcgccctgatagacggtttttcgccctttgacgttggagtccacgttctttaatagtggact
cttgttccaaactggaacaacactcaactctatctcgggctattcttttgatttataagggattttgccg
atttcggtctattggttaaaaaatgagctgatttaacaaaaatttaacgcgaattttaacaaaatattaa
cgtttacaattttatggtgcactctcagtacaatctgctctgatgccgcatagttaagccagccccgaca
cccgccaacacccgctgacgcgccctgacgggcttgtctgctcccggcatccgcttacagacaagctgtg
accgtctccgggagctgcatgtgtcagaggttttcaccgtcatcaccgaaacgcgcgagacgaaagggcc
tcgtgatacgcctatttttataggttaatgtcatgataataatggtttcttagacgtcaggtggcacttt
tcggggaaatgtgcgcggaacccctatttgtttatttttctaaatacattcaaatatgtatccgctcatg
agacaataaccctgataaatgcttcaataatattgaaaaaggaagagtatgagtattcaacatttccgtg
tcgcccttattccctttttgcggcattttgccttcctgtttttgctcacccagaaacgctggtgaaagt
aaaagatgctgaagatcagttgggtgcacgagtgggttacatcgaactggatctcaacagcggtaagatc
cttgagagttttcgccccgaagaacgttttccaatgatgagcacttttaaagttctgctatgtggcgcgg
tattatcccgtattgacgccgggcaagagcaactcggtcgccgcatacactattctcagaatgacttggt
tgagtactcaccagtcacagaaaagcatcttacggatggcatgacagtaagagaattatgcagtgctgcc
ataaccatgagtgataacactgcggccaacttacttctgacaacgatcggaggaccgaaggagctaaccg
ctttttgcacaacatgggggatcatgtaactcgccttgatcgttgggaaccggagctgaatgaagccat
accaaacgacgagcgtgacaccacgatgcctgtagcaatggcaacaacgttgcgcaaactattaactggc
gaactacttactctagcttcccggcaacaattaatagactggatggaggcggataaagttgcaggaccac
ttctgcgctcggcccttccggctggctggtttattgctgataaatctggagccggtgagcgtggaagccg
cggtatcattgcagcactggggccagatggtaagccctcccgtatcgtagttatctacacgacggggagt
caggcaactatggatgaacgaaatagacagatcgctgagataggtgcctcactgattaagcattggtaac
tgtcagaccaagtttactcatatatactttagattgatttaaaacttcatttttaatttaaaaggatcta
ggtgaagatccttttgataatctcatgaccaaaatcccttaacgtgagttttcgttccactgagcgtca
gaccccgtagaaaagatcaaaggatcttcttgagatccttttttttctgcgcgtaatctgctgcttgcaaa
caaaaaaaccaccgctaccagcggtggtttgtttgccggatcaagagctaccaactctttttccgaaggt
aactggcttcagcagagcgcagataccaaatactgttcttctagtgtagccgtagttaggccaccacttc
aagaactctgtagcaccgcctacatacctcgctctgctaatcctgttaccagtggctgctgccagtggcg
ataagtcgtgtcttaccgggttggactcaagacgatagttaccggataaggcgcagcggtcgggctgaac
ggggggttcgtgcacacagcccagcttggagcgaacgacctacaccgaactgagatacctacagcgtgag
ctatgagaaagcgccacgcttcccgaagggagaaaggcggacaggtatccggtaagcggcagggtcggaa
caggagagcgcacgagggagcttccagggggaaacgcctggtatctttatagtcctgtcgggtttcgcca
cctctgacttgagcgtcgatttttgtgatgctcgtcaggggggcggagcctatggaaaaacgccagcaac
gcggcctttttacggttcctggccttttgctggccttttgctcacatgtcctgcaggcagctgcgcgctc
gctcgctcactgaggccgcccgggcaaagcccgggcgtcgggcgacctttggtcgcccggcctcagtgag
cgagcgagcgcgcagagagggagtggccaactccatcactaggggttccttctaggtatagaaaagttgt
agttattaatagtaatcaattacggggtcattagttcatagcccatatatggagttccgcgttacataac
ttacggtaaatggcccgcctggctgaccgcccaacgacccccgcccattgacgtcaataatgacgtatgt
tcccatagtaacgccaatagggactttccattgacgtcaatgggtggagtatttacggtaaactgcccac
ttggcagtacatcaagtgtatcatatgccaagtacgccccctattgacgtcaatgacggtaaatggcccg

cctggcattatgcccagtacatgaccttatgggactttcctacttggcagtacatctacgtattagtcat
cgctattaccatggtgatgcggttttggcagtacatcaatgggcgtggatagcggtttgactcacgggga
tttccaagtctccaccccattgacgtcaatgggagtttgttttggcaccaaaatcaacgggactttccaa
aatgtcgtaacaactccgccccattgacgcaaatgggcggtaggcgtgtacggtgggaggtctatataag
cagagctggtttagtgaaccgtcagatccaagtttgtagggctagcgccaccatgcgctgttctccaggc
ggcgtgtggctcgccctggctgcttcccttctgcacgttagcctgcagggtgagttccagcgcaaactgt
ataaggagcttgttaagaattataacccccctggagcggccggtcgcaaatgattcccagccactgacagt
gtacttcagcctctccttgctgcagatcatggacgtggatgaaaagaaccaggtgctgaccactaatatt
tggttgcagatgtcctggaccgatcactacttgcagtggaatgtgagcgaatacccaggtgtaaagactg
taagattccctgacggccaaatctggaaaccagatatcctgctgtacaacagcgcagacgaaaggtttga
tgcaacatttcacaccaacgtgggagtcaattcttcaggccactgcctgtacctgccccctggaatcttc
aagtcctcatgctatatcgacgtccgctggtttcccttcgacgtccagcactgcaaactcaaattcggga
gctggagctacggcggatggagcctggatctgcaaatgcaggaggctgacatctctggttacatcccgaa
tggggagtgggaccttgtgggaatccccggtaaaagaagcgagcgattttatgaatgctgcaaagagccc
ttcccagatgtcaccttcacagtgaccatgcggagacgcatgggttattatctgatccaaatgtatatcc
caagcttgcttatagtgattttgtcatggatctccttctggattaatatggacgccgctccagctagggt
cggactgggcatcaccacagtgctgacaatgactactcagagctcaggcagccgagccagcttgcccaag
gtttcttacgtgaaggccatcgatatctggatggctgtctgccttctgtttgtcttcagcgcactgctgg
aatacgccgctgtcaattttgtgtctcgacagcataaagagctgttgcggttcagaagaaaacgacgcca
ccacaaagaggatgaggcaggagaaggacgcttcaactttagcgcctatggtatgggacctgcttgcctc
caggctaaagacggaatttccgtgaagggagccaacaatagcaacacaaccaacccacccccctgctccat
ctaagagcccggaggaaatgcgcaaactctttattcagagagcgaaaaagatcgacaaaatctcccggat
cggattccccatggctttcctgattttcaacatgttttattggatcatctacaagattgtgcgaagggag
gacgtacacaaccagtaagcctttcttgtacaaagtgggcccctctccctcccccccccctaacgttact
ggccgaagccgcttggaataaggccggtgtgcgtttgtctatatgttattttccaccatattgccgtctt
ttggcaatgtgagggcccggaaacctggccctgtcttcttgacgagcattcctaggggtctttcccctct
cgccaaaggaatgcaaggtctgttgaatgtcgtgaaggaagcagttcctctggaagcttcttgaagacaa
acaacgtctgtagcgacccttgcaggcagcggaacccccccacctggcgacaggtgcctctgcggccaaa
agccacgtgtataagatacacctgcaaaggcggcacaaccccagtgccacgttgtgagttggatagttgt
ggaaagagtcaaatggctctcctcaagcgtattcaacaaggggctgaaggatgcccagaaggtaccccat
tgtatgggatctgatctggggcctcggtacacatgctttacatgtgtttagtcgaggttaaaaaaacgtc
taggccccccgaaccacggggacgtggttttcctttgaaaaacacgatgataatatggccacaaccatgg
tgagcaagggcgccgagctgttcaccggcatcgtgcccatcctgatcgagctgaatggcgatgtgaatgg
ccacaagttcagcgtgagcggcgagggcgagggcgatgccacctacggcaagctgaccctgaagttcatc
tgcaccaccggcaagctgcctgtgccctggcccaccctggtgaccaccctgagctacggcgtgcagtgct
tctcacgctaccccgatcacatgaagcagcacgacttcttcaagagcgccatgcctgagggctacatcca
ggagcgcaccatcttcttcgaggatgacggcaactacaagtcgcgcgccgaggtgaagttcgagggcgat
accctggtgaatcgcatcgagctgaccggcaccgatttcaaggaggatggcaacatcctgggcaataaga
tggagtacaactacaacgcccacaatgtgtacatcatgaccgacaaggccaagaatggcatcaaggtgaa
cttcaagatccgccacaacatcgaggatggcagcgtgcagctggccgaccactaccagcagaataccccc
atcggcgatggccctgtgctgctgcccgataaccactacctgtccacccagagcgccctgtccaaggacc

ccaacgagaagcgcgatcacatgatctacttcggcttcgtgaccgccgccgccatcacccacggcatgga
tgagctgtacaagtga

CMV PSAM^4-GlyR IRES mCherry WPRE BGH pA

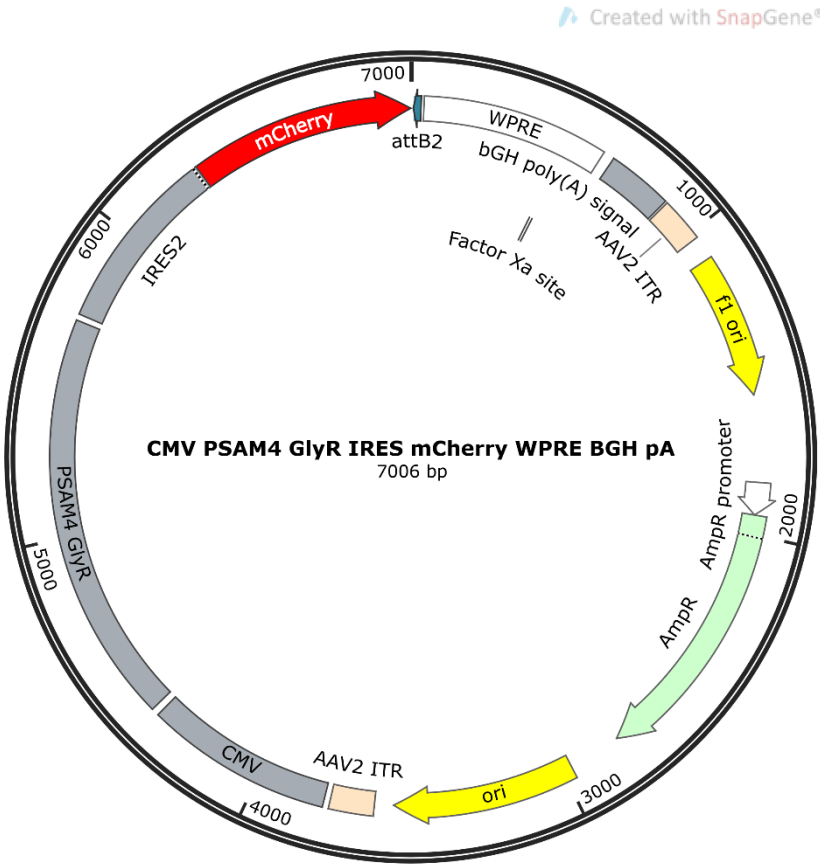

aagcggagacccagctttcttgtacaaagtgggaattccgataatcaacctctggattacaaaatttgtg
aaagattgactggtattcttaactatgttgctccttttacgctatgtggatacgctgctttaatgccttt
gtatcatgctattgcttcccgtatggctttcattttctcctccttgtataaatcctggttgctgtctctt
tatgaggagttgtggcccgttgtcaggcaacgtggcgtggtgtgcactgtgtttgctgacgcaacccccca
ctggttggggcattgccaccacctgtcagctcctttccgggactttcgctttccccctccctattgccac
ggcggaactcatcgccgcctgccttgcccgctgctggacaggggctcggctgttgggcactgacaattcc
gtggtgttgtcggggaagctgacgtcctttccatggctgctcgcctgtgttgccacctggattctgcgcg
ggacgtccttctgctacgtcccttcggccctcaatccagcggaccttccttcccgcggcctgctgccggc
tctgcggcctcttccgcgtcttcgccttcgccctcagacgagtcggatctccctttgggccgcctccccg
catcgggaattcctagagctcgctgatcagcctcgactgtgccttctagttgccagccatctgttgtttg
cccctcccccgtgccttccttgaccctggaaggtgccactcccactgtcctttcctaataaaatgaggaa
attgcatcgcattgtctgagtaggtgtcattctattctgggggggtggggtggggcaggacagcaagggg
aggattgggaagagaatagcaggcatgctggggagggccgcaggaacccctagtgatggagttggccact
ccctctctgcgcgctcgctcgctcactgaggccgggcgaccaaaggtcgcccgacgcccgggctttgccc
gggcggcctcagtgagcgagcgagcgcgcagctgcctgcaggggcgcctgatgcggtattttctccttac
gcatctgtgcggtatttcacaccgcatacgtcaaagcaaccatagtacgcgccctgtagcggcgcattaa
gcgcggcgggggtggtggttacgcgcagcgtgaccgctacacttgccagcgccttagcgcccgctccttt
cgctttcttcccttcctttctcgccacgttcgccggctttccccgtcaagctctaaatcgggggctccct

ttagggttccgatttagtgctttacggcacctcgaccccaaaaaacttgatttgggtgatggttcacgta
gtgggccatcgccctgatagacggtttttcgccctttgacgttggagtccacgttctttaatagtggact
cttgttccaaactggaacaacactcaactctatctcgggctattcttttgatttataagggattttgccg
atttcggtctattggttaaaaaatgagctgatttaacaaaaatttaacgcgaattttaacaaaatattaa
cgtttacaattttatggtgcactctcagtacaatctgctctgatgccgcatagttaagccagccccgaca
cccgccaacacccgctgacgcgccctgacgggcttgtctgctcccggcatccgcttacagacaagctgtg
accgtctccgggagctgcatgtgtcagaggttttcaccgtcatcaccgaaacgcgcgagacgaaagggcc
tcgtgatacgcctatttttataggttaatgtcatgataataatggtttcttagacgtcaggtggcacttt
tcggggaaatgtgcgcggaacccctatttgtttatttttctaaatacattcaaatatgtatccgctcatg
agacaataaccctgataaatgcttcaataatattgaaaaaggaagagtatgagtattcaacatttccgtg
tcgcccttattccctttttttgcggcattttgccttcctgtttttgctcacccagaaacgctggtgaaagt
aaaaagatgctgaagatcagttgggtgcacgagtgggttacatcgaactggatctcaacagcggtaagatc
cttgagagttttcgccccgaagaacgttttccaatgatgagcacttttaaagttctgctatgtggcgcgg
tattatcccgtattgacgccgggcaagagcaactcggtcgccgcatacactattctcagaatgacttggt
tgagtactcaccagtcacagaaaagcatcttacggatggcatgacagtaagagaattatgcagtgctgcc
ataaccatgagtgataacactgcggccaacttacttctgacaacgatcggaggaccgaaggagctaaccg
ctttttgcacaacatgggggatcatgtaactcgccttgatcgttgggaaccggagctgaatgaagccat
accaaacgacgagcgtgacaccacgatgcctgtagcaatggcaacaacgttgcgcaaactattaactggc
gaactacttactctagcttcccggcaacaattaatagactggatggaggcggataaagttgcaggaccac
ttctgcgctcggcccttccggctggctggtttattgctgataaatctggagccggtgagcgtggaagccg
cggtatcattgcagcactggggccagatggtaagccctcccgtatcgtagttatctacacgacggggagt
caggcaactatggatgaacgaaatagacagatcgctgagataggtgcctcactgattaagcattggtaac
tgtcagaccaagtttactcatatatactttagattgatttaaaacttcatttttaatttaaaaggatcta
ggtgaagatccttttttgataatctcatgaccaaaatcccttaacgtgagttttcgttccactgagcgtca
gaccccgtagaaaagatcaaaggatcttcttgagatccttttttttctgcgcgtaatctgctgcttgcaaa
caaaaaaaccaccgctaccagcggtggtttgtttgccggatcaagagctaccaactctttttccgaaggt
aactggcttcagcagagcgcagataccaaatactgttcttctagtgtagccgtagttaggccaccacttc
aagaactctgtagcaccgcctacatacctcgctctgctaatcctgttaccagtggctgctgccagtggcg
ataagtcgtgtcttaccgggttggactcaagacgatagttaccggataaggcgcagcggtcgggctgaac
ggggggttcgtgcacacagcccagcttggagcgaacgacctacaccgaactgagatacctacagcgtgag
ctatgagaaagcgccacgcttcccgaagggagaaaggcggacaggtatccggtaagcggcagggtcggaa
caggagagcgcacgagggagcttccagggggaaacgcctggtatctttatagtcctgtcgggtttcgcca
cctctgacttgagcgtcgatttttgtgatgctcgtcaggggggcggagcctatggaaaaacgccagcaac
gcggcctttttacggttcctggccttttgctggccttttgctcacatgtcctgcaggcagctgcgcgctc
gctcgctcactgaggccgcccgggcaaagcccgggcgtcgggcgacctttggtcgcccggcctcagtgag
cgagcgagcgcgcagagagggagtggccaactccatcactaggggttccttctaggtatagaaaagttgt
agttattaatagtaatcaattacggggtcattagttcatagcccatatatggagttccgcgttacataac
ttacggtaaatggcccgcctggctgaccgcccaacgacccccgcccattgacgtcaataatgacgtatgt
tcccatagtaacgccaatagggactttccattgacgtcaatgggtggagtatttacggtaaactgcccac
ttggcagtacatcaagtgtatcatatgccaagtacgccccctattgacgtcaatgacggtaaatggcccg
cctggcattatgcccagtacatgaccttatgggactttcctacttggcagtacatctacgtattagtcat
cgctattaccatggtgatgcggttttggcagtacatcaatgggcgtggatagcggtttgactcacgggga

tttccaagtctccaccccattgacgtcaatgggagtttgttttggcaccaaaatcaacgggactttccaa
aatgtcgtaacaactccgccccattgacgcaaatgggcggtaggcgtgtacggtgggaggtctatataag
cagagctggtttagtgaaccgtcagatccaagtttgtagggctagcgccaccatgcgctgttctccaggc
ggcgtgtggctcgccctggctgcttcccttctgcacgttagcctgcagggtgagttccagcgcaaactgt
ataaggagcttgttaagaattataacccccctggagcggccggtcgcaaatgattcccagccactgacagt
gtacttcagcctctccttgctgcagatcatggacgtggatgaaaagaaccaggtgctgaccactaatatt
tggttgcagatgtcctggaccgatcactacttgcagtggaatgtgagcgaatacccaggtgtaaagactg
taagattccctgacggccaaatctggaaaccagatatcctgctgtacaacagcgcagacgaaaggtttga
tgcaacatttcacaccaacgtgggagtcaattcttcaggccactgcctgtacctgccccctggaatcttc
aagtcctcatgctatatcgacgtccgctggtttcccttcgacgtccagcactgcaaactcaaattcggga
gctggagctacggcggatggagcctggatctgcaaatgcaggaggctgacatctctggttacatcccgaa
tggggagtgggaccttgtgggaatccccggtaaaagaagcgagcgattttatgaatgctgcaaagagccc
ttcccagatgtcaccttcacagtgaccatgcggagacgcatgggttattatctgatccaaatgtatatcc
caagcttgcttatagtgattttgtcatggatctccttctggattaatatggacgccgctccagctagggt
cggactgggcatcaccacagtgctgacaatgactactcagagctcaggcagccgagccagcttgcccaag
gtttcttacgtgaaggccatcgatatctggatggctgtctgccttctgtttgtcttcagcgcactgctgg
aatacgccgctgtcaattttgtgtctcgacagcataaagagctgttgcggttcagaagaaaacgacgcca
ccacaaagaggatgaggcaggagaaggacgcttcaactttagcgcctatggtatgggacctgcttgcctc
caggctaaagacggaatttccgtgaagggagccaacaatagcaacacaaccaacccacccccctgctccat
ctaagagcccggaggaaatgcgcaaactctttattcagagagcgaaaaagatcgacaaaatctcccggat
cggattccccatggctttcctgattttcaacatgttttattggatcatctacaagattgtgcgaagggag
gacgtacacaaccagtaagcctttcttgtacaaagtggcccctctccctcccccccccctaacgttactg
gccgaagccgcttggaataaggccggtgtgcgtttgtctatatgttatttccaccatattgccgtcttt
tggcaatgtgagggcccggaaacctggccctgtcttcttgacgagcattcctaggggtctttcccctctc
gccaaaggaatgcaaggtctgttgaatgtcgtgaaggaagcagttcctctggaagcttcttgaagacaaa
caacgtctgtagcgacccttgcaggcagcggaacccccacctggcgacaggtgcctctgcggccaaaa
gccacgtgtataagatacacctgcaaaggcggcacaaccccagtgccacgttgtgagttggatagttgtg
gaaagagtcaaatggctctcctcaagcgtattcaacaaggggctgaaggatgcccagaaggtaccccatt
gtatgggatctgatctggggcctcggtacacatgctttacatgtgtttagtcgaggttaaaaaaacgtct
aggcccccgaaccacggggacgtggttttcctttgaaaaacacgatgataatatggccacaaccatggt
gagcaagggcgaggaggataacatggccatcatcaaggagttcatgcgcttcaaggtgcacatggagggc
tccgtgaacggccacgagttcgagatcgagggcgagggcgagggccgcccctacgagggcacccagaccg
ccaagctgaaggtgaccaagggtggccccctgcccttcgcctgggacatcctgtcccctcagttcatgta
cggctccaaggcctacgtgaagcaccccgccgacatccccgactacttgaagctgtccttccccgagggc
ttcaagtgggagcgcgtgatgaacttcgaggacggcggcgtggtgaccgtgacccaggactcctccctgc
aggacggcgagttcatctacaaggtgaagctgcgcggcaccaacttcccctccgacggccccgtaatgca
gaagaagaccatgggctgggaggcctcctccgagcggatgtaccccgaggacggcgccctgaagggcgag
atcaagcagaggctgaagctgaaggacggcggccactacgacgctgaggtcaagaccacctacaaggcca
agaagcccgtgcagctgcccggcgcctacaacgtcaacatcaagttggacatcacctcccacaacgagga
ctacaccatcgtggaacagtacgaacgcgccgagggccgccactccaccggcggcatggacgagctgtac
aagtaa

Appendix 6

Tggggtctttgctcattacttgtacagctcgtccatgccgccggtggagtggcggccctcggcgcgttcg
tactgttccacgatggtgtagtcctcgttgtgggaggtgatgtccaacttgatgttgacgttgtaggcgc
cgggcagctgcacgggcttcttggccttgtaggtggtcttgacctcagcgtcgtagtggccgccgtcctt
cagcttcagcctctgcttgatctcgcccttcagggcgccgtcctcggggtacatccgctcggaggaggcc
tcccagcccatggtcttcttctgcattacggggccgtcggaggggaagttggtgccgcgcagcttcacct
tgtagatgaactcgccgtcctgcagggaggagtcctgggtcacggtcaccacgccgccgtcctcgaagtt
catcacgcgctcccacttgaagccctcggggaaggacagcttcaagtagtcggggatgtcggcggggtgc
ttcacgtaggccttggagccgtacatgaactgaggggacaggatgtcccaggcgaagggcaggggccac
ccttggtcaccttcagcttggcggtctgggtgccctcgtaggggcggccctcgccctcgccctcgatctc
gaactcgtggccgttcacggagccctccatgtgcaccttgaagcgcatgaactccttgatgatggccatg
ttatcctcctcgcccttgctcaccatgatcccccatggttg

9. References

Abdo, H., Li, L., Lallemend, F., Bachy, I., Xu, X. J., Rice, F. L., & Ernfors, P. (2011). Dependence on the transcription factor Shox2 for specification of sensory neurons conveying discriminative touch. *European Journal of Neuroscience*, *34*(10), 1529-1541.

Abrahamsen, B., Zhao, J., Asante, C. O., Cendan, C. M., Marsh, S., Martinez-Barbera, J. P., . . . Wood, J. N. (2008). The cell and molecular basis of mechanical, cold, and inflammatory pain. *Science*, *321*(5889), 702-705.

Abraira, V. E., Kuehn, E. D., Chirila, A. M., Springel, M. W., Toliver, A. A., Zimmerman, A. L., . . . Song, B. J. (2017). The cellular and synaptic architecture of the mechanosensory dorsal horn. *Cell*, *168*(1-2), 295-310.

Addgene. (2022). *ddPCR Titration of AAV Vectors*. https://www.addgene.org/protocols/aav-ddpcr-titration/

Adrian, E. D., & Zotterman, Y. (1926). The impulses produced by sensory nerve-endings: Part II. The response of a Single End-Organ. *J Physiol*, *61*(2), 151-171. https://doi.org/10.1113/jphysiol.1926.sp002281

Agarwal, N., Offermanns, S., & Kuner, R. (2004). Conditional gene deletion in primary nociceptive neurons of trigeminal ganglia and dorsal root ganglia. *Genesis*, *38*(3), 122-129. https://doi.org/10.1002/gene.20010

Aguirre, J., Del Moral, A., Cobo, I., Borgeat, A., & Blumenthal, S. (2012). The role of continuous peripheral nerve blocks. *Anesthesiology research and practice*, *2012*.

Aielli, F., Ponzetti, M., & Rucci, N. (2019). Bone Metastasis Pain, from the Bench to the Bedside. *Int J Mol Sci*, *20*(2). https://doi.org/10.3390/ijms20020280

Airan, R. D., Thompson, K. R., Fenno, L. E., Bernstein, H., & Deisseroth, K. (2009). Temporally precise in vivo control of intracellular signalling. *Nature*, *458*(7241), 1025-1029. https://doi.org/10.1038/nature07926

Akache, B., Grimm, D., Pandey, K., Yant, S. R., Xu, H., & Kay, M. A. (2006). The 37/67-kilodalton laminin receptor is a receptor for adeno-associated virus serotypes 8, 2, 3, and 9. *J Virol*, *80*(19), 9831-9836. https://doi.org/10.1128/jvi.00878-06

Akech, J., Wixted, J. J., Bedard, K., van der Deen, M., Hussain, S., Guise, T. A., . . . Lian, J. B. (2010). Runx2 association with progression of prostate cancer in patients: mechanisms mediating bone osteolysis and osteoblastic metastatic lesions. *Oncogene*, *29*(6), 811-821. https://doi.org/10.1038/onc.2009.389

Akopian, A. N., Sivilotti, L., & Wood, J. N. (1996). A tetrodotoxin-resistant voltage-gated sodium channel expressed by sensory neurons. *Nature*, *379*(6562), 257-262. https://doi.org/10.1038/379257a0

Akopian, A. N., Souslova, V., England, S., Okuse, K., Ogata, N., Ure, J., . . . Wood, J. N. (1999). The tetrodotoxin-resistant sodium channel SNS has a specialized function in pain pathways. *Nat Neurosci*, *2*(6), 541-548. https://doi.org/10.1038/9195

Alamri, A., Bron, R., Brock, J. A., & Ivanusic, J. J. (2015). Transient receptor potential cation channel subfamily V member 1 expressing corneal sensory neurons can be subdivided into at least three subpopulations [Original Research]. *Frontiers in Neuroanatomy*, *9*.

Alerasool, N., Segal, D., Lee, H., & Taipale, M. (2020). An efficient KRAB domain for CRISPRi applications in human cells. *Nature Methods*, *17*(11), 1093-1096. https://doi.org/10.1038/s41592-020-0966-x

Alexander, G. M., Rogan, S. C., Abbas, A. I., Armbruster, B. N., Pei, Y., Allen, J. A., . . . Roth, B. L. (2009). Remote control of neuronal activity in transgenic mice expressing evolved G protein-coupled receptors. *Neuron*, *63*(1), 27-39. https://doi.org/10.1016/j.neuron.2009.06.014

Alexander, R. B., Ponniah, S., Hasday, J., & Hebel, J. R. (1998). Elevated levels of proinflammatory cytokines in the semen of patients with chronic prostatitis/chronic pelvic pain syndrome. *Urology*, *52*(5), 744-749. https://doi.org/10.1016/s0090-4295(98)00390-2

Alhadeff, A. L., Su, Z., Hernandez, E., Klima, M. L., Phillips, S. Z., Holland, R. A., . . . Betley, J. N. (2018). A neural circuit for the suppression of pain by a competing need state. *Cell*, *173*(1), 140-152.

Allen, M. R., & Burr, D. B. (2014). Chapter 4 - Bone Modeling and Remodeling. In D. B. Burr & M. R. Allen (Eds.), *Basic and Applied Bone Biology* (pp. 75-90). Academic Press. https://doi.org/https://doi.org/10.1016/B978-0-12-416015-6.00004-6

Almeida, T. F., Roizenblatt, S., & Tufik, S. (2004). Afferent pain pathways: a neuroanatomical review. *Brain research*, *1000*(1-2), 40-56.
Aloe, L., Tuveri, M. A., Carcassi, U., & Levi-Montalcini, R. (1992). Nerve growth factor in the synovial fluid of patients with chronic arthritis [https://doi.org/10.1002/art.1780350315]. *Arthritis & Rheumatism*, *35*(3), 351-355. https://doi.org/https://doi.org/10.1002/art.1780350315
Alvarez-Leefmans, F. J., Gamiño, S. M., Giraldez, F., & Noguerón, I. (1988). Intracellular chloride regulation in amphibian dorsal root ganglion neurones studied with ion-selective microelectrodes. *J Physiol*, *406*, 225-246. https://doi.org/10.1113/jphysiol.1988.sp017378
Amr, Y. M., & Makharita, M. Y. (2014). Neurolytic sympathectomy in the management of cancer pain-time effect: a prospective, randomized multicenter study. *J Pain Symptom Manage*, *48*(5), 944-956.e942. https://doi.org/10.1016/j.jpainsymman.2014.01.015
Andersen, T. L., Boissy, P., Sondergaard, T. E., Kupisiewicz, K., Plesner, T., Rasmussen, T., . . . Delaissé, J. M. (2007). Osteoclast nuclei of myeloma patients show chromosome translocations specific for the myeloma cell clone: a new type of cancer-host partnership? *J Pathol*, *211*(1), 10-17. https://doi.org/10.1002/path.2078
Andersson, D. A., Gentry, C., Alenmyr, L., Killander, D., Lewis, S. E., Andersson, A., . . . Bevan, S. (2011). TRPA1 mediates spinal antinociception induced by acetaminophen and the cannabinoid Δ9-tetrahydrocannabiorcol. *Nature communications*, *2*(1), 1-11.
Arguello, F., Baggs, R. B., & Frantz, C. N. (1988). A murine model of experimental metastasis to bone and bone marrow. *Cancer Res*, *48*(23), 6876-6881.
Armbruster, B. N., Li, X., Pausch, M. H., Herlitze, S., & Roth, B. L. (2007). Evolving the lock to fit the key to create a family of G protein-coupled receptors potently activated by an inert ligand. *Proc Natl Acad Sci U S A*, *104*(12), 5163-5168. https://doi.org/10.1073/pnas.0700293104
Arnold, L. M. (2007). Duloxetine and other antidepressants in the treatment of patients with fibromyalgia. *Pain Med*, *8 Suppl 2*, S63-74. https://doi.org/10.1111/j.1526-4637.2006.00178.x
Arsenault, J., Ferrari, E., Niranjan, D., Cuijpers, S. A., Gu, C., Vallis, Y., . . . Davletov, B. (2013). Stapling of the botulinum type A protease to growth factors and neuropeptides allows selective targeting of neuroendocrine cells. *J Neurochem*, *126*(2), 223-233. https://doi.org/10.1111/jnc.12284
Asokan, A., Schaffer, D. V., & Samulski, R. J. (2012). The AAV vector toolkit: poised at the clinical crossroads. *Mol Ther*, *20*(4), 699-708. https://doi.org/10.1038/mt.2011.287
Atasoy, D., Aponte, Y., Su, H. H., & Sternson, S. M. (2008). A FLEX switch targets Channelrhodopsin-2 to multiple cell types for imaging and long-range circuit mapping. *J Neurosci*, *28*(28), 7025-7030. https://doi.org/10.1523/jneurosci.1954-08.2008
Atasoy, D., & Sternson, S. M. (2018). Chemogenetic Tools for Causal Cellular and Neuronal Biology. *Physiol Rev*, *98*(1), 391-418. https://doi.org/10.1152/physrev.00009.2017
Austin, P. J., Wu, A., & Moalem-Taylor, G. (2012). Chronic constriction of the sciatic nerve and pain hypersensitivity testing in rats. *J Vis Exp*(61). https://doi.org/10.3791/3393
Averill, S., McMahon, S. B., Clary, D. O., Reichardt, L. F., & Priestley, J. V. (1995). Immunocytochemical Localization of trkA Receptors in Chemically Identified Subgroups of Adult Rat Sensory Neurons [https://doi.org/10.1111/j.1460-9568.1995.tb01143.x]. *European Journal of Neuroscience*, *7*(7), 1484-1494. https://doi.org/https://doi.org/10.1111/j.1460-9568.1995.tb01143.x
Bae, J. Y., Kim, J. H., Cho, Y. S., Mah, W., & Bae, Y. C. (2015). Quantitative analysis of afferents expressing substance P, calcitonin gene-related peptide, isolectin B4, neurofilament 200, and Peripherin in the sensory root of the rat trigeminal ganglion [https://doi.org/10.1002/cne.23672]. *Journal of Comparative Neurology*, *523*(1), 126-138. https://doi.org/https://doi.org/10.1002/cne.23672
Bai, L., Lehnert, B. P., Liu, J., Neubarth, N. L., Dickendesher, T. L., Nwe, P. H., . . . Ginty, D. D. (2015). Genetic identification of an expansive mechanoreceptor sensitive to skin stroking. *Cell*, *163*(7), 1783-1795.
Balakrishnan, B., & Jayandharan, G. R. (2014). Basic biology of adeno-associated virus (AAV) vectors used in gene therapy. *Curr Gene Ther*, *14*(2), 86-100. https://doi.org/10.2174/1566523214666140302193709
Bangash, M. A., Alles, S. R. A., Santana-Varela, S., Millet, Q., Sikandar, S., De Clauser, L., . . . Sexton, J. E. (2018). Distinct transcriptional responses of mouse sensory neurons in models of human chronic pain conditions. *Wellcome open research*, *3*.

Barbera, L., Taylor, C., & Dudgeon, D. (2010). Why do patients with cancer visit the emergency department near the end of life? *Cmaj*, *182*(6), 563-568. https://doi.org/10.1503/cmaj.091187
Barnard, R. J., Elleder, D., & Young, J. A. (2006). Avian sarcoma and leukosis virus-receptor interactions: from classical genetics to novel insights into virus-cell membrane fusion. *Virology*, *344*(1), 25-29. https://doi.org/10.1016/j.virol.2005.09.021
Barnard, R. J., & Young, J. A. (2003). Alpharetrovirus envelope-receptor interactions. *Curr Top Microbiol Immunol*, *281*, 107-136. https://doi.org/10.1007/978-3-642-19012-4_3
Barragán-Iglesias, P., Rocha-González, H. I., Pineda-Farias, J. B., Murbartián, J., Godínez-Chaparro, B., Reinach, P. S., . . . Granados-Soto, V. (2014). Inhibition of peripheral anion exchanger 3 decreases formalin-induced pain. *European Journal of Pharmacology*, *738*, 91-100. https://doi.org/https://doi.org/10.1016/j.ejphar.2014.05.029
Barrangou, R., Fremaux, C., Deveau, H., Richards, M., Boyaval, P., Moineau, S., . . . Horvath, P. (2007). CRISPR provides acquired resistance against viruses in prokaryotes. *Science*, *315*(5819), 1709-1712. https://doi.org/10.1126/science.1138140
Barrios-Rodiles, M., & Chadee, K. (1998). Novel regulation of cyclooxygenase-2 expression and prostaglandin E2 production by IFN-gamma in human macrophages. *J Immunol*, *161*(5), 2441-2448.
Bartel, M. A., Weinstein, J. R., & Schaffer, D. V. (2012). Directed evolution of novel adeno-associated viruses for therapeutic gene delivery. *Gene Ther*, *19*(6), 694-700. https://doi.org/10.1038/gt.2012.20
Bartley, E. J., & Fillingim, R. B. (2013). Sex differences in pain: a brief review of clinical and experimental findings. *Br J Anaesth*, *111*(1), 52-58. https://doi.org/10.1093/bja/aet127
Basner-Tschakarjan, E., & Mingozzi, F. (2014). Cell-Mediated Immunity to AAV Vectors, Evolving Concepts and Potential Solutions. *Front Immunol*, *5*, 350. https://doi.org/10.3389/fimmu.2014.00350
Batalini, F., Gomes, M., I, F., Kuwae, F., Macanhan, G., & Pereira, J. L. B. (2017). Cancer complaints: The profile of patients from the emergency department of a Brazilian oncology teaching hospital. *F1000Res*, *6*, 1919. https://doi.org/10.12688/f1000research.12632.1
Bates, D., Schultheis, B. C., Hanes, M. C., Jolly, S. M., Chakravarthy, K. V., Deer, T. R., . . . Hunter, C. W. (2019). A Comprehensive Algorithm for Management of Neuropathic Pain. *Pain Med*, *20*(Suppl 1), S2-s12. https://doi.org/10.1093/pm/pnz075
Bautista, D. M., Siemens, J., Glazer, J. M., Tsuruda, P. R., Basbaum, A. I., Stucky, C. L., . . . Julius, D. (2007). The menthol receptor TRPM8 is the principal detector of environmental cold. *Nature*, *448*(7150), 204-208.
Beaulieu-Laroche, L., Christin, M., Donoghue, A., Agosti, F., Yousefpour, N., Petitjean, H., . . . Sharif-Naeini, R. (2020). TACAN Is an Ion Channel Involved in Sensing Mechanical Pain. *Cell*, *180*(5), 956-967.e917. https://doi.org/10.1016/j.cell.2020.01.033
Beerli, R. R., Dreier, B., & Barbas, C. F., 3rd. (2000). Positive and negative regulation of endogenous genes by designed transcription factors. *Proc Natl Acad Sci U S A*, *97*(4), 1495-1500. https://doi.org/10.1073/pnas.040552697
Behbehani, M. M., & Fields, H. L. (1979). Evidence that an excitatory connection between the periaqueductal gray and nucleus raphe magnus mediates stimulation produced analgesia. *Brain Res*, *170*(1), 85-93. https://doi.org/10.1016/0006-8993(79)90942-9
Bele, T., & Fabbretti, E. (2015). P2X receptors, sensory neurons and pain. *Current Medicinal Chemistry*, *22*(7), 845-850.
Bell, C. L., Gurda, B. L., Van Vliet, K., Agbandje-McKenna, M., & Wilson, J. M. (2012). Identification of the galactose binding domain of the adeno-associated virus serotype 9 capsid. *J Virol*, *86*(13), 7326-7333. https://doi.org/10.1128/jvi.00448-12
Bellahcène, A., Bachelier, R., Detry, C., Lidereau, R., Clézardin, P., & Castronovo, V. (2007). Transcriptome analysis reveals an osteoblast-like phenotype for human osteotropic breast cancer cells. *Breast Cancer Res Treat*, *101*(2), 135-148. https://doi.org/10.1007/s10549-006-9279-8
Ben-Ari, Y., Khalilov, I., Kahle, K. T., & Cherubini, E. (2012). The GABA excitatory/inhibitory shift in brain maturation and neurological disorders. *Neuroscientist*, *18*(5), 467-486. https://doi.org/10.1177/1073858412438697
Bennett, D. L., Clark, A. J., Huang, J., Waxman, S. G., & Dib-Hajj, S. D. (2019). The Role of Voltage-Gated Sodium Channels in Pain Signaling. *Physiol Rev*, *99*(2), 1079-1151. https://doi.org/10.1152/physrev.00052.2017
Bennett, D. L., & Woods, C. G. (2014). Painful and painless channelopathies. *Lancet Neurol*, *13*(6), 587-599. https://doi.org/10.1016/s1474-4422(14)70024-9

Berns, K. I., & Muzyczka, N. (2017). AAV: An Overview of Unanswered Questions. *Hum Gene Ther*, *28*(4), 308-313. https://doi.org/10.1089/hum.2017.048
Bessou, P., & Perl, E. R. (1969a). Response of cutaneous sensory units with unmyelinated fibers to noxious stimuli. *Journal of neurophysiology*, *32*(6), 1025-1043.
Bessou, P., & Perl, E. R. (1969b). Response of cutaneous sensory units with unmyelinated fibers to noxious stimuli. *J Neurophysiol*, *32*(6), 1025-1043. https://doi.org/10.1152/jn.1969.32.6.1025
Bhave, G., Zhu, W., Wang, H., Brasier, D. J., Oxford, G. S., & Gereau, R. W. t. (2002). cAMP-dependent protein kinase regulates desensitization of the capsaicin receptor (VR1) by direct phosphorylation. *Neuron*, *35*(4), 721-731. https://doi.org/10.1016/s0896-6273(02)00802-4
Bjurholm, A., Kreicbergs, A., Brodin, E., & Schultzberg, M. (1988). Substance P-and CGRP-immunoreactive nerves in bone. *Peptides*, *9*(1), 165-171.
Black, J. A., Hoeijmakers, J. G., Faber, C. G., Merkies, I. S., & Waxman, S. G. (2013). NaV1.7: stress-induced changes in immunoreactivity within magnocellular neurosecretory neurons of the supraoptic nucleus. *Mol Pain*, *9*, 39. https://doi.org/10.1186/1744-8069-9-39
Blair, N. T., & Bean, B. P. (2002). Roles of tetrodotoxin (TTX)-sensitive Na+ current, TTX-resistant Na+ current, and Ca2+ current in the action potentials of nociceptive sensory neurons. *J Neurosci*, *22*(23), 10277-10290.
Blaustein, M. P., & Lederer, W. J. (1999). Sodium/calcium exchange: its physiological implications. *Physiol Rev*, *79*(3), 763-854. https://doi.org/10.1152/physrev.1999.79.3.763
Bourinet, E., Alloui, A., Monteil, A., Barrère, C., Couette, B., Poirot, O., . . . Nargeot, J. (2005). Silencing of the Cav3.2 T-type calcium channel gene in sensory neurons demonstrates its major role in nociception [https://doi.org/10.1038/sj.emboj.7600515]. *The EMBO Journal*, *24*(2), 315-324. https://doi.org/https://doi.org/10.1038/sj.emboj.7600515
Boutin, S., Monteilhet, V., Veron, P., Leborgne, C., Benveniste, O., Montus, M. F., & Masurier, C. (2010). Prevalence of Serum IgG and Neutralizing Factors Against Adeno-Associated Virus (AAV) Types 1, 2, 5, 6, 8, and 9 in the Healthy Population: Implications for Gene Therapy Using AAV Vectors. *Human Gene Therapy*, *21*(6), 704-712. https://doi.org/10.1089/hum.2009.182
Bouza, A. A., & Isom, L. L. (2018). Voltage-Gated Sodium Channel β Subunits and Their Related Diseases. *Handb Exp Pharmacol*, *246*, 423-450. https://doi.org/10.1007/164_2017_48
Boyce, B. F., & Xing, L. (2008). Functions of RANKL/RANK/OPG in bone modeling and remodeling. *Arch Biochem Biophys*, *473*(2), 139-146. https://doi.org/10.1016/j.abb.2008.03.018
Brancaccio, M., Maywood, E. S., Chesham, J. E., Loudon, A. S., & Hastings, M. H. (2013). A Gq-Ca2+ axis controls circuit-level encoding of circadian time in the suprachiasmatic nucleus. *Neuron*, *78*(4), 714-728. https://doi.org/10.1016/j.neuron.2013.03.011
Bravo, L., Llorca-Torralba, M., Berrocoso, E., & Micó, J. A. (2019). Monoamines as Drug Targets in Chronic Pain: Focusing on Neuropathic Pain [Review]. *Frontiers in Neuroscience*, *13*.
Brazill, J. M., Beeve, A. T., Craft, C. S., Ivanusic, J. J., & Scheller, E. L. (2019). Nerves in Bone: Evolving Concepts in Pain and Anabolism. *J Bone Miner Res*, *34*(8), 1393-1406. https://doi.org/10.1002/jbmr.3822
Breivik, H., Collett, B., Ventafridda, V., Cohen, R., & Gallacher, D. (2006). Survey of chronic pain in Europe: prevalence, impact on daily life, and treatment. *Eur J Pain*, *10*(4), 287-333. https://doi.org/10.1016/j.ejpain.2005.06.009
Brenner, D. S., Golden, J. P., & Gereau, R. W. I. V. (2012). A Novel Behavioral Assay for Measuring Cold Sensation in Mice. *PLOS ONE*, *7*(6), e39765. https://doi.org/10.1371/journal.pone.0039765
Brierley, S. M., Hughes, P. A., Page, A. J., Kwan, K. Y., Martin, C. M., O'Donnell, T. A., . . . Liebregts, T. (2009). The ion channel TRPA1 is required for normal mechanosensation and is modulated by algesic stimuli. *Gastroenterology*, *137*(6), 2084-2095.
Brodowicz, T., Hadji, P., Niepel, D., & Diel, I. (2017). Early identification and intervention matters: A comprehensive review of current evidence and recommendations for the monitoring of bone health in patients with cancer. *Cancer Treatment Reviews*, *61*, 23-34. https://doi.org/https://doi.org/10.1016/j.ctrv.2017.09.008

Bron, R., Wood, R. J., Brock, J. A., & Ivanusic, J. J. (2014). Piezo2 expression in corneal afferent neurons [https://doi.org/10.1002/cne.23560]. *Journal of Comparative Neurology*, *522*(13), 2967-2979. https://doi.org/https://doi.org/10.1002/cne.23560
Brown, D. A., & Adams, P. R. (1980). Muscarinic suppression of a novel voltage-sensitive K+ current in a vertebrate neurone. *Nature*, *283*(5748), 673-676. https://doi.org/10.1038/283673a0
Brown, D. C., Iadarola, M. J., Perkowski, S. Z., Erin, H., Shofer, F., Laszlo, K. J., . . . Mannes, A. J. (2005). Physiologic and antinociceptive effects of intrathecal resiniferatoxin in a canine bone cancer model. *Anesthesiology*, *103*(5), 1052-1059. https://doi.org/10.1097/00000542-200511000-00020
Brunger, A. T., Choi, U. B., Lai, Y., Leitz, J., & Zhou, Q. (2018). Molecular mechanisms of fast neurotransmitter release. *Annual review of biophysics*, *47*, 469.
Bruno, F., Arcuri, D., Vozzo, F., Malvaso, A., Montesanto, A., & Maletta, R. (2022). Expression and Signaling Pathways of Nerve Growth Factor (NGF) and Pro-NGF in Breast Cancer: A Systematic Review. *Curr Oncol*, *29*(11), 8103-8120. https://doi.org/10.3390/curroncol29110640
Brzezicki, M. A., & Zakowicz, P. T. (2018). Mambalgins, the Venom-origin Peptides as a Potentially Novel Group of Analgesics: Mini Review. *CNS Neurol Disord Drug Targets*, *17*(2), 87-97. https://doi.org/10.2174/1871527317666171221110419
Burgess, P. R., & Perl, E. R. (1967). Myelinated afferent fibres responding specifically to noxious stimulation of the skin. *J Physiol*, *190*(3), 541-562. https://doi.org/10.1113/jphysiol.1967.sp008227
Burma, N. E., Leduc-Pessah, H., Fan, C. Y., & Trang, T. (2017). Animal models of chronic pain: advances and challenges for clinical translation. *Journal of neuroscience research*, *95*(6), 1242-1256.
Cai, S., Moutal, A., Yu, J., Chew, L. A., Isensee, J., Chawla, R., . . . Khanna, R. (2021). Selective targeting of NaV1.7 via inhibition of the CRMP2-Ubc9 interaction reduces pain in rodents. *Sci Transl Med*, *13*(619), eabh1314. https://doi.org/10.1126/scitranslmed.abh1314
Callaway, E. M. (2008). Transneuronal circuit tracing with neurotropic viruses. *Curr Opin Neurobiol*, *18*(6), 617-623. https://doi.org/10.1016/j.conb.2009.03.007
Cappariello, A., Maurizi, A., Veeriah, V., & Teti, A. (2014). The Great Beauty of the osteoclast. *Archives of Biochemistry and Biophysics*, *558*, 70-78. https://doi.org/https://doi.org/10.1016/j.abb.2014.06.017
Carton, J. M., Sauerwald, T., Hawley-Nelson, P., Morse, B., Peffer, N., Beck, H., . . . Sweet, R. (2007). Codon engineering for improved antibody expression in mammalian cells. *Protein Expr Purif*, *55*(2), 279-286. https://doi.org/10.1016/j.pep.2007.05.017
Casey, K. L. (2019). *Chasing Pain: The Search for a Neurobiological Mechanism of Pain*. Oxford University Press.
Caterina, M. J., Leffler, A., Malmberg, A. B., Martin, W. J., Trafton, J., Petersen-Zeitz, K. R., . . . Julius, D. (2000). Impaired nociception and pain sensation in mice lacking the capsaicin receptor. *Science*, *288*(5464), 306-313. https://doi.org/10.1126/science.288.5464.306
Caterina, M. J., Schumacher, M. A., Tominaga, M., Rosen, T. A., Levine, J. D., & Julius, D. (1997). The capsaicin receptor: a heat-activated ion channel in the pain pathway. *Nature*, *389*(6653), 816-824.
Catterall, W. A., Goldin, A. L., & Waxman, S. G. (2005). International Union of Pharmacology. XLVII. Nomenclature and structure-function relationships of voltage-gated sodium channels. *Pharmacological reviews*, *57*(4), 397-409.
Catterall, W. A., Perez-Reyes, E., Snutch, T. P., & Striessnig, J. (2005). International Union of Pharmacology. XLVIII. Nomenclature and structure-function relationships of voltage-gated calcium channels. *Pharmacological reviews*, *57*(4), 411-425.
Cavalli, E., Mammana, S., Nicoletti, F., Bramanti, P., & Mazzon, E. (2019). The neuropathic pain: An overview of the current treatment and future therapeutic approaches. *Int J Immunopathol Pharmacol*, *33*, 2058738419838383. https://doi.org/10.1177/2058738419838383
Cervero, F., & Wood, J. N. (2020). A History of Pain Research. *The Oxford Handbook of the Neurobiology of Pain*, 1.
Chakrabarti, S., Pattison, L. A., Doleschall, B., Rickman, R. H., Blake, H., Callejo, G., . . . Smith, E. S. J. (2020). Intraarticular Adeno-Associated Virus Serotype AAV-PHP.S-Mediated Chemogenetic Targeting of Knee-Innervating Dorsal Root Ganglion Neurons Alleviates Inflammatory Pain in Mice. *Arthritis Rheumatol*, *72*(10), 1749-1758. https://doi.org/10.1002/art.41314

Chakrabarti, S., Pattison, L. A., Singhal, K., Hockley, J. R. F., Callejo, G., & Smith, E. S. J. (2018). Acute inflammation sensitizes knee-innervating sensory neurons and decreases mouse digging behavior in a TRPV1-dependent manner. *Neuropharmacology*, *143*, 49-62.
Challis, R. C., Ravindra Kumar, S., Chan, K. Y., Challis, C., Beadle, K., Jang, M. J., . . . Gradinaru, V. (2019). Systemic AAV vectors for widespread and targeted gene delivery in rodents. *Nature Protocols*, *14*(2), 379-414. https://doi.org/10.1038/s41596-018-0097-3
Chan, H. Y., V, S., Xing, X., Kraus, P., Yap, S. P., Ng, P., . . . Lufkin, T. (2011). Comparison of IRES and F2A-based locus-specific multicistronic expression in stable mouse lines. *PLoS One*, *6*(12), e28885. https://doi.org/10.1371/journal.pone.0028885
Chan, K. Y., Jang, M. J., Yoo, B. B., Greenbaum, A., Ravi, N., Wu, W. L., . . . Gradinaru, V. (2017). Engineered AAVs for efficient noninvasive gene delivery to the central and peripheral nervous systems. *Nat Neurosci*, *20*(8), 1172-1179. https://doi.org/10.1038/nn.4593
Chang, J. C., Temple, G. F., Trecartin, R. F., & Kan, Y. W. (1979). Suppression of the nonsense mutation in homozygous β0 thalassaemia. *Nature*, *281*(5732), 602-603. https://doi.org/10.1038/281602a0
Chao, M. V. (2003). Neurotrophins and their receptors: A convergence point for many signalling pathways. *Nature Reviews Neuroscience*, *4*(4), 299-309. https://doi.org/10.1038/nrn1078
Chen, L., Huang, J., Zhao, P., Persson, A.-K., Dib-Hajj, F. B., Cheng, X., . . . Dib-Hajj, S. D. (2018). Conditional knockout of NaV1. 6 in adult mice ameliorates neuropathic pain. *Scientific reports*, *8*(1), 1-17.
Cheng, X., Dib-Hajj, S. D., Tyrrell, L., & Waxman, S. G. (2008). Mutation I136V alters electrophysiological properties of the Na(v)1.7 channel in a family with onset of erythromelalgia in the second decade. *Mol Pain*, *4*, 1. https://doi.org/10.1186/1744-8069-4-1
Cherubini, E., & Conti, F. (2001). Generating diversity at GABAergic synapses. *Trends Neurosci*, *24*(3), 155-162. https://doi.org/10.1016/s0166-2236(00)01724-0
Chesler, A. T., Szczot, M., Bharucha-Goebel, D., Čeko, M., Donkervoort, S., Laubacher, C., . . . Stanley, C. (2016). The role of PIEZO2 in human mechanosensation. *New England Journal of Medicine*, *375*(14), 1355-1364.
Chi, X. X., & Nicol, G. D. (2007). Manipulation of the potassium channel Kv1. 1 and its effect on neuronal excitability in rat sensory neurons. *Journal of neurophysiology*, *98*(5), 2683-2692.
Chia, Y. Y., Chow, L. H., Hung, C. C., Liu, K., Ger, L. P., & Wang, P. N. (2002). Gender and pain upon movement are associated with the requirements for postoperative patient-controlled iv analgesia: a prospective survey of 2,298 Chinese patients. *Can J Anaesth*, *49*(3), 249-255. https://doi.org/10.1007/bf03020523
Choi, J. S., & Waxman, S. G. (2011). Physiological interactions between Na(v)1.7 and Na(v)1.8 sodium channels: a computer simulation study. *J Neurophysiol*, *106*(6), 3173-3184. https://doi.org/10.1152/jn.00100.2011
Choi, V. W., McCarty, D. M., & Samulski, R. J. (2006). Host cell DNA repair pathways in adeno-associated viral genome processing. *J Virol*, *80*(21), 10346-10356. https://doi.org/10.1128/jvi.00841-06
Chow, S., Ding, K., Wan, B. A., Brundage, M., Meyer, R. M., Nabid, A., . . . Chow, E. (2017). Gender differences in pain and patient reported outcomes: a secondary analysis of the NCIC CTG SC. 23 randomized trial. *Annals of Palliative Medicine; Vol 6, Supplement 2 (December 04, 2017): Annals of Palliative Medicine¹*.
Chu, T., Shields, L. B. E., Zeng, W., Zhang, Y. P., Wang, Y., Barnes, G. N., . . . Cai, J. (2021). Dynamic glial response and crosstalk in demyelination-remyelination and neurodegeneration processes. *Neural Regen Res*, *16*(7), 1359-1368. https://doi.org/10.4103/1673-5374.300975
Chuang, H. H., Prescott, E. D., Kong, H., Shields, S., Jordt, S. E., Basbaum, A. I., . . . Julius, D. (2001). Bradykinin and nerve growth factor release the capsaicin receptor from PtdIns(4,5)P2-mediated inhibition. *Nature*, *411*(6840), 957-962. https://doi.org/10.1038/35082088
Clark, J. D., & Tempel, B. L. (1998). Hyperalgesia in mice lacking the Kv1. 1 potassium channel gene. *Neuroscience letters*, *251*(2), 121-124.
Cobos, E. J., Nickerson, C. A., Gao, F., Chandran, V., Bravo-Caparrós, I., González-Cano, R., . . . Seehus, C. R. (2018). Mechanistic differences in neuropathic pain modalities

revealed by correlating behavior with global expression profiling. *Cell reports*, *22*(5), 1301-1312.
Cole, J. S., & Patchell, R. A. (2008). Metastatic epidural spinal cord compression. *Lancet Neurol*, *7*(5), 459-466. https://doi.org/10.1016/s1474-4422(08)70089-9
Coleman, R. E. (2001). Metastatic bone disease: clinical features, pathophysiology and treatment strategies. *Cancer Treatment Reviews*, *27*(3), 165-176. https://doi.org/https://doi.org/10.1053/ctrv.2000.0210
Coleman, R. E., & Rubens, R. D. (1987). The clinical course of bone metastases from breast cancer. *Br J Cancer*, *55*(1), 61-66. https://doi.org/10.1038/bjc.1987.13
Connolly, V., Unwin, N., Sherriff, P., Bilous, R., & Kelly, W. (2000). Diabetes prevalence and socioeconomic status: a population based study showing increased prevalence of type 2 diabetes mellitus in deprived areas. *Journal of Epidemiology & Community Health*, *54*(3), 173-177.
Corder, G., Castro, D. C., Bruchas, M. R., & Scherrer, G. (2018). Endogenous and exogenous opioids in pain. *Annual review of neuroscience*, *41*, 453.
Corder, G., Tawfik, V. L., Wang, D., Sypek, E. I., Low, S. A., Dickinson, J. R., . . . Scherrer, G. (2017). Loss of μ opioid receptor signaling in nociceptors, but not microglia, abrogates morphine tolerance without disrupting analgesia. *Nat Med*, *23*(2), 164-173. https://doi.org/10.1038/nm.4262
Cortes-Altamirano, J. L., Olmos-Hernandez, A., Jaime, H. B., Carrillo-Mora, P., Bandala, C., Reyes-Long, S., & Alfaro-Rodríguez, A. (2018). Review: 5-HT1, 5-HT2, 5-HT3 and 5-HT7 Receptors and their Role in the Modulation of Pain Response in the Central Nervous System. *Curr Neuropharmacol*, *16*(2), 210-221. https://doi.org/10.2174/1570159x15666170911121027
Coste, B., Mathur, J., Schmidt, M., Earley, T. J., Ranade, S., Petrus, M. J., . . . Patapoutian, A. (2010). Piezo1 and Piezo2 Are Essential Components of Distinct Mechanically Activated Cation Channels. *Science*, *330*(6000), 55-60. https://doi.org/10.1126/science.1193270
Cotter, M. J., & Muruve, D. A. (2005). The induction of inflammation by adenovirus vectors used for gene therapy. *Front Biosci*, *10*, 1098-1105. https://doi.org/10.2741/1603
Coull, J. A., Boudreau, D., Bachand, K., Prescott, S. A., Nault, F., Sík, A., . . . De Koninck, Y. (2003). Trans-synaptic shift in anion gradient in spinal lamina I neurons as a mechanism of neuropathic pain. *Nature*, *424*(6951), 938-942. https://doi.org/10.1038/nature01868
Coward, K., Plumpton, C., Facer, P., Birch, R., Carlstedt, T., Tate, S., . . . Anand, P. (2000). Immunolocalization of SNS/PN3 and NaN/SNS2 sodium channels in human pain states. *Pain*, *85*(1-2), 41-50. https://doi.org/10.1016/s0304-3959(99)00251-1
Coward, P., Wada, H. G., Falk, M. S., Chan, S. D. H., Meng, F., Akil, H., & Conklin, B. R. (1998). Controlling signaling with a specifically designed Gi-coupled receptor. *Proceedings of the National Academy of Sciences*, *95*(1), 352-357. https://doi.org/10.1073/pnas.95.1.352
Cox, J. J., Reimann, F., Nicholas, A. K., Thornton, G., Roberts, E., Springell, K., . . . Woods, C. G. (2006). An SCN9A channelopathy causes congenital inability to experience pain. *Nature*, *444*(7121), 894-898. https://doi.org/10.1038/nature05413
Crook, R. J., Dickson, K., Hanlon, R. T., & Walters, E. T. (2014). Nociceptive sensitization reduces predation risk. *Curr Biol*, *24*(10), 1121-1125. https://doi.org/10.1016/j.cub.2014.03.043
Crowley, C., Spencer, S. D., Nishimura, M. C., Chen, K. S., Pitts-Meek, S., Armaninl, M. P., . . . Phillips, H. S. (1994). Mice lacking nerve growth factor display perinatal loss of sensory and sympathetic neurons yet develop basal forebrain cholinergic neurons. *Cell*, *76*(6), 1001-1011. https://doi.org/https://doi.org/10.1016/0092-8674(94)90378-6
Cummins, T. R., Black, J. A., Dib-Hajj, S. D., & Waxman, S. G. (2000). Glial-derived neurotrophic factor upregulates expression of functional SNS and NaN sodium channels and their currents in axotomized dorsal root ganglion neurons. *J Neurosci*, *20*(23), 8754-8761. https://doi.org/10.1523/jneurosci.20-23-08754.2000
Curtis, D. R., & Watkins, J. C. (1960). The excitation and depression of spinal neurones by structurally related amino acids. *J Neurochem*, *6*, 117-141. https://doi.org/10.1111/j.1471-4159.1960.tb13458.x
Czeschik, J. C., Hagenacker, T., Schäfers, M., & Büsselberg, D. (2008). TNF-α differentially modulates ion channels of nociceptive neurons. *Neuroscience Letters*, *434*(3), 293-298. https://doi.org/https://doi.org/10.1016/j.neulet.2008.01.070

Dai, Y. (2016). TRPs and pain. *Seminars in Immunopathology*, *38*(3), 277-291. https://doi.org/10.1007/s00281-015-0526-0

Dalkara, D., Byrne, L. C., Klimczak, R. R., Visel, M., Yin, L., Merigan, W. H., . . . Schaffer, D. V. (2013). In vivo-directed evolution of a new adeno-associated virus for therapeutic outer retinal gene delivery from the vitreous. *Sci Transl Med*, *5*(189), 189ra176. https://doi.org/10.1126/scitranslmed.3005708

Darios, F., Niranjan, D., Ferrari, E., Zhang, F., Soloviev, M., Rummel, A., . . . Davletov, B. (2010). SNARE tagging allows stepwise assembly of a multimodular medicinal toxin. *Proc Natl Acad Sci U S A*, *107*(42), 18197-18201. https://doi.org/10.1073/pnas.1007125107

Davis, J. B., Gray, J., Gunthorpe, M. J., Hatcher, J. P., Davey, P. T., Overend, P., . . . Sheardown, S. A. (2000). Vanilloid receptor-1 is essential for inflammatory thermal hyperalgesia. *Nature*, *405*(6783), 183-187. https://doi.org/10.1038/35012076

De Felice, M., Sanoja, R., Wang, R., Vera-Portocarrero, L., Oyarzo, J., King, T., . . . Porreca, F. (2011). Engagement of descending inhibition from the rostral ventromedial medulla protects against chronic neuropathic pain. *Pain*, *152*(12), 2701-2709. https://doi.org/10.1016/j.pain.2011.06.008

de Felipe, P., Luke, G. A., Hughes, L. E., Gani, D., Halpin, C., & Ryan, M. D. (2006). E unum pluribus: multiple proteins from a self-processing polyprotein. *Trends Biotechnol*, *24*(2), 68-75. https://doi.org/10.1016/j.tibtech.2005.12.006

DeFazio, R. A., Keros, S., Quick, M. W., & Hablitz, J. J. (2000). Potassium-Coupled Chloride Cotransport Controls Intracellular Chloride in Rat Neocortical Pyramidal Neurons. *The Journal of Neuroscience*, *20*(21), 8069. https://doi.org/10.1523/JNEUROSCI.20-21-08069.2000

Del Castillo, J., & Katz, B. (1954). Quantal components of the end-plate potential. *The Journal of physiology*, *124*(3), 560.

Deltcheva, E., Chylinski, K., Sharma, C. M., Gonzales, K., Chao, Y., Pirzada, Z. A., . . . Charpentier, E. (2011). CRISPR RNA maturation by trans-encoded small RNA and host factor RNase III. *Nature*, *471*(7340), 602-607. https://doi.org/10.1038/nature09886

Deng, L., Dourado, M., Reese, R. M., Huang, K., Shields, S. D., Stark, K. L., . . . Hackos, D. H. (2023). Nav1.7 is essential for nociceptor action potentials in the mouse in a manner independent of endogenous opioids. *Neuron*. https://doi.org/10.1016/j.neuron.2023.05.024

Denk, F., Bennett, D. L., & McMahon, S. B. (2017). Nerve Growth Factor and Pain Mechanisms. *Annual Review of Neuroscience*, *40*(1), 307-325. https://doi.org/10.1146/annurev-neuro-072116-031121

Dennett, D. C. (1993). *Consciousness explained*. Penguin uk.

Denny, C. A., Kheirbek, M. A., Alba, E. L., Tanaka, K. F., Brachman, R. A., Laughman, K. B., . . . Hen, R. (2014). Hippocampal memory traces are differentially modulated by experience, time, and adult neurogenesis. *Neuron*, *83*(1), 189-201. https://doi.org/10.1016/j.neuron.2014.05.018

Derry, S., Bell, R. F., Straube, S., Wiffen, P. J., Aldington, D., & Moore, R. A. (2019). Pregabalin for neuropathic pain in adults. *Cochrane Database of Systematic Reviews*(1). https://doi.org/10.1002/14651858.CD007076.pub3

Deuis, J. R., Dvorakova, L. S., & Vetter, I. (2017). Methods used to evaluate pain behaviors in rodents. *Frontiers in molecular neuroscience*, *10*, 284.

Deval, E., Gasull, X., Noël, J., Salinas, M., Baron, A., Diochot, S., & Lingueglia, E. (2010). Acid-Sensing Ion Channels (ASICs): Pharmacology and implication in pain. *Pharmacology & Therapeutics*, *128*(3), 549-558. https://doi.org/https://doi.org/10.1016/j.pharmthera.2010.08.006

Dhaka, A., Murray, A. N., Mathur, J., Earley, T. J., Petrus, M. J., & Patapoutian, A. (2007). TRPM8 is required for cold sensation in mice. *Neuron*, *54*(3), 371-378.

Dhandapani, R., Arokiaraj, C. M., Taberner, F. J., Pacifico, P., Raja, S., Nocchi, L., . . . Hussain, A. F. (2018). Control of mechanical pain hypersensitivity in mice through ligand-targeted photoablation of TrkB-positive sensory neurons. *Nature communications*, *9*(1), 1-14.

Diaz, A., & Dickenson, A. H. (1997). Blockade of spinal N-and P-type, but not L-type, calcium channels inhibits the excitability of rat dorsal horn neurones produced by subcutaneous formalin inflammation. *Pain*, *69*(1-2), 93-100.

Dib-Hajj, S. D., Binshtok, A. M., Cummins, T. R., Jarvis, M. F., Samad, T., & Zimmermann, K. (2009). Voltage-gated sodium channels in pain states: Role in pathophysiology and targets for treatment. *Brain Research Reviews*, *60*(1), 65-83. https://doi.org/https://doi.org/10.1016/j.brainresrev.2008.12.005

Djouhri, L., Fang, X., Okuse, K., Wood, J. N., Berry, C. M., & Lawson, S. N. (2003). The TTX-resistant sodium channel Nav1.8 (SNS/PN3): expression and correlation with membrane properties in rat nociceptive primary afferent neurons. *J Physiol*, *550*(Pt 3), 739-752. https://doi.org/10.1113/jphysiol.2003.042127

Dolphin, A. C. (2016). Voltage-gated calcium channels and their auxiliary subunits: physiology and pathophysiology and pharmacology. *The Journal of physiology*, *594*(19), 5369-5390.

Dong, B., Nakai, H., & Xiao, W. (2010). Characterization of genome integrity for oversized recombinant AAV vector. *Mol Ther*, *18*(1), 87-92. https://doi.org/10.1038/mt.2009.258

Donovan-Rodriguez, T., Urch, C. E., & Dickenson, A. H. (2006). Evidence of a role for descending serotonergic facilitation in a rat model of cancer-induced bone pain. *Neurosci Lett*, *393*(2-3), 237-242. https://doi.org/10.1016/j.neulet.2005.09.073

Du, X., Hao, H., Yang, Y., Huang, S., Wang, C., Gigout, S., . . . Edwards, I. (2017). Local GABAergic signaling within sensory ganglia controls peripheral nociceptive transmission. *The Journal of clinical investigation*, *127*(5), 1741-1756.

Duan, B., Cheng, L., Bourane, S., Britz, O., Padilla, C., Garcia-Campmany, L., . . . Ren, X. (2014). Identification of spinal circuits transmitting and gating mechanical pain. *Cell*, *159*(6), 1417-1432.

Duan, D., Yue, Y., Yan, Z., Yang, J., & Engelhardt, J. F. (2000). Endosomal processing limits gene transfer to polarized airway epithelia by adeno-associated virus. *J Clin Invest*, *105*(11), 1573-1587. https://doi.org/10.1172/jci8317

Dubin, Adrienne E., Schmidt, M., Mathur, J., Petrus, Matthew J., Xiao, B., Coste, B., & Patapoutian, A. (2012). Inflammatory Signals Enhance Piezo2-Mediated Mechanosensitive Currents. *Cell Reports*, *2*(3), 511-517. https://doi.org/https://doi.org/10.1016/j.celrep.2012.07.014

Dubuisson, D., & Dennis, S. G. (1977). The formalin test: A quantitative study of the analgesic effects of morphine, meperidine, and brain stem stimulation in rats and cats. *Pain*, *4*, 161-174. https://doi.org/https://doi.org/10.1016/0304-3959(77)90130-0

Dudley, H. R., & Spiro, D. (1961). THE FINE STRUCTURE OF BONE CELLS. *J Biophys Biochem Cytol*, *11*(3), 627-649. https://doi.org/10.1083/jcb.11.3.627

Duncan, G. (2017). The Meanings of 'Pain' in Historical, Social, and Political Context. *The Monist*, *100*(4), 514-531.

Dyer, D. P. (2020). Understanding the mechanisms that facilitate specificity, not redundancy, of chemokine-mediated leukocyte recruitment. *Immunology*, *160*(4), 336-344. https://doi.org/10.1111/imm.13200

Economides, A. N., Carpenter, L. R., Rudge, J. S., Wong, V., Koehler-Stec, E. M., Hartnett, C., . . . Stahl, N. (2003). Cytokine traps: multi-component, high-affinity blockers of cytokine action. *Nat Med*, *9*(1), 47-52. https://doi.org/10.1038/nm811

Edmonds, M. E., Clarke, M. B., Newton, S., Barrett, J., & Watkins, P. J. (1985). Increased Uptake of Bone Radiopharmaceutical in Diabetic Neuropathy. *QJM: An International Journal of Medicine*, *57*(3-4), 843-855. https://doi.org/10.1093/oxfordjournals.qjmed.a067929

Ehrengruber, M. U., Doupnik, C. A., Xu, Y., Garvey, J., Jasek, M. C., Lester, H. A., & Davidson, N. (1997). Activation of heteromeric G protein-gated inward rectifier K+ channels overexpressed by adenovirus gene transfer inhibits the excitability of hippocampal neurons. *Proceedings of the National Academy of Sciences*, *94*(13), 7070-7075. https://doi.org/10.1073/pnas.94.13.7070

Eide, P. K. (2000). Wind-up and the NMDA receptor complex from a clinical perspective. *Eur J Pain*, *4*(1), 5-15. https://doi.org/10.1053/eujp.1999.0154

Eiselé, J. L., Bertrand, S., Galzi, J. L., Devillers-Thiéry, A., Changeux, J. P., & Bertrand, D. (1993). Chimaeric nicotinic-serotonergic receptor combines distinct ligand binding and channel specificities. *Nature*, *366*(6454), 479-483. https://doi.org/10.1038/366479a0

Eisenach, J. C., DuPen, S., Dubois, M., Miguel, R., & Allin, D. (1995). Epidural clonidine analgesia for intractable cancer pain. The Epidural Clonidine Study Group. *Pain*, *61*(3), 391-399. https://doi.org/10.1016/0304-3959(94)00209-w

Eisenach, J. C., Hood, D. D., & Curry, R. (1998). Intrathecal, but not intravenous, clonidine reduces experimental thermal or capsaicin-induced pain and hyperalgesia in normal volunteers. *Anesth Analg*, *87*(3), 591-596. https://doi.org/10.1097/00000539-199809000-00018

Elliott, A. A., & Elliott, J. R. (1993). Characterization of TTX-sensitive and TTX-resistant sodium currents in small cells from adult rat dorsal root ganglia. *J Physiol*, *463*, 39-56. https://doi.org/10.1113/jphysiol.1993.sp019583

Elwood, R. W. (2011). Pain and suffering in invertebrates? *Ilar j*, *52*(2), 175-184. https://doi.org/10.1093/ilar.52.2.175
Emery, E. C., & Ernfors, P. (2018). Dorsal root ganglion neuron types and their functional specialization. In *The oxford handbook of the neurobiology of pain* (pp. 1-30). Oxford University Press London.
Emery, E. C., Luiz, A. P., & Wood, J. N. (2016). Nav1. 7 and other voltage-gated sodium channels as drug targets for pain relief. *Expert opinion on therapeutic targets*, *20*(8), 975-983.
Emery, E. C., & Wood, J. N. (2019). Somatosensation a la mode: plasticity and polymodality in sensory neurons. *Curr Opin Physiol*, *11*, 29-34. https://doi.org/10.1016/j.cophys.2019.04.014
Enomoto, M., Mantyh, P. W., Murrell, J., Innes, J. F., & Lascelles, B. D. X. (2019). Anti-nerve growth factor monoclonal antibodies for the control of pain in dogs and cats. *Veterinary Record*, *184*(1), 23. https://doi.org/10.1136/vr.104590
Faber, C. G., Hoeijmakers, J. G., Ahn, H. S., Cheng, X., Han, C., Choi, J. S., . . . Merkies, I. S. (2012). Gain of function Nav1.7 mutations in idiopathic small fiber neuropathy. *Ann Neurol*, *71*(1), 26-39. https://doi.org/10.1002/ana.22485
Faber, C. G., Lauria, G., Merkies, I. S., Cheng, X., Han, C., Ahn, H. S., . . . Waxman, S. G. (2012). Gain-of-function Nav1.8 mutations in painful neuropathy. *Proc Natl Acad Sci U S A*, *109*(47), 19444-19449. https://doi.org/10.1073/pnas.1216080109
Falk, S., & Dickenson, A. H. (2014). Pain and nociception: mechanisms of cancer-induced bone pain. *J Clin Oncol*, *32*(16), 1647-1654. https://doi.org/10.1200/jco.2013.51.7219
Farrell, M. S., Pei, Y., Wan, Y., Yadav, P. N., Daigle, T. L., Urban, D. J., . . . Roth, B. L. (2013). A Gαs DREADD Mouse for Selective Modulation of cAMP Production in Striatopallidal Neurons. *Neuropsychopharmacology*, *38*(5), 854-862. https://doi.org/10.1038/npp.2012.251
Fatt, P., & Katz, B. (1952). Spontaneous subthreshold activity at motor nerve endings. *The Journal of physiology*, *117*(1), 109.
Fayaz, A., Croft, P., Langford, R. M., Donaldson, L. J., & Jones, G. T. (2016). Prevalence of chronic pain in the UK: a systematic review and meta-analysis of population studies. *BMJ Open*, *6*(6), e010364. https://doi.org/10.1136/bmjopen-2015-010364
Feige, U., Hu, Y. L., Gasser, J., Campagnuolo, G., Munyakazi, L., & Bolon, B. (2000). Anti-interleukin-1 and anti-tumor necrosis factor-alpha synergistically inhibit adjuvant arthritis in Lewis rats. *Cell Mol Life Sci*, *57*(10), 1457-1470. https://doi.org/10.1007/pl00000629
Feil, S., Valtcheva, N., & Feil, R. (2009). Inducible cre mice. In *Gene knockout protocols* (pp. 343-363). Springer.
Ferrand, M., Da Rocha, S., Corre, G., Galy, A., & Boisgerault, F. (2015). Serotype-specific Binding Properties and Nanoparticle Characteristics Contribute to the Immunogenicity of rAAV1 Vectors. *Mol Ther*, *23*(6), 1022-1033. https://doi.org/10.1038/mt.2015.59
Ferrari, E., Maywood, E. S., Restani, L., Caleo, M., Pirazzini, M., Rossetto, O., . . . Davletov, B. (2011). Re-assembled botulinum neurotoxin inhibits CNS functions without systemic toxicity. *Toxins (Basel)*, *3*(4), 345-355. https://doi.org/10.3390/toxins3040345
Ferreira, S. H., Moncada, S. T., & Vane, J. R. (1971). Indomethacin and aspirin abolish prostaglandin release from the spleen. *Nature new biology*, *231*(25), 237-239.
Ferrini, F., Trang, T., Mattioli, T. A., Laffray, S., Del'Guidice, T., Lorenzo, L. E., . . . De Koninck, Y. (2013). Morphine hyperalgesia gated through microglia-mediated disruption of neuronal Cl^- homeostasis. *Nat Neurosci*, *16*(2), 183-192. https://doi.org/10.1038/nn.3295
Fertleman, C. R., Baker, M. D., Parker, K. A., Moffatt, S., Elmslie, F. V., Abrahamsen, B., . . . Rees, M. (2006). SCN9A mutations in paroxysmal extreme pain disorder: allelic variants underlie distinct channel defects and phenotypes. *Neuron*, *52*(5), 767-774. https://doi.org/10.1016/j.neuron.2006.10.006
Field, M. J., Li, Z., & Schwarz, J. B. (2007). Ca2+ channel α2-δ ligands for the treatment of neuropathic pain. *Journal of medicinal chemistry*, *50*(11), 2569-2575.
Fields, H. L. (2018). How expectations influence pain. *Pain*, *159*, S3-S10.
Fields, H. L., & Heinricher, M. M. (1985). Anatomy and physiology of a nociceptive modulatory system. *Philos Trans R Soc Lond B Biol Sci*, *308*(1136), 361-374. https://doi.org/10.1098/rstb.1985.0037
Finn, J. D., Hui, D., Downey, H. D., Dunn, D., Pien, G. C., Mingozzi, F., . . . High, K. A. (2010). Proteasome Inhibitors Decrease AAV2 Capsid derived Peptide Epitope Presentation on MHC Class I Following Transduction. *Molecular Therapy*, *18*(1), 135-142. https://doi.org/https://doi.org/10.1038/mt.2009.257

Finnerup, N. B., Kuner, R., & Jensen, T. S. (2020). Neuropathic Pain: From Mechanisms to Treatment. *Physiological Reviews*, *101*(1), 259-301. https://doi.org/10.1152/physrev.00045.2019
Fjell, J., Cummins, T. R., Dib-Hajj, S. D., Fried, K., Black, J. A., & Waxman, S. G. (1999). Differential role of GDNF and NGF in the maintenance of two TTX-resistant sodium channels in adult DRG neurons. *Brain Res Mol Brain Res*, *67*(2), 267-282. https://doi.org/10.1016/s0169-328x(99)00070-4
Flatters, S. J. L., Dougherty, P. M., & Colvin, L. A. (2017). Clinical and preclinical perspectives on chemotherapy-induced peripheral neuropathy (CIPN): a narrative review. *BJA: British Journal of Anaesthesia*, *119*(4), 737-749.
Florez-Paz, D., Bali, K. K., Kuner, R., & Gomis, A. (2016). A critical role for Piezo2 channels in the mechanotransduction of mouse proprioceptive neurons. *Scientific Reports*, *6*(1), 25923. https://doi.org/10.1038/srep25923
Franco, M. L., Melero, C., Sarasola, E., Acebo, P., Luque, A., Calatayud-Baselga, I., . . . Vilar, M. (2016). Mutations in TrkA Causing Congenital Insensitivity to Pain with Anhidrosis (CIPA) Induce Misfolding, Aggregation, and Mutation-dependent Neurodegeneration by Dysfunction of the Autophagic Flux. *J Biol Chem*, *291*(41), 21363-21374. https://doi.org/10.1074/jbc.M116.722587
Franzoso, G., Carlson, L., Xing, L., Poljak, L., Shores, E. W., Brown, K. D., . . . Siebenlist, U. (1997). Requirement for NF-kappaB in osteoclast and B-cell development. *Genes Dev*, *11*(24), 3482-3496. https://doi.org/10.1101/gad.11.24.3482
François, A., Schüetter, N., Laffray, S., Sanguesa, J., Pizzoccaro, A., Dubel, S., . . . Wood, J. N. (2015). The low-threshold calcium channel Cav3. 2 determines low-threshold mechanoreceptor function. *Cell reports*, *10*(3), 370-382.
Freburger, J. K., Holmes, G. M., Agans, R. P., Jackman, A. M., Darter, J. D., Wallace, A. S., . . . Carey, T. S. (2009). The rising prevalence of chronic low back pain. *Arch Intern Med*, *169*(3), 251-258. https://doi.org/10.1001/archinternmed.2008.543
Funk, K., Woitecki, A., Franjic-Würtz, C., Gensch, T., Möhrlen, F., & Frings, S. (2008). Modulation of chloride homeostasis by inflammatory mediators in dorsal root ganglion neurons. *Mol Pain*, *4*, 32. https://doi.org/10.1186/1744-8069-4-32
Furman, G. G. (1965). Comparison of models for subtractive and shunting lateral-inhibition in receptor-neuron fields. *Kybernetik*, *2*(6), 257-274. https://doi.org/10.1007/bf00274089
Galan, A., & Cervero, F. (2005). Painful stimuli induce in vivo phosphorylation and membrane mobilization of mouse spinal cord NKCC1 co-transporter. *Neuroscience*, *133*(1), 245-252. https://doi.org/10.1016/j.neuroscience.2005.02.025
Gallagher, J. P., Higashi, H., & Nishi, S. (1978). Characterization and ionic basis of GABA-induced depolarizations recorded in vitro from cat primary afferent neurones. *J Physiol*, *275*, 263-282. https://doi.org/10.1113/jphysiol.1978.sp012189
Gamba, G. (2005). Molecular physiology and pathophysiology of electroneutral cation-chloride cotransporters. *Physiol Rev*, *85*(2), 423-493. https://doi.org/10.1152/physrev.00011.2004
Gao, G., Vandenberghe, L. H., Alvira, M. R., Lu, Y., Calcedo, R., Zhou, X., & Wilson, J. M. (2004). Clades of Adeno-associated viruses are widely disseminated in human tissues. *J Virol*, *78*(12), 6381-6388. https://doi.org/10.1128/jvi.78.12.6381-6388.2004
Gao, Z. G., Duong, H. T., Sonina, T., Kim, S. K., Van Rompaey, P., Van Calenbergh, S., . . . Jacobson, K. A. (2006). Orthogonal activation of the reengineered A3 adenosine receptor (neoceptor) using tailored nucleoside agonists. *J Med Chem*, *49*(9), 2689-2702. https://doi.org/10.1021/jm050968b
Garneau, J. E., Dupuis, M., Villion, M., Romero, D. A., Barrangou, R., Boyaval, P., . . . Moineau, S. (2010). The CRISPR/Cas bacterial immune system cleaves bacteriophage and plasmid DNA. *Nature*, *468*(7320), 67-71. https://doi.org/10.1038/nature09523
Gasiunas, G., Barrangou, R., Horvath, P., & Siksnys, V. (2012). Cas9-crRNA ribonucleoprotein complex mediates specific DNA cleavage for adaptive immunity in bacteria. *Proc Natl Acad Sci U S A*, *109*(39), E2579-2586. https://doi.org/10.1073/pnas.1208507109
Gaskin, D. J., & Richard, P. (2012). The economic costs of pain in the United States. *J Pain*, *13*(8), 715-724. https://doi.org/10.1016/j.jpain.2012.03.009
Ghitani, N., Barik, A., Szczot, M., Thompson, J. H., Li, C., Le Pichon, C. E., . . . Chesler, A. T. (2017). Specialized mechanosensory nociceptors mediating rapid responses to hair pull. *Neuron*, *95*(4), 944-954.
Gilbert, L. A., Larson, M. H., Morsut, L., Liu, Z., Brar, G. A., Torres, S. E., . . . Qi, L. S. (2013). CRISPR-mediated modular RNA-guided regulation of transcription in eukaryotes. *Cell*, *154*(2), 442-451. https://doi.org/10.1016/j.cell.2013.06.044

Gingras, J., Smith, S., Matson, D. J., Johnson, D., Nye, K., Couture, L., . . . McDonough, S. I. (2014). Global Nav1.7 knockout mice recapitulate the phenotype of human congenital indifference to pain. *PLoS One*, *9*(9), e105895. https://doi.org/10.1371/journal.pone.0105895

Goetz, T., Arslan, A., Wisden, W., & Wulff, P. (2007). GABA(A) receptors: structure and function in the basal ganglia. *Prog Brain Res*, *160*, 21-41. https://doi.org/10.1016/s0079-6123(06)60003-4

Gold, M. S., & Gebhart, G. F. (2010). Nociceptor sensitization in pain pathogenesis. *Nat Med*, *16*(11), 1248-1257. https://doi.org/10.1038/nm.2235

Gold, M. S., Levine, J. D., & Correa, A. M. (1998). Modulation of TTX-R INa by PKC and PKA and their role in PGE2-induced sensitization of rat sensory neurons in vitro. *J Neurosci*, *18*(24), 10345-10355. https://doi.org/10.1523/jneurosci.18-24-10345.1998

Gold, M. S., Weinreich, D., Kim, C. S., Wang, R., Treanor, J., Porreca, F., & Lai, J. (2003). Redistribution of Na(V)1.8 in uninjured axons enables neuropathic pain. *J Neurosci*, *23*(1), 158-166. https://doi.org/10.1523/jneurosci.23-01-00158.2003

Goldstein, M. E., House, S. B., & Gainer, H. (1991). NF-L and peripherin immunoreactivities define distinct classes of rat sensory ganglion cells. *Journal of neuroscience research*, *30*(1), 92-104.

Gonçalves, N. P., Vægter, C. B., & Pallesen, L. T. (2018). Peripheral Glial Cells in the Development of Diabetic Neuropathy. *Front Neurol*, *9*, 268. https://doi.org/10.3389/fneur.2018.00268

Gough, P., & Myles, I. A. (2020). Tumor Necrosis Factor Receptors: Pleiotropic Signaling Complexes and Their Differential Effects [Review]. *Frontiers in Immunology*, *11*.

Gould, H. J., 3rd, Gould, T. N., England, J. D., Paul, D., Liu, Z. P., & Levinson, S. R. (2000). A possible role for nerve growth factor in the augmentation of sodium channels in models of chronic pain. *Brain Res*, *854*(1-2), 19-29. https://doi.org/10.1016/s0006-8993(99)02216-7

Gray, J. T., & Zolotukhin, S. (2011). Design and construction of functional AAV vectors. *Methods Mol Biol*, *807*, 25-46. https://doi.org/10.1007/978-1-61779-370-7_2

Gray, S. J., Foti, S. B., Schwartz, J. W., Bachaboina, L., Taylor-Blake, B., Coleman, J., . . . Samulski, R. J. (2011). Optimizing promoters for recombinant adeno-associated virus-mediated gene expression in the peripheral and central nervous system using self-complementary vectors. *Hum Gene Ther*, *22*(9), 1143-1153. https://doi.org/10.1089/hum.2010.245

Gregory, N. S., Harris, A. L., Robinson, C. R., Dougherty, P. M., Fuchs, P. N., & Sluka, K. A. (2013). An overview of animal models of pain: disease models and outcome measures. *The Journal of Pain*, *14*(11), 1255-1269.

Grieger, J. C., Soltys, S. M., & Samulski, R. J. (2016). Production of Recombinant Adeno-associated Virus Vectors Using Suspension HEK293 Cells and Continuous Harvest of Vector From the Culture Media for GMP FIX and FLT1 Clinical Vector. *Molecular Therapy*, *24*(2), 287-297. https://doi.org/https://doi.org/10.1038/mt.2015.187

Griesenbach, U., Pytel, K. M., & Alton, E. W. (2015). Cystic Fibrosis Gene Therapy in the UK and Elsewhere. *Hum Gene Ther*, *26*(5), 266-275. https://doi.org/10.1089/hum.2015.027

Groner, A. C., Meylan, S., Ciuffi, A., Zangger, N., Ambrosini, G., Dénervaud, N., . . . Trono, D. (2010). KRAB-zinc finger proteins and KAP1 can mediate long-range transcriptional repression through heterochromatin spreading. *PLoS Genet*, *6*(3), e1000869. https://doi.org/10.1371/journal.pgen.1000869

Gross, C. G. (2002). Genealogy of the "grandmother cell". *Neuroscientist*, *8*(5), 512-518. https://doi.org/10.1177/107385802237175

Grutter, T., de Carvalho, L. P., Dufresne, V., Taly, A., Edelstein, S. J., & Changeux, J. P. (2005). Molecular tuning of fast gating in pentameric ligand-gated ion channels. *Proc Natl Acad Sci U S A*, *102*(50), 18207-18212. https://doi.org/10.1073/pnas.0509024102

Gu, X., Zhang, J., Ma, Z., Wang, J., Zhou, X., Jin, Y., . . . Mei, F. (2010). The role of N-methyl-D-aspartate receptor subunit NR2B in spinal cord in cancer pain. *Eur J Pain*, *14*(5), 496-502. https://doi.org/10.1016/j.ejpain.2009.09.001

Guedon, J. G., Longo, G., Majuta, L. A., Thomspon, M. L., Fealk, M. N., & Mantyh, P. W. (2016). Dissociation between the relief of skeletal pain behaviors and skin hypersensitivity in a model of bone cancer pain. *Pain*, *157*(6), 1239-1247. https://doi.org/10.1097/j.pain.0000000000000514

Guenthner, C. J., Miyamichi, K., Yang, H. H., Heller, H. C., & Luo, L. (2013). Permanent genetic access to transiently active neurons via TRAP: targeted recombination in active populations. *Neuron*, *78*(5), 773-784. https://doi.org/10.1016/j.neuron.2013.03.025

Guise, T. A., Mohammad, K. S., Clines, G., Stebbins, E. G., Wong, D. H., Higgins, L. S., . . . Chirgwin, J. M. (2006). Basic mechanisms responsible for osteolytic and osteoblastic bone metastases. *Clin Cancer Res*, *12*(20 Pt 2), 6213s-6216s. https://doi.org/10.1158/1078-0432.ccr-06-1007

Guzmán, I., & Bosland, P. W. (2017). Sensory properties of chile pepper heat–and its importance to food quality and cultural preference. *Appetite*, *117*, 186-190.

Habib, A. M., Okorokov, A. L., Hill, M. N., Bras, J. T., Lee, M.-C., Li, S., . . . Houlden, H. (2019). Microdeletion in a FAAH pseudogene identified in a patient with high anandamide concentrations and pain insensitivity. *British journal of anaesthesia*, *123*(2), e249-e253.

Hamill, O. P., Marty, A., Neher, E., Sakmann, B., & Sigworth, F. J. (1981). Improved patch-clamp techniques for high-resolution current recording from cells and cell-free membrane patches. *Pflugers Arch*, *391*(2), 85-100. https://doi.org/10.1007/bf00656997

Hampf, M., & Gossen, M. (2007). Promoter Crosstalk Effects on Gene Expression. *Journal of Molecular Biology*, *365*(4), 911-920. https://doi.org/https://doi.org/10.1016/j.jmb.2006.10.009

Han, C., Estacion, M., Huang, J., Vasylyev, D., Zhao, P., Dib-Hajj, S. D., & Waxman, S. G. (2015). Human Na(v)1.8: enhanced persistent and ramp currents contribute to distinct firing properties of human DRG neurons. *J Neurophysiol*, *113*(9), 3172-3185. https://doi.org/10.1152/jn.00113.2015

Han, C., Vasylyev, D., Macala, L. J., Gerrits, M. M., Hoeijmakers, J. G., Bekelaar, K. J., . . . Waxman, S. G. (2014). The G1662S NaV1.8 mutation in small fibre neuropathy: impaired inactivation underlying DRG neuron hyperexcitability. *J Neurol Neurosurg Psychiatry*, *85*(5), 499-505. https://doi.org/10.1136/jnnp-2013-306095

Handwerker, H. O., Anton, F., Kocher, L., & Reeh, P. W. (1987). Nociceptor functions in intact skin and in neurogenic or non-neurogenic inflammation. *Acta physiologica Hungarica*, *69*(3-4), 333-342.

Hannibal, K. E., & Bishop, M. D. (2014). Chronic stress, cortisol dysfunction, and pain: a psychoneuroendocrine rationale for stress management in pain rehabilitation. *Physical therapy*, *94*(12), 1816-1825.

Hargreaves, K., Dubner, R., Brown, F., Flores, C., & Joris, J. (1988). A new and sensitive method for measuring thermal nociception in cutaneous hyperalgesia. *Pain*, *32*(1), 77-88. https://doi.org/10.1016/0304-3959(88)90026-7

Haroun, R., Wood, J. N., & Sikandar, S. (2022). Mechanisms of cancer pain. *Front Pain Res (Lausanne)*, *3*, 1030899. https://doi.org/10.3389/fpain.2022.1030899

Hasegawa, H., Abbott, S., Han, B.-X., Qi, Y., & Wang, F. (2007). Analyzing Somatosensory Axon Projections with the Sensory Neuron-Specific Advillin Gene. *The Journal of Neuroscience*, *27*(52), 14404. https://doi.org/10.1523/JNEUROSCI.4908-07.2007

Hastie, E., & Samulski, R. J. (2015). Adeno-associated virus at 50: a golden anniversary of discovery, research, and gene therapy success--a personal perspective. *Hum Gene Ther*, *26*(5), 257-265. https://doi.org/10.1089/hum.2015.025

Hatakeyama, S., Wakamori, M., Ino, M., Miyamoto, N., Takahashi, E., Yoshinaga, T., . . . Yoshizawa, T. (2001). Differential nociceptive responses in mice lacking the α1B subunit of N-type Ca2+ channels. *Neuroreport*, *12*(11), 2423-2427.

Hauge, E. M., Qvesel, D., Eriksen, E. F., Mosekilde, L., & Melsen, F. (2001). Cancellous bone remodeling occurs in specialized compartments lined by cells expressing osteoblastic markers. *J Bone Miner Res*, *16*(9), 1575-1582. https://doi.org/10.1359/jbmr.2001.16.9.1575

Hebben, M. (2018). Downstream bioprocessing of AAV vectors: Industrial challenges & regulatory requirements. *Cell Gene Ther. Insights*, *4*, 131-146.

Henry, J. L., Lalloo, C., & Yashpal, K. (2008). Central poststroke pain: an abstruse outcome. *Pain Res Manag*, *13*(1), 41-49. https://doi.org/10.1155/2008/754260

Hepp, R., Perraut, M., Chasserot-Golaz, S., Galli, T., Aunis, D., Langley, K., & Grant, N. J. (1999). Cultured glial cells express the SNAP-25 analogue SNAP-23. *Glia*, *27*(2), 181-187. https://doi.org/10.1002/(sici)1098-1136(199908)27:2<181::aid-glia8>3.0.co;2-9

Hernandez Bort, J. A. (2019). Challenges in the downstream process of gene therapy products. *Am Pharm Rev*, *22*(4), 25.

Hernandez, R. K., Wade, S. W., Reich, A., Pirolli, M., Liede, A., & Lyman, G. H. (2018). Incidence of bone metastases in patients with solid tumors: analysis of oncology electronic medical records in the United States. *BMC Cancer*, *18*(1), 44. https://doi.org/10.1186/s12885-017-3922-0

Hille, B. (1992). *Ionic channels of excitable membranes* (Vol. 21). Springer.

Hockley, J. R., Boundouki, G., Cibert-Goton, V., McGuire, C., Yip, P. K., Chan, C., . . . Bulmer, D. C. (2014). Multiple roles for NaV1.9 in the activation of visceral afferents by noxious inflammatory, mechanical, and human disease-derived stimuli. *Pain*, *155*(10), 1962-1975. https://doi.org/10.1016/j.pain.2014.06.015

Hodgkin, A. L., & Huxley, A. F. (1939). Action potentials recorded from inside a nerve fibre. *Nature*, *144*(3651), 710-711.

Hodgkin, A. L., & Huxley, A. F. (1952). A quantitative description of membrane current and its application to conduction and excitation in nerve. *The Journal of physiology*, *117*(4), 500.

Holden, J. E., Schwartz, E. J., & Proudfit, H. K. (1999). Microinjection of morphine in the A7 catecholamine cell group produces opposing effects on nociception that are mediated by alpha1- and alpha2-adrenoceptors. *Neuroscience*, *91*(3), 979-990. https://doi.org/10.1016/s0306-4522(98)00673-3

Hong, S., Morrow, T. J., Paulson, P. E., Isom, L. L., & Wiley, J. W. (2004). Early Painful Diabetic Neuropathy Is Associated with Differential Changes in Tetrodotoxin-sensitive and -resistant Sodium Channels in Dorsal Root Ganglion Neurons in the Rat *. *Journal of Biological Chemistry*, *279*(28), 29341-29350. https://doi.org/10.1074/jbc.M404167200

Horlbeck, M. A., Gilbert, L. A., Villalta, J. E., Adamson, B., Pak, R. A., Chen, Y., . . . Weissman, J. S. (2016). Compact and highly active next-generation libraries for CRISPR-mediated gene repression and activation. *eLife*, *5*, e19760. https://doi.org/10.7554/eLife.19760

Hsiao, E. C., Boudignon, B. M., Chang, W. C., Bencsik, M., Peng, J., Nguyen, T. D., . . . Nissenson, R. A. (2008). Osteoblast expression of an engineered Gs-coupled receptor dramatically increases bone mass. *Proceedings of the National Academy of Sciences*, *105*(4), 1209-1214. https://doi.org/10.1073/pnas.0707457105

Hsieh, M. T., Donaldson, L. F., & Lumb, B. M. (2015). Differential contributions of A- and C-nociceptors to primary and secondary inflammatory hypersensitivity in the rat. *Pain*, *156*(6), 1074-1083. https://doi.org/10.1097/j.pain.0000000000000151

Hua, T., Chen, B., Lu, D., Sakurai, K., Zhao, S., Han, B.-X., . . . Wang, F. (2020). General anesthetics activate a potent central pain-suppression circuit in the amygdala. *Nature Neuroscience*, *23*(7), 854-868. https://doi.org/10.1038/s41593-020-0632-8

Huang, J., Yang, Y., Dib-Hajj, S. D., van Es, M., Zhao, P., Salomon, J., . . . Waxman, S. G. (2014). Depolarized inactivation overcomes impaired activation to produce DRG neuron hyperexcitability in a Nav1.7 mutation in a patient with distal limb pain. *J Neurosci*, *34*(37), 12328-12340. https://doi.org/10.1523/jneurosci.2773-14.2014

Huang, J., Yang, Y., Zhao, P., Gerrits, M. M., Hoeijmakers, J. G., Bekelaar, K., . . . Waxman, S. G. (2013). Small-fiber neuropathy Nav1.8 mutation shifts activation to hyperpolarized potentials and increases excitability of dorsal root ganglion neurons. *J Neurosci*, *33*(35), 14087-14097. https://doi.org/10.1523/jneurosci.2710-13.2013

Hughes, S. W., Hickey, L., Hulse, R. P., Lumb, B. M., & Pickering, A. E. (2013). Endogenous analgesic action of the pontospinal noradrenergic system spatially restricts and temporally delays the progression of neuropathic pain following tibial nerve injury. *Pain*, *154*(9), 1680-1690. https://doi.org/10.1016/j.pain.2013.05.010

Hull, D. L. (1965). The effect of essentialism on taxonomy—two thousand years of stasis (I). *The British Journal for the Philosophy of Science*, *15*(60), 314-326.

Ibrahim, T., Flamini, E., Mercatali, L., Sacanna, E., Serra, P., & Amadori, D. (2010). Erratum: Pathogenesis of osteoblastic bone metastases from prostate cancer [https://doi.org/10.1002/cncr.25132]. *Cancer*, *116*(10), 2503-2503. https://doi.org/https://doi.org/10.1002/cncr.25132

Ikeda, R., Cha, M., Ling, J., Jia, Z., Coyle, D., & Gu, Jianguo G. (2014). Merkel Cells Transduce and Encode Tactile Stimuli to Drive Aβ-Afferent Impulses. *Cell*, *157*(3), 664-675. https://doi.org/https://doi.org/10.1016/j.cell.2014.02.026

Ikeda, R., & Gu, J. G. (2014). Piezo2 channel conductance and localization domains in Merkel cells of rat whisker hair follicles. *Neuroscience Letters*, *583*, 210-215. https://doi.org/https://doi.org/10.1016/j.neulet.2014.05.055

Ikeuchi, M., Kolker, S. J., & Sluka, K. A. (2009). Acid-sensing ion channel 3 expression in mouse knee joint afferents and effects of carrageenan-induced arthritis. *The journal of pain*, *10*(3), 336-342.

Indo, Y., Tsuruta, M., Hayashida, Y., Karim, M. A., Ohta, K., Kawano, T., . . . Matsuda, I. (1996). Mutations in the TRKA/NGF receptor gene in patients with congenital insensitivity to pain with anhidrosis. *Nature Genetics*, *13*(4), 485-488. https://doi.org/10.1038/ng0896-485

Inman, V. T., & deC. M. Saunders, J. B. (1944). REFERRED PAIN FROM SKELETAL STRUCTURES. *The Journal of Nervous and Mental Disease*, *99*(5).
Inoue, A., Ikoma, K., Morioka, N., Kumagai, K., Hashimoto, T., Hide, I., & Nakata, Y. (1999). Interleukin-1beta induces substance P release from primary afferent neurons through the cyclooxygenase-2 system. *J Neurochem*, *73*(5), 2206-2213.
International Pain Summit Of The International Association For The Study Of Pain. (2011). Declaration of Montréal: declaration that access to pain management is a fundamental human right. *J Pain Palliat Care Pharmacother*, *25*(1), 29-31. https://doi.org/10.3109/15360288.2010.547560
Isensee, J., Krahé, L., Moeller, K., Pereira, V., Sexton, J. E., Sun, X., . . . Hucho, T. (2017). Synergistic regulation of serotonin and opioid signaling contributes to pain insensitivity in Nav1.7 knockout mice. *Sci Signal*, *10*(461). https://doi.org/10.1126/scisignal.aah4874
Ishino, Y., Krupovic, M., & Forterre, P. (2018). History of CRISPR-Cas from Encounter with a Mysterious Repeated Sequence to Genome Editing Technology. *J Bacteriol*, *200*(7). https://doi.org/10.1128/jb.00580-17
Ivanova, A., Signore, M., Caro, N., Greene, N. D. E., Copp, A. J., & Martinez-Barbera, J. P. (2005). In vivo genetic ablation by Cre-mediated expression of diphtheria toxin fragment A. *genesis*, *43*(3), 129-135.
Jacus, M. O., Uebele, V. N., Renger, J. J., & Todorovic, S. M. (2012). Presynaptic Cav3. 2 channels regulate excitatory neurotransmission in nociceptive dorsal horn neurons. *Journal of Neuroscience*, *32*(27), 9374-9382.
Jaggi, A. S., Jain, V., & Singh, N. (2011). Animal models of neuropathic pain. *Fundamental & clinical pharmacology*, *25*(1), 1-28.
Jann, M. W., Lam, Y. W., & Chang, W. H. (1994). Rapid formation of clozapine in guinea-pigs and man following clozapine-N-oxide administration. *Archives internationales de pharmacodynamie et de therapie*, *328*(2), 243-250.
Jarvis, M. F., Scott, V. E., McGaraughty, S., Chu, K. L., Xu, J., Niforatos, W., . . . Xia, Z. (2014). A peripherally acting, selective T-type calcium channel blocker, ABT-639, effectively reduces nociceptive and neuropathic pain in rats. *Biochemical pharmacology*, *89*(4), 536-544.
Jean-Xavier, C., Pflieger, J. F., Liabeuf, S., & Vinay, L. (2006). Inhibitory postsynaptic potentials in lumbar motoneurons remain depolarizing after neonatal spinal cord transection in the rat. *J Neurophysiol*, *96*(5), 2274-2281. https://doi.org/10.1152/jn.00328.2006
Jensen, T. S., & Finnerup, N. B. (2014). Allodynia and hyperalgesia in neuropathic pain: clinical manifestations and mechanisms. *The Lancet Neurology*, *13*(9), 924-935.
Ji, R. R., Samad, T. A., Jin, S. X., Schmoll, R., & Woolf, C. J. (2002). p38 MAPK activation by NGF in primary sensory neurons after inflammation increases TRPV1 levels and maintains heat hyperalgesia. *Neuron*, *36*(1), 57-68. https://doi.org/10.1016/s0896-6273(02)00908-x
Jiang, H., Couto, L. B., Patarroyo-White, S., Liu, T., Nagy, D., Vargas, J. A., . . . Pierce, G. F. (2006). Effects of transient immunosuppression on adenoassociated, virus-mediated, liver-directed gene transfer in rhesus macaques and implications for human gene therapy. *Blood*, *108*(10), 3321-3328. https://doi.org/10.1182/blood-2006-04-017913
Jimenez-Andrade, J. M., Ghilardi, J. R., Castaneda-Corral, G., Kuskowski, M. A., & Mantyh, P. W. (2011). Preventive or late administration of anti-NGF therapy attenuates tumor-induced nerve sprouting, neuroma formation and cancer pain. *Pain*, *152*(11), 2564-2574. https://doi.org/10.1016/j.pain.2011.07.020
Jimi, E., Nakamura, I., Ikebe, T., Akiyama, S., Takahashi, N., & Suda, T. (1998). Activation of NF-kappaB is involved in the survival of osteoclasts promoted by interleukin-1. *J Biol Chem*, *273*(15), 8799-8805. https://doi.org/10.1074/jbc.273.15.8799
Jin, X., & Gereau, R. W. t. (2006). Acute p38-mediated modulation of tetrodotoxin-resistant sodium channels in mouse sensory neurons by tumor necrosis factor-alpha. *The Journal of neuroscience : the official journal of the Society for Neuroscience*, *26*(1), 246-255. https://doi.org/10.1523/JNEUROSCI.3858-05.2006
Jinek, M., Chylinski, K., Fonfara, I., Hauer, M., Doudna, J. A., & Charpentier, E. (2012). A programmable dual-RNA-guided DNA endonuclease in adaptive bacterial immunity. *Science*, *337*(6096), 816-821. https://doi.org/10.1126/science.1225829
Kaan, T. K. Y., Yip, P. K., Patel, S., Davies, M., Marchand, F., Cockayne, D. A., . . . McMahon, S. B. (2010). Systemic blockade of P2X3 and P2X2/3 receptors attenuates bone cancer pain behaviour in rats. *Brain*, *133*(9), 2549-2564. https://doi.org/10.1093/brain/awq194

Kaila, K., Price, T. J., Payne, J. A., Puskarjov, M., & Voipio, J. (2014). Cation-chloride cotransporters in neuronal development, plasticity and disease. *Nat Rev Neurosci*, *15*(10), 637-654. https://doi.org/10.1038/nrn3819
Kalva, S., Boeke, J. D., & Mita, P. (2018). Gibson Deletion: a novel application of isothermal in vitro recombination. *Biol Proced Online*, *20*, 2. https://doi.org/10.1186/s12575-018-0068-7
Kamioka, H., Honjo, T., & Takano-Yamamoto, T. (2001). A three-dimensional distribution of osteocyte processes revealed by the combination of confocal laser scanning microscopy and differential interference contrast microscopy. *Bone*, *28*(2), 145-149. https://doi.org/10.1016/s8756-3282(00)00421-x
Karashima, Y., Talavera, K., Everaerts, W., Janssens, A., Kwan, K. Y., Vennekens, R., . . . Voets, T. (2009). TRPA1 acts as a cold sensor in vitro and in vivo. *Proceedings of the National Academy of Sciences*, *106*(4), 1273-1278.
Karsenty, G., & Ferron, M. (2012). The contribution of bone to whole-organism physiology. *Nature*, *481*(7381), 314-320. https://doi.org/10.1038/nature10763
Kawabata, A. (2011). Prostaglandin E2 and pain--an update. *Biol Pharm Bull*, *34*(8), 1170-1173. https://doi.org/10.1248/bpb.34.1170
Kawasaki, Y., Xu, Z. Z., Wang, X., Park, J. Y., Zhuang, Z. Y., Tan, P. H., . . . Ji, R. R. (2008). Distinct roles of matrix metalloproteases in the early- and late-phase development of neuropathic pain. *Nat Med*, *14*(3), 331-336. https://doi.org/10.1038/nm1723
Kemp, T., Spike, R. C., Watt, C., & Todd, A. J. (1996). The mu-opioid receptor (MOR1) is mainly restricted to neurons that do not contain GABA or glycine in the superficial dorsal horn of the rat spinal cord. *Neuroscience*, *75*(4), 1231-1238. https://doi.org/10.1016/0306-4522(96)00333-8
Kerchner, G. A., Wilding, T. J., Li, P., Zhuo, M., & Huettner, J. E. (2001). Presynaptic kainate receptors regulate spinal sensory transmission. *J Neurosci*, *21*(1), 59-66. https://doi.org/10.1523/jneurosci.21-01-00059.2001
KG, H., K, K., MA, S., TH, L., JE, S., JR, G., . . . PW, M. (2005). A Blocking Antibody to Nerve Growth Factor Attenuates Skeletal Pain Induced by Prostate Tumor Cells Growing in Bone. *Cancer research*, *65*(20). https://doi.org/10.1158/0008-5472.CAN-05-0826
Khera, T., & Rangasamy, V. (2021). Cognition and Pain: A Review [Review]. *Frontiers in Psychology*, *12*.
Khodorova, A., Montmayeur, J. P., & Strichartz, G. (2009). Endothelin receptors and pain. *J Pain*, *10*(1), 4-28. https://doi.org/10.1016/j.jpain.2008.09.009
Khodorova, A., Navarro, B., Jouaville, L. S., Murphy, J. E., Rice, F. L., Mazurkiewicz, J. E., . . . Davar, G. (2003). Endothelin-B receptor activation triggers an endogenous analgesic cascade at sites of peripheral injury. *Nat Med*, *9*(8), 1055-1061. https://doi.org/10.1038/nm885
Kim, A. Y., Tang, Z., Liu, Q., Patel, K. N., Maag, D., Geng, Y., & Dong, X. (2008). Pirt, a phosphoinositide-binding protein, functions as a regulatory subunit of TRPV1. *Cell*, *133*(3), 475-485. https://doi.org/10.1016/j.cell.2008.02.053
Kim, Yu S., Chu, Y., Han, L., Li, M., Li, Z., LaVinka, Pamela C., . . . Dong, X. (2014). Central Terminal Sensitization of TRPV1 by Descending Serotonergic Facilitation Modulates Chronic Pain. *Neuron*, *81*(4), 873-887. https://doi.org/https://doi.org/10.1016/j.neuron.2013.12.011
Kitagawa, K., Uekusa, S., Matsuo, K., Moriyama, K., Yamamoto, T., Yada, Y., . . . Yoshio, T. (2021). Risk factors for clozapine-induced central nervous system abnormalities in Japanese patients with treatment-resistant schizophrenia. *Asian J Psychiatr*, *60*, 102652. https://doi.org/10.1016/j.ajp.2021.102652
Klinger-Gratz, P. P., Ralvenius, W. T., Neumann, E., Kato, A., Nyilas, R., Lele, Z., . . . Zeilhofer, H. U. (2018). Acetaminophen relieves inflammatory pain through CB1 cannabinoid receptors in the rostral ventromedial medulla. *Journal of Neuroscience*, *38*(2), 322-334.
Kong, D., Tong, Q., Ye, C., Koda, S., Fuller, P. M., Krashes, M. J., . . . Lowell, B. B. (2012). GABAergic RIP-Cre neurons in the arcuate nucleus selectively regulate energy expenditure. *Cell*, *151*(3), 645-657. https://doi.org/10.1016/j.cell.2012.09.020
Konietzny, F., Perl, E. R., Trevino, D., Light, A., & Hensel, H. (1981). Sensory experiences in man evoked by intraneural electrical stimulation of intact cutaneous afferent fibers. *Experimental Brain Research*, *42*(2), 219-222.
Koonin, E. V., Makarova, K. S., & Zhang, F. (2017). Diversity, classification and evolution of CRISPR-Cas systems. *Curr Opin Microbiol*, *37*, 67-78. https://doi.org/10.1016/j.mib.2017.05.008

Koyama, Y., Mizobata, T., Yamamoto, N., Hashimoto, H., Matsuda, T., & Baba, A. (1999). Endothelins stimulate expression of cyclooxygenase 2 in rat cultured astrocytes. *J Neurochem*, *73*(3), 1004-1011. https://doi.org/10.1046/j.1471-4159.1999.0731004.x

Kramer, K. M., Brock, J. A., Bloom, K., Moore, J. K., & Haber, J. E. (1994). Two different types of double-strand breaks in Saccharomyces cerevisiae are repaired by similar RAD52-independent, nonhomologous recombination events. *Molecular and Cellular Biology*, *14*(2), 1293-1301. https://doi.org/10.1128/mcb.14.2.1293-1301.1994

Kretschmer, T., Happel, L. T., England, J. D., Nguyen, D. H., Tiel, R. L., Beuerman, R. W., & Kline, D. G. (2002). Clinical Article Accumulation of PN1 and PN3 Sodium Channels in Painful Human Neuroma-Evidence from Immunocytochemistry. *Acta Neurochirurgica*, *144*(8), 803-810. https://doi.org/10.1007/s00701-002-0970-1

Krishtal, O. A., & Pidoplichko, V. I. (1981). A 'receptor'for protons in small neurons of trigeminal ganglia: possible role in nociception. *Neuroscience letters*, *24*(3), 243-246.

Kristiansen, K., Kroeze, W. K., Willins, D. L., Gelber, E. I., Savage, J. E., Glennon, R. A., & Roth, B. L. (2000). A Highly Conserved Aspartic Acid (Asp-155) Anchors the Terminal Amine Moiety of Tryptamines and Is Involved in Membrane Targeting of the 5-HT_{2A} Serotonin Receptor But Does Not Participate in Activation via a "Salt-Bridge Disruption" Mechanism. *Journal of Pharmacology and Experimental Therapeutics*, *293*(3), 735.

Kucharczyk, M. W., Chisholm, K. I., Denk, F., Dickenson, A. H., Bannister, K., & McMahon, S. B. (2020). The impact of bone cancer on the peripheral encoding of mechanical pressure stimuli. *PAIN*, *161*(8).

Kyranou, M., & Puntillo, K. (2012). The transition from acute to chronic pain: might intensive care unit patients be at risk? *Annals of Intensive Care*, *2*(1), 36. https://doi.org/10.1186/2110-5820-2-36

Labuz, D., Celik, M. Ö., Zimmer, A., & Machelska, H. (2016). Distinct roles of exogenous opioid agonists and endogenous opioid peptides in the peripheral control of neuropathy-triggered heat pain. *Scientific Reports*, *6*(1), 32799. https://doi.org/10.1038/srep32799

Laedermann, C. J., Abriel, H., & Decosterd, I. (2015). Post-translational modifications of voltage-gated sodium channels in chronic pain syndromes [Review]. *Frontiers in Pharmacology*, *6*.

Lagerström, M. C., Rogoz, K., Abrahamsen, B., Lind, A.-L., Ölund, C., Smith, C., . . . Kullander, K. (2011). A sensory subpopulation depends on vesicular glutamate transporter 2 for mechanical pain, and together with substance P, inflammatory pain. *Proceedings of the National Academy of Sciences*, *108*(14), 5789-5794.

Lamont, L. A., Tranquilli, W. J., & Grimm, K. A. (2000). Physiology of pain. *Veterinary Clinics: Small Animal Practice*, *30*(4), 703-728.

Langdahl, B., Ferrari, S., & Dempster, D. W. (2016). Bone modeling and remodeling: potential as therapeutic targets for the treatment of osteoporosis. In *Ther Adv Musculoskelet Dis* (Vol. 8, pp. 225-235). https://doi.org/10.1177/1759720x16670154

Langford, D. J., Bailey, A. L., Chanda, M. L., Clarke, S. E., Drummond, T. E., Echols, S., . . . LaCroix-Fralish, M. L. (2010). Coding of facial expressions of pain in the laboratory mouse. *Nature methods*, *7*(6), 447-449.

Lawson, S. N., Crepps, B., & Perl, E. R. (2002). Calcitonin gene-related peptide immunoreactivity and afferent receptive properties of dorsal root ganglion neurones in guinea-pigs. *The Journal of physiology*, *540*(3), 989-1002.

Lawson, S. N., Fang, X., & Djouhri, L. (2019). Nociceptor subtypes and their incidence in rat lumbar dorsal root ganglia (DRGs): focussing on C-polymodal nociceptors, Aβ-nociceptors, moderate pressure receptors and their receptive field depths. *Current opinion in physiology*, *11*, 125-146.

Lawson, S. N., McCarthy, P. W., & Prabhakar, E. (1996). Electrophysiological properties of neurones with CGRP-like immunoreactivity in rat dorsal root ganglia. *Journal of Comparative Neurology*, *365*(3), 355-366.

Lawson, S. N., & Waddell, P. J. (1991). Soma neurofilament immunoreactivity is related to cell size and fibre conduction velocity in rat primary sensory neurons. *The Journal of physiology*, *435*(1), 41-63.

Le Bars, D., Dickenson, A. H., & Besson, J. M. (1979). Diffuse noxious inhibitory controls (DNIC). II. Lack of effect on non-convergent neurones, supraspinal involvement and theoretical implications. *Pain*, *6*(3), 305-327. https://doi.org/10.1016/0304-3959(79)90050-2

Le Pichon, C. E., & Chesler, A. T. (2014). The functional and anatomical dissection of somatosensory subpopulations using mouse genetics. *Front Neuroanat*, *8*, 21. https://doi.org/10.3389/fnana.2014.00021
Ledford, H. (2020). CRISPR gene editing in human embryos wreaks chromosomal mayhem. In *Nature* (Vol. 583, pp. 17-18). https://doi.org/10.1038/d41586-020-01906-4
Lee, C., Lavoie, A., Liu, J., Chen, S. X., & Liu, B. H. (2020). Light Up the Brain: The Application of Optogenetics in Cell-Type Specific Dissection of Mouse Brain Circuits. *Front Neural Circuits*, *14*, 18. https://doi.org/10.3389/fncir.2020.00018
Lee, J. W., Siegel, S. M., & Oaklander, A. L. (2009). Effects of distal nerve injuries on dorsal-horn neurons and glia: relationships between lesion size and mechanical hyperalgesia. *Neuroscience*, *158*(2), 904-914. https://doi.org/10.1016/j.neuroscience.2008.10.010
Lee, K., & Boden, P. R. (1997). Characterization of the inward current induced by metabotropic glutamate receptor stimulation in rat ventromedial hypothalamic neurones. *J Physiol*, *504 (Pt 3)*(Pt 3), 649-663. https://doi.org/10.1111/j.1469-7793.1997.649bd.x
Leffler, A., Cummins, T. R., Dib-Hajj, S. D., Hormuzdiar, W. N., Black, J. A., & Waxman, S. G. (2002). GDNF and NGF reverse changes in repriming of TTX-sensitive Na(+) currents following axotomy of dorsal root ganglion neurons. *J Neurophysiol*, *88*(2), 650-658. https://doi.org/10.1152/jn.2002.88.2.650
Leffler, A., Mönter, B., & Koltzenburg, M. (2006). The role of the capsaicin receptor TRPV1 and acid-sensing ion channels (ASICS) in proton sensitivity of subpopulations of primary nociceptive neurons in rats and mice. *Neuroscience*, *139*(2), 699-709.
Leipold, E., Liebmann, L., Korenke, G. C., Heinrich, T., Gießelmann, S., Baets, J., . . . Hennings, J. C. (2013). A de novo gain-of-function mutation in SCN11A causes loss of pain perception. *Nature genetics*, *45*(11), 1399-1404.
Leite-Almeida, H., Valle-Fernandes, A., & Almeida, A. (2006). Brain projections from the medullary dorsal reticular nucleus: an anterograde and retrograde tracing study in the rat. *Neuroscience*, *140*(2), 577-595. https://doi.org/10.1016/j.neuroscience.2006.02.022
Levina, N., Tötemeyer, S., Stokes, N. R., Louis, P., Jones, M. A., & Booth, I. R. (1999). Protection of Escherichia coli cells against extreme turgor by activation of MscS and MscL mechanosensitive channels: identification of genes required for MscS activity. *Embo j*, *18*(7), 1730-1737. https://doi.org/10.1093/emboj/18.7.1730
Levine, D. N. (2007). Sherrington's "The Integrative action of the nervous system": a centennial appraisal. *J Neurol Sci*, *253*(1-2), 1-6. https://doi.org/10.1016/j.jns.2006.12.002
Levine, J., Gordon, N., & Fields, H. (1978). The mechanism of placebo analgesia. *The Lancet*, *312*(8091), 654-657.
Lewis, T., & Pochin, E. E. (1937). The double pain response of the human skin to a single stimulus. *Clin Sci*, *3*(67-76), 50.
Li, C., Sugam, J. A., Lowery-Gionta, E. G., McElligott, Z. A., McCall, N. M., Lopez, A. J., . . . Kash, T. L. (2016). Mu Opioid Receptor Modulation of Dopamine Neurons in the Periaqueductal Gray/Dorsal Raphe: A Role in Regulation of Pain. *Neuropsychopharmacology*, *41*(8), 2122-2132. https://doi.org/10.1038/npp.2016.12
Li, C., Wang, S., Chen, Y., & Zhang, X. (2018). Somatosensory neuron typing with high-coverage single-cell RNA sequencing and functional analysis. *Neuroscience bulletin*, *34*(1), 200-207.
Li, C.-L., Li, K.-C., Wu, D., Chen, Y., Luo, H., Zhao, J.-R., . . . Zhong, Y.-Q. (2016). Somatosensory neuron types identified by high-coverage single-cell RNA-sequencing and functional heterogeneity. *Cell research*, *26*(1), 83-102.
Li, L., Rutlin, M., Abraira, V. E., Cassidy, C., Kus, L., Gong, S., . . . Koerber, H. R. (2011). The functional organization of cutaneous low-threshold mechanosensory neurons. *Cell*, *147*(7), 1615-1627.
Li, P., Slimko, E. M., & Lester, H. A. (2002). Selective elimination of glutamate activation and introduction of fluorescent proteins into a Caenorhabditis elegans chloride channel. *FEBS Lett*, *528*(1-3), 77-82. https://doi.org/10.1016/s0014-5793(02)03245-3
Li, X., Zhao, X., Fang, Y., Jiang, X., Duong, T., Fan, C., . . . Kain, S. R. (1998). Generation of destabilized green fluorescent protein as a transcription reporter. *J Biol Chem*, *273*(52), 34970-34975. https://doi.org/10.1074/jbc.273.52.34970
Liberti, M. V., & Locasale, J. W. (2016). The Warburg Effect: How Does it Benefit Cancer Cells? *Trends Biochem Sci*, *41*(3), 211-218. https://doi.org/10.1016/j.tibs.2015.12.001
Lima, D., Albino-Teixeira, A., & Tavares, I. (2002). The caudal medullary ventrolateral reticular formation in nociceptive-cardiovascular integration. An experimental study in the rat. *Exp Physiol*, *87*(2), 267-274. https://doi.org/10.1113/eph8702354

Limberis, M. P., Vandenberghe, L. H., Zhang, L., Pickles, R. J., & Wilson, J. M. (2009). Transduction efficiencies of novel AAV vectors in mouse airway epithelium in vivo and human ciliated airway epithelium in vitro. *Mol Ther*, *17*(2), 294-301. https://doi.org/10.1038/mt.2008.261

Lino, C. A., Harper, J. C., Carney, J. P., & Timlin, J. A. (2018). Delivering CRISPR: a review of the challenges and approaches. *Drug Deliv*, *25*(1), 1234-1257. https://doi.org/10.1080/10717544.2018.1474964

Liu, X., Chung, K., & Chung, J. M. (1999). Ectopic discharges and adrenergic sensitivity of sensory neurons after spinal nerve injury. *Brain Res*, *849*(1-2), 244-247. https://doi.org/10.1016/s0006-8993(99)02165-4

Liu, X. D., Yang, J. J., Fang, D., Cai, J., Wan, Y., & Xing, G. G. (2014). Functional upregulation of nav1.8 sodium channels on the membrane of dorsal root Ganglia neurons contributes to the development of cancer-induced bone pain. *PLoS One*, *9*(12), e114623. https://doi.org/10.1371/journal.pone.0114623

Livak, K. J., & Schmittgen, T. D. (2001). Analysis of Relative Gene Expression Data Using Real-Time Quantitative PCR and the 2−ΔΔCT Method. *Methods*, *25*(4), 402-408. https://doi.org/https://doi.org/10.1006/meth.2001.1262

Loeser, J. D., & Treede, R. D. (2008). The Kyoto protocol of IASP Basic Pain Terminology. *Pain*, *137*(3), 473-477. https://doi.org/10.1016/j.pain.2008.04.025

Loyd, D. R., & Murphy, A. Z. (2009). The role of the periaqueductal gray in the modulation of pain in males and females: are the anatomy and physiology really that different? *Neural Plast*, *2009*, 462879. https://doi.org/10.1155/2009/462879

Lu, W., Dean-Clower, E., Doherty-Gilman, A., & Rosenthal, D. S. (2008). The value of acupuncture in cancer care. *Hematol Oncol Clin North Am*, *22*(4), 631-648, viii. https://doi.org/10.1016/j.hoc.2008.04.005

Lubejko, S. T., Graham, R. D., Livrizzi, G., Schaefer, R., Banghart, M. R., & Creed, M. C. (2022). The role of endogenous opioid neuropeptides in neurostimulation-driven analgesia. *Front Syst Neurosci*, *16*, 1044686. https://doi.org/10.3389/fnsys.2022.1044686

Lucas, O., Hilaire, C., Delpire, E., & Scamps, F. (2012). KCC3-dependent chloride extrusion in adult sensory neurons. *Mol Cell Neurosci*, *50*(3-4), 211-220. https://doi.org/10.1016/j.mcn.2012.05.005

Luyten, T., Welkenhuyzen, K., Roest, G., Kania, E., Wang, L., Bittremieux, M., . . . Bultynck, G. (2017). Resveratrol-induced autophagy is dependent on IP3Rs and on cytosolic Ca2+. *Biochimica et Biophysica Acta (BBA) - Molecular Cell Research*, *1864*(6), 947-956. https://doi.org/https://doi.org/10.1016/j.bbamcr.2017.02.013

Lyapustina, T., & Alexander, G. C. (2015). The prescription opioid addiction and abuse epidemic: how it happened and what we can do about it. *The Pharmaceutical Journal*, *294*(7865), 3-4.

MacDonald, D. I., Luiz, A. P., Iseppon, F., Millet, Q., Emery, E. C., & Wood, J. N. (2021). Silent cold-sensing neurons contribute to cold allodynia in neuropathic pain. *Brain*, *144*(6), 1711-1726. https://doi.org/10.1093/brain/awab086

MacDonald, D. I., Sikandar, S., Weiss, J., Pyrski, M., Luiz, A. P., Millet, Q., . . . Wood, J. N. (2021). A central mechanism of analgesia in mice and humans lacking the sodium channel Na(V)1.7. *Neuron*, *109*(9), 1497-1512.e1496. https://doi.org/10.1016/j.neuron.2021.03.012

Macdonald, R. L., & Botzolakis, E. J. (2010). Chapter 14 - GABAA Receptor Channels. In F. J. Alvarez-Leefmans & E. Delpire (Eds.), *Physiology and Pathology of Chloride Transporters and Channels in the Nervous System* (pp. 257-282). Academic Press. https://doi.org/https://doi.org/10.1016/B978-0-12-374373-2.00014-5

Macfarlane, G. J., Norrie, G., Atherton, K., Power, C., & Jones, G. T. (2009). The influence of socioeconomic status on the reporting of regional and widespread musculoskeletal pain: results from the 1958 British Birth Cohort Study. *Annals of the rheumatic diseases*, *68*(10), 1591-1595.

Madariaga-Mazón, A., Marmolejo-Valencia, A. F., Li, Y., Toll, L., Houghten, R. A., & Martinez-Mayorga, K. (2017). Mu-Opioid receptor biased ligands: A safer and painless discovery of analgesics? *Drug discovery today*, *22*(11), 1719-1729.

Madrid, R., De La Peña, E., Donovan-Rodriguez, T., Belmonte, C., & Viana, F. (2009). Variable threshold of trigeminal cold-thermosensitive neurons is determined by a balance between TRPM8 and Kv1 potassium channels. *Journal of Neuroscience*, *29*(10), 3120-3131.

Magnus, C. J., Lee, P. H., Atasoy, D., Su, H. H., Looger, L. L., & Sternson, S. M. (2011). Chemical and Genetic Engineering of Selective Ion Channel–Ligand Interactions. *Science*, *333*(6047), 1292-1296. https://doi.org/10.1126/science.1206606

Magnus, C. J., Lee, P. H., Bonaventura, J., Zemla, R., Gomez, J. L., Ramirez, M. H., . . . Sternson, S. M. (2019). Ultrapotent chemogenetics for research and potential clinical applications. *Science*, *364*(6436), eaav5282. https://doi.org/10.1126/science.aav5282

Maiarù, M., Leese, C., Certo, M., Echeverria-Altuna, I., Mangione, A. S., Arsenault, J., . . . Hunt, S. P. (2018). Selective neuronal silencing using synthetic botulinum molecules alleviates chronic pain in mice. *Science Translational Medicine*, *10*(450), eaar7384. https://doi.org/10.1126/scitranslmed.aar7384

Makarova, K. S., Wolf, Y. I., Alkhnbashi, O. S., Costa, F., Shah, S. A., Saunders, S. J., . . . Koonin, E. V. (2015). An updated evolutionary classification of CRISPR-Cas systems. In *Nat Rev Microbiol* (Vol. 13, pp. 722-736). https://doi.org/10.1038/nrmicro3569

Manole, A., Mannikko, R., Hanna, M. G., Kullmann, D. M., & Houlden, H. (2017). De novo KCNA2 mutations cause hereditary spastic paraplegia. *Annals of Neurology*, *81*(2), 326-328.

Mantyh, P. (2013). Bone cancer pain: causes, consequences, and therapeutic opportunities. *Pain*, *154 Suppl 1*, S54-s62. https://doi.org/10.1016/j.pain.2013.07.044

Mantyh, P. W., Clohisy, D. R., Koltzenburg, M., & Hunt, S. P. (2002). Molecular mechanisms of cancer pain. *Nature Reviews Cancer*, *2*(3), 201-209.

Mantyh, W. G., Jimenez-Andrade, J. M., Stake, J. I., Bloom, A. P., Kaczmarska, M. J., Taylor, R. N., . . . Mantyh, P. W. (2010). Blockade of nerve sprouting and neuroma formation markedly attenuates the development of late stage cancer pain. *Neuroscience*, *171*(2), 588-598. https://doi.org/10.1016/j.neuroscience.2010.08.056

Mao, S., Garzon-Muvdi, T., Di Fulvio, M., Chen, Y., Delpire, E., Alvarez, F. J., & Alvarez-Leefmans, F. J. (2012). Molecular and functional expression of cation-chloride cotransporters in dorsal root ganglion neurons during postnatal maturation. *J Neurophysiol*, *108*(3), 834-852. https://doi.org/10.1152/jn.00970.2011

Maquat, L. E., Kinniburgh, A. J., Rachmilewitz, E. A., & Ross, J. (1981). Unstable beta-globin mRNA in mRNA-deficient beta o thalassemia. *Cell*, *27*(3 Pt 2), 543-553. https://doi.org/10.1016/0092-8674(81)90396-2

Marcum, Z. A., & Hanlon, J. T. (2010). Recognizing the Risks of Chronic Nonsteroidal Anti-Inflammatory Drug Use in Older Adults. *Ann Longterm Care*, *18*(9), 24-27.

Margolin, J. F., Friedman, J. R., Meyer, W. K., Vissing, H., Thiesen, H. J., & Rauscher, F. J. (1994). Krüppel-associated boxes are potent transcriptional repression domains. *Proceedings of the National Academy of Sciences*, *91*(10), 4509-4513. https://doi.org/10.1073/pnas.91.10.4509

Marmigère, F., & Ernfors, P. (2007). Specification and connectivity of neuronal subtypes in the sensory lineage. *Nature Reviews Neuroscience*, *8*(2), 114-127. https://doi.org/10.1038/nrn2057

Martin, L. J., Acland, E. L., Cho, C., Gandhi, W., Chen, D., Corley, E., . . . Tohyama, S. (2019). Male-specific conditioned pain hypersensitivity in mice and humans. *Current Biology*, *29*(2), 192-201.

Mastakov, M. Y., Baer, K., Xu, R., Fitzsimons, H., & During, M. J. (2001). Combined Injection of rAAV with Mannitol Enhances Gene Expression in the Rat Brain. *Molecular Therapy*, *3*(2), 225-232. https://doi.org/https://doi.org/10.1006/mthe.2001.0246

Mattia, C., Savoia, G., Paoletti, F., Piazza, O., Albanese, D., Amantea, B., . . . Tufano, R. (2006). SIAARTI recommendations for analgo-sedation in intensive care unit. *Minerva Anestesiol*, *72*(10), 769-805.

Maurizi, A., & Rucci, N. (2018). The Osteoclast in Bone Metastasis: Player and Target. *Cancers*, *10*(7). https://doi.org/10.3390/cancers10070218

Mayer, D. K., Travers, D., Wyss, A., Leak, A., & Waller, A. (2011). Why do patients with cancer visit emergency departments? Results of a 2008 population study in North Carolina. *J Clin Oncol*, *29*(19), 2683-2688. https://doi.org/10.1200/jco.2010.34.2816

Mays, L. E., Wang, L., Lin, J., Bell, P., Crawford, A., Wherry, E. J., & Wilson, J. M. (2014). AAV8 induces tolerance in murine muscle as a result of poor APC transduction, T cell exhaustion, and minimal MHCI upregulation on target cells. *Mol Ther*, *22*(1), 28-41. https://doi.org/10.1038/mt.2013.134

Mays, L. E., & Wilson, J. M. (2011). The complex and evolving story of T cell activation to AAV vector-encoded transgene products. *Mol Ther*, *19*(1), 16-27. https://doi.org/10.1038/mt.2010.250

Mazzuca, M., Heurteaux, C., Alloui, A., Diochot, S., Baron, A., Voilley, N., . . . Cupo, A. (2007). A tarantula peptide against pain via ASIC1a channels and opioid mechanisms. *Nature neuroscience*, *10*(8), 943-945.
McCaffrey, G., Thompson, M. L., Majuta, L., Fealk, M. N., Chartier, S., Longo, G., & Mantyh, P. W. (2014). NGF blockade at early times during bone cancer development attenuates bone destruction and increases limb use. *Cancer Res*, *74*(23), 7014-7023. https://doi.org/10.1158/0008-5472.can-14-1220
McCarty, D. M. (2008). Self-complementary AAV vectors; advances and applications. *Mol Ther*, *16*(10), 1648-1656. https://doi.org/10.1038/mt.2008.171
McCarty, D. M., Monahan, P. E., & Samulski, R. J. (2001). Self-complementary recombinant adeno-associated virus (scAAV) vectors promote efficient transduction independently of DNA synthesis. *Gene Ther*, *8*(16), 1248-1254. https://doi.org/10.1038/sj.gt.3301514
McDonnell, A., Collins, S., Ali, Z., Iavarone, L., Surujbally, R., Kirby, S., & Butt, R. P. (2018). Efficacy of the Nav1.7 blocker PF-05089771 in a randomised, placebo-controlled, double-blind clinical study in subjects with painful diabetic peripheral neuropathy. *Pain*, *159*(8), 1465-1476. https://doi.org/10.1097/j.pain.0000000000001227
McEntire, D. M., Kirkpatrick, D. R., Dueck, N. P., Kerfeld, M. J., Smith, T. A., Nelson, T. J., . . . Agrawal, D. K. (2016). Pain transduction: a pharmacologic perspective. *Expert Rev Clin Pharmacol*, *9*(8), 1069-1080. https://doi.org/10.1080/17512433.2016.1183481
McIntosh, J. H., Cochrane, M., Cobbold, S., Waldmann, H., Nathwani, S. A., Davidoff, A. M., & Nathwani, A. C. (2012). Successful attenuation of humoral immunity to viral capsid and transgenic protein following AAV-mediated gene transfer with a non-depleting CD4 antibody and cyclosporine. *Gene Ther*, *19*(1), 78-85. https://doi.org/10.1038/gt.2011.64
McKay, B. E., McRory, J. E., Molineux, M. L., Hamid, J., Snutch, T. P., Zamponi, G. W., & Turner, R. W. (2006). CaV3 T-type calcium channel isoforms differentially distribute to somatic and dendritic compartments in rat central neurons. *European Journal of Neuroscience*, *24*(9), 2581-2594.
McKellar, Q. A., Midgley, D. M., Galbraith, E. A., Scott, E. W., & Bradley, A. (1992). Clinical and pharmacological properties of ivermectin in rabbits and guinea pigs. *Vet Rec*, *130*(4), 71-73. https://doi.org/10.1136/vr.130.4.71
Meents, J. E., Bressan, E., Sontag, S., Foerster, A., Hautvast, P., Rösseler, C., . . . Le, T. K. C. (2019). The role of Nav1. 7 in human nociceptors: insights from human induced pluripotent stem cell–derived sensory neurons of erythromelalgia patients. *Pain*, *160*(6), 1327.
Melzack, R., & Wall, P. D. (1965). Pain Mechanisms: A New Theory: A gate control system modulates sensory input from the skin before it evokes pain perception and response. *Science*, *150*(3699), 971-979.
Mendell, L. M. (1966). Physiological properties of unmyelinated fiber projection to the spinal cord. *Exp Neurol*, *16*(3), 316-332. https://doi.org/10.1016/0014-4886(66)90068-9
Mercadante, S., & Fulfaro, F. (2007). Management of painful bone metastases. *Curr Opin Oncol*, *19*(4), 308-314. https://doi.org/10.1097/CCO.0b013e3281214400
Merkel, S. F., Andrews, A. M., Lutton, E. M., Mu, D., Hudry, E., Hyman, B. T., . . . Ramirez, S. H. (2017). Trafficking of adeno-associated virus vectors across a model of the blood-brain barrier; a comparative study of transcytosis and transduction using primary human brain endothelial cells. *J Neurochem*, *140*(2), 216-230. https://doi.org/10.1111/jnc.13861
Metzger, D., & Feil, R. (1999). Engineering the mouse genome by site-specific recombination. *Current opinion in biotechnology*, *10*(5), 470-476.
Miao, X.-R., Gao, X.-F., Wu, J.-X., Lu, Z.-J., Huang, Z.-X., Li, X.-Q., . . . Yu, W.-F. (2010). Bilateral downregulation of Nav1.8 in dorsal root ganglia of rats with bone cancer pain induced by inoculation with Walker 256 breast tumor cells. *BMC Cancer*, *10*(1), 216. https://doi.org/10.1186/1471-2407-10-216
Michael, C. L., Laura, Z., David, K. M., & Irene, T. (2008). Identifying Brain Activity Specifically Related to the Maintenance and Perceptual Consequence of Central Sensitization in Humans. *The Journal of Neuroscience*, *28*(45), 11642. https://doi.org/10.1523/JNEUROSCI.2638-08.2008
Mijovic, A., & MacCabe, J. H. (2020). Clozapine-induced agranulocytosis. *Ann Hematol*, *99*(11), 2477-2482. https://doi.org/10.1007/s00277-020-04215-y
Millan, M. J. (2002). Descending control of pain. *Prog Neurobiol*, *66*(6), 355-474. https://doi.org/10.1016/s0301-0082(02)00009-6
Minett, M. S., Falk, S., Santana-Varela, S., Bogdanov, Y. D., Nassar, M. A., Heegaard, A. M., & Wood, J. N. (2014). Pain without nociceptors? Nav1.7-independent pain mechanisms. *Cell Rep*, *6*(2), 301-312. https://doi.org/10.1016/j.celrep.2013.12.033

Minett, M. S., Nassar, M. A., Clark, A. K., Passmore, G., Dickenson, A. H., Wang, F., . . . Wood, J. N. (2012). Distinct Nav1.7-dependent pain sensations require different sets of sensory and sympathetic neurons. *Nat Commun*, *3*, 791. https://doi.org/10.1038/ncomms1795

Minett, M. S., Pereira, V., Sikandar, S., Matsuyama, A., Lolignier, S., Kanellopoulos, A. H., . . . Wood, J. N. (2015). Endogenous opioids contribute to insensitivity to pain in humans and mice lacking sodium channel Nav1.7. *Nature Communications*, *6*(1), 8967. https://doi.org/10.1038/ncomms9967

Mishra, S., Bhatnagar, S., Goyal, G. N., Rana, S. P., & Upadhya, S. P. (2012). A comparative efficacy of amitriptyline, gabapentin, and pregabalin in neuropathic cancer pain: a prospective randomized double-blind placebo-controlled study. *Am J Hosp Palliat Care*, *29*(3), 177-182. https://doi.org/10.1177/1049909111412539

Miyazaki, T., Katagiri, H., Kanegae, Y., Takayanagi, H., Sawada, Y., Yamamoto, A., . . . Tanaka, S. (2000). Reciprocal role of ERK and NF-kappaB pathways in survival and activation of osteoclasts. *J Cell Biol*, *148*(2), 333-342. https://doi.org/10.1083/jcb.148.2.333

Mizusaki, B. E. P., & O'Donnell, C. (2021). Neural circuit function redundancy in brain disorders. *Current Opinion in Neurobiology*, *70*, 74-80. https://doi.org/https://doi.org/10.1016/j.conb.2021.07.008

Moayedi, M., & Davis, K. D. (2013). Theories of pain: from specificity to gate control. *J Neurophysiol*, *109*(1), 5-12. https://doi.org/10.1152/jn.00457.2012

Mohammed, Z. A., Doran, C., Grundy, D., & Nassar, M. A. (2017). Veratridine produces distinct calcium response profiles in mouse Dorsal Root Ganglia neurons. *Scientific Reports*, *7*(1), 45221. https://doi.org/10.1038/srep45221

Mohan, A., Fitzsimmons, B., Zhao, H. T., Jiang, Y., Mazur, C., Swayze, E. E., & Kordasiewicz, H. B. (2018). Antisense oligonucleotides selectively suppress target RNA in nociceptive neurons of the pain system and can ameliorate mechanical pain. *Pain*, *159*(1), 139-149. https://doi.org/10.1097/j.pain.0000000000001074

Molliver, D. C., Immke, D. C., Fierro, L., Paré, M., Rice, F. L., & McCleskey, E. W. (2005). ASIC3, an acid-sensing ion channel, is expressed in metaboreceptive sensory neurons. *Molecular pain*, *1*(1), 1-13.

Montal, M. (2010). Botulinum neurotoxin: a marvel of protein design. *Annu Rev Biochem*, *79*, 591-617. https://doi.org/10.1146/annurev.biochem.051908.125345

Morales-Aza, B. M., Chillingworth, N. L., Payne, J. A., & Donaldson, L. F. (2004). Inflammation alters cation chloride cotransporter expression in sensory neurons. *Neurobiol Dis*, *17*(1), 62-69. https://doi.org/10.1016/j.nbd.2004.05.010

Moreno, A. M., Alemán, F., Catroli, G. F., Hunt, M., Hu, M., Dailamy, A., . . . Mali, P. (2021). Long-lasting analgesia via targeted in situ repression of NaV1.7 in mice. *Science translational medicine*, *13*(584), eaay9056. https://doi.org/10.1126/scitranslmed.aay9056

Morgan, J. I., & Curran, T. (1989). Stimulus-transcription coupling in neurons: role of cellular immediate-early genes. *Trends Neurosci*, *12*(11), 459-462. https://doi.org/10.1016/0166-2236(89)90096-9

Muldoon, L. L., Nilaver, G., Kroll, R. A., Pagel, M. A., Breakefield, X. O., Chiocca, E. A., . . . Neuwelt, E. A. (1995). Comparison of intracerebral inoculation and osmotic blood-brain barrier disruption for delivery of adenovirus, herpesvirus, and iron oxide particles to normal rat brain. *Am J Pathol*, *147*(6), 1840-1851.

Mullard, A. (2022). Vertex's Na(V)1.8 inhibitor passes phase II pain point. In *Nat Rev Drug Discov* (Vol. 21, pp. 327). https://doi.org/10.1038/d41573-022-00070-w

Murphy, K. E., Shylo, N. A., Alexander, K. A., Churchill, A. J., Copperman, C., & García-García, M. J. (2016). The Transcriptional Repressive Activity of KRAB Zinc Finger Proteins Does Not Correlate with Their Ability to Recruit TRIM28. *PLOS ONE*, *11*(9), e0163555. https://doi.org/10.1371/journal.pone.0163555

Murthy, S. E., Loud, M. C., Daou, I., Marshall, K. L., Schwaller, F., Kühnemund, J., . . . Lewin, G. R. (2018). The mechanosensitive ion channel Piezo2 mediates sensitivity to mechanical pain in mice. *Science translational medicine*, *10*(462), eaat9897.

Muto, Y., Sakai, A., Sakamoto, A., & Suzuki, H. (2012). Activation of NK1 receptors in the locus coeruleus induces analgesia through noradrenergic-mediated descending inhibition in a rat model of neuropathic pain. *Br J Pharmacol*, *166*(3), 1047-1057. https://doi.org/10.1111/j.1476-5381.2011.01820.x

Mäkinen, P. I., Koponen, J. K., Kärkkäinen, A. M., Malm, T. M., Pulkkinen, K. H., Koistinaho, J., . . . Ylä-Herttuala, S. (2006). Stable RNA interference: comparison of U6 and H1

promoters in endothelial cells and in mouse brain. *J Gene Med*, *8*(4), 433-441. https://doi.org/10.1002/jgm.860
Nafe, J. P. (1929). A Quantitative Theory of Feeling. *The Journal of General Psychology*, *2*(2-3), 199-211. https://doi.org/10.1080/00221309.1929.9918059
Nagae, M., Hiraga, T., & Yoneda, T. (2007). Acidic microenvironment created by osteoclasts causes bone pain associated with tumor colonization. *J Bone Miner Metab*, *25*(2), 99-104. https://doi.org/10.1007/s00774-006-0734-8
Narahashi, T., Moore, J. W., & Scott, W. R. (1964). Tetrodotoxin blockage of sodium conductance increase in lobster giant axons. *The Journal of general physiology*, *47*(5), 965-974.
Naso, M. F., Tomkowicz, B., Perry, W. L., 3rd, & Strohl, W. R. (2017). Adeno-Associated Virus (AAV) as a Vector for Gene Therapy. *BioDrugs*, *31*(4), 317-334. https://doi.org/10.1007/s40259-017-0234-5
Nassar, M. A., Stirling, L. C., Forlani, G., Baker, M. D., Matthews, E. A., Dickenson, A. H., & Wood, J. N. (2004). Nociceptor-specific gene deletion reveals a major role for Nav1.7 (PN1) in acute and inflammatory pain. *Proc Natl Acad Sci U S A*, *101*(34), 12706-12711. https://doi.org/10.1073/pnas.0404915101
Nassar, M. A., Stirling, L. C., Forlani, G., Baker, M. D., Matthews, E. A., Dickenson, A. H., & Wood, J. N. (2004). Nociceptor-specific gene deletion reveals a major role for Nav1. 7 (PN1) in acute and inflammatory pain. *Proceedings of the National Academy of Sciences*, *101*(34), 12706-12711.
Naumer, M., Sonntag, F., Schmidt, K., Nieto, K., Panke, C., Davey, N. E., . . . Kleinschmidt, J. A. (2012). Properties of the adeno-associated virus assembly-activating protein. *J Virol*, *86*(23), 13038-13048. https://doi.org/10.1128/jvi.01675-12
Neher, E., & Sakmann, B. (1976). Single-channel currents recorded from membrane of denervated frog muscle fibres. *Nature*, *260*(5554), 799-802.
Nencini, S., & Ivanusic, J. (2017). Mechanically sensitive Aδ nociceptors that innervate bone marrow respond to changes in intra-osseous pressure. *J Physiol*, *595*(13), 4399-4415. https://doi.org/10.1113/jp273877
Nencini, S., Ringuet, M., Kim, D.-H., Chen, Y.-J., Greenhill, C., & Ivanusic, J. J. (2017). Mechanisms of nerve growth factor signaling in bone nociceptors and in an animal model of inflammatory bone pain. *Molecular Pain*, *13*, 1744806917697011. https://doi.org/10.1177/1744806917697011
Neumann, S., Doubell, T. P., Leslie, T., & Woolf, C. J. (1996). Inflammatory pain hypersensitivity mediated by phenotypic switch in myelinated primary sensory neurons. *Nature*, *384*(6607), 360-364. https://doi.org/10.1038/384360a0
NIDA. (2023). *Drug Overdose Death Rates*. https://nida.nih.gov/research-topics/trends-statistics/overdose-death-rates
Nie, L., Das Thakur, M., Wang, Y., Su, Q., Zhao, Y., & Feng, Y. (2010). Regulation of U6 promoter activity by transcriptional interference in viral vector-based RNAi. *Genomics Proteomics Bioinformatics*, *8*(3), 170-179. https://doi.org/10.1016/s1672-0229(10)60019-8
Nieuwenhuis, S., Forstmann, B. U., & Wagenmakers, E.-J. (2011). Erroneous analyses of interactions in neuroscience: a problem of significance. *Nature neuroscience*, *14*(9), 1105-1107.
Niggli, E., & Lederer, W. J. (1993). Activation of Na-Ca exchange current by photolysis of "caged calcium". *Biophys J*, *65*(2), 882-891. https://doi.org/10.1016/s0006-3495(93)81105-6
Nishimura, I., Uetsuki, T., Dani, S. U., Ohsawa, Y., Saito, I., Okamura, H., . . . Yoshikawa, K. (1998). Degeneration In Vivo of Rat Hippocampal Neurons by Wild-Type Alzheimer Amyloid Precursor Protein Overexpressed by Adenovirus-Mediated Gene Transfer. *The Journal of Neuroscience*, *18*(7), 2387. https://doi.org/10.1523/JNEUROSCI.18-07-02387.1998
Noël, J., Zimmermann, K., Busserolles, J., Deval, E., Alloui, A., Diochot, S., . . . Eschalier, A. (2009). The mechano-activated K+ channels TRAAK and TREK-1 control both warm and cold perception. *The EMBO journal*, *28*(9), 1308-1318.
Nuñez, J. K., Chen, J., Pommier, G. C., Cogan, J. Z., Replogle, J. M., Adriaens, C., . . . Weissman, J. S. (2021). Genome-wide programmable transcriptional memory by CRISPR-based epigenome editing. *Cell*, *184*(9), 2503-2519.e2517. https://doi.org/10.1016/j.cell.2021.03.025
Ochs, S. (2004). *A History of Nerve Functions: From Animal Spirits to Molecular Mechanisms*. Cambridge University Press. https://doi.org/DOI: 10.1017/CBO9780511546358

Okada-Ogawa, A., Porreca, F., & Meng, I. D. (2009). Sustained morphine-induced sensitization and loss of diffuse noxious inhibitory controls in dura-sensitive medullary dorsal horn neurons. *J Neurosci*, *29*(50), 15828-15835. https://doi.org/10.1523/jneurosci.3623-09.2009

Olson, W., Abdus-Saboor, I., Cui, L., Burdge, J., Raabe, T., Ma, M., & Luo, W. (2017). Sparse genetic tracing reveals regionally specific functional organization of mammalian nociceptors. *Elife*, *6*, e29507.

Ong, S. T., Li, F., Du, J., Tan, Y. W., & Wang, S. (2005). Hybrid cytomegalovirus enhancer-h1 promoter-based plasmid and baculovirus vectors mediate effective RNA interference. *Hum Gene Ther*, *16*(12), 1404-1412. https://doi.org/10.1089/hum.2005.16.1404

Oprée, A., & Kress, M. (2000). Involvement of the proinflammatory cytokines tumor necrosis factor-alpha, IL-1 beta, and IL-6 but not IL-8 in the development of heat hyperalgesia: effects on heat-evoked calcitonin gene-related peptide release from rat skin. *J Neurosci*, *20*(16), 6289-6293. https://doi.org/10.1523/jneurosci.20-16-06289.2000

Ossipov, M. H., Morimura, K., & Porreca, F. (2014). Descending pain modulation and chronification of pain. *Curr Opin Support Palliat Care*, *8*(2), 143-151. https://doi.org/10.1097/spc.0000000000000055

Paget, S. (1989). The distribution of secondary growths in cancer of the breast. 1889. *Cancer Metastasis Rev*, *8*(2), 98-101.

Pan, J., Lin, X. J., Ling, Z. H., & Cai, Y. Z. (2015). Effect of down-regulation of voltage-gated sodium channel Nav1.7 on activation of astrocytes and microglia in DRG in rats with cancer pain. *Asian Pac J Trop Med*, *8*(5), 405-411. https://doi.org/10.1016/s1995-7645(14)60352-7

Pancer, Z., & Cooper, M. D. (2006). THE EVOLUTION OF ADAPTIVE IMMUNITY. *Annual Review of Immunology*, *24*(1), 497-518. https://doi.org/10.1146/annurev.immunol.24.021605.090542

Parikh, V., Kozak, R., Martinez, V., & Sarter, M. (2007). Prefrontal acetylcholine release controls cue detection on multiple timescales. *Neuron*, *56*(1), 141-154. https://doi.org/10.1016/j.neuron.2007.08.025

Paulus, W., & Rothwell, J. C. (2016). Membrane resistance and shunting inhibition: where biophysics meets state-dependent human neurophysiology. *J Physiol*, *594*(10), 2719-2728. https://doi.org/10.1113/jp271452

Perl, E. R. (2007). Ideas about pain, a historical view. *Nat Rev Neurosci*, *8*(1), 71-80. https://doi.org/10.1038/nrn2042

Peters, C. M., Ghilardi, J. R., Keyser, C. P., Kubota, K., Lindsay, T. H., Luger, N. M., . . . Mantyh, P. W. (2005). Tumor-induced injury of primary afferent sensory nerve fibers in bone cancer pain. *Experimental Neurology*, *193*(1), 85-100. https://doi.org/https://doi.org/10.1016/j.expneurol.2004.11.028

Pfeffer, C. K., Stein, V., Keating, D. J., Maier, H., Rinke, I., Rudhard, Y., . . . Hübner, C. A. (2009). NKCC1-Dependent GABAergic Excitation Drives Synaptic Network Maturation during Early Hippocampal Development. *The Journal of Neuroscience*, *29*(11), 3419. https://doi.org/10.1523/JNEUROSCI.1377-08.2009

Pien, G. C., Basner-Tschakarjan, E., Hui, D. J., Mentlik, A. N., Finn, J. D., Hasbrouck, N. C., . . . High, K. A. (2009). Capsid antigen presentation flags human hepatocytes for destruction after transduction by adeno-associated viral vectors. *The Journal of Clinical Investigation*, *119*(6), 1688-1695. https://doi.org/10.1172/JCI36891

Pitcher, T., Sousa-Valente, J., & Malcangio, M. (2016). The monoiodoacetate model of osteoarthritis pain in the mouse. *JoVE (Journal of Visualized Experiments)*(111), e53746.

Plant, T. D., Zöllner, C., Kepura, F., Mousa, S. S., Eichhorst, J., Schaefer, M., . . . Oksche, A. (2007). Endothelin potentiates TRPV1 via ETA receptor-mediated activation of protein kinase C. *Mol Pain*, *3*, 35. https://doi.org/10.1186/1744-8069-3-35

Pogorzala, L. A., Mishra, S. K., & Hoon, M. A. (2013). The cellular code for mammalian thermosensation. *Journal of Neuroscience*, *33*(13), 5533-5541.

Polgár, E., Hughes, D. I., Arham, A. Z., & Todd, A. J. (2005). Loss of neurons from laminas I-III of the spinal dorsal horn is not required for development of tactile allodynia in the spared nerve injury model of neuropathic pain. *J Neurosci*, *25*(28), 6658-6666. https://doi.org/10.1523/jneurosci.1490-05.2005

Pomonis, J. D., Rogers, S. D., Peters, C. M., Ghilardi, J. R., & Mantyh, P. W. (2001). Expression and localization of endothelin receptors: implications for the involvement of peripheral glia in nociception. *J Neurosci*, *21*(3), 999-1006. https://doi.org/10.1523/jneurosci.21-03-00999.2001

Pope, J. E., Deer, T. R., Bruel, B. M., & Falowski, S. (2016). Clinical Uses of Intrathecal Therapy and Its Placement in the Pain Care Algorithm. *Pain Pract*, *16*(8), 1092-1106. https://doi.org/10.1111/papr.12438
Porreca, F., Burgess, S. E., Gardell, L. R., Vanderah, T. W., Malan, T. P., Jr., Ossipov, M. H., . . . Lai, J. (2001). Inhibition of neuropathic pain by selective ablation of brainstem medullary cells expressing the mu-opioid receptor. *J Neurosci*, *21*(14), 5281-5288. https://doi.org/10.1523/jneurosci.21-14-05281.2001
Porreca, F., Ossipov, M. H., & Gebhart, G. F. (2002). Chronic pain and medullary descending facilitation. *Trends Neurosci*, *25*(6), 319-325. https://doi.org/10.1016/s0166-2236(02)02157-4
Powell, S. K., Rivera-Soto, R., & Gray, S. J. (2015). Viral expression cassette elements to enhance transgene target specificity and expression in gene therapy. *Discov Med*, *19*(102), 49-57.
Price, T. J., Cervero, F., Gold, M. S., Hammond, D. L., & Prescott, S. A. (2009). Chloride regulation in the pain pathway. *Brain Res Rev*, *60*(1), 149-170. https://doi.org/10.1016/j.brainresrev.2008.12.015
Priest, B. T., Murphy, B. A., Lindia, J. A., Diaz, C., Abbadie, C., Ritter, A. M., . . . Martin, W. J. (2005). Contribution of the tetrodotoxin-resistant voltage-gated sodium channel NaV1.9 to sensory transmission and nociceptive behavior. *Proc Natl Acad Sci U S A*, *102*(26), 9382-9387. https://doi.org/10.1073/pnas.0501549102
Puchałowicz, K., Tarnowski, M., Baranowska-Bosiacka, I., Chlubek, D., & Dziedziejko, V. (2014). P2X and P2Y receptors—role in the pathophysiology of the nervous system. *Int J Mol Sci*, *15*(12), 23672-23704. https://doi.org/10.3390/ijms151223672
Pérez de Vega, M. J., Gómez-Monterrey, I., Ferrer-Montiel, A., & González-Muñiz, R. (2016). Transient Receptor Potential Melastatin 8 Channel (TRPM8) Modulation: Cool Entryway for Treating Pain and Cancer. *J Med Chem*, *59*(22), 10006-10029. https://doi.org/10.1021/acs.jmedchem.6b00305
Qi, L. S., Larson, M. H., Gilbert, L. A., Doudna, J. A., Weissman, J. S., Arkin, A. P., & Lim, W. A. (2013). Repurposing CRISPR as an RNA-guided platform for sequence-specific control of gene expression. *Cell*, *152*(5), 1173-1183. https://doi.org/10.1016/j.cell.2013.02.022
Qin, W., Li, Y., Liu, B., Liu, Y., Zhang, Y., Zhang, X., . . . Fan, B. (2020). Intrathecal morphine infusion therapy via a percutaneous port for refractory cancer pain in china: an efficacy, safety and cost utilization analysis. *Journal of Pain Research*, *13*, 231.
Qiu, F., Jiang, Y., Zhang, H., Liu, Y., & Mi, W. (2012). Increased expression of tetrodotoxin-resistant sodium channels Nav1.8 and Nav1.9 within dorsal root ganglia in a rat model of bone cancer pain. *Neurosci Lett*, *512*(2), 61-66. https://doi.org/10.1016/j.neulet.2012.01.069
Quenneville, S., Turelli, P., Bojkowska, K., Raclot, C., Offner, S., Kapopoulou, A., & Trono, D. (2012). The KRAB-ZFP/KAP1 system contributes to the early embryonic establishment of site-specific DNA methylation patterns maintained during development. *Cell Rep*, *2*(4), 766-773. https://doi.org/10.1016/j.celrep.2012.08.043
Raja, S. N., Carr, D. B., Cohen, M., Finnerup, N. B., Flor, H., Gibson, S., . . . Vader, K. (2020). The revised International Association for the Study of Pain definition of pain: concepts, challenges, and compromises. *Pain*, *161*(9), 1976-1982. https://doi.org/10.1097/j.pain.0000000000001939
Ramin, R., Christian Martin, G., Floris, P. J. G. L., Huub de, V., Judith, P., Sabine, V., . . . Niels, E. (2021). Dorsal Root Ganglia Macrophages Maintain Osteoarthritis Pain. *The Journal of Neuroscience*, *41*(39), 8249. https://doi.org/10.1523/JNEUROSCI.1787-20.2021
Ranade, S. S., Woo, S.-H., Dubin, A. E., Moshourab, R. A., Wetzel, C., Petrus, M., . . . Patapoutian, A. (2014). Piezo2 is the major transducer of mechanical forces for touch sensation in mice. *Nature*, *516*(7529), 121-125. https://doi.org/10.1038/nature13980
Randall, L. O. (1957). A method for measurement of analgesic activity on inflamed tissues. *Arch Int Pharmacodyn.*, *111*, 409-419.
Rapti, K., Louis-Jeune, V., Kohlbrenner, E., Ishikawa, K., Ladage, D., Zolotukhin, S., . . . Weber, T. (2012). Neutralizing antibodies against AAV serotypes 1, 2, 6, and 9 in sera of commonly used animal models. *Mol Ther*, *20*(1), 73-83. https://doi.org/10.1038/mt.2011.177
Ren, K., & Dubner, R. (2002). Descending modulation in persistent pain: an update. *Pain*, *100*(1-2), 1-6. https://doi.org/10.1016/s0304-3959(02)00368-8
Ren, K., & Torres, R. (2009). Role of interleukin-1beta during pain and inflammation. *Brain Res Rev*, *60*(1), 57-64. https://doi.org/10.1016/j.brainresrev.2008.12.020

Renganathan, M., Cummins, T. R., & Waxman, S. G. (2001). Contribution of Na(v)1.8 sodium channels to action potential electrogenesis in DRG neurons. *J Neurophysiol*, *86*(2), 629-640. https://doi.org/10.1152/jn.2001.86.2.629
Reuben, S. S., & Buvanendran, A. (2007). Preventing the development of chronic pain after orthopaedic surgery with preventive multimodal analgesic techniques. *JBJS*, *89*(6), 1343-1358.
Ried, M. U., Girod, A., Leike, K., Büning, H., & Hallek, M. (2002). Adeno-associated virus capsids displaying immunoglobulin-binding domains permit antibody-mediated vector retargeting to specific cell surface receptors. *J Virol*, *76*(9), 4559-4566. https://doi.org/10.1128/jvi.76.9.4559-4566.2002
Rigaud, M., Gemes, G., Barabas, M.-E., Chernoff, D. I., Abram, S. E., Stucky, C. L., & Hogan, Q. H. (2008). Species and strain differences in rodent sciatic nerve anatomy: Implications for studies of neuropathic pain. *PAIN*, *136*(1), 188-201. https://doi.org/https://doi.org/10.1016/j.pain.2008.01.016
Rodriguez, E., Sakurai, K., Xu, J., Chen, Y., Toda, K., Zhao, S., . . . Liedtke, W. (2017). A craniofacial-specific monosynaptic circuit enables heightened affective pain. *Nature neuroscience*, *20*(12), 1734-1743.
Romas, E., Gillespie, M. T., & Martin, T. J. (2002). Involvement of receptor activator of NFkappaB ligand and tumor necrosis factor-alpha in bone destruction in rheumatoid arthritis. *Bone*, *30*(2), 340-346. https://doi.org/10.1016/s8756-3282(01)00682-2
Roodman, G. D. (2004). Mechanisms of Bone Metastasis. *New England Journal of Medicine*, *350*(16), 1655-1664. https://doi.org/10.1056/NEJMra030831
Rose, J. A., Hoggan, M. D., & Shatkin, A. J. (1966). Nucleic acid from an adeno-associated virus: chemical and physical studies. *Proc Natl Acad Sci U S A*, *56*(1), 86-92. https://doi.org/10.1073/pnas.56.1.86
Roth, B. L. (2016). DREADDs for Neuroscientists. *Neuron*, *89*(4), 683-694. https://doi.org/10.1016/j.neuron.2016.01.040
Roza, C., Laird, J. M., Souslova, V., Wood, J. N., & Cervero, F. (2003). The tetrodotoxin-resistant Na+ channel Nav1.8 is essential for the expression of spontaneous activity in damaged sensory axons of mice. *J Physiol*, *550*(Pt 3), 921-926. https://doi.org/10.1113/jphysiol.2003.046110
Rucci, N. (2008). Molecular biology of bone remodelling. *Clin Cases Miner Bone Metab*, *5*(1), 49-56.
Rush, A. M., & Waxman, S. G. (2004). PGE2 increases the tetrodotoxin-resistant Nav1.9 sodium current in mouse DRG neurons via G-proteins. *Brain Res*, *1023*(2), 264-271. https://doi.org/10.1016/j.brainres.2004.07.042
Sabino, M. A., Ghilardi, J. R., Jongen, J. L., Keyser, C. P., Luger, N. M., Mach, D. B., . . . Mantyh, P. W. (2002). Simultaneous reduction in cancer pain, bone destruction, and tumor growth by selective inhibition of cyclooxygenase-2. *Cancer Res*, *62*(24), 7343-7349.
Sachdev, M., Gaínza-Lein, M., Tchapyjnikov, D., Jiang, Y.-H., Loddenkemper, T., & Mikati, M. A. (2017). Novel clinical manifestations in patients with KCNA2 mutations. *Seizure*, *51*, 74-76.
Sachs, D., Villarreal, C. F., Cunha, F. Q., Parada, C. A., & Ferreira, S. H. (2009). The role of PKA and PKCε pathways in prostaglandin E2-mediated hypernociception [https://doi.org/10.1111/j.1476-5381.2008.00093.x]. *British Journal of Pharmacology*, *156*(5), 826-834. https://doi.org/https://doi.org/10.1111/j.1476-5381.2008.00093.x
Safieh-Garabedian, B., Poole, S., Allchorne, A., Winter, J., & Woolf, C. J. (1995). Contribution of interleukin-1 beta to the inflammation-induced increase in nerve growth factor levels and inflammatory hyperalgesia. *Br J Pharmacol*, *115*(7), 1265-1275. https://doi.org/10.1111/j.1476-5381.1995.tb15035.x
Sakurai, K., Zhao, S., Takatoh, J., Rodriguez, E., Lu, J., Leavitt, A. D., . . . Wang, F. (2016). Capturing and Manipulating Activated Neuronal Ensembles with CANE Delineates a Hypothalamic Social-Fear Circuit. *Neuron*, *92*(4), 739-753. https://doi.org/10.1016/j.neuron.2016.10.015
Samad, T. A., Moore, K. A., Sapirstein, A., Billet, S., Allchorne, A., Poole, S., . . . Woolf, C. J. (2001). Interleukin-1beta-mediated induction of Cox-2 in the CNS contributes to inflammatory pain hypersensitivity. *Nature*, *410*(6827), 471-475. https://doi.org/10.1038/35068566
Samineni, V. K., Mickle, A. D., Yoon, J., Grajales-Reyes, J. G., Pullen, M. Y., Crawford, K. E., . . . Lai, H. H. (2017). Optogenetic silencing of nociceptive primary afferents reduces evoked and ongoing bladder pain. *Scientific reports*, *7*(1), 1-14.

Samulski, R. J., & Muzyczka, N. (2014). AAV-Mediated Gene Therapy for Research and Therapeutic Purposes. *Annu Rev Virol*, *1*(1), 427-451. https://doi.org/10.1146/annurev-virology-031413-085355
Saragiotto, B. T., Machado, G. C., Ferreira, M. L., Pinheiro, M. B., Abdel Shaheed, C., & Maher, C. G. (2016). Paracetamol for low back pain. *Cochrane Database Syst Rev*, *2016*(6), Cd012230. https://doi.org/10.1002/14651858.cd012230
Sarchielli, P., Mancini, M. L., Floridi, A., Coppola, F., Rossi, C., Nardi, K., . . . Calabresi, P. (2007). Increased levels of neurotrophins are not specific for chronic migraine: evidence from primary fibromyalgia syndrome. *J Pain*, *8*(9), 737-745. https://doi.org/10.1016/j.jpain.2007.05.002
Sasaki, K., Suzuki, M., Mieda, M., Tsujino, N., Roth, B., & Sakurai, T. (2011). Pharmacogenetic Modulation of Orexin Neurons Alters Sleep/Wakefulness States in Mice. *PLOS ONE*, *6*(5), e20360. https://doi.org/10.1371/journal.pone.0020360
Sattler, R., & Tymianski, M. (2001). Molecular mechanisms of glutamate receptor-mediated excitotoxic neuronal cell death. *Mol Neurobiol*, *24*(1-3), 107-129. https://doi.org/10.1385/mn:24:1-3:107
Sayilekshmy, M., Hansen, R. B., Delaissé, J. M., Rolighed, L., Andersen, T. L., & Heegaard, A. M. (2019). Innervation is higher above Bone Remodeling Surfaces and in Cortical Pores in Human Bone: Lessons from patients with primary hyperparathyroidism. *Sci Rep*, *9*(1), 5361. https://doi.org/10.1038/s41598-019-41779-w
Schmidt, R., Schmelz, M., Forster, C., Ringkamp, M., Torebjörk, E., & Handwerker, H. (1995). Novel classes of responsive and unresponsive C nociceptors in human skin. *J Neurosci*, *15*(1 Pt 1), 333-341. https://doi.org/10.1523/jneurosci.15-01-00333.1995
Schmitges, F. W., Radovani, E., Najafabadi, H. S., Barazandeh, M., Campitelli, L. F., Yin, Y., . . . Hughes, T. R. (2016). Multiparameter functional diversity of human C2H2 zinc finger proteins. *Genome Res*, *26*(12), 1742-1752. https://doi.org/10.1101/gr.209643.116
Schubert, V., Bouvier, D., & Volterra, A. (2011). SNARE protein expression in synaptic terminals and astrocytes in the adult hippocampus: a comparative analysis. *Glia*, *59*(10), 1472-1488. https://doi.org/10.1002/glia.21190
Schwei, M. J., Honore, P., Rogers, S. D., Salak-Johnson, J. L., Finke, M. P., Ramnaraine, M. L., . . . Mantyh, P. W. (1999). Neurochemical and cellular reorganization of the spinal cord in a murine model of bone cancer pain. *J Neurosci*, *19*(24), 10886-10897. https://doi.org/10.1523/jneurosci.19-24-10886.1999
Schäfers, M., & Sorkin, L. (2008). Effect of cytokines on neuronal excitability. *Neurosci Lett*, *437*(3), 188-193. https://doi.org/10.1016/j.neulet.2008.03.052
Seifert, R., & Wenzel-Seifert, K. (2002). Constitutive activity of G-protein-coupled receptors: cause of disease and common property of wild-type receptors. *Naunyn Schmiedebergs Arch Pharmacol*, *366*(5), 381-416. https://doi.org/10.1007/s00210-002-0588-0
Selman, C., & Swindell, W. R. (2018). Putting a strain on diversity. *The EMBO journal*, *37*(22), e100862.
Sevcik, M. A., Ghilardi, J. R., Peters, C. M., Lindsay, T. H., Halvorson, K. G., Jonas, B. M., . . . Mantyh, P. W. (2005). Anti-NGF therapy profoundly reduces bone cancer pain and the accompanying increase in markers of peripheral and central sensitization. *PAIN*, *115*(1).
Sevcik, M. A., Jonas, B. M., Lindsay, T. H., Halvorson, K. G., Ghilardi, J. R., Kuskowski, M. A., . . . Mantyh, P. W. (2006). Endogenous opioids inhibit early-stage pancreatic pain in a mouse model of pancreatic cancer. *Gastroenterology*, *131*(3), 900-910. https://doi.org/10.1053/j.gastro.2006.06.021
Seymour, B. (2019). Pain: a precision signal for reinforcement learning and control. *Neuron*, *101*(6), 1029-1041.
Shen, S., Bryant, K. D., Brown, S. M., Randell, S. H., & Asokan, A. (2011). Terminal N-linked galactose is the primary receptor for adeno-associated virus 9. *J Biol Chem*, *286*(15), 13532-13540. https://doi.org/10.1074/jbc.M110.210922
Shields, S. D., Ahn, H. S., Yang, Y., Han, C., Seal, R. P., Wood, J. N., . . . Dib-Hajj, S. D. (2012). Nav1.8 expression is not restricted to nociceptors in mouse peripheral nervous system. *Pain*, *153*(10), 2017-2030. https://doi.org/10.1016/j.pain.2012.04.022
Shiers, S., Funk, G., Cervantes, A., Horton, P., Dussor, G., Hennen, S., & Price, T. J. (2023). Na (V) 1.7 mRNA and protein expression in putative projection neurons of the human spinal dorsal horn. *bioRxiv*. https://doi.org/10.1101/2023.02.04.527110
Shmakov, S., Smargon, A., Scott, D., Cox, D., Pyzocha, N., Yan, W., . . . Koonin, E. V. (2017). Diversity and evolution of class 2 CRISPR-Cas systems. *Nat Rev Microbiol*, *15*(3), 169-182. https://doi.org/10.1038/nrmicro.2016.184

Sikandar, S., Minett, M. S., Millet, Q., Santana-Varela, S., Lau, J., Wood, J. N., & Zhao, J. (2018). Brain-derived neurotrophic factor derived from sensory neurons plays a critical role in chronic pain. *Brain*, *141*(4), 1028-1039.
Simard, J. M., Tarasov, K. V., & Gerzanich, V. (2007). Non-selective cation channels, transient receptor potential channels and ischemic stroke. *Biochim Biophys Acta*, *1772*(8), 947-957. https://doi.org/10.1016/j.bbadis.2007.03.004
Singhmar, P., Huo, X., Eijkelkamp, N., Berciano, S. R., Baameur, F., Mei, F. C., . . . Kavelaars, A. (2016). Critical role for Epac1 in inflammatory pain controlled by GRK2-mediated phosphorylation of Epac1. *Proceedings of the National Academy of Sciences*, *113*(11), 3036-3041. https://doi.org/10.1073/pnas.1516036113
Slimko, E. M., McKinney, S., Anderson, D. J., Davidson, N., & Lester, H. A. (2002). Selective Electrical Silencing of Mammalian Neurons In Vitro by the Use of Invertebrate Ligand-Gated Chloride Channels. *The Journal of Neuroscience*, *22*(17), 7373. https://doi.org/10.1523/JNEUROSCI.22-17-07373.2002
Smith, E. M., Pang, H., Cirrincione, C., Fleishman, S., Paskett, E. D., Ahles, T., . . . Shapiro, C. L. (2013). Effect of duloxetine on pain, function, and quality of life among patients with chemotherapy-induced painful peripheral neuropathy: a randomized clinical trial. *Jama*, *309*(13), 1359-1367. https://doi.org/10.1001/jama.2013.2813
Smith, E. S., & Lewin, G. R. (2009). Nociceptors: a phylogenetic view. *J Comp Physiol A Neuroethol Sens Neural Behav Physiol*, *195*(12), 1089-1106. https://doi.org/10.1007/s00359-009-0482-z
Smith, E. S., Omerbašić, D., Lechner, S. G., Anirudhan, G., Lapatsina, L., & Lewin, G. R. (2011). The molecular basis of acid insensitivity in the African naked mole-rat. *Science*, *334*(6062), 1557-1560. https://doi.org/10.1126/science.1213760
Smith-Edwards, K. M., DeBerry, J. J., Saloman, J. L., Davis, B. M., & Woodbury, C. J. (2016). Profound alteration in cutaneous primary afferent activity produced by inflammatory mediators. *Elife*, *5*. https://doi.org/10.7554/eLife.20527
Snutch, T. P. (2005). Targeting chronic and neuropathic pain: the N-type calcium channel comes of age. *NeuroRx*, *2*(4), 662-670.
Sonoda, E., Hochegger, H., Saberi, A., Taniguchi, Y., & Takeda, S. (2006). Differential usage of non-homologous end-joining and homologous recombination in double strand break repair. *DNA Repair (Amst)*, *5*(9-10), 1021-1029. https://doi.org/10.1016/j.dnarep.2006.05.022
Sorge, R. E., Martin, L. J., Isbester, K. A., Sotocinal, S. G., Rosen, S., Tuttle, A. H., . . . Kadoura, B. (2014). Olfactory exposure to males, including men, causes stress and related analgesia in rodents. *Nature methods*, *11*(6), 629-632.
Spagnuolo, M., & Blenner, M. (2021). Gene Excision by Dual-Guide CRISPR-Cas9. In I. Wheeldon & M. Blenner (Eds.), *Yarrowia lipolytica: Methods and Protocols* (pp. 85-94). Springer US. https://doi.org/10.1007/978-1-0716-1414-3_5
Stamboulian, S., Choi, J. S., Ahn, H. S., Chang, Y. W., Tyrrell, L., Black, J. A., . . . Dib-Hajj, S. D. (2010). ERK1/2 mitogen-activated protein kinase phosphorylates sodium channel Na(v)1.7 and alters its gating properties. *J Neurosci*, *30*(5), 1637-1647. https://doi.org/10.1523/jneurosci.4872-09.2010
Stannard, C. D. (2018). Where now for opioids in chronic pain? *Drug Ther Bull*, *56*(10), 118-122. https://doi.org/10.1136/dtb.2018.10.000007
Sternson, S. M., & Roth, B. L. (2014). Chemogenetic tools to interrogate brain functions. *Annu Rev Neurosci*, *37*, 387-407. https://doi.org/10.1146/annurev-neuro-071013-014048
Stirling, L. C., Forlani, G., Baker, M. D., Wood, J. N., Matthews, E. A., Dickenson, A. H., & Nassar, M. A. (2005). Nociceptor-specific gene deletion using heterozygous NaV1.8-Cre recombinase mice. *Pain*, *113*(1-2), 27-36. https://doi.org/10.1016/j.pain.2004.08.015
Stirling, L. C., Forlani, G., Baker, M. D., Wood, J. N., Matthews, E. A., Dickenson, A. H., & Nassar, M. A. (2005). Nociceptor-specific gene deletion using heterozygous NaV1. 8-Cre recombinase mice. *Pain*, *113*(1-2), 27-36.
Striessnig, J., Ortner, N. J., & Pinggera, A. (2015). Pharmacology of L-type Calcium Channels: Novel Drugs for Old Targets? In *Curr Mol Pharmacol* (Vol. 8, pp. 110-122). https://doi.org/10.2174/1874467208666150507105845
Sudres, M., Ciré, S., Vasseur, V., Brault, L., Da Rocha, S., Boisgérault, F., . . . Galy, A. (2012). MyD88 signaling in B cells regulates the production of Th1-dependent antibodies to AAV. *Mol Ther*, *20*(8), 1571-1581. https://doi.org/10.1038/mt.2012.101
Sutherland, M. L., Williams, S. H., Abedi, R., Overbeek, P. A., Pfaffinger, P. J., & Noebels, J. L. (1999). Overexpression of a Shaker-type potassium channel in mammalian central

nervous system dysregulates native potassium channel gene expression. *Proc Natl Acad Sci U S A*, *96*(5), 2451-2455. https://doi.org/10.1073/pnas.96.5.2451
Suzuki, T., Higgins, P. J., & Crawford, D. R. (2000). Control Selection for RNA Quantitation. *BioTechniques*, *29*(2), 332-337. https://doi.org/10.2144/00292rv02
Szczot, M., Pogorzala, L. A., Solinski, H. J., Young, L., Yee, P., Le Pichon, C. E., . . . Hoon, M. A. (2017). Cell-type-specific splicing of Piezo2 regulates mechanotransduction. *Cell reports*, *21*(10), 2760-2771.
Takahashi, K., & Ninomiya, T. (1987). Morphological changes of dorsal root ganglion cells in the process-forming period. *Prog Neurobiol*, *29*(4), 393-410. https://doi.org/10.1016/0301-0082(87)90020-7
Takazawa, T., & MacDermott, A. B. (2010). Synaptic pathways and inhibitory gates in the spinal cord dorsal horn. *Ann N Y Acad Sci*, *1198*, 153-158. https://doi.org/10.1111/j.1749-6632.2010.05501.x
Tan, Z. Y., Piekarz, A. D., Priest, B. T., Knopp, K. L., Krajewski, J. L., McDermott, J. S., . . . Cummins, T. R. (2014). Tetrodotoxin-resistant sodium channels in sensory neurons generate slow resurgent currents that are enhanced by inflammatory mediators. *J Neurosci*, *34*(21), 7190-7197. https://doi.org/10.1523/jneurosci.5011-13.2014
Tang, N. K. Y. (2018). Cognitive behavioural therapy in pain and psychological disorders: Towards a hybrid future. *Progress in Neuro-Psychopharmacology and Biological Psychiatry*, *87*, 281-289. https://doi.org/https://doi.org/10.1016/j.pnpbp.2017.02.023
Tarjan, D. R., Flavahan, W. A., & Bernstein, B. E. (2019). Epigenome editing strategies for the functional annotation of CTCF insulators. *Nat Commun*, *10*(1), 4258. https://doi.org/10.1038/s41467-019-12166-w
Tatsumi, S., Ishii, K., Amizuka, N., Li, M., Kobayashi, T., Kohno, K., . . . Ikeda, K. (2007). Targeted ablation of osteocytes induces osteoporosis with defective mechanotransduction. *Cell Metab*, *5*(6), 464-475. https://doi.org/10.1016/j.cmet.2007.05.001
Teichert, R. W., Memon, T., Aman, J. W., & Olivera, B. M. (2014). Using constellation pharmacology to define comprehensively a somatosensory neuronal subclass. *Proceedings of the National Academy of Sciences*, *111*(6), 2319-2324.
Ter Heegde, F., Luiz, A. P., Santana-Varela, S., Chessell, I. P., Welsh, F., Wood, J. N., & Chenu, C. (2019). Noninvasive mechanical joint loading as an alternative model for osteoarthritic pain. *Arthritis & Rheumatology*, *71*(7), 1078-1088.
Teti, A., & Zallone, A. (2009). Do osteocytes contribute to bone mineral homeostasis? Osteocytic osteolysis revisited. *Bone*, *44*(1), 11-16. https://doi.org/https://doi.org/10.1016/j.bone.2008.09.017
Teunissen, S. C., Wesker, W., Kruitwagen, C., de Haes, H. C., Voest, E. E., & de Graeff, A. (2007). Symptom prevalence in patients with incurable cancer: a systematic review. *J Pain Symptom Manage*, *34*(1), 94-104. https://doi.org/10.1016/j.jpainsymman.2006.10.015
Thakkar, B., & Acevedo, E. O. (2023). BDNF as a biomarker for neuropathic pain: Consideration of mechanisms of action and associated measurement challenges. *Brain and Behavior*, *13*(3), e2903. https://doi.org/https://doi.org/10.1002/brb3.2903
Thompson, K. J., Khajehali, E., Bradley, S. J., Navarrete, J. S., Huang, X. P., Slocum, S., . . . Tobin, A. B. (2018). DREADD Agonist 21 Is an Effective Agonist for Muscarinic-Based DREADDs in Vitro and in Vivo. *ACS Pharmacol Transl Sci*, *1*(1), 61-72. https://doi.org/10.1021/acsptsci.8b00012
Tian, S. X., Xu, T., Shi, R. Y., Cai, Y. Q., Wu, M. H., Zhen, S. J., . . . Liang, Y. (2023). Analgesic effect of electroacupuncture on bone cancer pain in rat model: the role of peripheral P2X3 receptor. *Purinergic Signal*, *19*(1), 13-27. https://doi.org/10.1007/s11302-022-09861-7
Todd, A. J. (2010). Neuronal circuitry for pain processing in the dorsal horn. *Nature Reviews Neuroscience*, *11*(12), 823-836.
Todd, A. J. (2017). Identifying functional populations among the interneurons in laminae I-III of the spinal dorsal horn. *Molecular pain*, *13*, 1744806917693003.
Todd, A. J., Wang, F., Todd, A. J., & Wang, F. (2018). Central nervous system pain pathways. In *The Oxford Handbook of the Neurobiology of Pain*. Oxford University Press Oxford, UK.
Tominaga, M., Caterina, M. J., Malmberg, A. B., Rosen, T. A., Gilbert, H., Skinner, K., . . . Julius, D. (1998). The cloned capsaicin receptor integrates multiple pain-producing stimuli. *Neuron*, *21*(3), 531-543. https://doi.org/10.1016/s0896-6273(00)80564-4

Tomlinson, R. E., Li, Z., Li, Z., Minichiello, L., Riddle, R. C., Venkatesan, A., & Clemens, T. L. (2017). NGF-TrkA signaling in sensory nerves is required for skeletal adaptation to mechanical loads in mice. *Proc Natl Acad Sci U S A*, *114*(18), E3632-e3641. https://doi.org/10.1073/pnas.1701054114

Tomlinson, R. E., Li, Z., Zhang, Q., Goh, B. C., Li, Z., Thorek, D. L. J., . . . Clemens, T. L. (2016). NGF-TrkA Signaling by Sensory Nerves Coordinates the Vascularization and Ossification of Developing Endochondral Bone. *Cell Rep*, *16*(10), 2723-2735. https://doi.org/10.1016/j.celrep.2016.08.002

Treede, R. D., Rief, W., Barke, A., Aziz, Q., Bennett, M. I., Benoliel, R., . . . Wang, S. J. (2015). A classification of chronic pain for ICD-11. *Pain*, *156*(6), 1003-1007. https://doi.org/10.1097/j.pain.0000000000000160

Tsantoulas, C., & McMahon, S. B. (2014). Opening paths to novel analgesics: the role of potassium channels in chronic pain. *Trends in neurosciences*, *37*(3), 146-158.

Tso, A. R., & Goadsby, P. J. (2017). Anti-CGRP monoclonal antibodies: the next era of migraine prevention? *Current treatment options in neurology*, *19*(8), 1-11.

Tsuda, M., Shigemoto-Mogami, Y., Koizumi, S., Mizokoshi, A., Kohsaka, S., Salter, M. W., & Inoue, K. (2003). P2X4 receptors induced in spinal microglia gate tactile allodynia after nerve injury. *Nature*, *424*(6950), 778-783.

Tuttle, A. H., Tohyama, S., Ramsay, T., Kimmelman, J., Schweinhardt, P., Bennett, G. J., & Mogil, J. S. (2015). Increasing placebo responses over time in US clinical trials of neuropathic pain. *Pain*, *156*(12), 2616-2626.

Uhrig, S., Coutelle, O., Wiehe, T., Perabo, L., Hallek, M., & Büning, H. (2012). Successful target cell transduction of capsid-engineered rAAV vectors requires clathrin-dependent endocytosis. *Gene Ther*, *19*(2), 210-218. https://doi.org/10.1038/gt.2011.78

Urban, M. O., & Gebhart, G. F. (1999). Supraspinal contributions to hyperalgesia. *Proc Natl Acad Sci U S A*, *96*(14), 7687-7692. https://doi.org/10.1073/pnas.96.14.7687

Urch, C. (2007). Normal Pain Transmission. *Rev Pain*, *1*(1), 2-6. https://doi.org/10.1177/204946370700100102

Urch, C. E., Donovan-Rodriguez, T., Gordon-Williams, R., Bee, L. A., & Dickenson, A. H. (2005). Efficacy of chronic morphine in a rat model of cancer-induced bone pain: behavior and in dorsal horn pathophysiology. *J Pain*, *6*(12), 837-845.

Urch, E. C., Donovan-Rodriguez, T., & Dickenson, H. A. (2003). Alterations in dorsal horn neurones in a rat model of cancer-induced bone pain. *Pain*, *106*(3), 347-356. https://doi.org/10.1016/j.pain.2003.08.002

Usoskin, D., Furlan, A., Islam, S., Abdo, H., Lönnerberg, P., Lou, D., . . . Kharchenko, P. V. (2015). Unbiased classification of sensory neuron types by large-scale single-cell RNA sequencing. *Nature neuroscience*, *18*(1), 145-153.

Uutela, P., Reinilä, R., Piepponen, P., Ketola, R. A., & Kostiainen, R. (2005). Analysis of acetylcholine and choline in microdialysis samples by liquid chromatography/tandem mass spectrometry. *Rapid Commun Mass Spectrom*, *19*(20), 2950-2956. https://doi.org/10.1002/rcm.2160

Valente, V., Teixeira, S. A., Neder, L., Okamoto, O. K., Oba-Shinjo, S. M., Marie, S. K., . . . Carlotti, C. G., Jr. (2009). Selection of suitable housekeeping genes for expression analysis in glioblastoma using quantitative RT-PCR. *BMC Mol Biol*, *10*, 17. https://doi.org/10.1186/1471-2199-10-17

van den Beuken-van Everdingen, M. H., de Rijke, J. M., Kessels, A. G., Schouten, H. C., van Kleef, M., & Patijn, J. (2007). Prevalence of pain in patients with cancer: a systematic review of the past 40 years. *Ann Oncol*, *18*(9), 1437-1449. https://doi.org/10.1093/annonc/mdm056

van den Beuken-van Everdingen, M. H. J., de Rijke, J. M., Kessels, A. G., Schouten, H. C., van Kleef, M., & Patijn, J. (2007). High prevalence of pain in patients with cancer in a large population-based study in The Netherlands. *Pain*, *132*(3), 312-320. https://doi.org/10.1016/j.pain.2007.08.022

Van den Eynden, J., Ali, S. S., Horwood, N., Carmans, S., Brône, B., Hellings, N., . . . Rigo, J. M. (2009). Glycine and glycine receptor signalling in non-neuronal cells. *Front Mol Neurosci*, *2*, 9. https://doi.org/10.3389/neuro.02.009.2009

Vanderah, T. W., Laughlin, T., Lashbrook, J. M., Nichols, M. L., Wilcox, G. L., Ossipov, M. H., . . . Porreca, F. (1996). Single intrathecal injections of dynorphin A or des-Tyr-dynorphins produce long-lasting allodynia in rats: blockade by MK-801 but not naloxone. *Pain*, *68*(2-3), 275-281.

Vandewauw, I., De Clercq, K., Mulier, M., Held, K., Pinto, S., Van Ranst, N., . . . Zimmermann, K. (2018). A TRP channel trio mediates acute noxious heat sensing. *Nature*, *555*(7698), 662-666.
Vanegas, H., & Schaible, H. G. (2004). Descending control of persistent pain: inhibitory or facilitatory? *Brain Res Brain Res Rev*, *46*(3), 295-309. https://doi.org/10.1016/j.brainresrev.2004.07.004
Viana, F., & Voets, T. (2019). Heat pain and cold pain. In *The Oxford handbook of the neurobiology of pain*. Oxford University Press Oxford.
Vissing, H., Meyer, W. K. H., Aagaard, L., Tommerup, N., & Thiesen, H. J. (1995). Repression of transcriptional activity by heterologous KRAB domains present in zinc finger proteins. *FEBS Letters*, *369*(2), 153-157. https://doi.org/https://doi.org/10.1016/0014-5793(95)00728-R
Voilley, N., de Weille, J., Mamet, J., & Lazdunski, M. (2001). Nonsteroid anti-inflammatory drugs inhibit both the activity and the inflammation-induced expression of acid-sensing ion channels in nociceptors. *Journal of Neuroscience*, *21*(20), 8026-8033.
von Moos, R., Body, J. J., Egerdie, B., Stopeck, A., Brown, J., Fallowfield, L., . . . Qian, Y. (2016). Pain and analgesic use associated with skeletal-related events in patients with advanced cancer and bone metastases. *Support Care Cancer*, *24*(3), 1327-1337. https://doi.org/10.1007/s00520-015-2908-1
Voscopoulos, C., & Lema, M. (2010). When does acute pain become chronic? *BJA: British Journal of Anaesthesia*, *105*(suppl_1), i69-i85. https://doi.org/10.1093/bja/aeq323
Wacnik, P. W., Eikmeier, L. J., Simone, D. A., Wilcox, G. L., & Beitz, A. J. (2005). Nociceptive characteristics of tumor necrosis factor-α in naive and tumor-bearing mice. *Neuroscience*, *132*(2), 479-491. https://doi.org/https://doi.org/10.1016/j.neuroscience.2004.12.035
Waldmann, R., Bassilana, F., de Weille, J., Champigny, G., Heurteaux, C., & Lazdunski, M. (1997). Molecular cloning of a non-inactivating proton-gated Na+ channel specific for sensory neurons. *Journal of Biological Chemistry*, *272*(34), 20975-20978.
Wall, P. D., & McMahon, S. B. (1985). Microneuronography and its relation to perceived sensation. A critical review. *Pain*, *21*(3), 209-229.
Wang, D., Tawfik, V. L., Corder, G., Low, S. A., François, A., Basbaum, A. I., & Scherrer, G. (2018). Functional Divergence of Delta and Mu Opioid Receptor Organization in CNS Pain Circuits. *Neuron*, *98*(1), 90-108.e105. https://doi.org/10.1016/j.neuron.2018.03.002
Wang, L., Calcedo, R., Wang, H., Bell, P., Grant, R., Vandenberghe, L. H., . . . Wilson, J. M. (2010). The pleiotropic effects of natural AAV infections on liver-directed gene transfer in macaques. *Mol Ther*, *18*(1), 126-134. https://doi.org/10.1038/mt.2009.245
Wang, X., Zhang, J., Eberhart, D., Urban, R., Meda, K., Solorzano, C., . . . Basbaum, A. I. (2013). Excitatory superficial dorsal horn interneurons are functionally heterogeneous and required for the full behavioral expression of pain and itch. *Neuron*, *78*(2), 312-324. https://doi.org/10.1016/j.neuron.2013.03.001
Watkins, L. R., & Maier, S. F. (1999). Implications of immune-to-brain communication for sickness and pain. *Proc Natl Acad Sci U S A*, *96*(14), 7710-7713. https://doi.org/10.1073/pnas.96.14.7710
Wedel, M. J. (2011). A monument of inefficiency: The presumed course of the recurrent laryngeal nerve in sauropod dinosaurs. *Acta Palaeontologica Polonica*, *57*(2), 251-256.
Weir, G. A., Middleton, S. J., Clark, A. J., Daniel, T., Khovanov, N., McMahon, S. B., & Bennett, D. L. (2017). Using an engineered glutamate-gated chloride channel to silence sensory neurons and treat neuropathic pain at the source. *Brain*, *140*(10), 2570-2585. https://doi.org/10.1093/brain/awx201
Weiss, J., Pyrski, M., Jacobi, E., Bufe, B., Willnecker, V., Schick, B., . . . Zufall, F. (2011). Loss-of-function mutations in sodium channel Nav1.7 cause anosmia. *Nature*, *472*(7342), 186-190. https://doi.org/10.1038/nature09975
Wende, H., Lechner, S. G., Cheret, C., Bourane, S., Kolanczyk, M. E., Pattyn, A., . . . Lewin, G. R. (2012). The transcription factor c-Maf controls touch receptor development and function. *Science*, *335*(6074), 1373-1376.
Werman, R., Davidoff, R. A., & Aprison, M. H. (1967). Is Glycine a Neurotransmitter ?: Inhibition of Motoneurones by Iontophoresis of Glycine. *Nature*, *214*(5089), 681-683. https://doi.org/10.1038/214681a0
Westenbroek, R. E., Hell, J. W., Warner, C., Dubel, S. J., Snutch, T. P., & Catterall, W. A. (1992). Biochemical properties and subcellular distribution of an N-type calcium hannel α1 subunit. *Neuron*, *9*(6), 1099-1115.

Whinn, K. S., Kaur, G., Lewis, J. S., Schauer, G. D., Mueller, S. H., Jergic, S., . . . Ghodke, H. (2019). Nuclease dead Cas9 is a programmable roadblock for DNA replication. *Scientific Reports*, *9*(1), 13292. https://doi.org/10.1038/s41598-019-49837-z
Wickersham, I. R., Lyon, D. C., Barnard, R. J., Mori, T., Finke, S., Conzelmann, K. K., . . . Callaway, E. M. (2007). Monosynaptic restriction of transsynaptic tracing from single, genetically targeted neurons. *Neuron*, *53*(5), 639-647. https://doi.org/10.1016/j.neuron.2007.01.033
Wilcox, C. E., Mayer, A. R., Teshiba, T. M., Ling, J., Smith, B. W., Wilcox, G. L., & Mullins, P. G. (2015). The Subjective Experience of Pain: an FMRI Study of Percept-related Models and Functional Connectivity. *Pain Med*, *16*(11), 2121-2133. https://doi.org/10.1111/pme.12785
Wilke, B. U., Kummer, K. K., Leitner, M. G., & Kress, M. (2020). Chloride – The Underrated Ion in Nociceptors [Review]. *Frontiers in Neuroscience*, *14*.
Wong, G. Y., & Gavva, N. R. (2009). Therapeutic potential of vanilloid receptor TRPV1 agonists and antagonists as analgesics: Recent advances and setbacks. *Brain Res Rev*, *60*(1), 267-277. https://doi.org/10.1016/j.brainresrev.2008.12.006
Woo, S.-H., Lukacs, V., de Nooij, J. C., Zaytseva, D., Criddle, C. R., Francisco, A., . . . Patapoutian, A. (2015). Piezo2 is the principal mechanotransduction channel for proprioception. *Nature Neuroscience*, *18*(12), 1756-1762. https://doi.org/10.1038/nn.4162
Woo, S.-H., Ranade, S., Weyer, A. D., Dubin, A. E., Baba, Y., Qiu, Z., . . . Patapoutian, A. (2014). Piezo2 is required for Merkel-cell mechanotransduction. *Nature*, *509*(7502), 622-626. https://doi.org/10.1038/nature13251
Wood, J. N. (2015). From plant extract to molecular panacea: a commentary on Stone (1763)'An account of the success of the bark of the willow in the cure of the agues'. *Philosophical Transactions of the Royal Society B: Biological Sciences*, *370*(1666), 20140317.
Wood, J. N. (2020). *The Oxford Handbook of the Neurobiology of Pain*. Oxford University Press.
Woolf, C. J. (1983). Evidence for a central component of post-injury pain hypersensitivity. *Nature*, *306*(5944), 686-688.
Woolf, C. J. (1984). Long term alterations in the excitability of the flexion reflex produced by peripheral tissue injury in the chronic decerebrate rat. *Pain*, *18*(4), 325-343.
Woolf, C. J. (2018). Pain amplification—a perspective on the how, why, when, and where of central sensitization. *Journal of Applied Biobehavioral Research*, *23*(2), e12124.
Woolf, C. J., & Thompson, S. W. N. (1991). The induction and maintenance of central sensitization is dependent on N-methyl-D-aspartic acid receptor activation; implications for the treatment of post-injury pain hypersensitivity states. *Pain*, *44*(3), 293-299.
Wright, A. (2011). A Criticism of the IASPs Definition of Pain. *Journal of Consciousness Studies*, *18*(9-10).
Wu, J., Yan, Z., Li, Z., Qian, X., Lu, S., Dong, M., . . . Yan, N. (2016). Structure of the voltage-gated calcium channel Cav1. 1 at 3.6 Å resolution. *Nature*, *537*(7619), 191-196.
Wu, Z., Asokan, A., & Samulski, R. J. (2006). Adeno-associated virus serotypes: vector toolkit for human gene therapy. *Mol Ther*, *14*(3), 316-327. https://doi.org/10.1016/j.ymthe.2006.05.009
Xia, X. G., Zhou, H., Ding, H., Affar el, B., Shi, Y., & Xu, Z. (2003). An enhanced U6 promoter for synthesis of short hairpin RNA. *Nucleic Acids Res*, *31*(17), e100. https://doi.org/10.1093/nar/gng098
Xiong, J., Onal, M., Jilka, R. L., Weinstein, R. S., Manolagas, S. C., & O'Brien, C. A. (2011). Matrix-embedded cells control osteoclast formation. *Nat Med*, *17*(10), 1235-1241. https://doi.org/10.1038/nm.2448
Xiong, Z.-G., Zhu, X.-M., Chu, X.-P., Minami, M., Hey, J., Wei, W.-L., . . . Simon, R. P. (2004). Neuroprotection in Ischemia: Blocking Calcium-Permeable Acid-Sensing Ion Channels. *Cell*, *118*(6), 687-698. https://doi.org/https://doi.org/10.1016/j.cell.2004.08.026
Xu, M., Kontinen, V. K., & Kalso, E. (1999). Endogenous noradrenergic tone controls symptoms of allodynia in the spinal nerve ligation model of neuropathic pain. *Eur J Pharmacol*, *366*(1), 41-45. https://doi.org/10.1016/s0014-2999(98)00910-8
Yalcin, I., Megat, S., Barthas, F., Waltisperger, E., Kremer, M., Salvat, E., & Barrot, M. (2014). The sciatic nerve cuffing model of neuropathic pain in mice. *J Vis Exp*(89). https://doi.org/10.3791/51608
Yanagisawa, Y., Furue, H., Kawamata, T., Uta, D., Yamamoto, J., Furuse, S., . . . Yoshimura, M. (2010). Bone cancer induces a unique central sensitization through synaptic

changes in a wide area of the spinal cord. *Molecular Pain*, *6*. https://doi.org/10.1186/1744-8069-6-38
Yang, J., Zhang, J., Yang, H., Li, K., Lei, X., & Xu, C. (2016). The potential role of Piezo2 in the mediation of visceral sensation. *Neuroscience Letters*, *630*, 158-163. https://doi.org/https://doi.org/10.1016/j.neulet.2016.07.058
Yang, Y., Zhang, J., Gao, Q., Bo, J., & Ma, Z. (2017). Etanercept attenuates thermal and mechanical hyperalgesia induced by bone cancer. *Exp Ther Med*, *13*(5), 2565-2569. https://doi.org/10.3892/etm.2017.4260
Yao, P., Ding, Y., Wang, Z., Ma, J., Hong, T., Zhu, Y., . . . Pan, S. (2016). Impacts of anti-nerve growth factor antibody on pain-related behaviors and expressions of opioid receptor in spinal dorsal horn and dorsal root ganglia of rats with cancer-induced bone pain. *Mol Pain*, *12*. https://doi.org/10.1177/1744806916644928
Yeo, N. C., Chavez, A., Lance-Byrne, A., Chan, Y., Menn, D., Milanova, D., . . . Church, G. M. (2018). An enhanced CRISPR repressor for targeted mammalian gene regulation. *Nature Methods*, *15*(8), 611-616. https://doi.org/10.1038/s41592-018-0048-5
Yoneda, T., Sasaki, A., & Mundy, G. R. (1994). Osteolytic bone metastasis in breast cancer. *Breast Cancer Res Treat*, *32*(1), 73-84. https://doi.org/10.1007/bf00666208
You, H. J., Lei, J., Sui, M. Y., Huang, L., Tan, Y. X., Tjølsen, A., & Arendt-Nielsen, L. (2010). Endogenous descending modulation: spatiotemporal effect of dynamic imbalance between descending facilitation and inhibition of nociception. *J Physiol*, *588*(Pt 21), 4177-4188. https://doi.org/10.1113/jphysiol.2010.196923
Yu, D., Thakor, D. K., Han, I., Ropper, A. E., Haragopal, H., Sidman, R. L., . . . Teng, Y. D. (2013). Alleviation of chronic pain following rat spinal cord compression injury with multimodal actions of huperzine A. *Proceedings of the National Academy of Sciences*, *110*(8), E746-E755. https://doi.org/10.1073/pnas.1300083110
Zamponi, G. W., Gandini, M. A., & Snutch, T. P. (2018). Voltage-Gated Calcium Channels: Molecular Targets for Treating Chronic Pain.
Zamponi, G. W., Striessnig, J., Koschak, A., & Dolphin, A. C. (2015). The physiology, pathology, and pharmacology of voltage-gated calcium channels and their future therapeutic potential. *Pharmacological reviews*, *67*(4), 821-870.
Zeisel, A., Hochgerner, H., Lönnerberg, P., Johnsson, A., Memic, F., Van Der Zwan, J., . . . La Manno, G. (2018). Molecular architecture of the mouse nervous system. *Cell*, *174*(4), 999-1014.
Zemelman, B. V., Nesnas, N., Lee, G. A., & Miesenböck, G. (2003). Photochemical gating of heterologous ion channels: Remote control over genetically designated populations of neurons. *Proceedings of the National Academy of Sciences*, *100*(3), 1352-1357. https://doi.org/10.1073/pnas.242738899
Zhang, F., Wang, Y., Liu, Y., Han, H., Zhang, D., Fan, X., . . . Zhang, H. (2019). Transcriptional Regulation of Voltage-Gated Sodium Channels Contributes to GM-CSF-Induced Pain. *The Journal of Neuroscience*, *39*(26), 5222. https://doi.org/10.1523/JNEUROSCI.2204-18.2019
Zhang, H., Craciun, L. C., Mirshahi, T., Rohács, T., Lopes, C. M., Jin, T., & Logothetis, D. E. (2003). PIP(2) activates KCNQ channels, and its hydrolysis underlies receptor-mediated inhibition of M currents. *Neuron*, *37*(6), 963-975. https://doi.org/10.1016/s0896-6273(03)00125-9
Zhang, H., Yang, B., Mu, X., Ahmed, S. S., Su, Q., He, R., . . . Gao, G. (2011). Several rAAV vectors efficiently cross the blood-brain barrier and transduce neurons and astrocytes in the neonatal mouse central nervous system. *Mol Ther*, *19*(8), 1440-1448. https://doi.org/10.1038/mt.2011.98
Zhang, L., Berta, T., Xu, Z. Z., Liu, T., Park, J. Y., & Ji, R. R. (2011). TNF-α contributes to spinal cord synaptic plasticity and inflammatory pain: Distinct role of TNF receptor subtype 1 and 2. *Pain*, *152*(2), 419-427. https://doi.org/10.1016/j.pain.2010.11.014
Zhang, N., & Bevan, M. J. (2011). CD8(+) T cells: foot soldiers of the immune system. *Immunity*, *35*(2), 161-168. https://doi.org/10.1016/j.immuni.2011.07.010
Zhang, R. X., Liu, B., Li, A., Wang, L., Ren, K., Qiao, J. T., . . . Lao, L. (2008). Interleukin 1beta facilitates bone cancer pain in rats by enhancing NMDA receptor NR-1 subunit phosphorylation. *Neuroscience*, *154*(4), 1533-1538. https://doi.org/10.1016/j.neuroscience.2008.04.072
Zhang, X. F., Zhu, C. Z., Thimmapaya, R., Choi, W. S., Honore, P., Scott, V. E., . . . Shieh, C. C. (2004). Differential action potentials and firing patterns in injured and uninjured small dorsal root ganglion neurons after nerve injury. *Brain Res*, *1009*(1-2), 147-158. https://doi.org/10.1016/j.brainres.2004.02.057

Zhao, G. Q., Zhang, Y., Hoon, M. A., Chandrashekar, J., Erlenbach, I., Ryba, N. J., & Zuker, C. S. (2003). The receptors for mammalian sweet and umami taste. *Cell*, *115*(3), 255-266. https://doi.org/10.1016/s0092-8674(03)00844-4

Zheng, C., & Baum, B. J. (2008). Evaluation of promoters for use in tissue-specific gene delivery. *Methods Mol Biol*, *434*, 205-219. https://doi.org/10.1007/978-1-60327-248-3_13

Zhou, X., Wang, L., Hasegawa, H., Amin, P., Han, B.-X., Kaneko, S., . . . Wang, F. (2010). Deletion of PIK3C3/Vps34 in sensory neurons causes rapid neurodegeneration by disrupting the endosomal but not the autophagic pathway. *Proceedings of the National Academy of Sciences*, *107*(20), 9424-9429.

Zhou, X., Xiao, Z., Xu, Y., Zhang, Y., Tang, D., Wu, X., . . . Liu, Z. (2017). Electrophysiological and Pharmacological Analyses of Nav1.9 Voltage-Gated Sodium Channel by Establishing a Heterologous Expression System [Original Research]. *Frontiers in Pharmacology*, *8*.

Zhou, Z., Davar, G., & Strichartz, G. (2002). Endothelin-1 (ET-1) selectively enhances the activation gating of slowly inactivating tetrodotoxin-resistant sodium currents in rat sensory neurons: a mechanism for the pain-inducing actions of ET-1. *J Neurosci*, *22*(15), 6325-6330. https://doi.org/10.1523/jneurosci.22-15-06325.2002

Zotterman, Y. (1936). Specific action potentials in the lingual nerve of cat. *Skandinavisches Archiv Für Physiologie*, *75*(3), 105-119.

Zotterman, Y. (1939). Touch, pain and tickling: an electro-physiological investigation on cutaneous sensory nerves. *The Journal of physiology*, *95*(1), 1.